

Reference Equations of State for the Thermodynamic Properties of Fluid Phase *n*-Butane and Isobutane

D. Bücker^{a)} and W. Wagner^{b)}

Lehrstuhl für Thermodynamik, Ruhr-Universität Bochum, D-44780 Bochum, Germany

(Received 23 June 2004; revised manuscript received 3 January 2005; accepted 26 January 2005; published online 2 June 2006)

New formulations for the thermodynamic properties of fluid phase *n*-butane and isobutane in the form of fundamental equations explicit in the Helmholtz energy are presented. The functional form of the correlation equations for the residual parts was developed simultaneously for both substances considering data for the thermodynamic properties of ethane, propane, *n*-butane, and isobutane. Each contains 25 coefficients which were fitted to selected data for the thermal and caloric properties of the respective fluid both in the single-phase region and on the vapor–liquid phase boundary. This work provides information on the available experimental data for the thermodynamic properties of *n*- and isobutane, and presents all details of the new formulations. The new equations of state describe the $p\rho T$ surfaces with uncertainties in density of 0.02% (coverage factor $k=2$ corresponding to a confidence level of about 95%) from the melting line up to temperatures of 340 K and pressures of 12 MPa. The available reliable data sets in other regions are represented within their experimental uncertainties. The primary data, to which the equation for *n*-butane was fitted, cover the fluid region from the melting line to temperatures of 575 K and pressures of 69 MPa. The equation for isobutane was fitted to primary data that cover the fluid region from the melting line to temperatures of 575 K and pressures of 35 MPa. Beyond the range described by experimental data, the equations yield reasonable extrapolation behavior up to very high temperatures and pressures. In addition to the equations of state, independent equations for the vapor pressures, the saturated-liquid and saturated-vapor densities, and the melting pressures are given. Tables of thermodynamic properties calculated from the new formulations are listed in Appendix 2. Additionally, a preliminary equation of state for propane is presented that was developed in the course of the simultaneous optimization. This equation has the same functional form as the equations of state for *n*- and isobutane. © 2006 American Institute of Physics. [DOI: 10.1063/1.1901687]

Key words: caloric properties; density; equation of state; fundamental equation; isobutane; multiproperty fitting; *n*-butane; propane; property tables; simultaneous optimization; thermal properties; thermodynamic properties; vapor–liquid phase boundary.

Contents

1. Introduction.....	935	2.6. Saturated-Vapor Density.....	940
1.1. Background.....	935	2.7. Caloric Data on the Vapor–Liquid Phase Boundary.....	941
1.2. Previous Equations of State.....	935	3. Data for the Single-Phase Region.....	942
1.3. Notes on the Values of Temperature Used in this Paper.....	936	3.1. <i>n</i> -Butane.....	943
2. Phase Equilibria of <i>n</i> - and Isobutane.....	936	3.1.1. Thermal Properties.....	943
2.1. Triple Point.....	937	3.1.2. Isochoric Heat Capacities.....	944
2.2. Critical Point.....	937	3.1.3. Isobaric Heat Capacities of the Real Fluid.....	945
2.3. Melting Pressure.....	937	3.1.4. Ideal-Gas Isobaric Heat Capacities....	945
2.4. Vapor Pressure.....	937	3.1.5. Speeds of Sound.....	946
2.5. Saturated-Liquid Density.....	939	3.2. Isobutane.....	946
		3.2.1. Thermal Properties.....	946
		3.2.2. Isobaric Heat Capacities of the Real Fluid.....	947
		3.2.3. Ideal-Gas Isobaric Heat Capacities....	948
		3.2.4. Speeds of Sound.....	949
		4. The New Equations of State.....	949
		4.1. The Equations for the Helmholtz Energy of	

^{a)}Current address: E.ON Energy Projects GmbH, Denisstr. 2, D-80335 München, Germany.

^{b)}Author to whom correspondence should be addressed; electronic mail: wagner@thermo.ruhr-uni-bochum.de

© 2006 American Institute of Physics.

the Ideal Gas.....	950	of <i>n</i> -butane.....	939
4.2. The Equations for the Residual Part of the Helmholtz Energy.....	950	7. Summary of the data sets for the vapor pressure of isobutane.....	939
4.2.1. Fitting the Coefficients.....	950	8. Parameters for the vapor-pressure equations of <i>n</i> - and isobutane, Eq. (2.2).....	939
4.2.2. Optimizing the Functional Form.....	952	9. Parameters for the saturated-liquid density equations of <i>n</i> - and isobutane, Eq. (2.3).....	940
4.2.3. Selected Database.....	954	10. Summary of the data sets for the saturated-liquid density of <i>n</i> -butane.....	940
4.2.4. The Equations for the Residual Part α^r	954	11. Summary of the data sets for the saturated-liquid density of isobutane.....	941
5. Comparison of the Simultaneously Optimized Equations of State with Experimental Data.....	956	12. Summary of the data sets for the saturated-vapor density of <i>n</i> -butane.....	941
5.1. The Vapor-Liquid Phase Boundary of <i>n</i> -Butane.....	957	13. Summary of the data sets for the saturated-vapor density of isobutane.....	941
5.1.1. Thermal Properties.....	957	14. Parameters for the saturated-vapor density equations of <i>n</i> - and isobutane, Eq. (2.4).....	942
5.1.2. Caloric Properties.....	958	15. Summary of the data sets for caloric properties on the vapor-liquid phase boundary of <i>n</i> -butane.....	942
5.2. The Single-Phase Region of <i>n</i> -Butane.....	958	16. Summary of the data sets for caloric properties on the vapor-liquid phase boundary of isobutane.....	943
5.2.1. $p\rho T$ Data.....	958	17. Summary of the $p\rho T$ data sets for <i>n</i> -butane that were assigned to group 1. Uncertainties are given where the original articles contain such estimates. Uncertainty values in parentheses were estimated by ourselves.....	944
5.2.2. Virial Coefficients.....	959	18. Summary of the $p\rho T$ data sets for <i>n</i> -butane that were assigned to groups 2 and 3.....	944
5.2.3. Isochoric Heat Capacity.....	959	19. Summary of the data sets for the second and third virial coefficients of <i>n</i> -butane.....	944
5.2.4. Isobaric Heat Capacity.....	959	20. Details on the data for the isochoric heat capacity of <i>n</i> -butane that were assigned to group 1. Uncertainties are given as estimated by the authors. Uncertainty values in parentheses were estimated by ourselves.....	945
5.2.5. Speed of Sound.....	961	21. Summary of the available data sets for the isobaric heat capacity of <i>n</i> -butane. Uncertainties are given as estimated by the authors.....	946
5.3. The Vapor-Liquid Phase Boundary of Isobutane.....	963	22. Summary of the data sets for the isobaric heat capacity of <i>n</i> -butane in the ideal-gas state. Uncertainties are given where the original articles contain such estimates.....	946
5.3.1. Thermal Properties.....	963	23. Summary of the data sets for the speed of sound of <i>n</i> -butane that were assigned to group 1. Uncertainties are given where the original articles contain such estimates. Uncertainty values in parentheses were estimated by ourselves.....	947
5.3.2. Caloric Properties.....	964	24. Summary of the data sets for the speed of sound of <i>n</i> -butane that were assigned to group 3.....	947
5.4. The Single-Phase Region of Isobutane.....	965	25. Corrections applied to the speed of sound data measured by Ewing <i>et al.</i> (1988).....	947
5.4.1. $p\rho T$ Data.....	965	26. Summary of the $p\rho T$ data sets for isobutane that were assigned to group 1. Uncertainty values in parentheses were estimated by ourselves.....	948
5.4.2. Virial Coefficients.....	966	27. Summary of the $p\rho T$ data sets for isobutane that	
5.4.3. Isobaric Heat Capacity.....	967		
5.4.4. Speed of Sound.....	967		
5.5. Extrapolation Behavior.....	968		
5.5.1. High Pressures and High Temperatures.....	968		
5.5.2. Ideal Curves.....	969		
6. Estimated Uncertainty of Calculated Properties.....	969		
7. Recommendations for Improving the Basis of the Experimental Data for <i>n</i> - and Isobutane.....	970		
8. Acknowledgments.....	971		
9. Appendix 1: The Simultaneously Optimized Equation of State for Propane.....	972		
10. Appendix 2: Tables of Thermodynamic Properties of <i>n</i> - and Isobutane.....	974		
11. References.....	1017		

List of Tables

1. Information on selected equations of state for <i>n</i> - and isobutane.....	936
2. Available data for the triple-point temperatures of <i>n</i> - and isobutane.....	937
3. Parameters for the characteristic points on the vapor-liquid phase boundaries of <i>n</i> - and isobutane.....	937
4. Available data for the critical points of <i>n</i> - and isobutane. Uncertainties are given where the original articles contain such estimates.....	938
5. Parameters for the melting-pressure equations of <i>n</i> - and isobutane, Eq. (2.1).....	938
6. Summary of the data sets for the vapor pressure	
of <i>n</i> -butane.....	939
7. Summary of the data sets for the vapor pressure of isobutane.....	939
8. Parameters for the vapor-pressure equations of <i>n</i> - and isobutane, Eq. (2.2).....	939
9. Parameters for the saturated-liquid density equations of <i>n</i> - and isobutane, Eq. (2.3).....	940
10. Summary of the data sets for the saturated-liquid density of <i>n</i> -butane.....	940
11. Summary of the data sets for the saturated-liquid density of isobutane.....	941
12. Summary of the data sets for the saturated-vapor density of <i>n</i> -butane.....	941
13. Summary of the data sets for the saturated-vapor density of isobutane.....	941
14. Parameters for the saturated-vapor density equations of <i>n</i> - and isobutane, Eq. (2.4).....	942
15. Summary of the data sets for caloric properties on the vapor-liquid phase boundary of <i>n</i> -butane.....	942
16. Summary of the data sets for caloric properties on the vapor-liquid phase boundary of isobutane.....	943
17. Summary of the $p\rho T$ data sets for <i>n</i> -butane that were assigned to group 1. Uncertainties are given where the original articles contain such estimates. Uncertainty values in parentheses were estimated by ourselves.....	944
18. Summary of the $p\rho T$ data sets for <i>n</i> -butane that were assigned to groups 2 and 3.....	944
19. Summary of the data sets for the second and third virial coefficients of <i>n</i> -butane.....	944
20. Details on the data for the isochoric heat capacity of <i>n</i> -butane that were assigned to group 1. Uncertainties are given as estimated by the authors. Uncertainty values in parentheses were estimated by ourselves.....	945
21. Summary of the available data sets for the isobaric heat capacity of <i>n</i> -butane. Uncertainties are given as estimated by the authors.....	946
22. Summary of the data sets for the isobaric heat capacity of <i>n</i> -butane in the ideal-gas state. Uncertainties are given where the original articles contain such estimates.....	946
23. Summary of the data sets for the speed of sound of <i>n</i> -butane that were assigned to group 1. Uncertainties are given where the original articles contain such estimates. Uncertainty values in parentheses were estimated by ourselves.....	947
24. Summary of the data sets for the speed of sound of <i>n</i> -butane that were assigned to group 3.....	947
25. Corrections applied to the speed of sound data measured by Ewing <i>et al.</i> (1988).....	947
26. Summary of the $p\rho T$ data sets for isobutane that were assigned to group 1. Uncertainty values in parentheses were estimated by ourselves.....	948
27. Summary of the $p\rho T$ data sets for isobutane that	

were assigned to groups 2 and 3.....	948	energy of propane, Eqs. (4.5) and (4.6).....	971
28. Summary of the data sets for the second and third virial coefficients of isobutane.....	949	42. Coefficients of the equation of the residual part α^r of the dimensionless Helmholtz energy of propane, Eq. (4.12).....	971
29. Summary of the data sets for the isobaric heat capacity of isobutane that were assigned to group 1. Uncertainties are given where the original articles contain such estimates. Uncertainty values in parentheses were estimated by ourselves.....	949	43. Coefficients for the correlation equations for the thermal properties on the vapor–liquid phase boundary of propane, Eqs. (9.2)–(9.4).....	971
30. Summary of the data sets for the isobaric heat capacity of isobutane that were assigned to group 3.....	950	44. Thermodynamic properties of <i>n</i> -butane on the vapor–liquid phase boundary as a function of temperature.....	974
31. Summary of the data sets for the isobaric heat capacity of isobutane in the ideal-gas state. Uncertainties are given where the original articles contain such estimates.....	950	45. Thermodynamic properties of <i>n</i> -butane in the single-phase region.....	980
32. Summary of the data for the speed of sound of isobutane that were assigned to group 1. Uncertainty values in parentheses were estimated by ourselves.....	951	46. Thermodynamic properties of isobutane on the vapor–liquid phase boundary as a function of temperature.....	996
33. Relations of thermodynamic properties to the ideal-gas part α° , Eq. (4.6), and the residual part α^r , Eq. (4.12), of the dimensionless Helmholtz energy and their derivatives.....	951	47. Thermodynamic properties of isobutane in the single-phase region.....	1003
34. Coefficients of the correlation equations for the ideal-gas isobaric heat capacity c_p and the ideal-gas part α° of the dimensionless Helmholtz energy of <i>n</i> - and isobutane, Eqs. (4.5) and (4.6).....	952		
35. The ideal-gas part α° , Eq. (4.6), of the dimensionless Helmholtz energy and its derivatives.....	952		
36. Summary of the selected data for thermodynamic properties of <i>n</i> - and isobutane that were used in the simultaneous optimization and nonlinear fit of the residual parts α^r of <i>n</i> - and isobutane, Eq. (4.12).....	953		
37. Summary of the experimental data for thermodynamic properties of ethane that were used in the simultaneous optimization of the residual parts α^r of <i>n</i> - and isobutane, Eq. (4.12).....	954		
38. Summary of the experimental data for thermodynamic properties of propane that were used in the simultaneous optimization of the residual parts α^r of <i>n</i> - and isobutane, Eq. (4.12).....	955		
39. Coefficients and exponents of the equation of the residual part α^r of the dimensionless Helmholtz energy of <i>n</i> - and isobutane, Eq. (4.12).....	955		
40. The residual part, α^r , Eq. (4.12), of the dimensionless Helmholtz energy and its derivatives.....	956		
41. Coefficients for the correlation equations for the ideal-gas isobaric heat capacity c_p and the ideal-gas part α° of the dimensionless Helmholtz			

List of Figures

1. Absolute deviations and percentage deviations $100\Delta p_s/p_s = 100(p_{s,\text{exp}} - p_{s,\text{calc}})/p_{s,\text{exp}}$ of experimental data for the vapor pressure p_s of <i>n</i> -butane from values calculated from the vapor-pressure equation, Eq. (2.2).....	939
2. Absolute deviations and percentage deviations $100\Delta p_s/p_s = 100(p_{s,\text{exp}} - p_{s,\text{calc}})/p_{s,\text{exp}}$ of experimental data for the vapor pressure p_s of isobutane from values calculated from the vapor-pressure equation, Eq. (2.2). In order not to overcrowd the diagram for $T > 310$ K, from the data of Miyamoto <i>et al.</i> (2004) only about every second data point is plotted.....	940
3. Percentage deviations $100\Delta\rho'/\rho' = 100(\rho'_{\text{exp}} - \rho'_{\text{calc}})/\rho'_{\text{exp}}$ of experimental data for the saturated-liquid density ρ' of <i>n</i> -butane from values calculated from the equation for the saturated-liquid density, Eq. (2.3).....	940
4. Percentage deviations $100\Delta\rho'/\rho' = 100(\rho'_{\text{exp}} - \rho'_{\text{calc}})/\rho'_{\text{exp}}$ of experimental data for the saturated-liquid density ρ' of isobutane from values calculated from the equation for the saturated-liquid density, Eq. (2.3).....	941
5. Percentage deviations $100\Delta\rho''/\rho'' = 100(\rho''_{\text{exp}} - \rho''_{\text{calc}})/\rho''_{\text{exp}}$ of the selected data for the saturated-vapor density ρ'' of <i>n</i> -butane from values calculated from the equation for the saturated-vapor density, Eq. (2.4).....	942
6. Percentage deviations $100\Delta\rho''/\rho'' = 100(\rho''_{\text{exp}} - \rho''_{\text{calc}})/\rho''_{\text{exp}}$ of the selected data for the saturated-vapor density ρ'' of isobutane from values calculated from the equation for the saturated-vapor density, Eq. (2.4).....	942
7. Distribution of the experimental $p\rho T$ data for <i>n</i> -butane used to develop the residual part of the equation of state, Eq. (4.1), in a $p-T$ diagram.....	943

8. Distribution of the experimental data for the caloric properties of <i>n</i> -butane used to develop the residual part of the equation of state, Eq. (4.1), in a <i>p-T</i> diagram.	945	
9. Distribution of the experimental <i>pρT</i> data for isobutane used to develop the residual part of the equation of state, Eq. (4.1), in a <i>p-T</i> diagram.	948	
10. Distribution of the experimental data for the caloric properties of isobutane used to develop the residual part of the equation of state, Eq. (4.1), in a <i>p-T</i> diagram.	949	
11. Absolute deviations and percentage deviations [$100\Delta y/y = 100(y_{\text{exp}} - y_{\text{calc}})/y_{\text{exp}}$ with $y = p_s, \rho', \rho''$] of the selected thermal data for <i>n</i> -butane at saturation from values calculated from the equation of state, Eq. (4.1). Values calculated from the ancillary equations, Eqs. (2.2)–(2.4), and from the equations of state of Miyamoto and Watanabe (2001) and of Younglove and Ely (1987) are plotted for comparison.	957	
12. Percentage deviations [$100\Delta y/y = 100(y_{\text{exp}} - y_{\text{calc}})/y_{\text{exp}}$ with $y = w', c_\sigma$] of data for the speed of sound in saturated-liquid <i>n</i> -butane and for the heat capacity along the saturated-liquid line of <i>n</i> -butane from values calculated from the equation of state, Eq. (4.1). Values calculated from the equations of state of Miyamoto and Watanabe (2001) and of Younglove and Ely (1987) are plotted for comparison.	957	
13. Percentage density deviations of highly accurate <i>pρT</i> data for <i>n</i> -butane from values calculated from the equation of state, Eq. (4.1). Values calculated from the equations of state of Miyamoto and Watanabe (2001) and of Younglove and Ely (1987) are plotted for comparison.	959	
14. Percentage density deviations of <i>pρT</i> data for <i>n</i> -butane assigned to groups 1 and 2 at pressures up to 4 MPa from values calculated from the equation of state, Eq. (4.1). Values calculated from the equations of state of Miyamoto and Watanabe (2001) and of Younglove and Ely (1987) are plotted for comparison.	960	
15. Percentage density deviations of <i>pρT</i> data for <i>n</i> -butane assigned to groups 1 and 2 from values calculated from the equation of state, Eq. (4.1). Values calculated from the equations of state of Miyamoto and Watanabe (2001) and of Younglove and Ely (1987) are plotted for comparison.	960	
16. Percentage pressure deviations $100\Delta p/p = 100(p_{\text{exp}} - p_{\text{calc}})/p_{\text{exp}}$ of <i>pρT</i> data for <i>n</i> -butane on a near-critical isotherm from values calculated from the equation of state, Eq. (4.1). Values calculated from the equations of state of Miyamoto and Watanabe (2001) and of Younglove and Ely (1987) are plotted for comparison.	961	
17. Representation of data for the second virial coefficient of <i>n</i> -butane at temperatures up to 600 K. The plotted lines correspond to values calculated from the equation of state, Eq. (4.1), and from the equations of state of Miyamoto and Watanabe (2001) and of Younglove and Ely (1987).	961	
18. Representation of data for the third virial coefficient of <i>n</i> -butane at temperatures up to 600 K. The plotted lines correspond to values calculated from the equation of state, Eq. (4.1), and from the equations of state of Miyamoto and Watanabe (2001) and of Younglove and Ely (1987).	961	
19. Percentage deviations of isochoric heat capacity data for <i>n</i> -butane measured by Magee and Lüdecke (1998) from values calculated from the equation of state, Eq. (4.1). Values calculated from the equations of state of Miyamoto and Watanabe (2001) and of Younglove and Ely (1987) are plotted for comparison.	962	
20. Percentage deviations $\Delta c_p/c_p = (c_{p,\text{exp}} - c_{p,\text{calc}})/c_{p,\text{exp}}$ of isobaric heat capacity data for <i>n</i> -butane from values calculated from the equation of state, Eq. (4.1). Values calculated from the equations of state of Miyamoto and Watanabe (2001) and of Younglove and Ely (1987) are plotted for comparison.	962	
21. Percentage deviations of speed of sound data for <i>n</i> -butane in the liquid and supercritical region from values calculated from the equation of state, Eq. (4.1). Values calculated from the equations of state of Miyamoto and Watanabe (2001) and of Younglove and Ely (1987) are plotted for comparison.	962	
22. Percentage deviations of speed of sound data for <i>n</i> -butane in the gaseous region from values calculated from the equation of state, Eq. (4.1). Values calculated from the equations of state of Miyamoto and Watanabe (2001) and of Younglove and Ely (1987) are plotted for comparison.	963	

23. Absolute deviations and percentage deviations [$100\Delta y/y = 100(y_{\text{exp}} - y_{\text{calc}})/y_{\text{exp}}$ with $y = p_s, \rho', \rho''$] of the selected thermal data for isobutane at saturation from values calculated from the equation of state, Eq. (4.1). Values calculated from the ancillary equations, Eqs. (2.2)–(2.4), and from the equations of state of Miyamoto and Watanabe (2002) and of Younglove and Ely (1987) are plotted for comparison.	963	967
24. Percentage deviations $100\Delta c_\sigma/c_\sigma = 100(c_{\sigma,\text{exp}} - c_{\sigma,\text{calc}})/c_{\sigma,\text{exp}}$ of data for the heat capacity along the saturated-liquid line of isobutane from values calculated from the equation of state, Eq. (4.1). Values calculated from the equations of state of Miyamoto and Watanabe (2002) and of Younglove and Ely (1987) are plotted for comparison.	964	968
25. Percentage density deviations of highly accurate $p\rho T$ data for isobutane from values calculated from the equation of state, Eq. (4.1). Values calculated from the equations of state of Miyamoto and Watanabe (2002) and of Younglove and Ely (1987) are plotted for comparison.	964	968
26. Percentage density deviations of $p\rho T$ data for isobutane assigned to groups 1 and 2 from values calculated from the equation of state, Eq. (4.1). Values calculated from the equations of state of Miyamoto and Watanabe (2002) and of Younglove and Ely (1987) are plotted for comparison.	965	
27. Percentage pressure deviations $100\Delta p/p = 100(p_{\text{exp}} - p_{\text{calc}})/p_{\text{exp}}$ of $p\rho T$ data for isobutane on a near-critical isotherm from values calculated from the equation of state, Eq. (4.1). Values calculated from the equations of state of Miyamoto and Watanabe (2002) and of Younglove and Ely (1987) are plotted for comparison.	966	969
28. Representation of data for the second virial coefficient of isobutane at temperatures up to 600 K. The plotted lines correspond to values calculated from the equation of state, Eq. (4.1), and from the equations of state of Miyamoto and Watanabe (2002) and of Younglove and Ely (1987).	966	969
29. Representation of data for the third virial coefficient of isobutane at temperatures up to 450 K. The plotted lines correspond to values calculated from the equation of state, Eq. (4.1), and from the equations of state of Miyamoto and Watanabe (2002) and of Younglove and Ely (1987).	967	970
30. Percentage deviations of isobaric heat capacity data for isobutane assigned to group 1 from values calculated from the equation of state, Eq. (4.1). Values calculated from the equations of state of Miyamoto and Watanabe (2002) and of Younglove and Ely (1987) are plotted for comparison.		
31. Percentage deviations of speed of sound data for isobutane in the gaseous region from values calculated from the equation of state, Eq. (4.1). Values calculated from the equations of state of Miyamoto and Watanabe (2002) and of Younglove and Ely (1987) are plotted for comparison.		
32. Absolute plot of three isotherms of $p\rho T$ data for <i>n</i> -butane in a $p-T$ diagram up to very high pressures. The plotted lines correspond to values calculated from the equation of state, Eq. (4.1), and from the equations of state of Miyamoto and Watanabe (2001) and of Younglove and Ely (1987).		
33. Absolute plot of three isotherms of $p\rho T$ data for isobutane in a $p-T$ diagram up to very high pressures. The plotted lines correspond to values calculated from the equation of state, Eq. (4.1), and from the equations of state of Miyamoto and Watanabe (2002) and of Younglove and Ely (1987).		
34. “Ideal curves” for <i>n</i> -butane in a double logarithmic p/p_c vs T/T_c diagram. The curves correspond to values calculated from the equation of state, Eq. (4.1), and from the equations of state of Miyamoto and Watanabe (2001) and of Younglove and Ely (1987). The area marked in gray corresponds to the region where Eq. (4.1) was fitted to experimental data.		
35. “Ideal curves” for isobutane in a double logarithmic p/p_c vs T/T_c diagram. The curves correspond to values calculated from the equation of state, Eq. (4.1), and from the equations of state of Miyamoto and Watanabe (2002) and of Younglove and Ely (1987). The area marked in gray corresponds to the region where Eq. (4.1) was fitted to experimental data.		
36. Tolerance diagram for densities of <i>n</i> -butane calculated from the equation of state, Eq. (4.1). For the extended critical region, the uncertainty in pressure is given.		
37. Tolerance diagram for isobaric and isochoric heat capacities of <i>n</i> -butane calculated from the equation of state, Eq. (4.1).		969
38. Tolerance diagram for speeds of sound of <i>n</i> -butane calculated from the equation of state, Eq. (4.1).		970
39. Tolerance diagram for densities of isobutane calculated from the equation of state, Eq. (4.1). For the extended critical region, the		

uncertainty in pressure is given.	970	<i>s</i>	Specific entropy
40. Tolerance diagram for isobaric and isochoric heat capacities of isobutane calculated from the equation of state, Eq. (4.1).	970	<i>t</i>	Temperature exponent
41. Tolerance diagram for speeds of sound of isobutane calculated from the equation of state, Eq. (4.1).	970	<i>T</i>	Thermodynamic temperature, ITS-90
42. Absolute deviations and percentage deviations [$100\Delta y/y = 100(y_{\text{exp}} - y_{\text{calc}})/y_{\text{exp}}$ with $y = p, \rho', \rho''$] of highly accurate thermal data for propane at saturation from values calculated from the equation of state, Eq. (4.1). Values calculated from the ancillary equations, Eqs. (9.2)–(9.4), and from the equations of state of Miyamoto and Watanabe (2000) and of Younglove and Ely (1987) are plotted for comparison.	971	<i>u</i>	Specific internal energy
43. Percentage density deviations of highly accurate $p\rho T$ data for propane (95–380 K) from values calculated from the equation of state, Eq. (4.1). Values calculated from the equations of state of Miyamoto and Watanabe (2000) and of Younglove and Ely (1987) are plotted for comparison.	972	<i>v</i>	Specific volume
44. Percentage density deviations of highly accurate $p\rho T$ data for propane (400–520 K) from values calculated from the equation of state, Eq. (4.1). Values calculated from the equations of state of Miyamoto and Watanabe (2000) and of Younglove and Ely (1987) are plotted for comparison.	973	<i>w</i>	Speed of sound
		<i>x,y,z</i>	Any thermodynamic property
		<i>Z</i>	Compression factor [$Z = p/(\rho RT)$]

Greek symbols

α	Dimensionless Helmholtz energy [$\alpha = a/(RT)$]
$\beta, \varepsilon, \gamma, \eta, \theta$	Adjustable parameters
χ^2	Sum of squares
X^{*2}	Quality criterion in the simultaneous optimization
δ	Reduced density ($\delta = \rho/\rho_c$)
δ_T	Isothermal throttling coefficient [$\delta_T = (\partial h/\partial p)_T$]
Δ	Difference in any quantity
Δh^ν	Enthalpy of vaporization
ϑ	Transformed temperature ($\vartheta = 1 - T/T_c$)
μ	Joule-Thomson coefficient [$\mu = (\partial T/\partial p)_h$]
ρ	Mass density
σ^2	Variance
τ	Inverse reduced temperature ($\tau = T_c/T$)

Superscripts

*	Reduced
o	Ideal-gas state
r	Residual contribution
'	Saturated-liquid state
"	Saturated-vapor state
-	Vector

Subscripts

At some reference state	
Based on ITS-90	
b	At the normal boiling point
c	At the critical point
calc	Calculated
exp	Experimental
h	Isenthalpic
i,j	Indices
m	Denotes a state on the melting curve
p	Isobaric
s	Denotes a state on the vapor-pressure curve
s	Isentropic
σ	Along the saturated-liquid line
t	At the triple point
tot	Total
subst	Substance specific
T	Isothermal
v	Isochoric

Nomenclature

Symbol	Physical quantity
<i>a</i>	Specific Helmholtz energy
<i>B</i>	Second virial coefficient
<i>C</i>	Third virial coefficient
<i>c</i>	Density exponent
<i>c_p</i>	Specific isobaric heat capacity
<i>c_v</i>	Specific isochoric heat capacity
<i>c_σ</i>	Specific heat capacity along the saturated-liquid line
<i>d</i>	Density exponent
<i>f_{wt}, f_{subst}</i>	Arbitrary weighting factors
<i>g</i>	Specific Gibbs energy
<i>h</i>	Specific enthalpy
<i>i,j,k,m</i>	Serial numbers
<i>J</i>	Number of different properties considered in the fit
<i>K</i>	Number of substances considered in the simultaneous optimization
<i>M</i>	Molar mass, number of data for a given property
<i>n</i>	Adjustable coefficient
<i>p</i>	Pressure
<i>R</i>	Specific gas constant
<i>R_m</i>	Molar gas constant

Physical Constants and Characteristic Properties of *n*- and Isobutane

Molar mass	$M = 58.12220 \text{ g mol}^{-1}$	(Coplen 2001)
Universal gas constant	$R_m = 8.314472 \text{ J mol}^{-1} \text{ K}^{-1}$	(Mohr and Taylor 1999)
Specific gas constant	$R = 0.14305157 \text{ kJ kg}^{-1} \text{ K}^{-1}$	
Reference state		
Temperature	$T_0 = 298.15 \text{ K}$	
Pressure	$p_0 = 0.101325 \text{ MPa}$	
Specific entropy	$s_0 = 0 \text{ kJ kg}^{-1} \text{ K}^{-1}$	
Specific enthalpy	$h_0 = 0 \text{ kJ kg}^{-1}$	

For the thermal properties at the critical point and the triple point see Table 3.

1. Introduction

1.1. Background

Due to their broad range of industrial and scientific applications, the need for accurate values of the thermodynamic properties of normal (*n*-) and isobutane is unquestioned. The increasing concern about green house impacts has opened new applications as alternative refrigerants and thus created new demands for highly accurate property values, albeit the flammability of the hydrocarbons to date limits their use as refrigerants to rather small devices. This work is part of an international collaboration between the Ruhr University in Bochum and the National Institute of Standards and Technology in Boulder to characterize the properties of ethane (Bücker and Wagner, 2006), propane (Lemmon *et al.*, unpublished), and the butanes (this work).

For the first three members of the alkane series, namely methane, ethane, and propane, a great number of accurate experimental data are available over broad ranges of temperature and pressure. For the butanes, however, the data situation is not quite as promising. While the thermal properties have been investigated with unmatched accuracy at temperatures up to 340 K and pressures up to 12 MPa by Glos *et al.* (2004), precise data at higher temperatures and pressures are scarce. In some parts of the fluid region, experimental results for caloric properties are missing completely.

The inhomogeneous data situation on the one hand, and the need for very accurate and consistent property values on the other hand, demand for precise yet numerically very stable equations of state. Very accurate equations can be developed with the aid of sophisticated procedures for the optimization of the functional form, see e.g., Setzmann and Wagner (1989). Nevertheless, due to the great flexibility of these algorithms, a comprehensive and consistent database is required to individually optimize the functional form of an equation of state for one particular substance. Span *et al.* (1998) overcame these constraints with a modified algorithm that optimizes the functional form of the correlation equation by simultaneously considering data for different yet physically related substances. Span and Wagner (2003a, 2003b, 2003c) applied the simultaneous optimization to the very general classes of polar and nonpolar substances thus developing generalized equations of state for numerous fluids. These equations yield reliable results even for substances with very restricted data sets. However, the relatively small

number of terms, the limited flexibility of the functional form, and the broad variety of substances that were considered in the development of the equations confine their scope to technical applications with moderate demands on accuracy.

In the present work, we seek to combine the flexibility of the individual optimization and the stability of the simultaneous algorithm by applying the simultaneous optimization to a very small number of physically similar substances, namely ethane, propane, *n*-butane, and isobutane. While the main focus was set on *n*- and isobutane, the comprehensive and accurate data sets for the thermodynamic properties of ethane and propane were utilized to stabilize the optimization and to provide the algorithm with the necessary information in regions where no data or only dubious values are available for the butanes. The equations of state presented here for the butanes are equally able to represent even the most accurate data within their experimental uncertainties and to yield reliable results in sparsely measured regions. Additionally, the equations extrapolate reasonably up to extreme conditions of temperature and pressure (see Sec. 5.5) at least with respect to basic properties such as density, fugacity, and enthalpy.

1.2. Previous Equations of State

Selected equations of state which describe large parts of the fluid region and which were commonly used in industrial or scientific applications during the last 20 years are summarized in Table 1. The equations published by Span and Wagner (2003a, 2003b), Miyamoto and Watanabe (2001, 2002), and Younglove and Ely (1987) were fitted to data for thermal and caloric properties. The remaining equations were fitted to thermal data only.

Until now, the equations of state of the modified Benedict–Webb–Rubin (MBWR) type established by Younglove and Ely (1987) have been most commonly used for the thermodynamic properties of *n*- and isobutane. Little indication of the data used to fit the coefficients was given, but the authors most probably had all existent data available. Due to their functional form the equations are not suitable for extrapolation.

Recently, Miyamoto and Watanabe (2001, 2002) published equations of state in terms of the Helmholtz energy. The data used for setting up the equations basically correspond to the data discussed in Secs. 2 and 3 of this work, excluding the highly accurate data for the thermal properties in the homog-

TABLE 1. Information on selected equations of state for *n*- and isobutane

Authors	Year	Temperature range (K)	Pressure range (MPa)	Structure of the equation	Number of coefficients
Equations of state for <i>n</i> -butane					
Span & Wagner	2003 ^{a,b}	135–693	0–69	Helmholtz energy	12
Miyamoto & Watanabe	2001	135–589	0–69	Helmholtz energy	19
Sychev <i>et al.</i>	1995	135–589	0–69	Compression factor	53
Polt <i>et al.</i>	1992	140–589	0–30	Pressure explicit	20
Younglove & Ely	1987	135–500	0–70	Pressure explicit	32
Haynes & Goodwin	1982	135–700	0–70	Pressure explicit	15 ^a
Equations of state for isobutane					
Span & Wagner	2003 ^{a,b}	114–573	0–106	Helmholtz energy	12
Miyamoto & Watanabe	2002	114–537	0–35	Helmholtz energy	19
Polt <i>et al.</i>	1992	120–498	0–35	Pressure explicit	20
Younglove & Ely	1987	114–600	0–35	Pressure explicit	32
Waxman & Gallagher	1983	250–600	0–40	Helmholtz energy	34
Goodwin & Haynes	1982	114–700	0–70	Pressure explicit	15 ^a

^aValues are calculated iteratively from equations for the thermal properties on the vapor–liquid phase boundary and from an additional correlation equation. The total number of terms in the equations is 15.

enous phase and on the phase boundaries measured by Glos *et al.* (2004). The data obtained by Beattie *et al.* (1939b, 1949) in the near-critical region of the butanes were not included.

As discussed in Sec. 1.1, Span and Wagner (2003a, 2003b) introduced a simultaneously optimized functional form for a broad range of nonpolar fluids, including the butanes. These equations are designed strictly for technical applications and do not compete with highly accurate reference equations of state. Data from the recent high precision measurements of the thermal properties by Funke *et al.* (2002a, 2002b) and Claus *et al.* (2003) were not available when the simultaneously optimized equations were set up.

Each of the aforementioned equations has several of the following disadvantages:

- (1) accurate data for the thermodynamic properties of the butanes are not represented within their experimental uncertainty;
- (2) unreasonable behavior is observed in regions with a poor data situation;
- (3) extrapolation to temperatures and pressures outside the range of validity yields unreasonable results; and
- (4) the temperature values do not correspond to the current International Temperature Scale of 1990 (ITS-90).

In this paper, new equations of state for *n*- and isobutane are presented to overcome these shortcomings. The thermodynamic surfaces of both alkanes in the range covered by reliable experimental data are described within the experimental uncertainties. The new equations were developed using current multiproperty-fitting procedures and a state-of-the-art simultaneous optimization algorithm.

1.3. Notes on the Values of Temperature used in this Paper

- (1) All correlation equations presented in this article refer to the ITS-90.

- (2) No distinction is made between the thermodynamic temperature T and the temperature T_{90} of the currently valid International Temperature Scale of 1990 (ITS-90) (see Preston-Thomas 1990).
- (3) Temperature values of available experimental data referring to older temperature scales were converted to ITS-90. The conversion from the IPTS-68 temperature scale to ITS-90 temperatures was carried out based on conversion equations given by Rusby *et al.* (1991). Data corresponding to the IPTS-48 temperature scale were converted to IPTS-68 according to the procedure given by Bedford and Kirby (1969).
- (4) Values calculated from literature equations that are used in the corresponding figures for comparison purposes, were, if necessary, converted from their original temperature scale to ITS-90 values.

2. Phase Equilibria of *n*- and Isobutane

In the following sections we review the experimental data available for the thermodynamic properties on the vapor–liquid coexistence lines and on the melting lines of the butanes. Simple correlation equations that were developed by Glos *et al.* (2004) and by ourselves are given for the thermal properties. To facilitate the readers access to the data situation we generally classified the data sets into three groups. The assignment considers the uncertainty of the data, the size of the data set, the covered temperature range, and the data situation of the corresponding property in the relevant region. Group 1 includes all the data used for the development of the corresponding correlation equation. Reliable data sets that fall behind the quality of group 1 data, with respect to at least one of the aspects mentioned above, may still be very useful for comparisons. These data are assigned to group 2. All other data sets are assigned to group 3 and are not taken into consideration here. Nevertheless, these data may contain valuable information. Our ranking is determined by the quality relative to the best available reference data rather than by

TABLE 2. Available data for the triple-point temperatures of *n*- and isobutane

Authors	T_t (K)
<i>n</i> -Butane	
Glos <i>et al.</i> (2004)	134.895 ± 0.02
Das <i>et al.</i> (1973a)	134.87
Klipping & Schmidt (1965)	134.83
Rossini <i>et al.</i> (1953)	134.8
Aston & Messerly (1940)	134.8
Huffman <i>et al.</i> (1931)	134.1
Isobutane	
Glos <i>et al.</i> (2004)	113.730 ± 0.005
Das <i>et al.</i> (1973b)	113.56
Rossini <i>et al.</i> (1953)	113.57
Francis (1941)	113.75
Aston <i>et al.</i> (1940)	113.75
Parks <i>et al.</i> (1937)	113.2

any kind of absolute level of quality, and data that do not contribute to the level of accuracy aspired to here may be useful for other purposes.

2.1. Triple Point

Table 2 summarizes the available values for the temperature at the gas–solid–liquid triple points of *n*- and isobutane. From the description of the experiments, especially in the older articles, it is not always clear whether the reported temperatures are really triple-point values or melting temperatures at standard pressure. The values reported by Das *et al.* (1973a, 1973b) were used for the development of equations of state of Goodwin and Haynes (1982), Haynes and Goodwin (1982), and Younglove and Ely (1987). The only reliable values, however, are the data of Glos *et al.* (2004), which we used in this work.

No experimental data are available for the triple-point pressure of the butanes. We hence adopted the values that are obtained from the respective vapor-pressure equations (see Sec. 2.4) by inserting the appropriate triple-point temperature. The values of the triple-point parameters thus established are given in Table 3 for both butanes.

2.2. Critical Point

The critical-point parameters of the butanes have been investigated by numerous authors. A summary of the available data is given in Table 4. The values for *n*-butane recom-

mended by Ambrose and Tsonopoulos (1995) are based on the values reported by Younglove and Ely (1987) and Beattie *et al.* (1939b). They agree with the parameters reported by Conolly (1962), Kratzke *et al.* (1982), Brunner (1988), and Holcomb *et al.* (1995) within reasonable uncertainties and have been adopted in this work. For isobutane, we used the parameters reported by Levelt Sengers *et al.* (1983). These values were established by a re-evaluation of results obtained by Beattie *et al.* (1949) and appear to be the most reliable values available, even though the reported uncertainties are quite optimistic. Table 3 compiles the critical point parameters of *n*- and isobutane used in this work.

2.3. Melting Pressure

The only experimental data available for the melting pressures of the butanes were obtained by Reeves *et al.* (1964). The values are presented in graphs. The reported pressures reach up to 900 MPa for both alkanes. While Reeves *et al.* (1964) observed only one solid phase of *n*-butane over the entire pressure range, they report a second solid phase of isobutane occurring at approximately 370 MPa, causing a solid–solid–liquid triple point. Haynes and Goodwin (1982) and Goodwin and Haynes (1982) established the parameters of the Simon equation based on these data. We readjusted these parameters to suit the triple-point parameters used in this work. The equation reads

$$\frac{p_m}{p_t} = 1 + n \left[\left(\frac{T}{T_t} \right)^{\theta} - 1 \right], \quad (2.1)$$

with the parameters for *n*- and isobutane given in Table 5. The equation for isobutane represents the data of Reeves *et al.* (1964) only up to the solid–solid–liquid triple point at roughly 370 MPa. It should be noted that Eq. (2.1) for isobutane is not consistent with density measurements performed by Haynes (1983b) in that some of the liquid-density data points at low temperatures (120 K) actually fall on the solid side of Eq. (2.1). A more reliable description of the melting pressure of isobutane, and thus a more precise description of the range of validity of the new fundamental equation of state, will be possible once new measurements of the melting pressure are available.

2.4. Vapor Pressure

The earliest measurements of the vapor pressure date back to the beginning of the last century. Summaries of the available data are given in Table 6 for *n*-butane and in Table 7 for isobutane. A number of data sets are consistent with each other within 0.5% in vapor pressure, but only the values reported by Glos *et al.* (2004) can be considered to be group 1 data. Since these data only cover temperatures up to 340 K, data of inferior quality had to be considered at higher temperatures. The correlation equation used in the present work for the vapor pressure of *n*-butane was developed by Glos

TABLE 3. Parameters for the characteristic points on the vapor–liquid phase boundaries of *n*- and isobutane

	<i>n</i> -Butane	Isobutane
Triple point		
T_t /K	134.895	113.73
p_t /Pa	0.653	0.0219
Critical point		
T_c /K	425.125	407.81
p_c /MPa	3.796	3.629
ρ_c /(kg m ⁻³)	228	225.5

TABLE 4. Available data for the critical points of *n*- and isobutane. Uncertainties are given where the original articles contain such estimates

Authors	Method	T_c (K)	p_c (MPa)	ρ_c /(kg m ⁻³)
<i>n</i> -Butane				
Ambrose & Tsonopoulos (1995)	A	425.12±0.1	3.796±0.01	228±3
Holcomb <i>et al.</i> (1995)	B	425.12		229.2
Li & Kiran (1988)	C	424.6	3.8	221
Brunner (1988)	C	425.06±0.1	3.793±0.005	
Younglove & Ely (1987)	A	425.125	3.796	227.84
Kratzke <i>et al.</i> (1982)	D	425.105 ^a	3.78385	
Haynes & Goodwin (1982)	A	425.12 ^b	3.7960	227.85
Das <i>et al.</i> (1973a)	A	425.12	3.797	228
Kay (1970)	C	425.4	3.798	228±1
Kreglewski & Kay (1969)	C	425.32	3.798	228
Kay (1964)	C	425.3	3.8	
Connolly (1962)	C	425.106	3.7845	
Kay (1941)	C	425.4	3.793	228
Beattie <i>et al.</i> (1939b)	D	425.15	3.797	225±2
Harand (1935)	C	426.8		
Seibert & Burrell (1915)	C	426.4	3.615	
Visser (1913)	C	424	3.8	
Kuenen (1911)	C	424	3.8	
Isobutane				
Daubert (1996)	A	407.8±0.5	3.640±0.05	224±3
Younglove & Ely (1987)	A	407.82	3.640	224.4
Leveld Sengers <i>et al.</i> (1983)	C	407.81±0.02	3.629±0.002	225.5±2
Waxman & Gallagher (1983)	A	407.818	3.6306	227
Goodwin & Haynes (1982)	A	407.82	3.640	224.36
Das <i>et al.</i> (1973b)	A	408.1	3.65	221
Connolly (1962)	C	407.15	3.70	
Beattie <i>et al.</i> (1949)	D	408.11	3.65	221
Gilliland & Scheeline (1940)	C	407.6	3.69	
Harand (1935)	C	407		
Seibert & Burrell (1915)	C	406.8	3.702	

^aValue adopted from Connolly (1962) and transformed from IPTS-68 to ITS-90.

^bValue adopted from Das *et al.* (1973a).

Methods used to determine the critical parameters:

- A Equation of state/evaluation of published data.
- B Evaluation of measurements of the saturated-vapor and saturated-liquid densities in the critical region.
- C Disappearance of the meniscus.
- D Evaluation of $p\rho T$ measurements.

et al. (2004). The parameters of the corresponding equation for isobutane were established in this work. For both substances, the vapor-pressure equation reads

$$\ln\left(\frac{p_s}{p_c}\right) = \frac{T_c}{T} (n_1 \vartheta^{\theta_1} + n_2 \vartheta^{\theta_2} + n_3 \vartheta^{\theta_3} + n_4 \vartheta^{\theta_4}) \quad (2.2)$$

with $\vartheta = 1 - T/T_c$. The values of the critical parameters T_c and p_c in Eq. (2.2) correspond to the values given in Table 3. The other parameters and coefficients for the equation are given in Table 8.

Comparisons of experimental results for the vapor pressure of *n*-butane and values calculated from Eq. (2.2) are

TABLE 5. Parameters for the melting-pressure equations of *n*- and isobutane, Eq. (2.1)

	<i>n</i> -Butane	Isobutane
n	5.585582364×10^8	1.953637130×10^9
θ	2.206	6.12

shown in Fig. 1. The diagram is divided into two parts. On the left hand side, absolute deviations are given for temperatures below 230 K and on the right hand side, percentage deviations are shown for higher temperatures. The results reported by Kratzke *et al.* (1982) and by Kay (1940) do not appear to be more accurate than other group 2 data. They were used in the fit of Eq. (2.2) because no other reliable data are available above 340 K. Data that deviate from the reference values reported by Glos *et al.* (2004) by more than 0.5% were assigned to group 3. With very few exceptions, the group 2 vapor pressures deviate from the reference data towards higher values. It seems reasonable to assume that this effect is caused by lower boiling impurities. Based on the available experimental data, we expect the uncertainties in vapor pressure of *n*-butane calculated from Eq. (2.2) to be less than 5 Pa at temperatures below 230 K, less than 0.4% above 340 K, and less than 0.03% between these temperatures.

Figure 2 illustrates the representation of group 1 and 2

TABLE 6. Summary of the data sets for the vapor pressure of *n*-butane

Authors	Number of data	Temperature range (K)	Group
Glos <i>et al.</i> (2004)	23	135–310	1
Kayukawa (2002)	11	240–380	3
Sako & Horiguchi (1997)	22	301–316	2
Holcomb <i>et al.</i> (1995)	22	250–410	3
Gainar & Anitescu (1992)	12	300–352	3
Machin & Golding (1989)	195	173–280	3
Weber (1989)	4	309–394	2
Holldorf & Knapp (1988)	20	258–357	2
Hsu <i>et al.</i> (1985)	3	319–378	3
Weber (1985)	3	250–280	3
Kratzke <i>et al.</i> (1982)	12	320–423	1–2
Flebbe <i>et al.</i> (1982)	12	278–358	2
Martinez-Ortiz & Manlay (1978)	12	278–344	2
Laurance & Swift (1974)	3	310–339	3
Carruth & Kobayashi (1973)	14	135–213	3
Kahre (1973)	2	288–328	3
Kay (1970)	3	389–425	1–2
Hirata & Suda (1966)	25	303–401	3
Carmichael <i>et al.</i> (1962)	26	311–380	3
Connolly (1962)	7	344–425	2
Tickner & Lossing (1951)	13	135–196	3
Mertes & Colburn (1947)	8	293–394	3
Wackher <i>et al.</i> (1945)	10	205–279	3
Olds <i>et al.</i> (1944)	4	311–411	2
Kay (1940)	20	325–425	3
Aston & Messerly (1940)	11	195–273	3
Beattie <i>et al.</i> (1939b)	4	348–423	2
Sage <i>et al.</i> (1937a)	7	294–394	3
Dana <i>et al.</i> (1926)	19	255–331	3
Burrell & Robertson (1915a)	17	173–273	3
Seibert & Burrell (1915)	10	303–403	3

TABLE 7. Summary of the data sets for the vapor pressure of isobutane

Authors	Number of data	Temperature range (K)	Group
Glos <i>et al.</i> (2004)	24	120–340	1
Miyamoto <i>et al.</i> (2004) ^a	28	310–407	2
Kayukawa (2002)	18	240–380	3
Ewing & Goodwin (1991)	28	255–323	3
Weber (1989)	4	311–394	3
Weber (1985)	4	250–280	3
Waxman & Gallagher (1983)	16	298–398	1–2
Martinez-Ortiz & Manley (1978)	10	277–344	2
Steele <i>et al.</i> (1976)	10	277–344	2
Kahre (1973)	5	277–329	3
Carmichael <i>et al.</i> (1962)	26	311–380	3
Hirata & Suda (1966)	29	295–407	3
Connolly (1962)	6	344–407	2
Tickner & Lossing (1951)	13	121–187	3
Beattie <i>et al.</i> (1949)	5	303–398	3
Mertes & Colburn (1947)	8	293–394	3
Wackher <i>et al.</i> (1945)	9	206–263	3
Gilliland & Scheeline (1940)	5	352–407	3
Aston <i>et al.</i> (1940)	9	188–261	2
Sage & Lacey (1938)	7	294–394	3
Dana <i>et al.</i> (1926)	20	249–353	3
Seibert & Burrell (1915)	10	303–393	3
Burrell & Robertson (1915b)	15	158–260	3

^aThese data were only available after the development of the vapor-pressure equation, Eq. (2.2), and the new equation of state, Eq. (4.1), for isobutane.TABLE 8. Parameters for the vapor-pressure equations of *n*- and isobutane, Eq. (2.2)

	<i>n</i> -Butane	Isobutane
<i>n</i> ₁	−7.17616903	−6.85093103
<i>n</i> ₂	2.53635336	1.36543198
<i>n</i> ₃	−2.07532869	−1.32542691
<i>n</i> ₄	−2.82241113	−2.56190994
θ_1	1	1
θ_2	1.5	1.5
θ_3	2	2.5
θ_4	4.5	4.5

data for the vapor pressure of isobutane by Eq. (2.2). Again, the diagram is divided into two parts, with absolute deviations shown in the low-temperature part and percentage deviations shown for higher temperatures. The data reported by Waxman and Gallagher (1983) agree with the reference values measured by Glos *et al.* (2004) within 0.2% and were selected to complete the database used to establish the parameters of Eq. (2.2). Data sets that remain within 0.5% of the selected data were assigned to group 2. Similarly to the results for *n*-butane, we expect the uncertainties of vapor pressures of isobutane calculated from Eq. (2.2) to be less than 5 Pa at temperatures below 200 K, less than 0.4% above 340 K, and less than 0.03% inbetween.

2.5. Saturated-Liquid Density

The data reported by Glos *et al.* (2004) describe the saturated-liquid density of *n*- and isobutane with the highest possible accuracy at temperatures up to 340 K. The expected experimental uncertainties are less than 0.03%. Beyond that temperature, accurate results are lacking, so that inferior data had to be used additionally to set up the respective correlation equations. For both fluids, the equation for the saturated-liquid density is given by

$$\left(\frac{\rho'}{\rho_c} - 1 \right) = n_1 \vartheta^{\theta_1} + n_2 \vartheta^{\theta_2} + n_3 \vartheta^{\theta_3} + n_4 \vartheta^{\theta_4}, \quad (2.3)$$

with $\vartheta = 1 - T/T_c$. The critical parameters T_c and ρ_c correspond to the values given in Table 3, while the other coeffi-

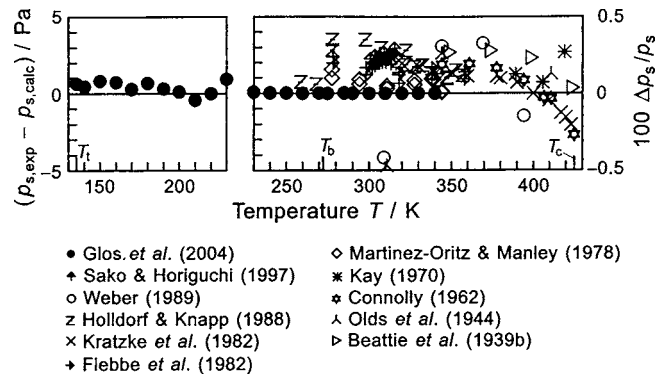


FIG. 1. Absolute deviations and percentage deviations $100\Delta p_s/p_s = 100(p_{s,\text{exp}} - p_{s,\text{calc}})/p_{s,\text{exp}}$ of experimental data for the vapor pressure p_s of *n*-butane from values calculated from the vapor-pressure equation, Eq. (2.2).

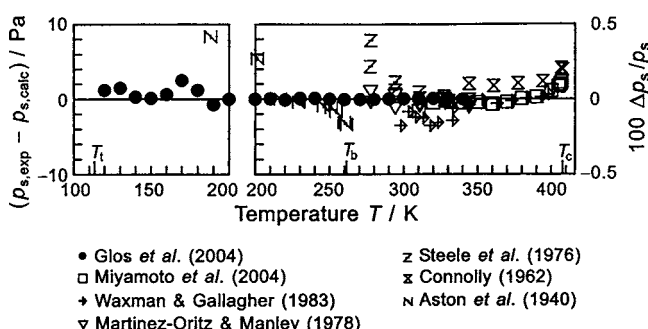


Fig. 2. Absolute deviations and percentage deviations $100\Delta p_s / p_s = 100(p_{s,\text{exp}} - p_{s,\text{calc}})/p_{s,\text{exp}}$ of experimental data for the vapor pressure p_s of isobutane from values calculated from the vapor-pressure equation, Eq. (2.2). In order not to overcrowd the diagram for $T > 310$ K, from the data of Miyamoto *et al.* (2004) only about every second data point is plotted.

stants and parameters are compiled in Table 9. For both fluids, Eq. (2.3) represents the experimental data within their uncertainties.

Table 10 summarizes the published data sets for *n*-butane. Almost all data available from the literature agree with the values of Glos *et al.* (2004) within 0.5% and were assigned to group 2. To establish the parameters of Eq. (2.3), the results obtained by Holcomb *et al.* (1995) were used above 340 K, and values from the work of Kay (1940) were used above 400 K as a complement for the data of Glos *et al.* (2004). The representation of the groups 1 and 2 data by Eq. (2.3) is shown in Fig. 3.

For isobutane, a number of experimental results agree with the reference data of Glos *et al.* (2004) within 0.15%. These data were assigned to group 2. Nevertheless, the only reliable experimental saturated-liquid densities at temperatures above 340 K are only a few values reported by Sliwinski (1969), reaching up to 368 K. To establish the parameters of Eq. (2.3) we additionally used values near the critical point that were calculated from a scaled equation of state by Levelt Sengers *et al.* (1983). No reliable estimate can be given here for the uncertainties of these values. Percentage deviations of the data calculated by Levelt Sengers *et al.* (1983) and the experimental data assigned to groups 1 and 2 from values calculated from Eq. (2.3) are shown in Fig. 4. All available data sets are summarized in Table 11.

TABLE 9. Parameters for the saturated-liquid density equations of *n*- and isobutane, Eq. (2.3)

	<i>n</i> -Butane	Isobutane
n_1	1.97874515	2.04025104
n_2	0.856799510	0.850874089
n_3	-0.341871887	-0.479052281
n_4	0.304337558	0.348201252
θ_1	0.345	0.355
θ_2	1	1
θ_3	1.5	4/3
θ_4	3	7/3

TABLE 10. Summary of the data sets for the saturated-liquid density of *n*-butane

Authors	Number of data	Temperature range (K)	Group
Glos <i>et al.</i> (2004)	23	135–340	1
Kayukawa (2002)	11	240–380	3
Holcomb <i>et al.</i> (1995)	18	316–410	1–2
Kaminishi <i>et al.</i> (1988)	12	273–323	2
Hsu <i>et al.</i> (1985)	3	319–377	2
Orrit & Laupretre (1978)	50	135–275	2
Haynes (1983a)	11	135–300	2
Haynes & Hiza (1977)	12	135–300	2
McClune (1976)	17	143–173	2
Kahre (1973)	4	288–328	2
Sliwinski (1969)	10	283–368	2
Connolly (1956)	2	293–298	2
Olds <i>et al.</i> (1944)	4	311–411	2
Carney (1942)	10	272–323	2
NGAA (1942)	13	226–333	2
Benoliel (1941)	18	213–293	2
Kay (1940)	20	325–425	1–2
van der Vet (1937)	9	283–323	2
Sage <i>et al.</i> (1937a)	7	294–394	3
Coffin & Maass (1928)	19	239–305	2
Dana <i>et al.</i> (1926)	8	273–329	2

2.6. Saturated-Vapor Density

The few data sets available for the saturated-vapor density of *n*- and isobutane are summarized in Tables 12 and 13, respectively. Glos *et al.* (2004) obtained high precision data at temperatures from 270 to 340 K for *n*-butane, and from 260 to 340 K for isobutane. We assume the experimental uncertainties of these values to be less than 0.03% generally, with somewhat higher uncertainties at the low temperature end. At lower temperatures, no experimental data are available. Glos *et al.* (2004) therefore determined reliable densities from virial equations of state with relative uncertainties comparable to those of their experimental vapor pressure

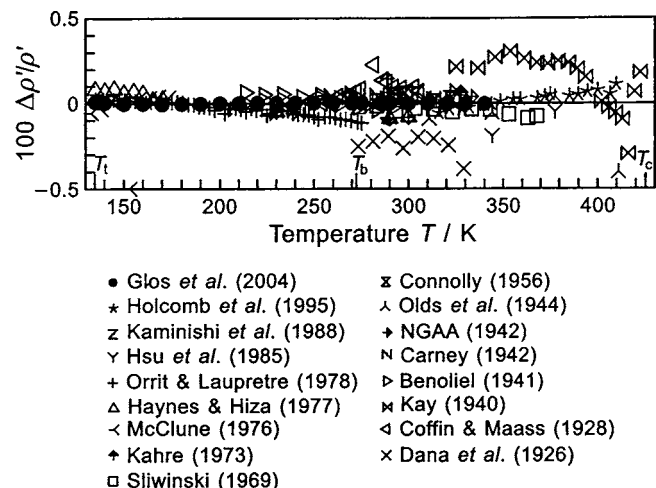


Fig. 3. Percentage deviations $100\Delta\rho'/\rho' = 100(\rho'_{\text{exp}} - \rho'_{\text{calc}})/\rho'_{\text{exp}}$ of experimental data for the saturated-liquid density ρ' of *n*-butane from values calculated from the equation for the saturated-liquid density, Eq. (2.3).

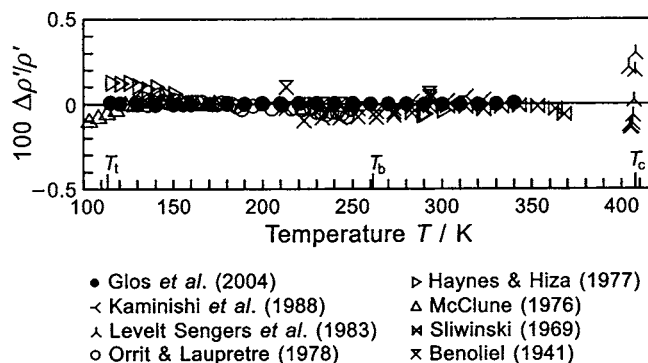


Fig. 4. Percentage deviations $100\Delta\rho'/\rho'=100(\rho'_{\text{exp}}-\rho'_{\text{calc}})/\rho'_{\text{exp}}$ of experimental data for the saturated-liquid density ρ' of isobutane from values calculated from the equation for the saturated-liquid density, Eq. (2.3).

data. Above 340 K no accurate data are available. We used the following equation for the saturated-vapor densities of *n*- and isobutane:

$$\ln\left(\frac{\rho''}{\rho_c}\right) = \frac{T_c}{T}(n_1\vartheta^{\theta_1} + n_2\vartheta^{\theta_2} + n_3\vartheta^{\theta_3} + n_4\vartheta^{\theta_4}), \quad (2.4)$$

with $\vartheta=1-T/T_c$. The critical parameters in Eq. (2.4) correspond to the values listed in Table 3, the other parameters are given in Table 14.

To establish the parameters of Eq. (2.4) for *n*-butane, we used the data reported by Glos *et al.* (2004), complemented by values from the work of Sliwinski (1969) and Kay (1940) at temperatures above 340 K. No experimental data are available for the saturated-vapor density of isobutane above 368 K. Therefore, similarly to the proceeding technique for the

TABLE 11. Summary of the data sets for the saturated-liquid density of isobutane

Authors	Number of data	Temperature range (K)	Group
Glos <i>et al.</i> (2004)	24	115–340	1
Kayukawa (2002)	17	240–380	3
Kaminishi <i>et al.</i> (1988)	6	273–323	2
Levett Sengers <i>et al.</i> (1983)	9 ^a	404–408	—
Masui <i>et al.</i> (1982)	5	309–335	3
Orrit & Laupretre (1978)	36	129–249	2
Haynes & Hiza (1977)	12	115–300	2
McClune (1976)	17	123–173	2
Rodosevich & Miller (1973)	3	114–120	3
Kahre (1973)	10	277–327	3
Sliwinski (1969)	10	283–368	1–2
Beattie <i>et al.</i> (1949)	5	303–398	3
Wackher <i>et al.</i> (1945)	2	223–273	3
NGAA (1942)	14	228–333	3
Carney (1942)	19	245–323	3
Benoliel (1941)	18	213–293	2
Morris <i>et al.</i> (1939)	12	311–378	3
Sage & Lacey (1938)	7	294–394	3
van der Vet (1937)	9	283–323	3
Coffin & Maass (1928)	17	245–305	3
Dana <i>et al.</i> (1926)	8	273–329	3

^aValues calculated from a scaled equation of state.

TABLE 12. Summary of the data sets for the saturated-vapor density of *n*-butane

Authors	Number of data	Temperature range (K)	Group
Glos <i>et al.</i> (2004)	9 ^a	270–340	1
Holcomb <i>et al.</i> (1995)	18	316–410	2
Hsu <i>et al.</i> (1985)	3	319–377	2
Sliwinski (1969)	10	283–368	2
Olds <i>et al.</i> (1944)	4	311–411	2
Kay (1940)	20	325–425	1–2
Sage <i>et al.</i> (1937a)	7	294–394	2
Dana <i>et al.</i> (1926)	8	281–321	2

^aAdditionally, 17 values have been calculated from a virial equation for temperatures from 140 to 300 K.

saturated-liquid density, we used values calculated from a scaled equation of state by Levett Sengers *et al.* (1983) in addition to the experimental data. Comparisons of the available data and saturated-vapor densities calculated from Eq. (2.4) are shown in Fig. 5 for *n*-butane and in Fig. 6 for isobutane. The inconsistencies between the reference data reported by Glos *et al.* (2004) and the other data sets are evident. All experimental data are represented by the new correlations within their uncertainties.

2.7. Caloric Data on the Vapor–Liquid Phase Boundary

No ancillary equations have been developed for the caloric properties on the vapor–liquid phase boundaries of *n*- or isobutane, but there are data sets for caloric properties on the saturated-liquid line that were assigned to group 1. These data were used in the development of the new equations of state [Eq. (4.1)]. The available data sets are summarized in Table 15 for *n*-butane and in Table 16 for isobutane.

Measurements of the speed of sound in saturated-liquid *n*-butane were performed by Niepmann (1984) using the pulse-echo technique. The reported experimental uncertainties are 0.2% in speed of sound. The inherent scatter of the data however suggests that this value corresponds to the reproducibility rather than to the total uncertainty of the data. All data from the investigation were considered in the development of the new equation of state.

TABLE 13. Summary of the data sets for the saturated-vapor density of isobutane

Authors	Number of data	Temperature range (K)	Group
Glos <i>et al.</i> (2004)	9 ^a	260–340	1
Kayukawa (2002)	1	260	3
Levett Sengers <i>et al.</i> (1983)	9 ^b	403–407	—
Sliwinski (1969)	10	283–368	2
Sage & Lacey (1938)	7	294–394	3
Dana <i>et al.</i> (1926)	6	273–313	3

^aAdditionally, 13 values have been calculated from a virial equation for temperatures from 140 to 250 K.

^bValues calculated from a scaled equation of state.

TABLE 14. Parameters for the saturated-vapor density equations of *n*- and isobutane, Eq. (2.4)

	<i>n</i> -Butane	Isobutane
n_1	-2.07770057	-2.12933323
n_2	-3.08362490	-2.93790085
n_3	-0.485645266	-0.894410860
n_4	-3.83167519	-3.46343707
θ_1	0.345	0.355
θ_2	5/6	5/6
θ_3	19/6	19/6
θ_4	25/6	26/6

Aside from two older sources containing experimental results for the heat capacity along the saturated-liquid line of *n*-butane, a recent study of this property, performed by Magee and Lüddecke (1998), is available. The results cover a broad range of temperatures and make an important contribution to the description of the caloric properties of saturated-liquid *n*-butane. The authors report the experimental uncertainties c_σ to be less than 0.7%. However, the data apparently are not consistent with data for the thermal properties measured by Glos *et al.* (2004) (see also Secs. 3.1.2, 5.1.2, and 5.2.3).

The relation between the dimensionless Helmholtz energy and c_σ contains the first derivative of the vapor pressure (see Table 33). Direct inclusion of this property in the nonlinear fit therefore involves an interlocked relation to the Maxwell criterion as given by Eqs. (4.2a)–(4.2c). To avoid numerical problems, the specific heat capacities along the saturated-liquid line have been transformed into specific heat capacities at saturated-liquid densities according to

$$c'_p(T) = c_\sigma(T) - \frac{T}{\rho'^2} \frac{\left(\frac{\partial p}{\partial T}\right)_\rho \frac{dp_s}{dT}}{\left(\frac{\partial p}{\partial \rho}\right)_T}. \quad (2.5)$$

The loss of accuracy associated with this transformation is

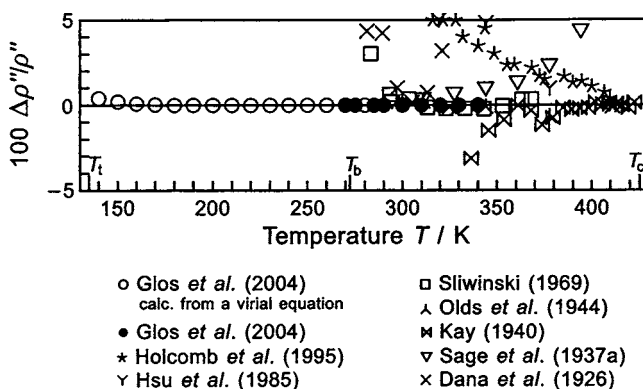


FIG. 5. Percentage deviations $100\Delta\rho''/\rho''=100(\rho''_{\text{exp}}-\rho''_{\text{calc}})/\rho''_{\text{exp}}$ of the selected data for the saturated-vapor density ρ'' of *n*-butane from values calculated from the equation for the saturated-vapor density, Eq. (2.4).

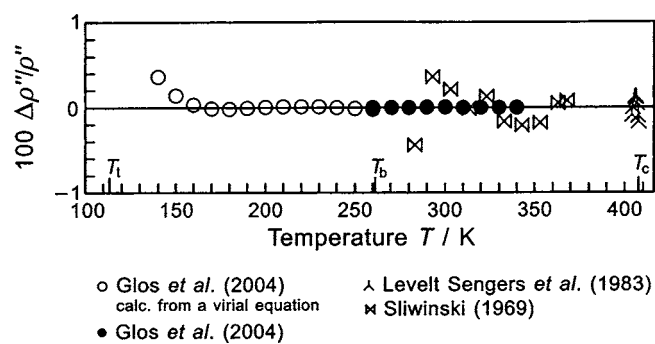


FIG. 6. Percentage deviations $100\Delta\rho''/\rho''=100(\rho''_{\text{exp}}-\rho''_{\text{calc}})/\rho''_{\text{exp}}$ of the selected data for the saturated-vapor density ρ'' of isobutane from values calculated from the equation for the saturated-vapor density, Eq. (2.4).

negligible at low temperatures or if accurate preliminary equations are used to calculate the fraction in Eq. (2.5).

For isobutane, only very old data are available for caloric properties on the phase boundary. In the absence of recent data, two data sets for the heat capacity along the saturated-liquid line, published by Aston *et al.* (1940) and by Parks *et al.* (1937), were used in the development of the new equation of state.

The enthalpy of vaporization of *n*- and isobutane has been investigated in a few early studies. This property is linked directly to the vapor pressure and the densities of the saturated liquid and the saturated vapor by the equation of Clausius–Clapeyron. Since these properties are accurately known in the temperature range covered by experimental results, no data for the enthalpy of vaporization were taken into account in the development of the new equations of state.

3. Data for the Single-Phase Region

This section presents experimental data sets for the thermodynamic properties of the butanes in the homogeneous fluid region. General information on all available data sets and more detailed information on the data selected for the development of the new equations of state are presented in the following tables. Similar to Sec. 2, the data have been classified into three groups where appropriate.

The uncertainties given in the tables usually correspond to estimates reported by the authors. In some studies, however, the stated uncertainties appear overly optimistic or no esti-

TABLE 15. Summary of the data sets for caloric properties on the vapor-liquid phase boundary of *n*-butane

Authors	Number of data			Temperature range (K)	Group
	w'	c_σ	Δh^v		
Magee & Lüddecke (1998)	—	100	—	139–317	1
Niepmann (1984)	19	—	—	200–360	1
Aston & Messerly (1940)	—	21	1	142–274	3
Huffmann <i>et al.</i> (1931)	—	8	—	142–316	3
Dana <i>et al.</i> (1926)	—	—	8	274–297	3

TABLE 16. Summary of the data sets for caloric properties on the vapor–liquid phase boundary of isobutane

Authors	Number of data		Temperature range (K)	Group
	c_σ	Δh^ν		
Aston <i>et al.</i> (1940)	25		116–257	1
Aston <i>et al.</i> (1940)		1	261	3
Parks <i>et al.</i> (1937)	19	—	115–258	1
Dana <i>et al.</i> (1926)	11	10	261–292	3

mates are given at all. In these cases, we had to estimate more realistic values for the uncertainties. In the tables, these values are presented in parentheses.

3.1. *n*-Butane

3.1.1. Thermal Properties

The thermal properties of *n*-butane at temperatures from 140 to 340 K and pressures up to 12 MPa have been measured recently by Glos *et al.* (2004) using a two-sinker densimeter, which is probably the most accurate technique available today. The reported purity of the specimen is 99.98%. The total uncertainty in density given by Glos *et al.* for their $p\rho T$ data of *n*-butane is less than 0.02%. However, for low gas densities from 2 to 10 kg m⁻³ the uncertainty rises up to 0.1% in density. Details on the experimental setup are given by Kleinrahm and Wagner (1986), Händel *et al.* (1992), and Wagner and Kleinrahm (2004). Primarily, these data give the most accurate description of the $p\rho T$ surface of liquid *n*-butane, but additionally, they provide precise information on the thermal behavior in the gas phase and can be used to validate other data sets in these regions.

All other experimental data available for the thermal properties of *n*-butane are of substantially lower accuracy than the data reported by Glos *et al.* (2004). The fluid region is covered with reliable data at temperatures up to 573 K and pressures up to 69 MPa. All data that were used to establish the new fundamental equation are shown in a $p-T$ diagram in Fig. 7, while details on the selected data sets are given in Table 17. The data sets that were assigned to groups 2 and 3 are summarized in Table 18.

At low temperatures and high pressures, Golovskii *et al.* (1978a) obtained liquid densities using a piezometer. The values were published by Sychev *et al.* (1995). The total uncertainties in density are reported to be 0.05%, but the measured densities are approximately 0.05%–0.1% lower than densities reported by Glos *et al.* (2004). The data are especially important at pressures above 12 MPa, where no other accurate $p\rho T$ data are available.

The region of supercritical pressures was investigated comprehensively in a pycnometric study by Olds *et al.* (1944). The data agree with the reference values reported by Glos *et al.* (2004) within 0.2%, which is consistent with the uncertainties estimated by the authors. We assume the actual

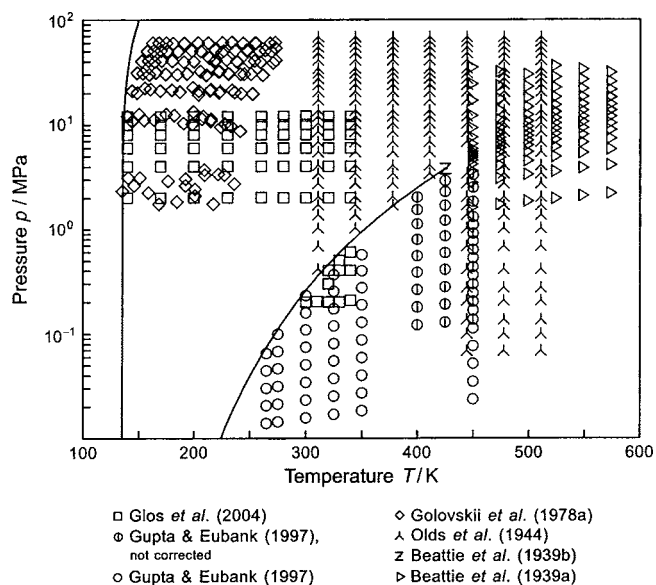


FIG. 7. Distribution of the experimental $p\rho T$ data for *n*-butane used to develop the residual part of the equation of state, Eq. (4.1), in a $p-T$ diagram.

uncertainties at higher temperatures to be 0.4% in density. At temperatures from 340 to 420 K and at supercritical pressures, no other reliable data are available.

Beattie and co-workers published two data sets for the thermal properties of *n*-butane both of which were obtained using pycnometric techniques. While one data set (Beattie *et al.* 1939b) describes only a very narrow range of temperature and pressure around the critical point, the other work (Beattie *et al.* 1939a) contains values over a larger part of the liquid, gaseous, and supercritical regions. These data are the only description of the near-critical region of *n*-butane thus far.

Gupta and Eubank (1997) performed measurements on gaseous *n*-butane using the Burnett method. The article contains data of two different measuring runs. The data of the first measuring run were not corrected for effects of adsorption and were classified reliable only for temperatures above 375 K by the authors. The results of the second measuring run are given after a correction for effects of adsorption and hence are claimed to be reliable over the entire temperature range, i.e., from 265 to 450 K. No estimates are given for the experimental uncertainties of the measured densities, but from comparisons to the data reported by Glos *et al.* (2004) we conclude that the total uncertainties of the data from the second measuring run are probably 0.2% at the lower temperatures, slightly increasing to about 0.3% at the higher temperatures, while the reliable data from the first measuring run appear to be accurate to only within 0.5%.

Another investigation of the liquid region worth mentioning was performed by Haynes (1983a) using a magnetic suspension densimeter. These data were not used to establish the new equation of state because they deviate systematically from the data measured by Glos *et al.* (2004). This offset increases with pressure and reaches approximately +0.3% in

TABLE 17. Summary of the $p\rho T$ data sets for *n*-butane that were assigned to group 1. Uncertainties are given where the original articles contain such estimates. Uncertainty values in parentheses were estimated by ourselves

Authors	Number of data		Temperature range (K)	Pressure range (MPa)	Total uncertainty in density
	Total	Selected			
Glos <i>et al.</i> (2004)	65	65	140–340	0.2–12	0.01%–0.02%
Gupta & Eubank (1997)	114	78	265–450	0.01–1.1	(0.2%)
Golovskii <i>et al.</i> (1978a)	122	122	135–273	1.7–61	0.05% (0.15%)
Olds <i>et al.</i> (1944)	217	182	311–511	0.07–69	0.2% (0.4%)
Beattie <i>et al.</i> (1939a)	116	102	423–573	1.5–36	(0.4%)
Beattie <i>et al.</i> (1939b)	95	95	425.05–425.25	3.77–3.82	(0.2%) ^a

^aUncertainty in pressure.

density on some isotherms. The data obtained by Golovskii *et al.* (1978a) are in better alignment with the densities reported by Glos *et al.* (2004) and thus were preferred in this work.

Data from two recent investigations were not considered in the development of the new equation of state. Kiran and Sen (1992) obtained data in simultaneous measurements of viscosity and density. The measuring technique and the calibration procedure described in the paper do not seem to be appropriate for accurate density measurements. We therefore chose the data of Olds *et al.* (1944) which cover the entire range investigated by Kiran and Sen (1992). The data measured by Kayukawa (2002) were not available when the equations presented in this work were set up. The results were obtained using a vibrating tube densimeter and show deviations from highly accurate density values of up to 0.3% in the liquid region and more than 1% in the gaseous region. The inner consistency of data obtained in one single measuring run (i.e., along a specific isotherm) is much better than this, but data from different measuring runs systematically deviate from each other and from reliable data by the other authors.

Values of the virial coefficients are usually established by isothermal fits to $p\rho T$ measurements or by evaluation of equations of state. Hence, these data do not generally contain any new information which is not given by the genuine $p\rho T$ values. Table 19 summarizes the available data sets for the second and third virial coefficients of *n*-butane. None of these data were used in the development of the equation of state presented in this work.

TABLE 18. Summary of the $p\rho T$ data sets for *n*-butane that were assigned to groups 2 and 3

Authors	Number of data	Temperature range (K)	Pressure range (MPa)	Group
Kayukawa (2002)	150	240–380	0.05–7	2–3
Kiran & Sen (1992)	100	323–443	13–69	2
Haynes (1983a)	105	140–300	1.7–36.1	2
Kay (1940)	453	311–589	0.2–8.3	3
Sage <i>et al.</i> (1937a)	154	294–394	0.1–20.7	3

3.1.2. Isochoric Heat Capacities

One single data set, established by Magee and Lüddecke (1998), is available for the isochoric heat capacity of fluid phase *n*-butane. The data are shown in a p - T diagram in Fig. 8, together with the other selected data for the calorific properties of *n*-butane. Just like the data for the heat capacity on the saturated-liquid line from the same investigation (see Sec. 2.7) we found the data in the homogenous region to be inconsistent with the $p\rho T$ values measured by Glos *et al.* (2004). No preliminary equation could represent both data sets within the uncertainties reported by the respective authors, and there was a clear interrelation between the representation of the thermal data on the one hand and the heat capacity data on the other hand. We believe the data of Glos *et al.* (2004) to be free of appreciable systematic errors and thus accepted small systematic deviations of the heat capacity data from values calculated with the new equation of state. These systematic offsets remain in the order of magni-

TABLE 19. Summary of the data sets for the second and third virial coefficients of *n*-butane

Authors	Number of data		Temperature range (K)
	B	C	
Glos <i>et al.</i> (2004)	9	—	270–340
Gupta & Eubank (1997)	9	6	265–450
Ababio <i>et al.</i> (1994)	4	4	318–348
Ewing <i>et al.</i> (1988)	8	8	250–320
Browstow <i>et al.</i> (1979)	5	—	322–347
Bottomley & Nairn (1977)	24	—	316–580
Strein <i>et al.</i> (1971)	10	—	296–498
Jones & Kay (1967)	8	—	368–498
Bottomley & Spurling (1964)	8	—	273–426
Huff & Reed (1963)	8	—	283–510
Kappallo <i>et al.</i> (1963)	7	—	244–321
Tripp & Dunlap (1962)	3	—	283–323
McGlashan & Potter (1962)	12	—	296–413
Connolly (1962)	7	7	344–444
Gunn (1958)	8	4	344–511
Hamann & McManamey (1953)	14	—	303–423
Hirschfelder <i>et al.</i> (1942)	7	—	423–573
Beattie & Stockmayer (1942)	7	—	423–573

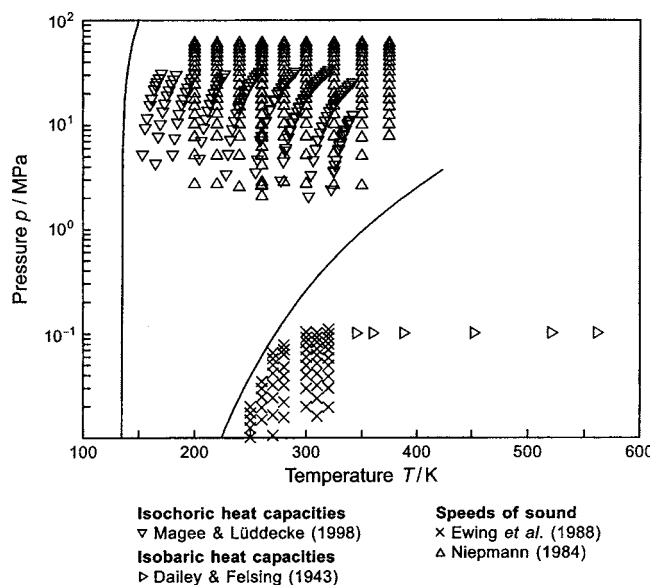


FIG. 8. Distribution of the experimental data for the caloric properties of *n*-butane used to develop the residual part of the equation of state, Eq. (4.1), in a p - T diagram.

tude of the uncertainty estimates given by Magee and Lüddecke (1998) (see Sec. 5.1.2). Details on the data are given in Table 20.

3.1.3. Isobaric Heat Capacities of the Real Fluid

The experimental results available for the isobaric heat capacity of fluid phase *n*-butane were published at least 60 years ago. The four data sets are confined to results in the gas phase at atmospheric pressure. In this region, the heat capacity is determined basically by the ideal-gas heat capacity and the thermal properties of the real gas, both of which are known to a good degree of accuracy. The experimental data therefore do not contribute significantly to the knowledge of the thermodynamic properties of *n*-butane. Only the results of Dailey and Felsing (1943), which include data at temperatures up to 673 K, were selected for the development of the new equation of state and are shown in Fig. 8. All data sets are summarized in Table 21.

3.1.4. Ideal-Gas Isobaric Heat Capacities

Data for the isobaric heat capacity of *n*-butane in the ideal-gas state were used in this work to set up the equation for the Helmholtz energy of the ideal gas given in Sec. 4.1. Two different approaches are commonly used to establish

such data. The first method uses experimental data for caloric properties extrapolated to the limit of zero density. Major sources of uncertainties are the measurements themselves and the extrapolation of real fluid data to the ideal-gas values. The temperature range where such data are available is restricted to the operating range of the corresponding experimental setups. For *n*-butane, three data sets have been established in this way. Dailey and Felsing (1943) measured isobaric heat capacities of the real gas and extrapolated the values directly to the ideal-gas state. Ewing *et al.* (1988) and Colgate *et al.* (1990) measured values for real-gas speeds of sound via spherical resonators and extrapolated these to obtain speeds of sound at zero density. Such data can be transformed to ideal-gas isobaric heat capacities by the relation

$$w^\circ = \sqrt{\left(\frac{c_p^\circ}{c_p^\circ - R}\right)RT}. \quad (3.1)$$

An error analysis yields

$$\frac{\Delta c_p^\circ}{c_p^\circ} = 2\left(1 - \frac{c_p^\circ}{R}\right)\frac{\Delta w^\circ}{w^\circ}. \quad (3.2)$$

Thus the ideal-gas isobaric heat capacities are very sensitive to uncertainties of the extrapolated speeds of sound. Deviations between the results of Ewing *et al.* (1988) and Colgate *et al.* (1990) reach up to 2% in heat capacity. These deviations are equivalent to inconsistencies of approximately 0.1% in the speed of sound.

The second method to determine the heat capacity of ideal gases uses theoretical approaches that depend on molecular constants measured by spectroscopy. Such property models usually consider contributions from molecular translation, rotation, and vibration. For more complex polyatomic molecules, like the butanes, internal rotation has to be considered as well. For *n*-butane, the uncertainties of ideal-gas heat capacity data calculated from such models arise mainly from a lack of knowledge about the effects of internal rotation. Chen *et al.* (1975) thoroughly examined these effects and calculated values for the isobaric heat capacity at temperatures up to 1500 K. Additional results from their calculations were published by Kurnik and Barduhn (1978). Thus far, these data are the most reliable source of information about the caloric properties of *n*-butane in the ideal-gas state. Older investigations that were performed by Schäfer and Auer (1961) and by Rossini *et al.* (1953) were based on calculations by Pitzer (1944) and have to be considered obsolete.

Because of the severe discrepancies between the data obtained by extrapolation of experimental results, we chose to

TABLE 20. Details on the data for the isochoric heat capacity of *n*-butane that were assigned to group 1. Uncertainties are given as estimated by the authors. Uncertainty values in parentheses were estimated by ourselves

Authors	Number of data		Temperature range (K)	Density range/(kg m ⁻³)	Total uncertainty in isochoric heat capacity
	Total	Selected			
Magee & Lüddecke (1998)	148	148	153–342	2–30	0.7% (2%)

TABLE 21. Summary of the available data sets for the isobaric heat capacity of *n*-butane. Uncertainties are given as estimated by the authors

Authors	Number of data		Temperature range (K)	Pressure range (MPa)	Total uncertainty in isobaric heat capacity
	Total	Selected			
Dailey & Felsing (1943)	8	8	344–693	0.10	1%
Dobratz (1941)	4	—	294–444	0.10	data assigned to group 3
Sage <i>et al.</i> (1937b)	8	—	294–411	0.10	data assigned to group 3
Beeck (1936)	4	—	273–573	0.10	data assigned to group 3

establish the equation for the ideal-gas part of the Helmholtz energy exclusively on the data published by Chen *et al.* (1975). Information on the available data sets is given in Table 22.

3.1.5. Speeds of Sound

Four experimental investigations of the speed of sound in fluid *n*-butane are available. Two of them, performed by Ewing *et al.* (1988) and Niepmann (1984) were considered in the development of the new equation of state. The data sets are summarized in Table 23 and shown in a *p*–*T* diagram in Fig. 8. The remaining two studies are compiled in Table 24.

Ewing *et al.* (1988) used a spherical resonator to obtain speeds of sound in gaseous *n*-butane at low pressures. As we discussed in the preceding section, these values are not consistent with the function for the ideal-gas Helmholtz energy presented in this work. For every isotherm investigated by Ewing *et al.* (1988), we assessed these inconsistencies by extrapolating the experimental speeds of sound to zero pressure and subtracting the resulting value from the corresponding speed of sound calculated from our equation for the ideal-gas Helmholtz energy [Eq. (4.5)]. The experimental speeds of sound were then “corrected” by this difference to be consistent with Eq. (4.5), and the corrected values were used to develop the equation for the residual part [Eq. (4.12)]. The corrections that were applied to the data on the individual isotherms are given in Table 25.

At supercritical pressures and liquid-like densities, Niepmann (1984) performed measurements of the speed of sound using the pulse-echo technique. The total uncertainties are reported to be 0.2% in the speed of sound, but plots of the

data reveal an inherent scatter of up to 0.25%. Additionally, there is a systematic leap in the speeds of sound occurring around 20–35 MPa on most of the investigated isotherms. This leap is in the order of 0.2% and might be caused by a switch of the pressure measuring system. We therefore assumed the total uncertainties of the data to be approximately 0.5% in speed of sound.

3.2. Isobutane

3.2.1. Thermal Properties

Similar to *n*-butane, the thermal properties of isobutane have recently been investigated by Glos *et al.* (2004) using a two-sinker densimeter. The purity of the sample is reported to be 99.98%, and the total uncertainties of the measured density values are given to be between 0.01% and 0.02% except for lower gas densities where the uncertainties rise up to 0.1%. These data undoubtedly make up the most accurate description of the thermal properties of isobutane available. Most of the measurements have been performed in the liquid region at sub- and supercritical pressures. Additionally, some values have been obtained in the gas phase. These data provide an important basis for the development of the new equation of state and were used as a reference to assess the quality of other data sets.

Another important study was performed by Waxman and Gallagher (1983) and Waxman (1980) on a Burnett apparatus. The data were obtained at gaseous and supercritical states. Both data sets were measured during the same investigation, but only some of the values were published by Waxman and Gallagher (1983). The purity of the specimen is

TABLE 22. Summary of the data sets for the isobaric heat capacity of *n*-butane in the ideal-gas state. Uncertainties are given where the original articles contain such estimates

Authors	Number of data	Temperature range (K)	Total uncertainty	Measured property
Data calculated from models based on spectroscopic data				
Kurnik & Barduhn (1978)	24	160–390	—	—
Chen <i>et al.</i> (1975)	36 ^a	0–1500	—	—
Schäfer & Auer (1961)	18	200–1500	—	—
Rossini <i>et al.</i> (1953)	19	0–1500	—	—
Data extrapolated from experimental results				
Colgate <i>et al.</i> (1990)	3	298–348	—	w
Ewing <i>et al.</i> (1988)	8	250–320	0.0025%–0.02%	w
Dailey & Felsing (1943)	8	345–693	1%	<i>c</i> _p

^aThese data were used to fit the correlation equation for the ideal-gas heat capacity, Eq. (4.5).

TABLE 23. Summary of the data sets for the speed of sound of *n*-butane that were assigned to group 1. Uncertainties are given where the original articles contain such estimates. Uncertainty values in parentheses were estimated by ourselves

Authors	Number of data		Temperature range (K)	Pressure range (MPa)	Total uncertainty in speed of sound
	Total	Selected			
Ewing <i>et al.</i> (1988)	66	66	250–320	0.005–0.1	(0.1%)
Niepmann (1984)	230	227	200–375	2–60	0.2% (0.5%)

given as 99.98%, while no estimates are reported for the uncertainties of the data. We assume the total uncertainties of the measured densities to be generally less than 0.1%, with significantly higher uncertainties close to the phase boundary and near the critical point.

Beattie *et al.* (1949, 1950) published two data sets for the thermal properties of isobutane. The first investigation focused on the critical region, whereas the latter work was concerned with the liquid, gaseous, and supercritical regions. The densities were measured with a piezometer. Neither the purity of the sample nor estimates for the uncertainties of the results are given.

Liquid densities at temperatures up to 300 K and pressures up to 35 MPa have been measured by Haynes (1983b) with a magnetic suspension densimeter. The purity of the isobutane is reported as 99.9%, the total uncertainties of the densities are estimated to be less than 0.1%. The measured densities are systematically higher than the values reported by Glos *et al.* (2004) and these deviations increase with pressure. Analogous discrepancies can be observed for *n*-butane (see Sec. 3.1.1). Unlike the data situation for *n*-butane, no other reliable data for the thermal properties of isobutane are available above 12 MPa. For this reason, the data above this pressure were used to establish the new equation of state, assuming rather high uncertainties of 0.5% for the densities.

The results of two early studies by Morris *et al.* (1939) and Sage and Lacey (1938) were not considered in the development of the new equation of state. Both data sets are inconsistent with the results reported by the other authors. A very small data set consisting of only five values at 55 MPa that were established by Gonzalez and Lee (1966) to support their viscosity measurements was also disregarded because of the low quality of the data. All selected data are shown in a *p*–*T* diagram in Fig. 9. Additional information on these data is given in Table 26, while the remaining data sets are summarized in Table 27.

Kayukawa (2002) obtained density values using a vibrating tube densimeter. The data were not available when the

TABLE 24. Summary of the data sets for the speed of sound of *n*-butane that were assigned to group 3

Authors	Number of data	Temperature range (K)	Pressure range (MPa)	Group
Rao (1971)	15	143–268	0.1	3
M'Hirsi (1958)	— ^a	311–511	0.1–90	3

^aData presented in graphs only.

equations presented in this work were set up. Similar to the corresponding values for *n*-butane, the inner consistency of data obtained in one single measuring run (i.e., along a specific isotherm) is quite good, while data from different measuring runs systematically deviate from each other and from reliable data of others. The systematic deviations from highly accurate values are generally within 0.8% for liquid-region densities and more than 1% for gas-phase data.

No data for the thermal virial coefficients of isobutane are available beyond the range of parameters covered by *p*, *T* data. However, we could increase the quality of the new equation of state with respect to the speed of sound by including eight values for the second virial coefficient that were obtained by Ewing and Goodwin (1991) from an evaluation of their speed of sound data. All data sets available for the second and third virial coefficients of isobutane are summarized in Table 28.

3.2.2. Isobaric Heat Capacities of the Real Fluid

With the exception of the work of Ernst and Büscher (1970), all experimental data for the isobaric heat capacity of isobutane stem from investigations that were performed before 1950. The range covered by these *c*, *p* data is confined to the subcritical gas phase. Since only few data for the caloric properties are available at all, three of the data sets were included in the development of the new equation of state. They are summarized in Table 29 and shown in a *p*–*T* diagram in Fig. 10, together with the selected data for the speed of sound. The other data sets are compiled in Table 30.

The most recent data set, established by Ernst and Büscher (1970), comprises pressures up to 0.7 MPa. No particulars are given on the purity of the isobutane sample. A total error of 0.1% is reported, which apparently corresponds to the

TABLE 25. Corrections applied to the speed of sound data measured by Ewing *et al.* (1988)

<i>T</i> (K)	$(w_{\text{calc}} - w_{\text{exp}})/w_{\text{exp}}$
250	-0.00069
260	-0.00079
270	-0.00080
280	-0.00080
300	-0.00071
310	-0.00085
320	-0.00090

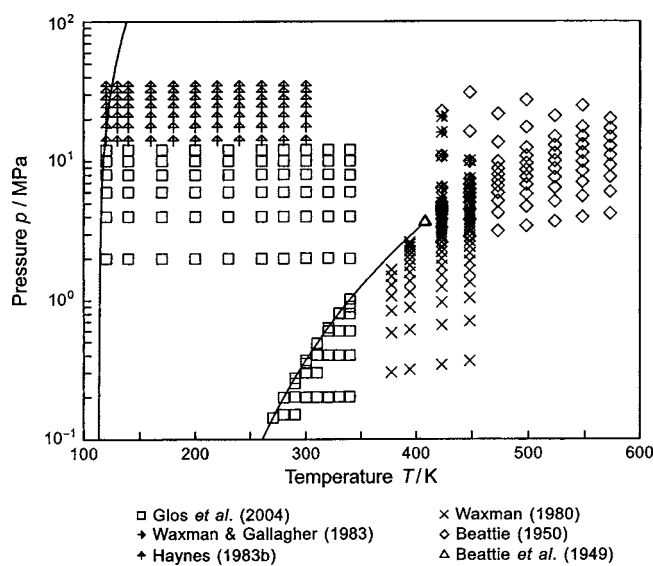


FIG. 9. Distribution of the experimental $p\varphi T$ data for isobutane used to develop the residual part of the equation of state, Eq. (4.1), in a p - T diagram.

reproducibility. These data are the most important source of information on the caloric properties of isobutane in the real-gas state.

Wacker *et al.* (1947) measured isobaric heat capacities at pressures up to 0.5 MPa. The purity of the sample is reported to be 99.85%. The estimated uncertainties of less than 0.07% in heat capacity appear by far too optimistic. The heat capacities are consistent with the data reported by Ernst and Büscher (1970) to within approximately 0.3%.

Dailey and Felsing (1943) used a calorimeter operating at atmospheric pressure. Their isobutane sample had a purity of approximately 99%. Their results were used in this work because they appear to be reliable within the estimated uncertainties and because they include values at temperatures not covered by any other investigation.

Two more data sets, published by Sage and Lacey (1938) and Sage *et al.* (1937b), were not included in the development of the new equation of state. The results of both studies deviate seriously from the values reported by the aforementioned authors.

TABLE 27. Summary of the $p\varphi T$ data sets for isobutane that were assigned to groups 2 and 3

Authors	Number of data	Temperature range (K)	Pressure range (MPa)	Group
Kayukawa (2002)	258	240–380	0.03–7	2–3
Gonzalez & Lee (1966)	5	311–444	55.2	2
Morris <i>et al.</i> (1939)	162	311–511	0.7–34.5	3
Sage & Lacey (1938)	177	294–394	0.07–20.7	3

3.2.3. Ideal-Gas Isobaric Heat Capacities

The data situation for the ideal-gas isobaric heat capacity of isobutane is very similar to the situation for *n*-butane. The determination of values based on molecular constants is less complicated because the isobutane molecule can be well approximated as three independently rotating methyl groups. The available data sets are compiled in Table 31.

To additionally get a better agreement with experimental data, Chen *et al.* (1975) included an empirical parameter in their calculations that was adjusted to data reported by Ernst and Büscher (1970), Wacker *et al.* (1947), and Dailey and Felsing (1943). Earlier works based on molecular constants were performed by Schäfer and Auer (1961) and Rossini *et al.* (1953) both of which depend on calculations by Pitzer (1944) and have to be considered as obsolete. The equation for the ideal-gas heat capacity [Eq. (4.5)] and thus the equation for the ideal-gas part of the Helmholtz energy [Eq. (4.6)] were established based on the data reported by Chen *et al.* (1975).

Ewing and Goodwin (1991) and Colgate *et al.* (1990) determined values for the ideal-gas heat capacity by evaluation of experimental speed of sound data, as described in Sec. 3.1.4. The heat capacities reported by Ewing and Goodwin (1991) agree within 0.45% with the data calculated by Chen *et al.* (1975), while the values reported by Colgate *et al.* (1990) are up to 3% smaller than any other reported data. The remaining data sets that have been mentioned above were obtained by extrapolation of experimental real-gas isobaric heat capacities and are consistent with the values reported by Chen *et al.* (1975).

TABLE 26. Summary of the $p\varphi T$ data sets for isobutane that were assigned to group 1. Uncertainty values in parentheses were estimated by ourselves

Authors	Number of data		Temperature range (K)	Pressure range (MPa)	Total uncertainty in density
	Total	Selected			
Glos <i>et al.</i> (2004)	82	82	120–340	0.15–12	0.01%–0.02%
Haynes (1983b)	156	91	120–300	1.7–35	(0.5%)
Waxman & Gallagher (1983)	27	27	423–448	3.5–21	(0.1%–0.2%)
Waxman (1980)	85	85	378–448	0.3–21	(0.1%–0.2%)
Beattie <i>et al.</i> (1950)	75	75	423–573	2.6–31	(0.4%)
Beattie <i>et al.</i> (1949)	174	174	407–408	3.61–3.67	(0.2%) ^a

^aUncertainty in pressure.

TABLE 28. Summary of the data sets for the second and third virial coefficients of isobutane

Authors	No. of data		Temperature range (K)
	B	C	
Glos <i>et al.</i> (2004)	9	—	260–340
Ewing & Goodwin (1991)	8 ^a	8	251–319
Waxman & Gallagher (1983)	4	4	377–448
Kumar (1979)	11	—	273–511
Strein <i>et al.</i> (1971)	11	—	296–494
Huff & Reed (1963)	6	—	344–510
Connolly (1962)	7	7	344–444
Gunn (1958)	6	—	344–511
Schäfer <i>et al.</i> (1974)	6	—	295–511

^aThese data were included in the development of the new equation of state.

3.2.4. Speeds of Sound

One single data set containing experimental results for the speed of sound of isobutane is available. The data were obtained by Ewing and Goodwin (1991) with a spherical resonator and cover the gaseous region at low pressures and densities. Standard deviations of less than 0.003% are given for the squared speed of sound, but in view of the reported sample purity of only 99.9% these estimates appear to be optimistic. The data are shown in a *p*–*T* diagram in Fig. 10, while additional information is given in Table 32. The data were used to set up the new equation of state although they provide little information that goes beyond the ideal-gas part of the Helmholtz energy.

4. The New Equations of State

The equations of state for *n*-butane and isobutane presented here are fundamental equations explicit in the Helmholtz energy α as a function of density ρ and temperature T . These equations are expressed in dimensionless form, $\alpha = \alpha/(RT)$, and are separated into two parts, an ideal-gas part α° and a residual part α^r that accounts for intermolecular forces, so that

$$\frac{\alpha(\rho, T)}{RT} = \alpha(\delta, \tau) = \alpha^\circ(\delta, \tau) + \alpha^r(\delta, \tau), \quad (4.1)$$

where $\delta = \rho/\rho_c$ is the reduced density and $\tau = T_c/T$ is the inverse reduced temperature. For *n*-butane the critical density is $\rho_c = 228 \text{ kg m}^{-3}$ and the critical temperature is $T_c = 425.125 \text{ K}$; for isobutane it is $\rho_c = 225.5 \text{ kg m}^{-3}$ and T_c

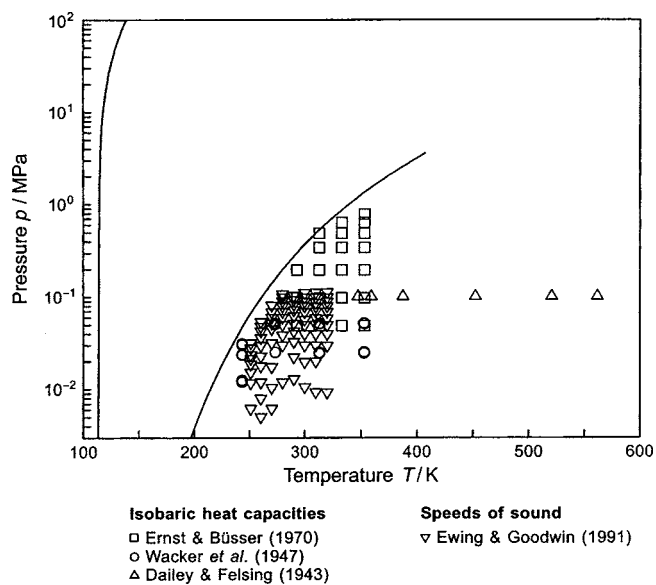


FIG. 10. Distribution of the experimental data for the caloric properties of isobutane used to develop the residual part of the equation of state, Eq. (4.1), in a *p*–*T* diagram.

= 407.81 K. For both butanes the specific gas constant amounts to $R = 0.143\,051\,57 \text{ kJ kg}^{-1} \text{ K}^{-1}$. The ideal-gas part α° and the residual part α^r of the dimensionless Helmholtz energy α are given by Eqs. (4.6) and (4.12).

Since Eq. (4.1) is an equation of state in the form of a fundamental equation, all thermodynamic properties can be calculated using combinations of α° and α^r and their derivatives. These relations are given in Table 33 for the thermodynamic properties considered in this paper. At a given temperature, the vapor pressure and the saturated-liquid and saturated-vapor densities can be obtained by simultaneously solving the phase-equilibrium conditions:

$$\frac{p_s}{RT} = \rho' [1 + \delta' \alpha_\delta^r(\delta', \tau)], \quad (4.2a)$$

$$\frac{p_s}{RT} = \rho'' [1 + \delta'' \alpha_\delta^r(\delta'', \tau)], \quad (4.2b)$$

$$\frac{p_s}{RT} \left(\frac{1}{\rho''} - \frac{1}{\rho'} \right) - \ln \left(\frac{\rho'}{\rho''} \right) = \alpha^r(\delta', \tau) - \alpha^r(\delta'', \tau); \quad (4.2c)$$

for the meaning of α_δ^r see the footnote a) in Table 33.

TABLE 29. Summary of the data sets for the isobaric heat capacity of isobutane that were assigned to group 1. Uncertainties are given where the original articles contain such estimates. Uncertainty values in parentheses were estimated by ourselves

Authors	Number of data		Temperature range (K)	Pressure range (MPa)	Total uncertainty in isobaric heat capacity
	Total	Selected			
Ernst & Büsser (1970)	21	21	293–353	0.04–0.7	0.1% (0.3%)
Wacker <i>et al.</i> (1947)	37	37	243–353	0.1–0.5	0.07% (0.5%–1%)
Dailey & Felsing (1943)	8	8	347–693	0.1	1% (1.5%)

TABLE 30. Summary of the data sets for the isobaric heat capacity of isobutane that were assigned to group 3

Authors	Number of data	Temperature range (K)	Pressure range (MPa)	Group
Sage & Lacey (1938)	59	294–394	0.1–2.5	3
Sage <i>et al.</i> (1937b)	10	294–444	0.101325	3

4.1. The Equations for the Helmholtz Energy of the Ideal Gas

The Helmholtz energy of the ideal gas is given by

$$\alpha^\circ(\rho, T) = h^\circ(T) - RT - Ts^\circ(\rho, T). \quad (4.3)$$

The enthalpy $h^\circ(T)$ and the entropy $s^\circ(\rho, T)$ of the ideal gas can be derived from an equation for the ideal-gas isobaric heat capacity $c_p^\circ(T)$. Replacing h° and s° in Eq. (4.3) by the appropriate expressions yields

$$\begin{aligned} \alpha^\circ(\rho, T) = & \int_{T_0}^T c_p^\circ dT + h_0^\circ - RT - T \left[\int_{T_0}^T \frac{c_p^\circ - R}{T} dT \right. \\ & \left. - R \ln\left(\frac{\rho}{\rho_0}\right) + s_0^\circ \right], \end{aligned} \quad (4.4)$$

where all variables with the index “0” refer to an arbitrary reference state. We set the enthalpy and the entropy to zero at $T_0 = 298.15$ K and $p_0 = 0.101325$ MPa. The corresponding ideal-gas density is given by $\rho_0 = p_0/(RT_0)$.

The new correlation equations for the ideal-gas isobaric heat capacities of n - and isobutane have the following functional form:

$$\frac{c_p^\circ(T)}{R} = 1 + n_3^\circ + \sum_{i=4}^7 n_i^\circ (\theta_i^\circ \tau)^2 \frac{\exp(-\theta_i^\circ \tau)}{[\exp(-\theta_i^\circ \tau) - 1]^2}. \quad (4.5)$$

For both substances, the coefficients n_i° and parameters θ_i° of Eq. (4.5) were fitted to the respective data reported by Chen *et al.* (1975), and are given in Table 34. With these coefficients and parameters, Eq. (4.5) reproduces the input data for either substance within 0.03%.

The expression for the Helmholtz energy of the ideal gas can be derived by inserting Eq. (4.5) into Eq. (4.4) and carrying out the integration

$$\begin{aligned} \alpha^\circ = & \ln(\delta) + n_1^\circ + n_2^\circ \tau + n_3^\circ \ln(\tau) \\ & + \sum_{i=4}^7 n_i^\circ \ln[1 - \exp(-\theta_i^\circ \tau)], \end{aligned} \quad (4.6)$$

for the definition of δ and τ see Eq. (4.1). The coefficients n_i° and parameters θ_i° are given in Table 34 for both substances. The integration constants n_1° and n_2° were chosen to give zero for the ideal-gas enthalpy at $T_0 = 298.15$ K and the ideal-gas entropy at $T_0 = 298.15$ K and $p_0 = 0.101325$ MPa. Table 35 compiles the derivatives of the ideal-gas part α° required for the calculation of thermodynamic properties.

4.2. The Equations for the Residual Part of the Helmholtz Energy

Unlike the ideal-gas part of the Helmholtz energy, no physically founded models are available that accurately describe the thermodynamic behavior of real fluids over a wide range of density and pressure. Therefore, empirical descriptions of the residual Helmholtz energy were developed in this work. State-of-the-art procedures were used to establish the mathematical structure of the correlation equations and to adjust the coefficients. Although certain demands on the functional form as formulated by Span and Wagner (1997) were considered, the terms in the equations are basically empirical.

4.2.1. Fitting the Coefficients

Once a certain functional form has been chosen for the residual part of the Helmholtz energy $\alpha^r(\delta, \tau, \bar{n})$, data for J different properties z_j (e.g., pressure, speed of sound, etc.) can be used to determine the coefficients n_i (expressed as vector \bar{n}) by minimizing the following sum of squares:

$$\chi^2 = \sum_{j=1}^J \chi_j^2 = \sum_{j=1}^J \sum_{m=1}^M \left[\frac{[z_{\text{exp}} - z_{\text{calc}}(x_{\text{exp}}, y_{\text{exp}}, \bar{n})]^2}{\sigma_{\text{tot}}^2} \right]_{j,m}, \quad (4.7)$$

TABLE 31. Summary of the data sets for the isobaric heat capacity of isobutane in the ideal-gas state. Uncertainties are given where the original articles contain such estimates

Authors	Number of data	Temperature range (K)	Total uncertainty	Measured property
Data calculated from models based on spectroscopic data				
Chen <i>et al.</i> (1975)	44 ^a	0–1500	—	—
Schäfer & Auer (1961)	19	200–1500	—	—
Rossini <i>et al.</i> (1953)	19	0–1500	—	—
Data extrapolated from experimental results				
Ewing & Goodwin (1991)	8	251–320	0.003%–0.02%	w
Colgate <i>et al.</i> (1990)	3	298–348	—	w
Ernst & Büsser (1970)	4	293–353	0.2%	c_p
Wacker <i>et al.</i> (1947)	4	243–353	0.11%	c_p
Dailey & Felsing (1943)	8	348–693	1%	c_p

^aThese data were used to fit the correlation equation for the ideal-gas heat capacity, Eq. (4.5).

TABLE 32. Summary of the data for the speed of sound of isobutane that were assigned to group 1. Uncertainty values in parentheses were estimated by ourselves

Authors	Number of data		Temperature range (K)	Pressure range (MPa)	Total uncertainty in speed of sound
	Total	Selected			
Ewing & Goodwin (1991)	79	79	251–320	0.006–0.11	(0.1%)

where M_j is the number of data points used for the j th property, z_{exp} the experimental value for any property z , and z_{calc} the value for this property calculated from the equation for α^r with the parameter vector \bar{n} at x_{exp} and y_{exp} . The independent variables x and y may vary for the different properties. When data for different properties are included in the development of a correlation equation, the residual $\Delta z = (z_{\text{exp}} - z_{\text{calc}})$ of Eq. (4.7) has to be reduced with an appropriate measure for the uncertainty of the data point. From the Gaussian error propagation formula, the uncertainty of a measured data point can be calculated as

$$\sigma_{\text{exp}}^2 = \left[\frac{\partial \Delta z}{\partial x} \right]_{y,z}^2 \sigma_x^2 + \left[\frac{\partial \Delta z}{\partial y} \right]_{x,z}^2 \sigma_y^2 + \left[\frac{\partial \Delta z}{\partial z} \right]_{x,y}^2 \sigma_z^2, \quad (4.8)$$

where σ_x , σ_y , and σ_z are the isolated uncertainties of the single variables x , y , and z , respectively. The partial derivatives have to be calculated from a preliminary equation of state. In some instances, the calculated weights were modified by arbitrary multiplicative factors f_{wt} to increase or reduce the influence of a particular data set on the overall representation of the surface. In this way, the disproportion-

TABLE 33. Relations of thermodynamic properties to the ideal-gas part α° , Eq. (4.6), and the residual part α^r , Eq. (4.12), of the dimensionless Helmholtz energy and their derivatives^{a,b}

Property	Relation
Pressure $p = \rho^2 (\partial a / \partial \rho)_T$	$\frac{p(\delta, \tau)}{\rho R T} = 1 + \delta \alpha_\delta^r$
Entropy $s = -(\partial a / \partial T)_v$	$\frac{s(\delta, \tau)}{R} = \tau(\alpha_\tau^\circ + \alpha_\tau^r) - \alpha^\circ - \alpha^r$
Internal energy $u = a + T s$	$\frac{u(\delta, \tau)}{R T} = \tau(\alpha_\tau^\circ + \alpha_\tau^r)$
Enthalpy $h = u + p v$	$\frac{h(\delta, \tau)}{R T} = 1 + \tau(\alpha_\tau^\circ + \alpha_\tau^r) + \delta \alpha_\delta^r$
Gibbs free energy $g = h - T s$	$\frac{g(\delta, \tau)}{R T} = 1 + \alpha^\circ + \alpha^r + \delta \alpha_\delta^r$
Isochoric heat capacity $c_v = (\partial u / \partial T)_v$	$\frac{c_v(\delta, \tau)}{R} = -\tau^2(\alpha_{\tau\tau}^\circ + \alpha_{\tau\tau}^r)$
Isobaric heat capacity $c_p = (\partial h / \partial T)_p$	$\frac{c_p(\delta, \tau)}{R} = -\tau^2(\alpha_{\tau\tau}^\circ + \alpha_{\tau\tau}^r) + \frac{(1 + \delta \alpha_\delta^r - \delta \tau \alpha_{\delta\tau}^r)^2}{1 + 2 \delta \alpha_\delta^r + \delta^2 \alpha_{\delta\delta}^r}$
Saturated-liquid heat capacity $c_\sigma(T) = (\partial h / \partial T)_p + T(\partial p / \partial T)_v \cdot (dp_s / dT) / (-\rho^2(\partial p / \partial \rho)_T) _{\rho=\rho'}$	$\frac{c_\sigma(\tau)}{R} = -\tau^2(\alpha_{\tau\tau}^\circ + \alpha_{\tau\tau}^r) + \frac{1 + \delta' \alpha_\delta^r - \delta' \tau \alpha_{\delta\tau}^r}{1 + 2 \delta' \alpha_\delta^r + \delta'^2 \alpha_{\delta\delta}^r} \cdot \left[(1 + \delta' \alpha_\delta^r - \delta' \tau \alpha_{\delta\tau}^r) - \frac{1}{\rho_c R \delta'} \frac{dp_s}{dT} \right]^c$
Speed of sound $w = (\partial p / \partial \rho)_s^{1/2}$	$\frac{w^2(\delta, \tau)}{R T} = 1 + 2 \delta \alpha_\delta^r + \delta^2 \alpha_{\delta\delta}^r - \frac{(1 + \delta \alpha_\delta^r - \delta \tau \alpha_{\delta\tau}^r)^2}{\tau^2(\alpha_{\tau\tau}^\circ + \alpha_{\tau\tau}^r)}$
Joule-Thomson coefficient $\mu = (\partial T / \partial p)_h$	$\mu(\delta, \tau) R \rho = \frac{-(\delta \alpha_\delta^r + \delta^2 \alpha_{\delta\delta}^r + \delta \tau \alpha_{\delta\tau}^r)}{(1 + \delta \alpha_\delta^r - \delta \tau \alpha_{\delta\tau}^r)^2 - \tau^2(\alpha_{\tau\tau}^\circ + \alpha_{\tau\tau}^r)(1 + 2 \delta \alpha_\delta^r + \delta^2 \alpha_{\delta\delta}^r)}$
Isothermal throttling coefficient $\delta_T = (\partial h / \partial p)_T$	$\delta_T(\delta, \tau) \rho = \frac{1 + \delta \alpha_\delta^r - \delta \tau \alpha_{\delta\tau}^r}{1 + 2 \delta \alpha_\delta^r + \delta^2 \alpha_{\delta\delta}^r}$
Second virial coefficient $B(T) = \lim_{\rho \rightarrow 0} (\partial Z / \partial \rho)_T$	$B(\tau) \rho_c = \lim_{\delta \rightarrow 0} \alpha_\delta^r(\delta, \tau)$
Third virial coefficient $C(T) = \lim_{\rho \rightarrow 0} \left[\frac{1}{2} (\partial^2 Z / \partial \rho^2)_T \right]$	$C(\tau) \rho_c^2 = \lim_{\delta \rightarrow 0} \alpha_{\delta\delta}^r(\delta, \tau)$

^a $\alpha_\delta^r = [\partial \alpha^r / \partial \delta]_\tau$, $\alpha_{\delta\delta}^r = [\partial^2 \alpha^r / \partial \delta^2]_\tau$, $\alpha_\tau^r = [\partial \alpha^r / \partial \tau]_\delta$, $\alpha_{\tau\tau}^r = [\partial^2 \alpha^r / \partial \tau^2]_\delta$, $\alpha_{\delta\tau}^r = [\partial^2 \alpha^r / \partial \delta \partial \tau]$, $\alpha_\tau^\circ = [\partial \alpha^\circ / \partial \tau]_\delta$, $\alpha_{\tau\tau}^\circ = [\partial^2 \alpha^\circ / \partial \tau^2]_\delta$.

^b For the specific gas constant R see Eq. (4.1).

^c $dp_s / dT = [\rho'' \cdot \rho' / (\rho'' - \rho')] R [\ln(\rho''/\rho') + \alpha^r(\tau, \delta'') - \alpha^r(\tau, \delta') - \tau(\alpha_\tau^r(\tau, \delta'') - \alpha_\tau^r(\tau, \delta'))]$.

TABLE 34. Coefficients of the correlation equations for the ideal-gas isobaric heat capacity c_p° and the ideal-gas part α° of the dimensionless Helmholtz energy of n - and isobutane, Eqs. (4.5) and (4.6)

i	n -Butane	Isobutane
n_1°	12.54882924	11.60865546
n_2°	-5.46976878	-5.29450411
n_3°	3.24680487	3.05956619
n_4°	5.54913289	4.94641014
n_5°	11.4648996	4.09475197
n_6°	7.59987584	15.6632824
n_7°	9.66033239	9.73918122
θ_4°	0.7748404445	0.9512779015
θ_5°	3.3406025522	2.3878958853
θ_6°	4.9705130961	4.3469042691
θ_7°	9.9755537783	10.3688586351

ate influence of single data sets that were assigned overly optimistic uncertainties by the corresponding authors could be avoided. The total variance of a data point in Eq. (4.7) then reads

$$\sigma_{\text{tot}}^2 = \sigma_{\text{exp}}^2 / f_{\text{wt}}^2. \quad (4.9)$$

The procedure to determine the coefficient vector \bar{n} by minimizing the sum of squares [Eq. (4.7)] is called multiproperty fitting and generally leads to the problem of iteratively solving a system of nonlinear equations. However, if every property z considered in the fit depends on the same independent variables as the correlation function (in this work, this is the Helmholtz energy with the independent variables temperature and density), and if the mathematical relations between z and the correlation function or its derivatives are linear for all considered properties, the system to be solved becomes a linear system of normal equations and can be solved straightforwardly. Data for properties that fulfill the abovementioned conditions are called "linear" data. For functions in terms of the Helmholtz energy, such properties are, e.g., $p(T, \rho)$ and $c_v(T, \rho)$ (see Table 33). If one or both of the conditions are not fulfilled, complicated and time-consuming nonlinear algorithms have to be used to minimize the sum of squares. Such "nonlinear" properties are, e.g., $w(T, \rho)$ and $c_p(T, \rho)$. The optimization procedure that we used to establish the functional form of the new correlation

equations for the residual part α^r uses strictly linear algorithms. To include data for nonlinear properties in these algorithms, they have to be transformed to linear data with the help of preliminary equations. Details on such linearization procedures are given by Setzmann and Wagner (1991) and Tegeler *et al.* (1997). At the end of the optimization, after the functional form was chosen, the final values of the coefficients n_i were determined in a nonlinear fit directly considering both linear and nonlinear data. The residua used in the linear and nonlinear algorithms correspond to common formulations recently explained by Span (2000).

4.2.2. Optimizing the Functional Form

The predominant objective of the advancement of sophisticated algorithms to optimize the functional form of equations of state [see Wagner (1974), Ewers and Wagner (1982), Setzmann and Wagner (1989), or Tegeler *et al.* (1997)] has always been to improve the accuracy of the formulation with regard to the representation of highly accurate data. The high accuracy of the established formulation is intimately connected to a high flexibility of the applied optimization algorithm, therefore large and reliable data sets are required to confine the optimization to reasonable solutions. As it was shown in Secs. 2 and 3, however, the data situation for the butanes is very inhomogeneous. While the thermal properties in large parts of the fluid region are described within the highest attainable accuracy by experimental data, reliable values of the caloric properties are scarce, and in several regions the definition of even the thermal properties is poor. To establish equations for the butanes that are accurate enough to describe the high precision data within the small experimental uncertainties, yet numerically stable enough to yield reasonable results in poorly surveyed regions, we used a so-called "simultaneous" optimization algorithm to develop the mathematical structure of the correlation function for α^r .

This algorithm, developed by Span *et al.* (1998), considers data sets for different substances concurrently. Instead of choosing the formulation that yields the best description of a

TABLE 35. The ideal-gas part α° , Eq. (4.6), of the dimensionless Helmholtz energy and its derivatives^a

α°	=	$\ln \delta$	+	n_1°	+	$n_2^\circ \tau$	+	$n_3^\circ \ln \tau$	+	$\sum_{i=4}^7 n_i^\circ \ln(1 - e^{-\theta_i^\circ \tau})$
α_δ°	=	$1/\delta$	+	0	+	0	+	0	+	0
$\alpha_{\delta\delta}^\circ$	=	$-1/\delta^2$	+	0	+	0	+	0	+	0
α_τ°	=	0	+	0	+	n_2°	+	n_3° / τ	+	$\sum_{i=4}^7 n_i^\circ \theta_i^\circ [(1 - e^{-\theta_i^\circ \tau})^{-1} - 1]$
$\alpha_{\tau\tau}^\circ$	=	0	+	0	+	0	-	$-n_3^\circ / \tau^2$	-	$\sum_{i=4}^7 n_i^\circ (\theta_i^\circ)^2 e^{-\theta_i^\circ \tau} (1 - e^{-\theta_i^\circ \tau})^{-2}$
$\alpha_{\delta\tau}^\circ$	=	0	+	0	+	0	+	0	+	0

^a $\alpha_\delta^\circ = [\partial \alpha^\circ / \partial \delta]_\tau$, $\alpha_{\delta\delta}^\circ = [\partial^2 \alpha^\circ / \partial \delta^2]_\tau$, $\alpha_\tau^\circ = [\partial \alpha^\circ / \partial \tau]_\delta$, $\alpha_{\tau\tau}^\circ = [\partial^2 \alpha^\circ / \partial \tau^2]_\delta$, $\alpha_{\delta\tau}^\circ = [\partial^2 \alpha^\circ / \partial \delta \partial \tau]$.

TABLE 36. Summary of the selected data for thermodynamic properties of *n*- and isobutane that were used in the simultaneous optimization and nonlinear fit of the residual parts α^r of *n*- and isobutane, Eq. (4.12)

Property	n-Butane			Isobutane		
	For details see	Number of data		For details see	Number of data	
		Simultaneous optimization	Nonlinear fit		Simultaneous optimization	Nonlinear fit
$p(\rho, T)$	Table 17	644	644	Table 26	534	534
$p_s(T)$		144 ^a			147 ^a	
$p'(T)$		144 ^a			147 ^a	
$p''(T)$		144 ^a			147 ^a	
$p_s(T)$	Table 6		23	Table 7		31
$p'(T)$	Table 10		23	Table 11		43
$p''(T)$	Table 12		26	Table 13		31
$B(T)$				Table 28	8	8
$c_v(\rho, T)$	Table 20	148	148			
$c_p(\rho, T)$	Table 21	8 ^b	8	Table 29	66 ^b	66
$c'_p(T)$	Table 15	100 ^b	100	Table 16	44 ^b	44
$w(p, T)$	Table 23	293 ^b	293	Table 32	79 ^b	79
$w'(T)$	Table 15	19 ^b	19			

^aLinearized solution of the Maxwell criterion using data calculated from the ancillary equations, Eqs. (2.2) to (2.4) (see Wagner 1972).

^bLinearized data used in the linear optimization procedure (see Setzmann and Wagner 1991).

single fluid, the simultaneous optimization chooses the one that yields the best results for all fluids on average. The key idea is that if the considered fluids are typical representatives of a certain group of fluids, equations of state using the simultaneously optimized functional form can be fitted to data sets of other fluids from the same group without significant disadvantages. In this way, the benefits of optimized functional forms can be utilized for many fluids, even if the available data sets are not sufficient to optimize a functional form using substance specific strategies. Span and Wagner (2003a, 2003b, 2003c) applied this algorithm to establish short functional forms for equations which are able to satisfy advanced technical demands on accuracy for the groups of typical polar and nonpolar substances.

In this work we applied the simultaneous algorithm to develop reference quality equations of state. Therefore, we only considered very few but physically very similar substances. Besides *n*- and isobutane we also included the lighter alkanes ethane and propane in the optimization. Comprehensive and very accurate data sets are available for both substances. These additional data sets confine the optimization algorithm to reasonable results where reliable information on the butanes is missing.

Details on the optimization algorithm are given by Span *et al.* (1998) and Span and Wagner (2003a). However, we used a slightly different quality criterion X^{*2} for the simultaneous optimization. In the adaptation of the algorithm we used, X^{*2} is calculated by summing the reduced and weighted sums of square χ_k^{*2} of the individual substances:

$$X^{*2} = \sum_{k=1}^K \chi_k^{*2} = \sum_{k=1}^K f_{\text{subst}, k} \frac{\chi_k^2}{M_k}, \quad (4.10)$$

where the sum of squares χ_k^2 specific for substance k is reduced by the number of data considered for k , M_k . An ar-

bitrary weighting factor $f_{\text{subst}, k}$ is assigned to each sum of squares so that the influence of the substances on the optimization can be set individually. The individual sums of squares are calculated as described in the preceding section [see Eq. (4.7)].

The bank of terms that built the basis for the development of the new equations of state

$$\begin{aligned} \alpha^r = & \sum_{i=1}^4 \sum_{j=0}^{16} n_{ij} \delta^i \tau^{j/4} + \exp(-\delta) \sum_{i=1}^8 \sum_{j=0}^8 n_{ij} \delta^i \tau^{j/2} \\ & + \exp(-\delta^2) \sum_{i=1}^8 \sum_{j=0}^8 n_{ij} \delta^i \tau^{j/2} \\ & + \exp(-\delta^3) \sum_{i=1}^8 \sum_{j=4}^{16} n_{ij} \delta^i \tau^j \\ & + \exp(-\delta^4) \sum_{i=2}^{10} \sum_{j=0}^{10} n_{ij} \delta^i \tau^{2j} \\ & + \sum_{i=1}^{84} n_i \delta^{d_i} \tau^{t_i} \exp[-\eta_i(\delta - \varepsilon_i)^2 - \beta_i(\tau - \gamma_i)^2], \end{aligned} \quad (4.11)$$

comprises a total of 528 terms, including 68 simple polynomial terms, 376 polynomials combined with exponential functions, and 84 modified Gaussian bell-shaped terms as introduced by Setzmann and Wagner (1991) to improve the representation of data in the critical region. The parameters of these terms covered the ranges $1 \leq d_i \leq 3$, $0 \leq t_i \leq 3$, $10 \leq \eta_i \leq 20$, $150 \leq \beta_i \leq 250$, $0.85 \leq \varepsilon_i \leq 1$, $1.13 \leq \gamma_i \leq 1.16$. The density and temperature exponents of the remaining terms in

TABLE 37. Summary of the experimental data for thermodynamic properties of ethane that were used in the simultaneous optimization of the residual parts α^r of *n*- and isobutane, Eq. (4.12)

Property	Authors	Number of data		Temperature range (K)	Pressure range (MPa)
		Total	Selected		
$p\rho T$	Funke <i>et al.</i> (2002a)	356	356	140–340	0.2–12
	Funke <i>et al.</i> (2002b)	203	203	303–305	4.7–4.9
	Claus <i>et al.</i> (2003)	168	168	240–520	1–30
	Mansoorian <i>et al.</i> (1981)	91	91	323–473	0.04–5.4
	Golovskii <i>et al.</i> (1978b)	112	57	92–270	1.2–60
	Straty & Tsumura (1976)	477	153	92–320	0.4–38
	Pal <i>et al.</i> (1976)	267	58	157–344	0.52–73
	Douslin & Harrison (1973)	298	58	248–623	1.2–41
	Tsiklis <i>et al.</i> (1972)	75	75	323–673	200–900
	Beattie <i>et al.</i> (1939c)	82	20	323–548	6.1–36
B	Funke <i>et al.</i> (2002a)	14	14	240–340	—
p_s	Funke <i>et al.</i> (2002b)	44	44	90–305	—
ρ'	Funke <i>et al.</i> (2002b)	42	42	90–305	—
ρ''	Funke <i>et al.</i> (2002b)	32	32 ^a	90–305	—
c_v	Haase & Tillmann (1994)	11	11	305–317	202 ^b
	Roder (1976)	209	209	110–329	48–610 ^b
	Berestov <i>et al.</i> (1973)	24	3	305–306	206 ^b
c_p	Ernst & Hochberg (1989)	52	52	303–393	0.3–53
	Bender (1982)	36	36	233–298	0.1–1.5
w	Estrada-Alexanders & Trusler (1997)	186	186	220–450	0.01–10
	Trusler & Costa Gomez (1996)	52	7	250–350	0.03–20
	Boyes (1992)	71	51	210–360	0.02–1
	Lemming (1989)	163	127	223–351	0.02–0.6
	Tsumura & Straty (1977)	154	154	100–323	3.6–37
w'	Tsumura & Straty (1977)	55	55	90–305	—
	Vangeel (1976)	55	55	98–288	—
c_σ	Roder (1976)	106	106	93–301	—

^aAdditionally, 12 values were calculated from a virial equation. These data were also used.

^bFor isochoric heat capacity data, the density range in kg m^{-3} is given instead of the pressure range.

Eq. (4.7) were chosen according to recommendations given by Span and Wagner (1997) to ensure reliable extrapolation behavior of the formulations.

4.2.3. Selected Database

The experimental data that were selected to establish the new equations of state for the butanes have been presented in Secs. 2 and 3. Table 36 gives a brief summary of the data used in the simultaneous optimization procedure and in the final nonlinear fit of the individual coefficient sets. The data sets selected for the thermodynamic properties of ethane and propane are summarized in Tables 37 and 38, respectively. A detailed discussion of the data situation for ethane is given by Bücker and Wagner (2006). In addition to the experimental data, several data have been generated for the exclusive use in the simultaneous optimization algorithm. These are:

(1) A total of 232 data for the isobaric heat capacity of ethane and 81 data for the isobaric heat capacity of propane calculated from preliminary equations to ensure a numerically reliable linearization of the experimental speeds of sound published by Estrada-Alexanders and Trusler (1997), Tsumura and Straty (1977), and Younglove (1981). Details on such linearization procedures are given by Setzmann and Wagner (1991), Tegeler *et al.* (1997), and Wagner and Prüß (2002).

(2) 144 data for *n*-butane, 147 data for isobutane, and 147 data for propane, calculated from the ancillary equations, Eqs. (2.2)–(2.4) and Eqs. (9.2)–(9.4), respectively. 224 data calculated from similar equations for ethane published by Funke *et al.* (2002b). These (T_s, p_s, ρ', ρ'') data are needed for a linearized solution of the phase-equilibrium condition (Maxwell criterion) (see Wagner 1972).

4.2.4. The Equations for the Residual Part α^r

From the bank of terms as formulated in Eq. (4.11), the simultaneous optimization algorithm selected the final functional form for the residual Helmholtz energy given by

$$\begin{aligned} \alpha^r = & \sum_{i=1}^7 n_i \delta^{d_i} \tau^{t_i} + \sum_{i=8}^{23} n_i \delta^{d_i} \tau^{t_i} \exp(-\delta^{c_i}) \\ & + \sum_{i=24}^{25} n_i \delta^{d_i} \tau^{t_i} \exp[-\eta_i(\delta - \varepsilon_i)^2 - \beta_i(\tau - \gamma_i)^2], \end{aligned} \quad (4.12)$$

for the definition of δ and τ see Eq. (4.1). The final values of the coefficients n_i were determined by nonlinear fits and are given together with the other parameters in Table 39. Note that only the coefficients are different for the individual substances, while the other parameters were determined simul-

TABLE 38. Summary of the experimental data for thermodynamic properties of propane that were used in the simultaneous optimization of the residual parts α^r of *n*- and isobutane, Eq. (4.12)

Property	Authors	Number of data		Temperature range (K)	Pressure range (MPa)
		Total	Selected		
$p\rho T$	Glos <i>et al.</i> (2004)	72	72	95–340	0.2–12
	Glos <i>et al.</i> (2004), Appendix	130	130	340–520	2–30
	Kratzke & Müller (1984)	54	54	247–491	2–61
	Haynes (1983c)	196	196	90–300	0.6–38
	Thomas & Harrison (1982)	803	78	258–623	0.5–40
	Ely & Kobayashi (1978)	222	31	166–324	0.1–43
	Rodosevich & Miller (1973)	4	4	91–115	0.01–0.05
	Dawson & McKetta (1960)	18	18	243–348	0.05–0.18
	Glos <i>et al.</i> (2004)	24	24	110–340	—
	Kratzke & Müller (1984)	5	5	300–357	—
p_s	Kratzke (1980)	14	14	312–368	—
	Glos <i>et al.</i> (2004)	27	27	90–340	—
ρ'	Thomas & Harrison (1982)	22	9	258–369	—
	Glos <i>et al.</i> (2004)	12	12 ^a	230–340	—
ρ''	Thomas & Harrison (1982)	11	9	323–369	—
	Abdulagatov <i>et al.</i> (1997)	37	37	305–369	—
c_v', c_v''	Trusler & Zarari (1996)	68	68	225–375	0.01–0.84
	Niepmann (1984)	222	221	200–323	0.2–61
	Younglove (1981)	162	162	90–300	1.92–35
w'	Niepmann (1984)	19	19	200–325	—
	Ernst & Büscher (1970)	36	36	293–353	0.05–1.37
c_p	Yesavage <i>et al.</i> (1968)	199	187	166–422	1.7–14

^aAdditionally, 19 values were calculated from a virial equation. These data were also used.

TABLE 39. Coefficients and exponents of the equation of the residual part α^r of the dimensionless Helmholtz energy of *n*- and isobutane, Eq. (4.12)

<i>i</i>	Substance specific coefficients n_i		Simultaneously optimized functional form						
	<i>n</i> -Butane	Isobutane	c_i	d_i	t_i				
1	$0.25536998241635 \times 10^1$	$0.20686820727966 \times 10^1$	—	1	0.50				
2	$-0.44585951806696 \times 10^1$	$-0.36400098615204 \times 10^1$	—	1	1.00				
3	0.82425886369063	0.51968754427244	—	1	1.50				
4	0.11215007011442	0.17745845870123	—	2	0.00				
5	$-0.35910933680333 \times 10^{-1}$	-0.12361807851599	—	3	0.50				
6	$0.16790508518103 \times 10^{-1}$	$0.45145314010528 \times 10^{-1}$	—	4	0.50				
7	$0.32734072508724 \times 10^{-1}$	$0.30476479965980 \times 10^{-1}$	—	4	0.75				
8	0.95571232982005	0.75508387706302	1	1	2.00				
9	$-0.10003385753419 \times 10^1$	-0.85885381015629	1	1	2.50				
10	$0.85581548803855 \times 10^{-1}$	$0.36324009830684 \times 10^{-1}$	1	2	2.50				
11	$-0.25147918369616 \times 10^{-1}$	$-0.19548799450550 \times 10^{-1}$	1	7	1.50				
12	$-0.15202958578918 \times 10^{-2}$	$-0.44452392904960 \times 10^{-2}$	1	8	1.00				
13	$0.47060682326420 \times 10^{-2}$	$0.46410763666460 \times 10^{-2}$	1	8	1.50				
14	$-0.97845414174006 \times 10^{-1}$	$-0.71444097992825 \times 10^{-1}$	2	1	4.00				
15	$-0.48317904158760 \times 10^{-1}$	$-0.80765060030713 \times 10^{-1}$	2	2	7.00				
16	0.17841271865468	0.15560460945053	2	3	3.00				
17	$0.18173836739334 \times 10^{-1}$	$0.20318752160332 \times 10^{-2}$	2	3	7.00				
18	-0.11399068074953	-0.10624883571689	2	4	3.00				
19	$0.19329896666669 \times 10^{-1}$	$0.39807690546305 \times 10^{-1}$	2	5	1.00				
20	$0.11575877401010 \times 10^{-2}$	$0.16371431292386 \times 10^{-1}$	2	5	6.00				
21	$0.15253808698116 \times 10^{-3}$	$0.53212200682628 \times 10^{-3}$	2	10	0.00				
22	$-0.43688558458471 \times 10^{-1}$	$-0.78681561156387 \times 10^{-2}$	3	2	6.00				
23	$-0.82403190629989 \times 10^{-2}$	$-0.30981191888963 \times 10^{-2}$	3	6	13.00				
<i>i</i>	<i>n</i> -Butane	Isobutane	c_i	d_i	t_i				
24	$-0.28390056949441 \times 10^{-1}$	$-0.42276036810382 \times 10^{-1}$	—	1	2.00				
25	$0.14904666224681 \times 10^{-2}$	$-0.53001044558079 \times 10^{-2}$	—	2	0.00				
<i>i</i>	<i>n</i> -Butane	Isobutane	c_i	d_i	t_i	η_i	β_i	ε_i	γ_i
24	$-0.28390056949441 \times 10^{-1}$	$-0.42276036810382 \times 10^{-1}$	—	1	2.00	10	150	0.85	1.16
25	$0.14904666224681 \times 10^{-2}$	$-0.53001044558079 \times 10^{-2}$	—	2	0.00	10	200	1.00	1.13

TABLE 40. The residual part, α^r , Eq. (4.12), of the dimensionless Helmholtz energy and its derivatives^a

$$\begin{aligned}
\alpha^r &= \sum_{i=1}^7 n_i \delta^{d_i} \tau^{t_i} + \sum_{i=8}^{23} n_i \delta^{d_i} \tau^{t_i} e^{-\delta^{c_i}} + \sum_{i=24}^{25} n_i \delta^{d_i} \tau^{t_i} e^{-\eta_i(\delta-\varepsilon_i)^2 - \beta_i(\tau-\gamma_i)^2} \\
\alpha_{\delta}^r &= \sum_{i=1}^7 n_i d_i \delta^{d_i-1} \tau^{t_i} + \sum_{i=8}^{23} n_i e^{-\delta^{c_i}} [\delta^{d_i-1} \tau^{t_i} (d_i - c_i \delta^{c_i})] + \sum_{i=24}^{25} n_i \delta^{d_i} \tau^{t_i} e^{-\eta_i(\delta-\varepsilon_i)^2 - \beta_i(\tau-\gamma_i)^2} \left[\frac{d_i}{\delta} - 2\eta_i(\delta-\varepsilon_i) \right] \\
\alpha_{\delta\delta}^r &= \sum_{i=1}^7 n_i d_i (d_i - 1) \delta^{d_i-2} \tau^{t_i} + \sum_{i=8}^{23} n_i e^{-\delta^{c_i}} [\delta^{d_i-2} \tau^{t_i} ((d_i - c_i \delta^{c_i}) (d_i - 1 - c_i \delta^{c_i}) - c_i^2 \delta^{c_i})] + \sum_{i=24}^{25} n_i \tau^{t_i} e^{-\eta_i(\delta-\varepsilon_i)^2 - \beta_i(\tau-\gamma_i)^2} \\
&\quad \cdot [-2\eta_i \delta^{d_i} + 4\eta_i^2 \delta^{d_i} (\delta-\varepsilon_i)^2 - 4d_i \eta_i \delta^{d_i-1} (\delta-\varepsilon_i) + d_i (d_i - 1) \delta^{d_i-2}] \\
\alpha_{\tau}^r &= \sum_{i=1}^7 n_i t_i \delta^{d_i} \tau^{t_i-1} + \sum_{i=8}^{23} n_i t_i \delta^{d_i} \tau^{t_i-1} e^{-\delta^{c_i}} + \sum_{i=24}^{25} n_i \delta^{d_i} \tau^{t_i} e^{-\eta_i(\delta-\varepsilon_i)^2 - \beta_i(\tau-\gamma_i)^2} \left[\frac{t_i}{\tau} - 2\beta_i(\tau-\gamma_i) \right] \\
\alpha_{\tau\tau}^r &= \sum_{i=1}^7 n_i t_i (t_i - 1) \delta^{d_i} \tau^{t_i-2} + \sum_{i=8}^{23} n_i t_i (t_i - 1) \delta^{d_i} \tau^{t_i-2} e^{-\delta^{c_i}} + \sum_{i=24}^{25} n_i \delta^{d_i} \tau^{t_i} e^{-\eta_i(\delta-\varepsilon_i)^2 - \beta_i(\tau-\gamma_i)^2} \left[\left(\frac{t_i}{\tau} - 2\beta_i(\tau-\gamma_i) \right)^2 - \frac{t_i}{\tau^2} - 2\beta_i \right] \\
\alpha_{\delta\tau}^r &= \sum_{i=1}^7 n_i d_i t_i \delta^{d_i-1} \tau^{t_i-1} + \sum_{i=8}^{23} n_i t_i \delta^{d_i-1} \tau^{t_i-1} (d_i - c_i \delta^{c_i}) e^{-\delta^{c_i}} + \sum_{i=24}^{25} n_i \delta^{d_i} \tau^{t_i} e^{-\eta_i(\delta-\varepsilon_i)^2 - \beta_i(\tau-\gamma_i)^2} \left[\frac{d_i}{\delta} - 2\eta_i(\delta-\varepsilon_i) \right] \left[\frac{t_i}{\tau} - 2\beta_i(\tau-\gamma_i) \right]
\end{aligned}$$

^a $\alpha_{\delta}^r = [\partial \alpha^r / \partial \delta]_{\tau}$, $\alpha_{\delta\delta}^r = [\partial^2 \alpha^r / \partial \delta^2]_{\tau}$, $\alpha_{\tau}^r = [\partial \alpha^r / \partial \tau]_{\delta}$, $\alpha_{\tau\tau}^r = [\partial^2 \alpha^r / \partial \tau^2]_{\delta}$, $\alpha_{\delta\tau}^r = [\partial^2 \alpha^r / \partial \delta \partial \tau]$.

taneously and are valid for all substances considered in the optimization. The derivatives of the residual part α^r , needed for the property calculations, are presented in Table 40.

The new equations of state for *n*- and isobutane, Eq. (4.1) in combination with the formulations for α° , Eq. (4.6), and the formulations for α^r , Eq. (4.12), were constrained to the critical parameters given in Table 3, and to the first and second derivatives of pressure with respect to density being zero at the critical point.

The range of validity of the new equations of state for *n*-butane and isobutane [Eq. (4.1)] is based on the region from which reliable experimental data were used to develop the equation. Thus, the range of validity is defined by the following region in temperature and pressure:

134.895 K $\leq T \leq$ 575 K and $p \leq 69$ MPa for *n*-butane, and

113.730 K $\leq T \leq$ 575 K and $p \leq 35$ MPa for isobutane, with the lowest temperature corresponding to the triple-point temperature. Naturally, the melting line delimits the range of validity (see Sec. 2.3). In this range clear statements about the uncertainty of the equation of state can be made. The estimations for the uncertainties are given in Sec. 6.

The equation can also be used outside the range of validity, however, with greater uncertainties (see also Sec. 5.5).

The functional form for α^r developed in this work [Eq. (4.12)] has been optimized simultaneously for ethane, propane, *n*-butane, and isobutane. Thus, using the right set of coefficients and reducing parameters together with the appropriate equation for α° , Eq. (4.1) can be used to calculate properties of ethane and propane as well. We do not give the required coefficients and parameters for ethane here, because the comprehensive and highly accurate data available for this substance cannot be represented adequately using the relatively simple mathematical structure of Eq. (4.12). An indi-

vidually optimized reference equation of state for ethane that adequately describes even the most precise data sets has just been developed by ourselves (see Bücker and Wagner 2006). This equation should be used to calculate accurate property values for ethane. For propane, an accurate reference equation of state is being developed at the National Institute for Standards and Technology at present. Once this equation is published by Lemmon *et al.* (unpublished), it should be used as the exclusive source for accurate property data for propane. To bridge the time gap until then, we recommend using the simultaneously optimized equation for propane and therefore summarize the required coefficients and parameters in Sec. 9. Their values have been established considering highly accurate data for the thermal properties of propane (see Glos *et al.* 2004). Accordingly, the equation of state presented here yields a better representation of the thermodynamic properties than it has been possible until now. However, we want to emphasize that this equation will be superseded by the upcoming equation of state individually optimized for propane.

5. Comparison of the Simultaneously Optimized Equations of State with Experimental Data

This section gives a discussion of the quality of the new equations of state for *n*- and isobutane. The comparisons with selected experimental data are shown separately for each substance. At the end of this section, the extrapolation behavior of the new formulations is briefly illustrated. Most figures also show calculated values from the equations of state published by Miyamoto and Watanabe (2001, 2002) and by Younglove and Ely (1987). These equations will also be referred to as the Miyamoto equations and the Younglove equations. The equations of Younglove and Ely (1987) have

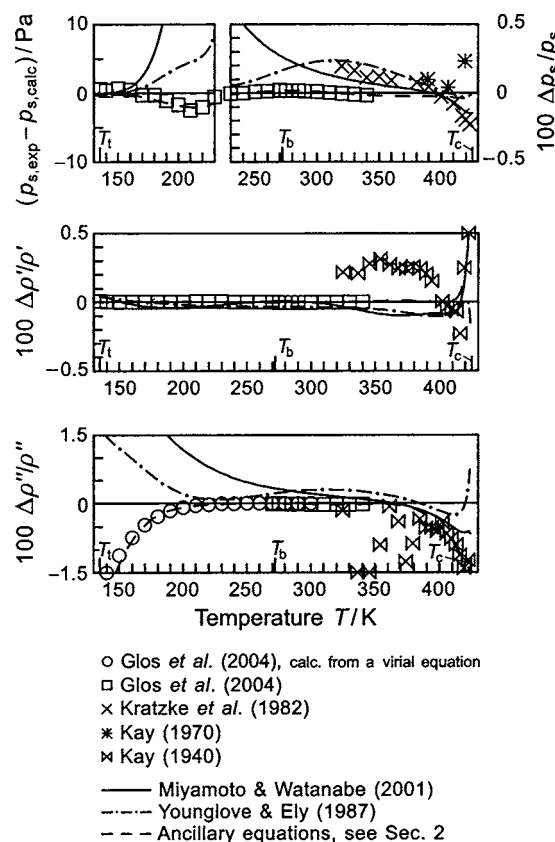


FIG. 11. Absolute deviations and percentage deviations [$100\Delta y/y = 100(y_{\text{exp}} - y_{\text{calc}})/y_{\text{exp}}$ with $y = p_s, \rho', \rho''$] of the selected thermal data for *n*-butane at saturation from values calculated from the equation of state, Eq. (4.1). Values calculated from the ancillary equations, Eqs. (2.2)–(2.4), and from the equations of state of Miyamoto and Watanabe (2001) and of Younglove and Ely (1987) are plotted for comparison.

been commonly accepted as a reference for the thermodynamic properties of *n*- and isobutane. Since they are based on the International Practical Temperature Scale of 1968 (IPTS-68), temperature values were converted to the IPTS-68 scale before values were calculated from these equations (see also Sec. 1.3).

5.1. The Vapor–Liquid Phase Boundary of *n*-Butane

5.1.1. Thermal Properties

The thermal properties of *n*-butane have been measured to a satisfactory accuracy only at temperatures up to 340 K. Comparisons between selected experimental results and values calculated from Eq. (4.1) are given in Fig. 11 for the vapor pressure and the saturated-liquid and saturated-vapor densities. The inconsistencies between the different data sets at temperatures above 340 K are well recognizable. Values calculated from the equations of state of Miyamoto and Watanabe (2001), of Younglove and Ely (1987), and from the ancillary equations given in Sec. 2 [Eqs. (2.2)–(2.4)] are shown for comparison.

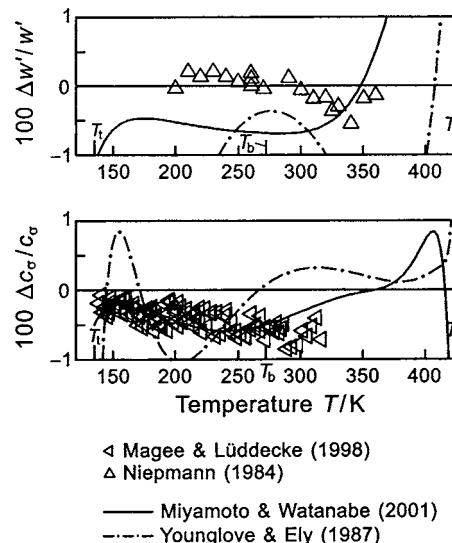


FIG. 12. Percentage deviations [$100\Delta y/y = 100(y_{\text{exp}} - y_{\text{calc}})/y_{\text{exp}}$ with $y = w', c_\sigma$] of data for the speed of sound in saturated-liquid *n*-butane and for the heat capacity along the saturated-liquid line of *n*-butane from values calculated from the equation of state, Eq. (4.1). Values calculated from the equations of state of Miyamoto and Watanabe (2001) and of Younglove and Ely (1987) are plotted for comparison.

The upper diagram, showing the representation of vapor-pressure data, is divided in two parts. At temperatures below 220 K absolute deviations are shown instead of the percentage deviations which are given in the other diagrams. Due to the small values of the vapor pressure at these low temperatures, absolute deviations are more significant than the divergent percentage deviations. The highly accurate data measured by Glos *et al.* (2004) are reproduced with maximum deviations of less than $(0.02\% + 5 \text{ Pa})$ and thus within the expected experimental uncertainties.

The Miyamoto equation cannot reproduce these data adequately. The deviations clearly exceed the uncertainties and increase to more than $+0.5\%$ at 240 K. This disagreement arises from the different data used to establish the equations. Miyamoto and Watanabe (2001) used unpublished data measured at the National Institute for Standards and Technology which are consistent with the heat capacity values measured by Magee and Lüddecke (1998) but apparently disagree with the data reported by Glos *et al.* (2004). We also assume these differences to be the reason for the differences in the representation of the isochoric heat capacity and the heat capacity along the saturated-liquid line (see Secs. 5.2.3 and 5.1.2, respectively). Similarly, the equation of state of Younglove and Ely (1987) does not represent the reference data of Glos *et al.* (2004) appropriately. The maximum deviations of the calculated vapor pressures however remain within 0.25% .

All considered equations of state are able to represent the saturated-liquid densities measured by Glos *et al.* (2004) with maximum deviations of less than 0.05% . Only Eq. (4.1), however, reproduces these values within 0.008% , which is certainly within their experimental uncertainties. The few reference data for the saturated-vapor density of *n*-butane are reproduced within 0.028% by the new equation

of state. Saturated-vapor densities calculated from either the Miyamoto or the Younglove equation deviate by up to 0.3% from the densities measured by Glos *et al.* (2004). The great relative deviations between the values calculated from a virial equation by Glos *et al.* (2004), and values calculated from the other equations of state are due to the small values of the saturated-vapor densities at low temperatures.

A reliable assessment of the quality of the different equations above 340 K is restricted by the poor quality of the available data. Data on this part of the phase boundaries were assigned only minor weights in the development of the new equation of state. The ancillary equations give a slightly better representation of the experimental data on the phase boundary than the new equation of state. However, if thermodynamically consistent values for all properties on the phase boundary are desired, data should be calculated from Eq. (4.1).

5.1.2. Caloric Properties

Figure 12 gives comparisons between selected experimental data for caloric properties of saturated-liquid *n*-butane and values calculated from Eq. (4.1). The upper diagram shows speeds of sound measured by Niepmann (1984). With the exception of one datum, the new fundamental equation of state represents all values within 0.4% in the speed of sound. At temperatures from 200 to 300 K, values calculated from the Miyamoto equation are systematically lower than the measured speeds of sound, with an almost constant deviation of -0.7% . The Younglove equation yields values that are up to 2.5% lower than the experimental results.

The lower diagram in Fig. 12 shows deviations between data for the heat capacity along the saturated-liquid line measured by Magee and Lüddecke (1998) and values calculated from Eq. (4.1). The experimental data are systematically lower than the values calculated from the new equation of state, with an average deviation of approximately -0.4% in heat capacity. Although the data additionally exhibit an inherent scatter of roughly 0.2%–0.3%, 95 out of the 100 reported data are reproduced within the experimental uncertainties which are reported to be 0.7%. The Miyamoto equation yields a good representation of these data at temperatures from 140 to 290 K, reproducing the heat capacities within their scatter. At higher temperatures, the measured values are systematically lower than values calculated from the Miyamoto equation, with differences up to -0.7% . The equation of Younglove and Ely (1987) is not as able to reproduce the data appropriately.

The experimental results of Magee and Lüddecke (1998) are apparently not consistent with values of the vapor pressure measured by Glos *et al.* (2004). To obtain preliminary equations that were able to reproduce the heat capacities along the saturated-liquid line reported by Magee and Lüddecke (1998) within their scatter, we had to assign them disproportionate weights. Equations of state developed in this way exhibited significant systematic errors with regard to the representation of vapor pressures and the $p\rho T$ data measured

by Glos *et al.* (2004). The representation of the speeds of sound measured by Niepmann (1984) deteriorated also, but the resulting deviations appeared to be less systematic. We consider the results of Glos *et al.* (2004) to be most reliable. While calorimetric measurements generally are very susceptible to systematic perturbations, the measurements of thermal properties on the phase boundary and in the single-phase region using the two-sinker method have proven to yield reference quality results free of considerable systematic errors for many years. Nevertheless, we appreciate that the measurements of Magee and Lüddecke (1998) contribute very important information on the caloric properties of *n*-butane.

5.2. The Single-Phase Region of *n*-Butane

5.2.1. $p\rho T$ Data

The results of the measurements performed by Glos *et al.* (2004) describe the thermal properties of *n*-butane at temperatures from 95 to 340 K and pressures up to 12 MPa with the highest accuracy attainable to date. Figure 13 shows the representation of the new $p\rho T$ data by Eq. (4.1). Except for two data at 340 K, all data are represented with maximum deviations of less than 0.01% and thus clearly within the small experimental uncertainties. The comparisons point out the high performance of Eq. (4.1) in this important fluid region. Densities calculated from the equations of state of Miyamoto and Watanabe (2001) and Younglove and Ely (1987) show appreciably different plots in some regions. However, the deviations from the measured densities are generally less than 0.05%.

Outside of the range of the data covered by the measurements of Glos *et al.* (2004), the data situation is inhomogeneous. Figure 14 gives comparisons between selected data at pressures up to 4 MPa and values calculated from Eq. (4.1). In this region, reliable data are available that mutually agree to within 0.4% in density. The performance of the different equations regarding the representation of these data is very similar. The data of Gupta and Eubank (1997) which are marked “not corrected” in the figures are results from the first measuring run and were not corrected for adsorption effects (see Sec. 3.1.1). Their quality is obviously inferior to the corrected results of the second measuring run. However, since they were obtained independently, they were included in the development of the new equation of state where no other reliable data were available. Uncorrected data at pressures below 0.1 MPa were not used, since they are clearly inconsistent with the other data sets. A better representation of the data between 0.5 and 2 MPa would have been possible only by assigning them unreasonable weights. All preliminary equations that were fitted to such data sets revealed significant weaknesses in the remaining regions.

Comparisons of the new equation of state with $p\rho T$ data at higher pressures are given in Fig. 15. Note the different scales used for the percentage deviations in the diagrams for temperatures below and above 400 K. The systematic errors inherent in the data reported by Haynes (1983a) and the poor

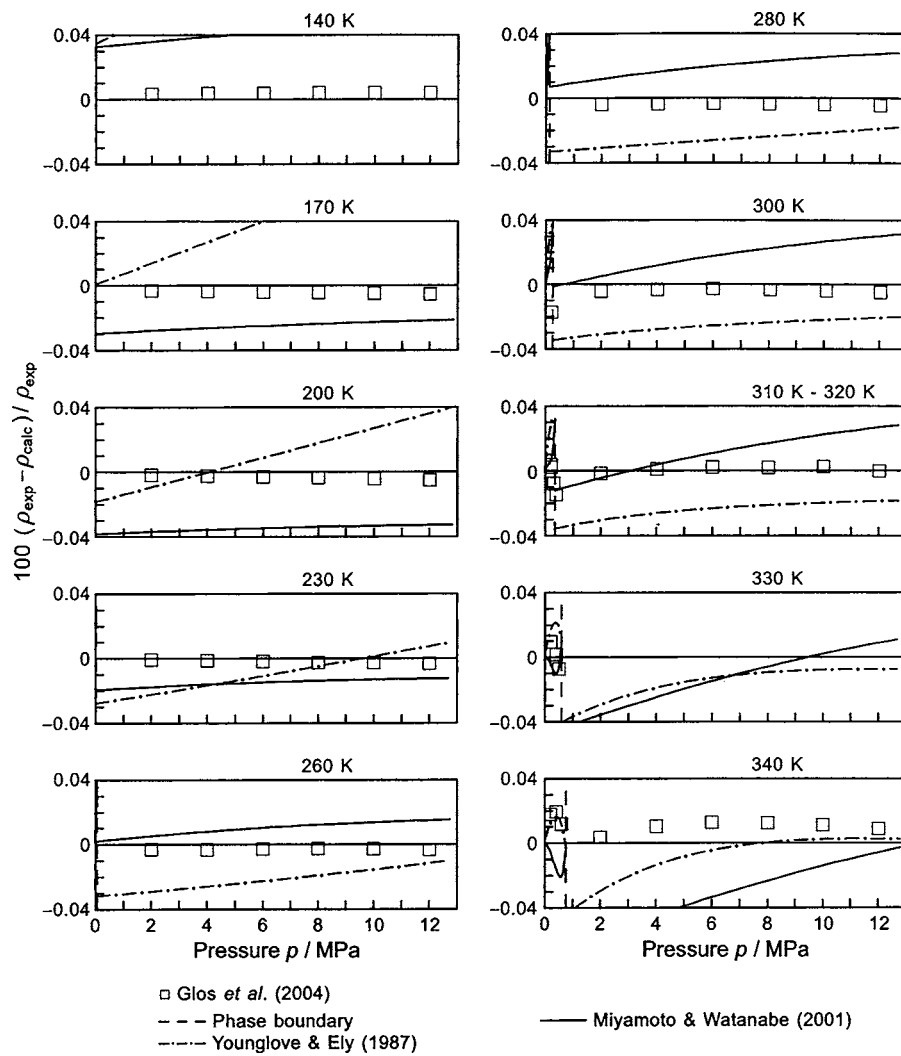


FIG. 13. Percentage density deviations of highly accurate $p\rho T$ data for *n*-butane from values calculated from the equation of state, Eq. (4.1). Values calculated from the equations of state of Miyamoto and Watanabe (2001) and of Younglove and Ely (1987) are plotted for comparison.

quality of the measurements performed by Kiran and Sen (1992) have been discussed in Sec. 3.1.1. The diagram displaying temperatures from 230 to 240 K reveals the small but systematic misalignment between the data of Golovskii *et al.* (1978a) and the data of Glos *et al.* (2004). At temperatures below approximately 400 K, the different data sets classified as reliable mutually agree at least within 0.4% in density and are reproduced accordingly by Eq. (4.1) and by the Miyamoto equation. The equation of state of Younglove and Ely (1987) follows the data reported by Haynes (1983a) and therefore cannot reproduce all data within the estimated experimental uncertainties. The diagrams on the right hand side of Fig. 15 show temperatures above 400 K. In this region, the inconsistencies between the different data sets become very large so that the performance of the equations cannot be verified properly. All data are reproduced within their mutual consistency. With the exception of the data reported by Beattie *et al.* (1939a) on the 423 K isotherm, this consistency is better than 1.5% in density, generally much better.

The new equation of state reproduces the data measured by Beattie *et al.* (1939b) in the critical region with an average absolute deviation of 0.012% in pressure. Figure 16

shows comparisons of the measured pressures on a near-critical isotherm with values calculated from Eq. (4.1). The offset of the values calculated from the Miyamoto equation is due to the different choice of critical parameters.

5.2.2. Virial Coefficients

No data for the second or third virial coefficients of *n*-butane were used in the development of the new fundamental equation of state. Nevertheless, Eq. (4.1) yields reasonable plots of these properties. Figure 17 shows absolute values of selected data for the second virial coefficient B . Additionally, values calculated from the new equation of state, from the Miyamoto equation, and from the Younglove equation are plotted as lines. All equations yield very similar plots of the second virial coefficient over the entire temperature range.

The corresponding diagram for the third virial coefficient C is shown in Fig. 18. Again, the values calculated from Eq. (4.1) show a thermodynamically correct plot, yielding the expected maximum and the succeeding sharp decrease towards low temperatures. Compared to the data obtained from

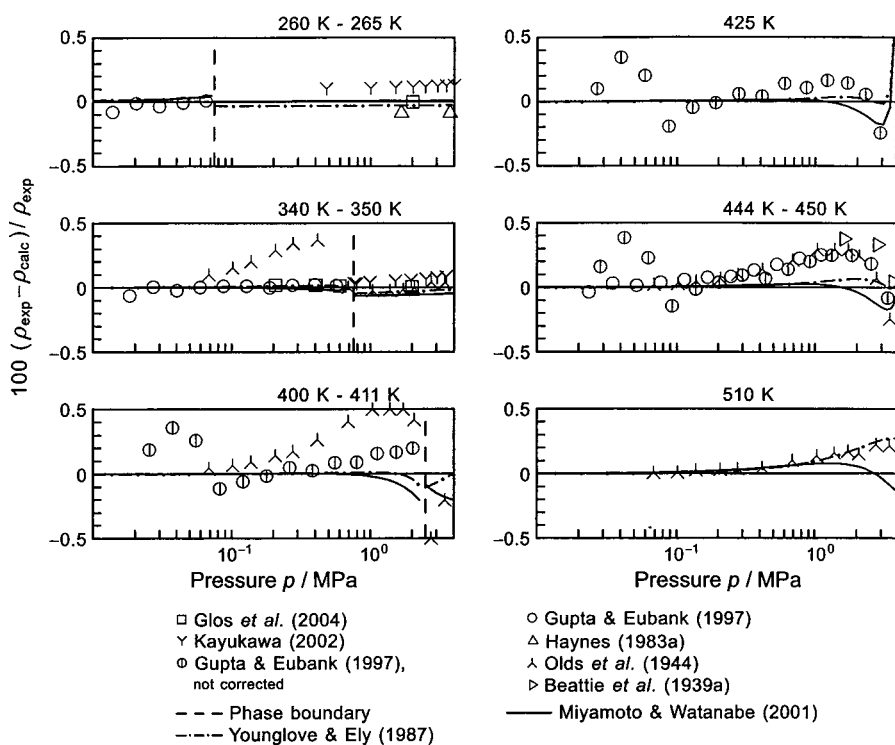


FIG. 14. Percentage density deviations of $p\rho T$ data for *n*-butane assigned to groups 1 and 2 at pressures up to 4 MPa from values calculated from the equation of state, Eq. (4.1). Values calculated from the equations of state of Miyamoto and Watanabe (2001) and of Younglove and Ely (1987) are plotted for comparison.

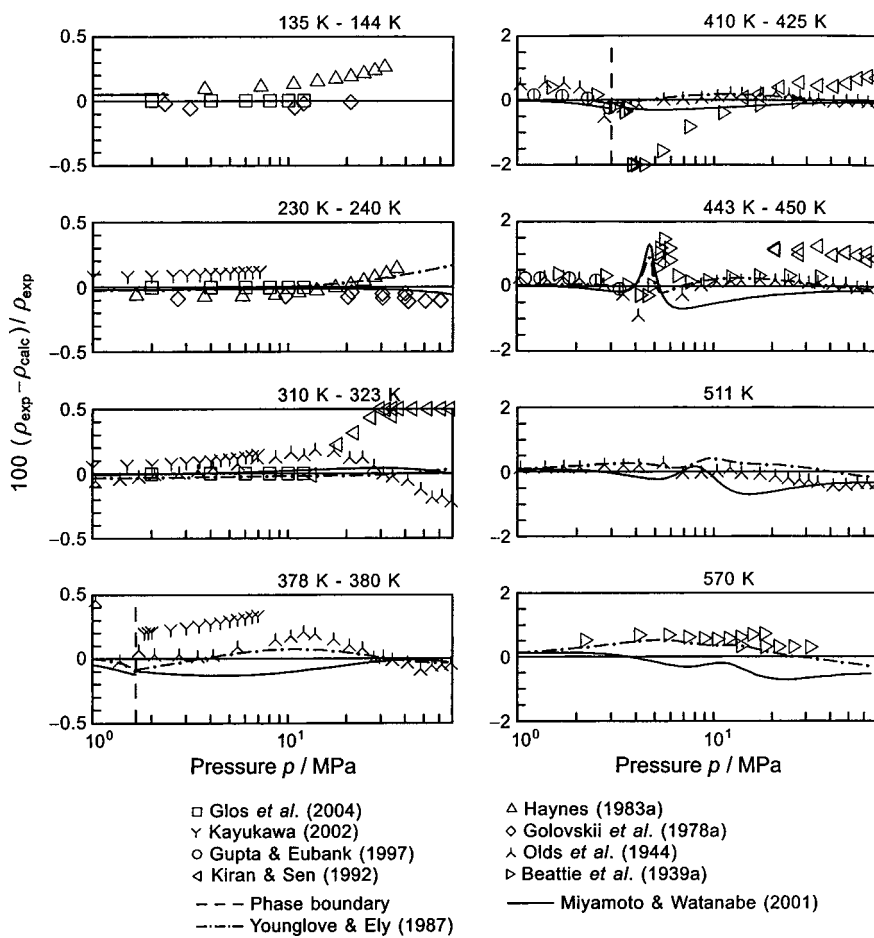


FIG. 15. Percentage density deviations of $p\rho T$ data for *n*-butane assigned to groups 1 and 2 from values calculated from the equation of state, Eq. (4.1). Values calculated from the equations of state of Miyamoto and Watanabe (2001) and of Younglove and Ely (1987) are plotted for comparison.

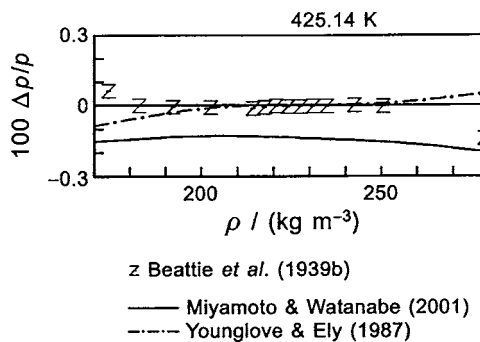


FIG. 16. Percentage pressure deviations $100\Delta p/p = 100(p_{\text{exp}} - p_{\text{calc}})/p_{\text{exp}}$ of $p\rho T$ data for *n*-butane on a near-critical isotherm from values calculated from the equation of state, Eq. (4.1). Values calculated from the equations of state of Miyamoto and Watanabe (2001) and of Younglove and Ely (1987) are plotted for comparison.

measurements, the absolute maximum of the third virial coefficient calculated from Eq. (4.1) is slightly smaller. The equation of Younglove and Ely (1987) yields a maximum at somewhat lower temperature than predicted by the literature data, while the equation of Miyamoto and Watanabe (2001) does not produce a maximum within the expected temperature range at all.

5.2.3. Isochoric Heat Capacity

Percentage deviations of the data for the isochoric heat capacity measured by Magee and Lüdecke (1998) from values calculated with Eq. (4.1) are illustrated in Fig. 19. As we discussed in Sec. 5.1.2 for the heat capacities along the saturated liquid line, the data are apparently not consistent with data for the thermal properties of *n*-butane measured by Glos *et al.* (2004). The deviations are less than the reported experimental uncertainties of 0.7% in c_v for the vast majority

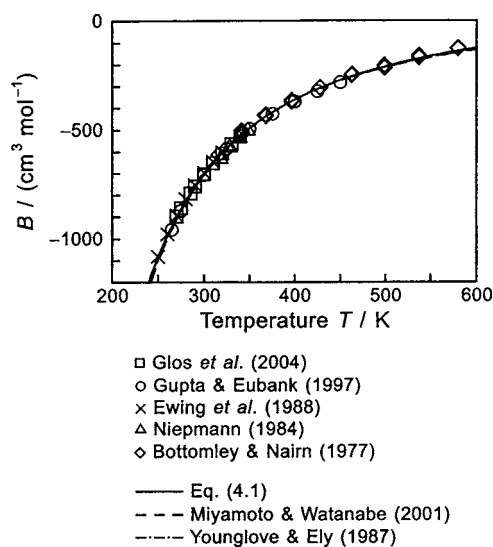


FIG. 17. Representation of data for the second virial coefficient of *n*-butane at temperatures up to 600 K. The plotted lines correspond to values calculated from the equation of state, Eq. (4.1), and from the equations of state of Miyamoto and Watanabe (2001) and of Younglove and Ely (1987).

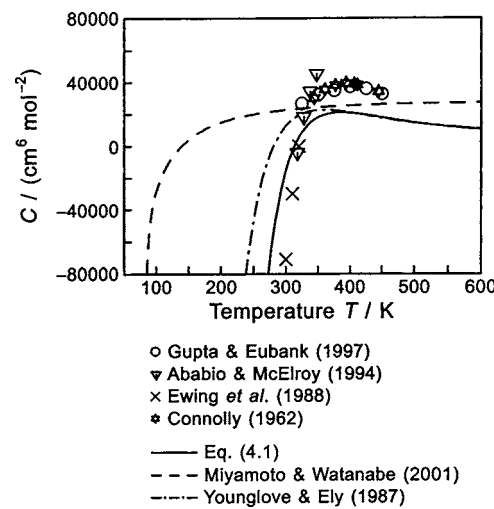


FIG. 18. Representation of data for the third virial coefficient of *n*-butane at temperatures up to 600 K. The plotted lines correspond to values calculated from the equation of state, Eq. (4.1), and from the equations of state of Miyamoto and Watanabe (2001) and of Younglove and Ely (1987).

of the data. Systematic deviations exceeding these uncertainties can be observed only at the lowest investigated densities below 580 kg m^{-3} . The clear scatter actually seems to indicate higher experimental uncertainties.

Miyamoto and Watanabe (2001) developed their equation using not only the isochoric heat capacities reported by Magee and Lüdecke (1998), but also unpublished data for the vapor pressure of *n*-butane which are consistent with the caloric property values. The highly accurate vapor pressures measured by Glos *et al.* (2004) were not yet available. Nevertheless, the Miyamoto equation can only reproduce the experimental heat capacities with systematic deviations comparable to the results of the new equation of state. The values calculated at higher densities deviate appreciably from the experimental data, while the representation improves towards lower densities. When the equation of state of Younglove and Ely (1987) was published, no reliable data for the isochoric heat capacity were available. Accordingly, the results from the equation differ greatly from the measured values.

5.2.4. Isobaric Heat Capacity

The only experimental data included in the development of Eq. (4.1) are values measured by Dailey and Felsing (1943). Comparisons of these data with values calculated from the new equation of state are shown in Fig. 20. All considered equations of state reproduce the data clearly within their experimental uncertainties, which basically indicates the consistency of the ideal-gas parts used in the different equations.

5.2.5. Speed of Sound

The speeds of sound measured by Niepmann (1984), in combination with the heat capacity data reported by Magee and Lüdecke (1998), are the most important source of in-

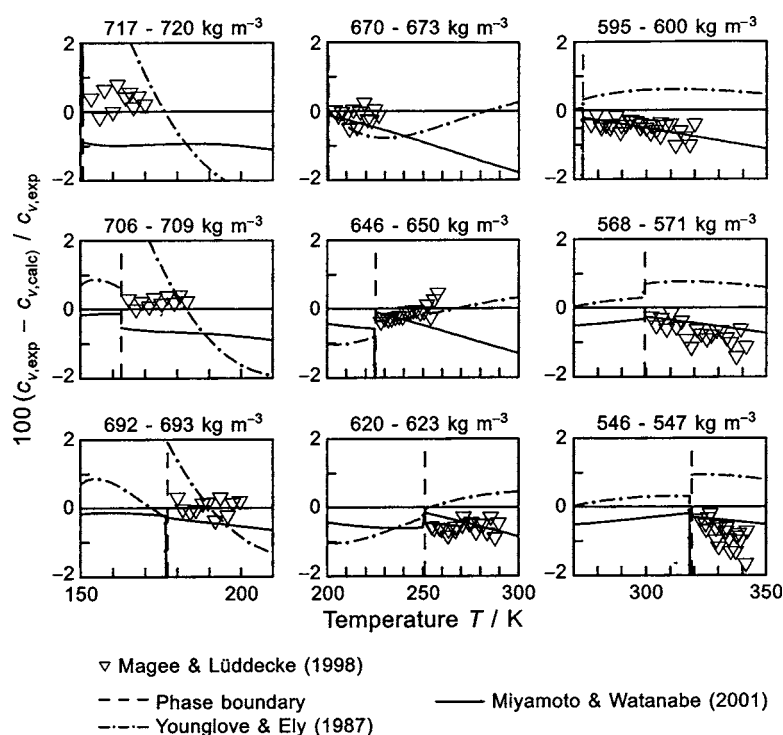


FIG. 19. Percentage deviations of isochoric heat capacity data for *n*-butane measured by Magee and Lüddecke (1998) from values calculated from the equation of state, Eq. (4.1). Values calculated from the equations of state of Miyamoto and Watanabe (2001) and of Younglove and Ely (1987) are plotted for comparison.

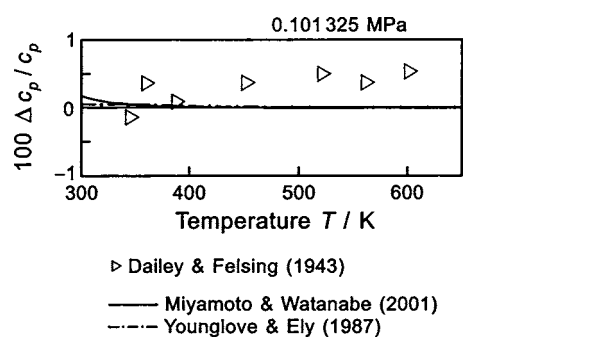


FIG. 20. Percentage deviations $\Delta c_p / c_p = (c_{p,\text{exp}} - c_{p,\text{calc}}) / c_{p,\text{exp}}$ of isobaric heat capacity data for *n*-butane from values calculated from the equation of state, Eq. (4.1). Values calculated from the equations of state of Miyamoto and Watanabe (2001) and of Younglove and Ely (1987) are plotted for comparison.

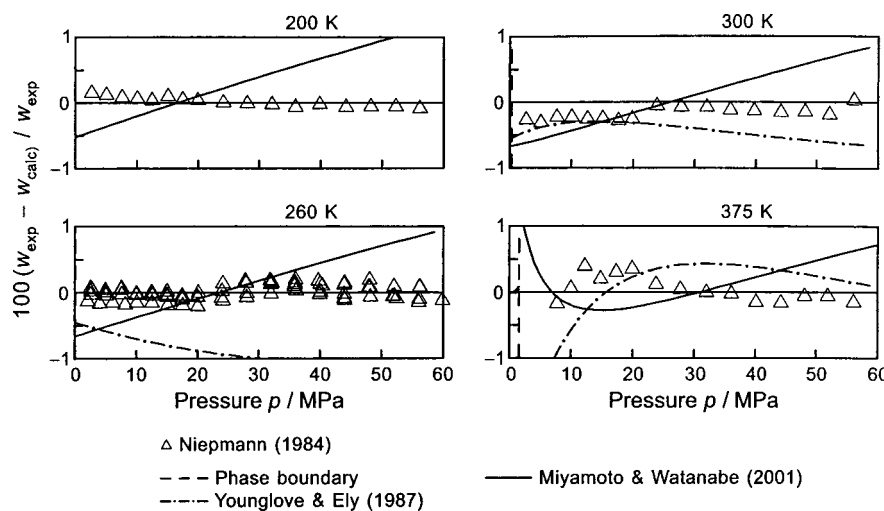


FIG. 21. Percentage deviations of speed of sound data for *n*-butane in the liquid and supercritical region from values calculated from the equation of state, Eq. (4.1). Values calculated from the equations of state of Miyamoto and Watanabe (2001) and of Younglove and Ely (1987) are plotted for comparison.

formation on the caloric properties of liquid *n*-butane available. Figure 21 illustrates the representation of the measured speeds of sound by the different equations of state on four typical isotherms. Only Eq. (4.1) reproduces all the data within the experimental uncertainties, while neither the Miyamoto equation nor the Younglove equation can follow the run of the data. Maximum deviations between values calculated from the Miyamoto equation and the experimental results rarely exceed 1% at the speed of sound, while similar deviations for the Younglove equation reach up to 3% at lower temperatures.

As described in Sec. 3.1.5, the values of the speed of sound obtained by Ewing *et al.* (1988) were corrected to attain consistency with the ideal-gas part α° used in this work. Comparisons between these corrected values and the new

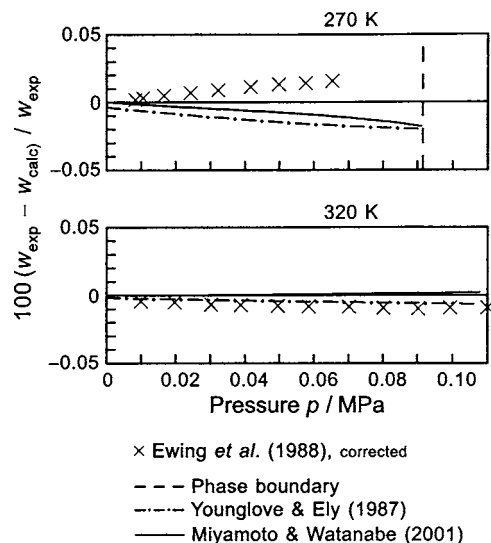


FIG. 22. Percentage deviations of speed of sound data for *n*-butane in the gaseous region from values calculated from the equation of state, Eq. (4.1). Values calculated from the equations of state of Miyamoto and Watanabe (2001) and of Younglove and Ely (1987) are plotted for comparison.

fundamental equation are given in Fig. 22. The diagrams show typical isotherms and document the good representation of the corrected values by all of the considered equations of state.

5.3. The Vapor–Liquid Phase Boundary of Isobutane

5.3.1. Thermal Properties

The phase boundary of isobutane is only partially described by experimental results. Only the vapor pressure has been investigated experimentally over the entire temperature range. We therefore utilized data calculated from a scaled fundamental equation by Levelt Sengers *et al.* (1983) for the saturated-vapor and saturated-liquid densities in the critical region of isobutane to complement the data base, similar to the development of the ancillary equations (see Secs. 2.5 and 2.6). Deviations of selected data of the thermal properties on the phase boundary from values calculated with Eq. (4.1) are shown in Fig. 23. As in the corresponding figure for *n*-butane (see Sec. 5.1.1) the diagram for the vapor pressure has been divided into two parts, with absolute deviations for temperatures below 200 K, and percentage deviations for higher temperatures. The reason for this subdivision is again the very small absolute values of this property at low temperatures.

Equation (4.1) reproduces the highly accurate vapor pressures measured by Glos *et al.* (2004) with maximum deviations of less than ($0.01\% + 3 \text{ Pa}$) which is clearly within the expected experimental uncertainties. The values reported by Waxman and Gallagher (1983)—the only reliable data available at temperatures above 340 K—are also reproduced within their uncertainties, especially in view of the deviations between these data and the values reported by Glos *et al.* (2004).

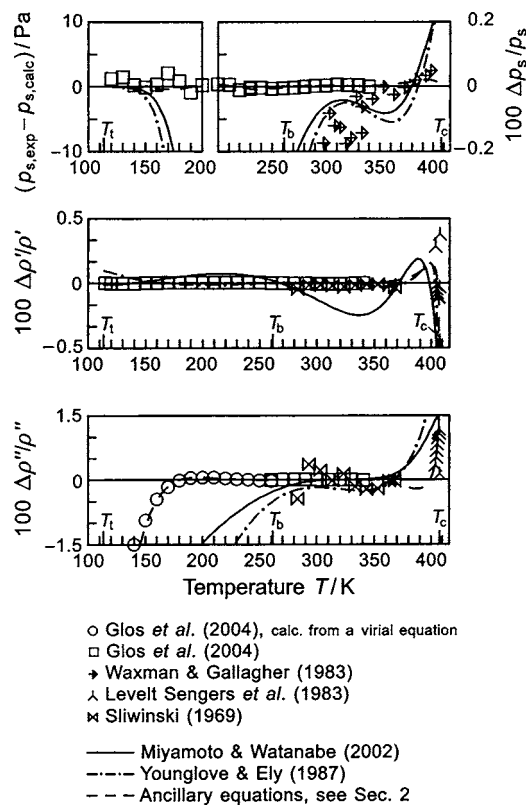


FIG. 23. Absolute deviations and percentage deviations [$100\Delta y/y = 100(y_{\text{exp}} - y_{\text{calc}})/y_{\text{exp}}$ with $y = p_s, \rho', \rho''$] of the selected thermal data for isobutane at saturation from values calculated from the equation of state, Eq. (4.1). Values calculated from the ancillary equations, Eqs. (2.2)–(2.4), and from the equations of state of Miyamoto and Watanabe (2002) and of Younglove and Ely (1987) are plotted for comparison.

Neither the equation of state of Miyamoto and Watanabe (2002) nor the one of Younglove and Ely (1987) is able to reproduce the new experimental results adequately. The measured values are systematically higher than the calculated vapor pressures, with maximum deviations of approximately 1.5% for the Miyamoto equation and up to 3% for the Younglove equation, considering only data at temperatures above 200 K.

The saturated-liquid densities reported by Glos *et al.* (2003) are reproduced within 0.01% by the new equation of state. Densities measured by Sliwinski (1969) are slightly lower than the high-accuracy data and are represented adequately by the new equation of state. The values calculated from the scaled equation of state of Levelt Sengers *et al.* (1983) agree with the corresponding values calculated from Eq. (4.1) within 0.5%, but they can only give a rough estimate of the shape of the phase equilibrium curve and may not be used for a reliable assessment of the performance of other empirical equations of state.

The deviations between the highly accurate saturated-liquid densities measured by Glos *et al.* (2004) and values calculated from the Younglove equation remain within 0.02% over a large temperature range. Only at temperatures below 150 K are the calculated values too high. The equation of state of Miyamoto and Watanabe (2002), however, does

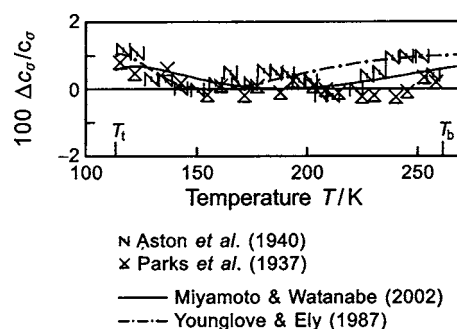


FIG. 24. Percentage deviations $100\Delta c_\sigma/c_\sigma = 100(c_{\sigma,\text{exp}} - c_{\sigma,\text{calc}})/c_{\sigma,\text{exp}}$ of data for the heat capacity along the saturated-liquid line of isobutane from values calculated from the equation of state, Eq. (4.1). Values calculated from the equations of state of Miyamoto and Watanabe (2002) and of Younglove and Ely (1987) are plotted for comparison.

not yield a satisfying representation of the experimental data. The calculated values oscillate around the measured densities, with maximum deviations of 0.3%. We can see no reason for this poor performance, since Miyamoto and Watanabe (2002) used reliable data for the saturated-liquid densities.

The poor data situation for the saturated-vapor density of isobutane is appreciable in Fig. 23. The experimental data of Glos *et al.* (2004) and Sliwinski (1969) are reproduced by Eq. (4.1) with maximum deviations of 0.004% and 0.5%, respectively, which is well within the experimental uncertainties. The data calculated from a virial equation of state agree with the corresponding results from Eq. (4.1) within 0.7 g m^{-3} , and the maximum difference between the values calculated from the scaled equation of state of Levelt Sengers *et al.* (1983) and from Eq. (4.1) is +1.2%. The Miyamoto equation and the Younglove equation both reproduce the data reported by Sliwinski (1969) appropriately, but neither of them is able to represent the data measured by Glos *et al.* (2004) within their small experimental uncertainties.

5.3.2. Caloric Properties

The heat capacities along the saturated liquid line reported by Aston *et al.* (1940) and Parks *et al.* (1937) are the only fairly reasonable data for caloric properties of saturated isobutane available, even though relatively large experimental uncertainties have to be attributed to these early measurements. As Fig. 24 illustrates, all of the considered equations of state adequately reproduce the experimental results.

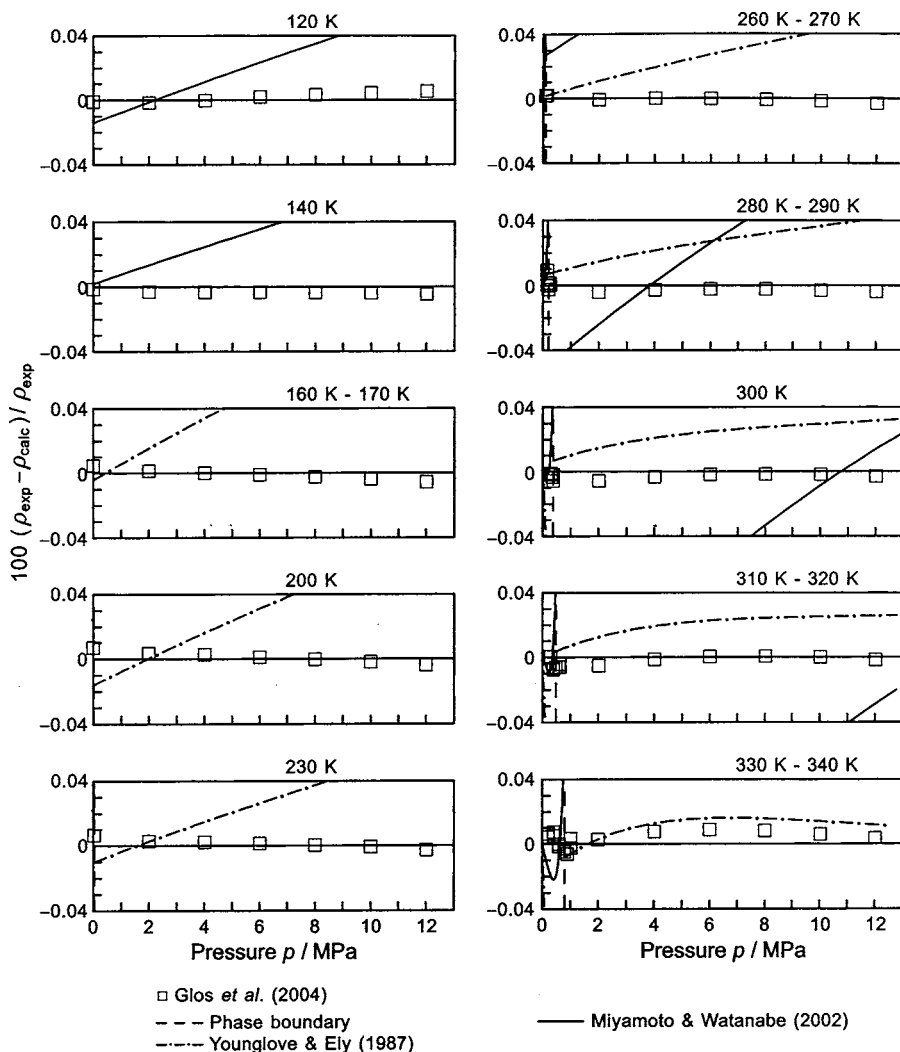


FIG. 25. Percentage density deviations of highly accurate $p\rho T$ data for isobutane from values calculated from the equation of state, Eq. (4.1). Values calculated from the equations of state of Miyamoto and Watanabe (2002) and of Younglove and Ely (1987) are plotted for comparison.

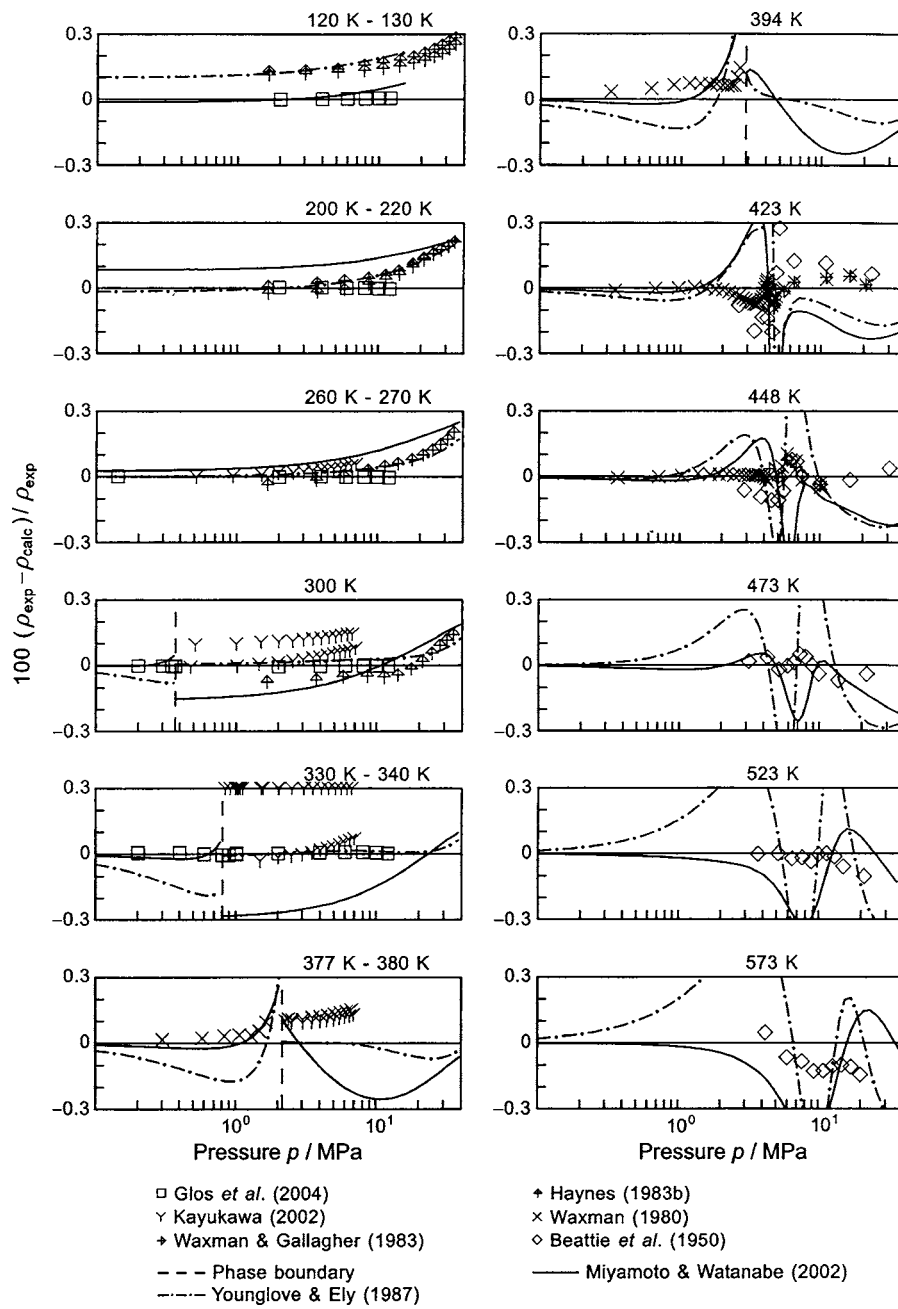


FIG. 26. Percentage density deviations of $p\rho T$ data for isobutane assigned to groups 1 and 2 from values calculated from the equation of state, Eq. (4.1). Values calculated from the equations of state of Miyamoto and Watanabe (2002) and of Younglove and Ely (1987) are plotted for comparison.

5.4. The Single-Phase Region of Isobutane

5.4.1. $p\rho T$ Data

Just as for *n*-butane, the results of the measurements performed by Glos *et al.* (2004) redefine the $p\rho T$ surface of isobutane at temperatures from 95 to 340 K and pressures up to 12 MPa with the highest achievable accuracy. Figure 25 shows the percentage density deviations of these data from values calculated with Eq. (4.1). All data are represented with maximum deviations of less than 0.01% which is well within the experimental uncertainties. Figure 25 illustrates the high performance of the new equation of state in the liquid and gaseous region.

The equations of state of Miyamoto and Watanabe (2002) and of Younglove and Ely (1987) cannot reproduce the experimental data properly. Values calculated from either of these equations differ from the measured densities by up to 0.3%. Although the main reason for these deviations may be the different data sets used in the development of the respective correlations, we could not reach satisfactory agreement with the data even by refitting the coefficients of the equations. This reveals the limitations of the functional forms of both equations of state, neither of which was optimized for isobutane.

Figure 26 shows comparisons of values calculated from Eq. (4.1) with experimental data that were assigned to groups 1 and 2 (see Tables 26 and 27). The $p\rho T$ data of Haynes

(1983b) deviate systematically from the highly accurate data of Glos *et al.* (2004), where the deviations clearly increase with increasing pressure. Therefore, only very small weights were assigned to these data in the development of the equation of state. Due to the simultaneous optimization, Eq. (4.1) is numerically very stable in this range of temperature and pressure and we do believe the values calculated from the new equation of state to be distinctly more reliable than the experimental values.

The results of the Burnett measurements performed by Waxman (1980) and Waxman and Gallagher (1983) are generally reproduced well within 0.1% in density. Only isolated values near the phase boundary are slightly outside this margin, but the actual uncertainties of the data are probably higher when approaching the saturation curve. The Miyamoto equation of state yields a good representation of these data only at the lowest investigated temperature, which is 377 K. At higher temperatures, the densities calculated from this equation systematically deviate to higher values when approaching the saturated-vapor line, with maximum deviations reaching more than 0.3% at subcritical temperatures. At supercritical states, the calculated densities oscillate around the experimental data showing even higher maximum deviations. Similarly, the equation of state of Younglove and Ely (1987) is not able to represent the measurements satisfactorily. The deviations of densities calculated from the Younglove equation exceed the uncertainties of the data over the entire temperature range.

The work of Beattie *et al.* (1950) is the only source of reliable experimental $p\rho T$ data at temperatures above 448 K. The data are represented with maximum deviations of less than 0.3% in density by Eq. (4.1). We abandoned an even better representation of these data due to the following reasons. On the one hand, we assume the data to be reproduced well within their experimental uncertainties, while on the other an overfitting of data at the edge of the fitting range can cause severe deficiencies in the extrapolation behavior of the correlation function. Neither the Miyamoto equation nor the Younglove equation achieves a similar representation of the data reported by Beattie *et al.* (1950). For both equations, the maximum differences between calculated and measured densities are beyond 0.4%.

In the critical region, pressures calculated from Eq. (4.1) agree with experimental results of Beattie *et al.* (1949) within 0.1%. Percentage pressure deviations of these data from values calculated from the new equation of state are shown in Fig. 27. The appreciable deviations of pressures calculated from the equations of state of Miyamoto and Watanabe (2002) and Younglove and Ely (1987) are due to the different choice of critical parameters. We adopted values reported by Levelt Sengers *et al.* (1983) while both the other equations were developed using values established by Goodwin and Haynes (1982).

5.4.2. Virial Coefficients

The values for the second virial coefficient that were obtained from speed of sound measurements by Ewing and

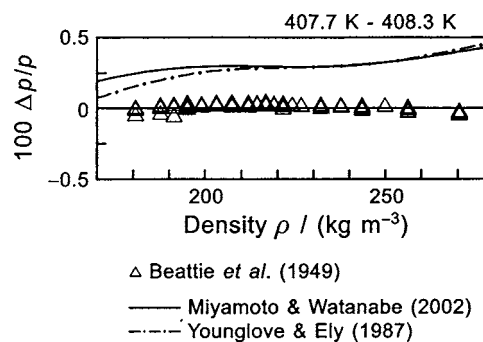


FIG. 27. Percentage pressure deviations $100\Delta p/p = 100(p_{\text{exp}} - p_{\text{calc}})/p_{\text{exp}}$ of $p\rho T$ data for isobutane on a near-critical isotherm from values calculated from the equation of state, Eq. (4.1). Values calculated from the equations of state of Miyamoto and Watanabe (2002) and of Younglove and Ely (1987) are plotted for comparison.

Goodwin (1991) are the only virial coefficient data that were used to establish Eq. (4.1). Figure 28 shows absolute values of the second virial coefficient that are available from the literature. Values calculated from Eq. (4.1), from the Miyamoto equation, and from the Younglove equation are plotted as lines. All considered equations of state yield reasonable plots of this property and agree well with the virial coefficients reported by Glos *et al.* (2004) and Ewing and Goodwin (1991).

Figure 29 shows the equivalent diagram for the third virial coefficient. The few available data clearly indicate a maximum value of the virial coefficient between 350 and 450 K which is reproduced only by Eq. (4.1). The plots of the third virial coefficients produced by the two other equations of state seem to be faulty and are not supported by the available data.

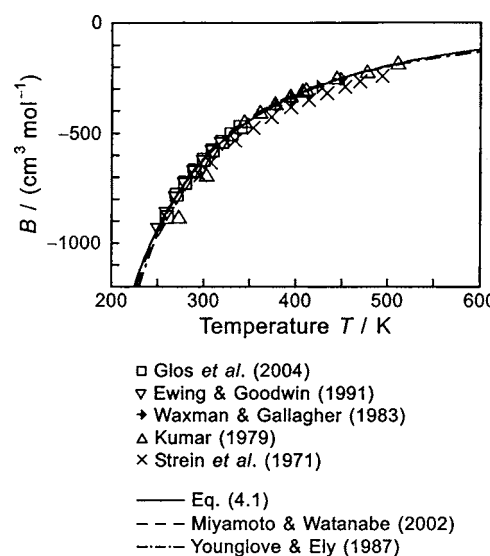


FIG. 28. Representation of data for the second virial coefficient of isobutane at temperatures up to 600 K. The plotted lines correspond to values calculated from the equation of state, Eq. (4.1), and from the equations of state of Miyamoto and Watanabe (2002) and of Younglove and Ely (1987).

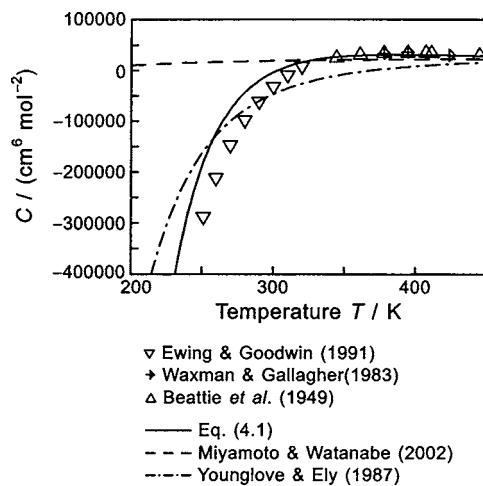
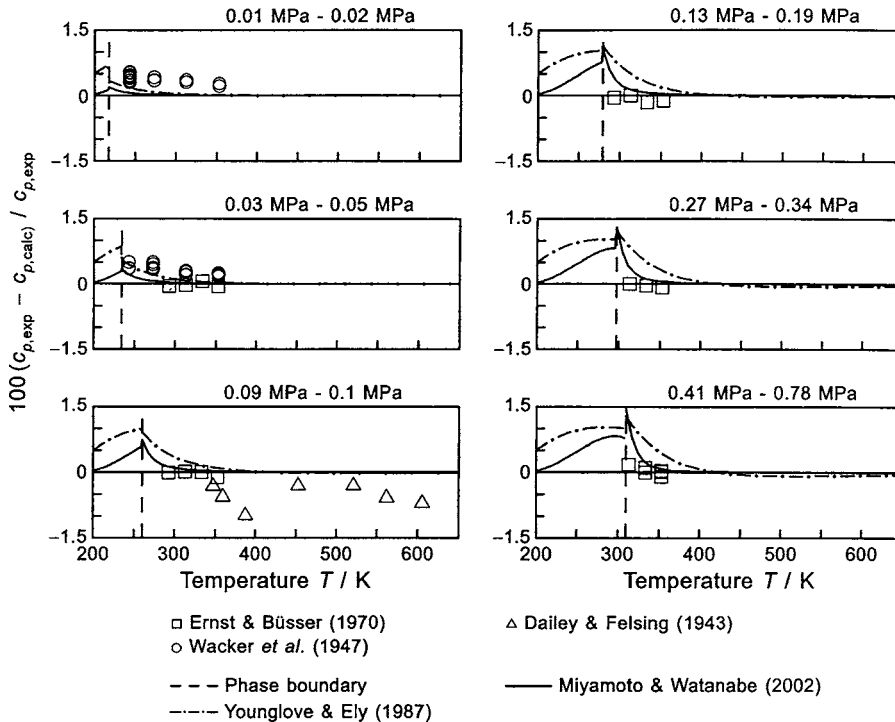


FIG. 29. Representation of data for the third virial coefficient of isobutane at temperatures up to 450 K. The plotted lines correspond to values calculated from the equation of state, Eq. (4.1), and from the equations of state of Miyamoto and Watanabe (2002) and of Younglove and Ely (1987).

5.4.3. Isobaric Heat Capacity

Comparisons between experimental data and values calculated from the new equation of state are shown for the isobaric heat capacity in Fig. 30. The heat capacities measured by Ernst and Büscher (1970), which are the most reliable values available, are represented with maximum deviations of less than 0.18% which is clearly within the experimental uncertainty. Maximum deviations are less than 0.6% for the heat capacities reported by Wacker *et al.* (1947) and less than



1% for the values reported by Dailey and Felsing (1943). For both data sets, the agreement is obviously within the experimental uncertainties.

The equations of Miyamoto and Watanabe (2002) and of Younglove and Ely (1987) can only reproduce the two older data sets within their experimental uncertainties. Both equations fail to adequately represent the data reported by Ernst and Büscher (1970). As Fig. 30 shows, the discrepancies between experimental data and calculated values increase in the vicinity of the phase boundary, which is a clear hint that the real-gas effects are not reproduced correctly.

5.4.4. Speed of Sound

The only available data for the speed of sound in the gaseous region of isobutane were measured at very low densities and are therefore basically useful to verify the ideal-gas part of the Helmholtz energy inherent in the equation of state (see also Sec. 3.1.4). Percentage deviations of the measured speeds of sound from values calculated with Eq. (4.1) are shown in Fig. 31. The new equation of state reproduces all data within very small allowances of less than 0.02%. Since the ideal-gas part α° , Eq. (4.6), was fitted to data for the ideal-gas isobaric heat capacity reported by Chen *et al.* (1975), the deviations that are visible in Fig. 31 correspond essentially to discrepancies between the two data sets. Since the influence of the real-gas behavior increases with pressure, an incorrect residual part α^r would lead to deviations that also increase with pressure. Therefore, the consistency of the offset between the experimental speeds of sound and the values calculated from Eq. (4.1) confirms the accuracy of the residual part. The equation of state of Miyamoto and

FIG. 30. Percentage deviations of isobaric heat capacity data for isobutane assigned to group 1 from values calculated from the equation of state, Eq. (4.1). Values calculated from the equations of state of Miyamoto and Watanabe (2002) and of Younglove and Ely (1987) are plotted for comparison.

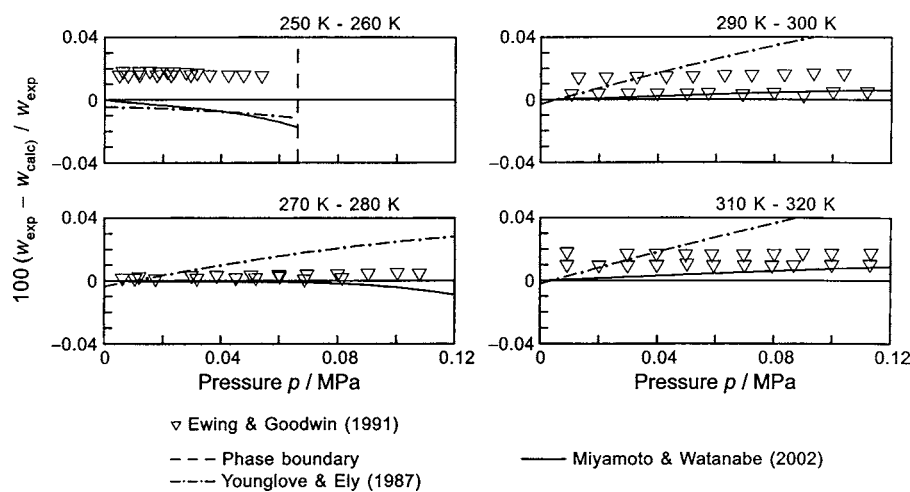


FIG. 31. Percentage deviations of speed of sound data for isobutane in the gaseous region from values calculated from the equation of state, Eq. (4.1). Values calculated from the equations of state of Miyamoto and Watanabe (2002) and of Younglove and Ely (1987) are plotted for comparison.

Watanabe (2002) also reproduces the data with reasonable constant deviations. Speeds of sound calculated from the Younglove equation, however, deviate increasingly from the experimental data and thus reveal more substantial incongruities.

5.5. Extrapolation Behavior

5.5.1. High Pressures and High Temperatures

No experimental data for the thermodynamic properties of *n*- and isobutane are available beyond 70 MPa and 700 K. In the simultaneous optimization, $p\rho T$ data for ethane were used that cover pressures up to 900 MPa. Outside these limits, no data were included in the development of the new equations of state. Figures 32 and 33 show $p-\rho$ diagrams for *n*- and isobutane at very high pressures, with some high-temperature isotherms calculated from the simultaneously

optimized equations of state, from the Miyamoto equations, and from the Younglove equations. Equation (4.1) yields reasonable plots of the isotherms over the entire range of parameters. The isotherms calculated from the equations of state of Miyamoto and Watanabe (2001, 2002) also show thermodynamically sound behavior, although the calculated pressures appear to be far too large, considering results from reference equations of state for other substances. The different isotherms calculated from the equations of state of Younglove and Ely (1987), however, intersect at densities of approximately $1000\text{--}1400 \text{ kg m}^{-3}$ and continue in reverse order beyond the point of intersection. This behavior is obviously wrong and prevents a reasonable extrapolation of these equations.

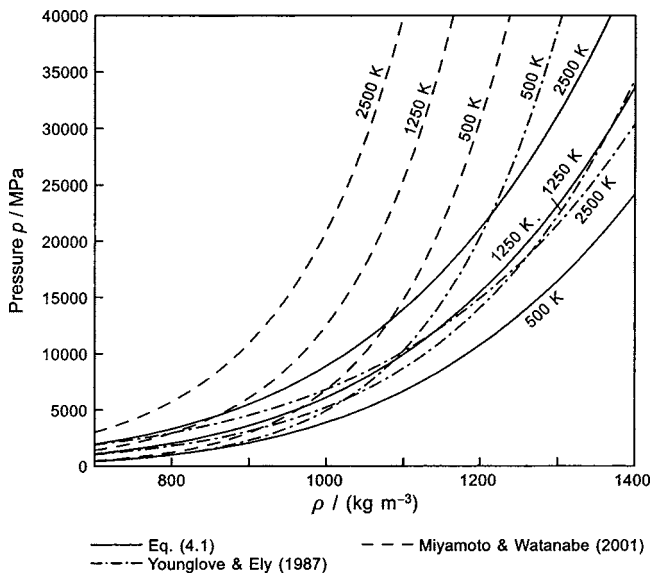


FIG. 32. Absolute plot of three isotherms of $p\rho T$ data for *n*-butane in a $p-T$ diagram up to very high pressures. The plotted lines correspond to values calculated from the equation of state, Eq. (4.1), and from the equations of state of Miyamoto and Watanabe (2001) and of Younglove and Ely (1987).

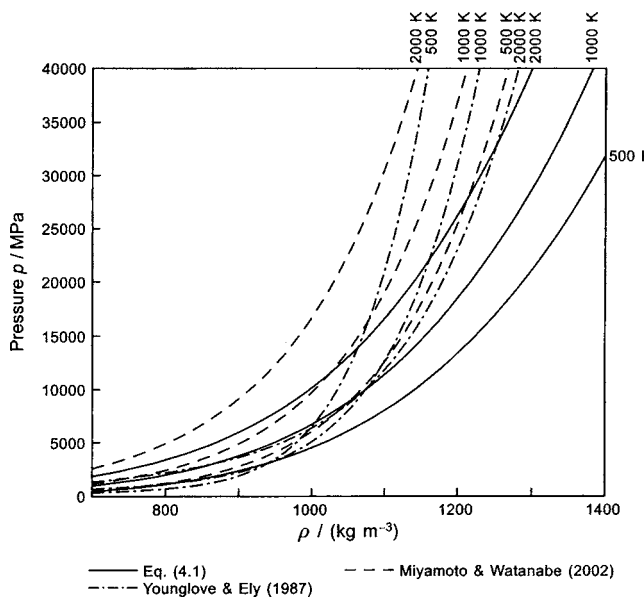


FIG. 33. Absolute plot of three isotherms of $p\rho T$ data for isobutane in a $p-T$ diagram up to very high pressures. The plotted lines correspond to values calculated from the equation of state, Eq. (4.1), and from the equations of state of Miyamoto and Watanabe (2002) and of Younglove and Ely (1987).

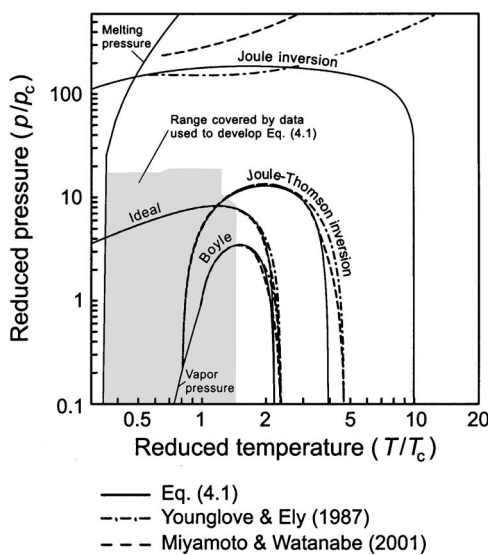


FIG. 34. “Ideal curves” for *n*-butane in a double logarithmic p/p_c vs T/T_c diagram. The curves correspond to values calculated from the equation of state, Eq. (4.1), and from the equations of state of Miyamoto and Watanabe (2001) and of Younglove and Ely (1987). The area marked in gray corresponds to the region where Eq. (4.1) was fitted to experimental data.

5.5.2. Ideal Curves

Ideal curves are frequently used to assess the extrapolation behavior of equations of state. We consider ideal curves of the compression factor and its first derivatives, namely the classical ideal curve ($Z=1$), the Boyle curve [$(\partial Z/\partial p)_T = 0$], the Joule–Thomson inversion curve [$(\partial Z/\partial T)_p = 0$], and the Joule inversion curve [$(\partial Z/\partial T)_p \neq 0$]. The plots of these characteristic curves, calculated from Eq. (4.1) and from the other considered equations of state, are shown in

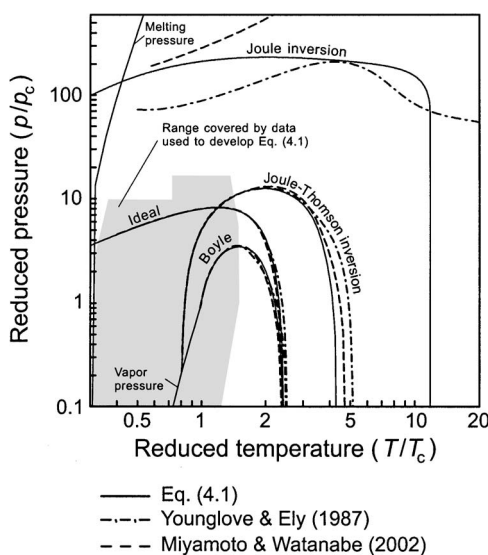


FIG. 35. “Ideal curves” for isobutane in a double logarithmic p/p_c vs T/T_c diagram. The curves correspond to values calculated from the equation of state, Eq. (4.1), and from the equations of state of Miyamoto and Watanabe (2002) and of Younglove and Ely (1987). The area marked in gray corresponds to the region where Eq. (4.1) was fitted to experimental data.

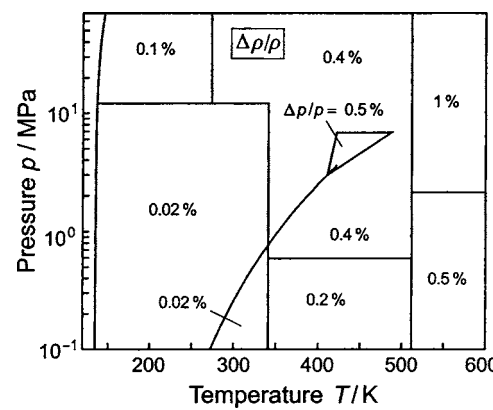


FIG. 36. Tolerance diagram for densities of *n*-butane calculated from the equation of state, Eq. (4.1). For the extended critical region, the uncertainty in pressure is given.

Figs. 34 and 35 for *n*- and isobutane, respectively. No quantitative information should be drawn from the diagrams, but it is recognizable that the plots of the curves calculated from Eq. (4.1) show reasonable shapes with no sharp inflection points or random oscillations. The curves intersect the abscissa at reduced temperatures that compare well to results for other well measured substances (see Span and Wagner 1997). The equations of state of Miyamoto and Watanabe (2001, 2002) and of Younglove and Ely (1987) produce reasonable plots for only three of the ideal curves. The shapes of the Joule inversion curves are not plausible and there are no intersections with the abscissa, indicating that extrapolating these equations to high temperatures may give misleading results.

6. Estimated Uncertainty of Calculated Properties

The most reliable basis to estimate uncertainties of calculated property values is comparisons with experimental data. Where such data are missing, estimations are based on an assessment of the real-gas effects, on analyses of the thermodynamic relations between the investigated property and

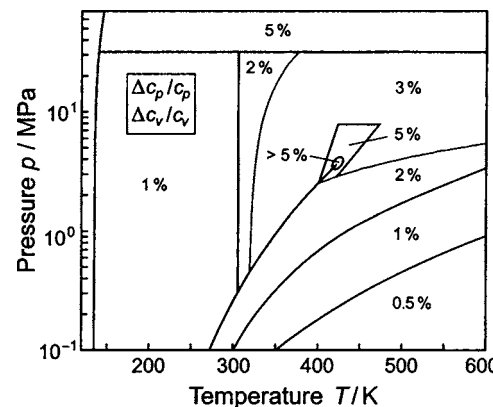


FIG. 37. Tolerance diagram for isobaric and isochoric heat capacities of *n*-butane calculated from the equation of state, Eq. (4.1).

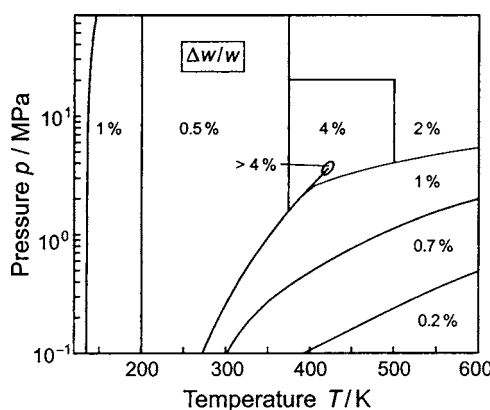


FIG. 38. Tolerance diagram for speeds of sound of *n*-butane calculated from the equation of state, Eq. (4.1).

properties with a more reliable experimental basis, and on comparisons of the results from different thermodynamic property models. Estimates for the uncertainty of calculated densities, speeds of sounds, and isochoric and isobaric heat capacities have been established. They are given in tolerance diagrams in Figs. 36–38 for *n*-butane and in Figs. 39–41 for isobutane.

According to the results of the assessment of the extrapolation behavior presented in Sec. 5.5, Eq. (4.1) should yield reasonable results outside its range of validity at least for basic thermodynamic properties like pressure, density, and enthalpy. In particular, we believe that extrapolating Eq. (4.1) for isobutane to pressures up to 70 MPa only slightly increases the uncertainty of calculated $p\rho T$ properties. One should be more careful when extrapolating Eq. (4.1) with regard to caloric properties for which second derivatives of the equation of state are needed, for example, heat capacities and speeds of sound. The uncertainties of these extrapolated properties might be clearly higher than those of the basic properties.

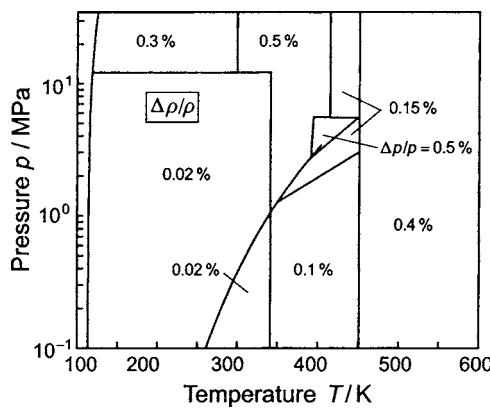


FIG. 39. Tolerance diagram for densities of isobutane calculated from the equation of state, Eq. (4.1). For the extended critical region, the uncertainty in pressure is given.

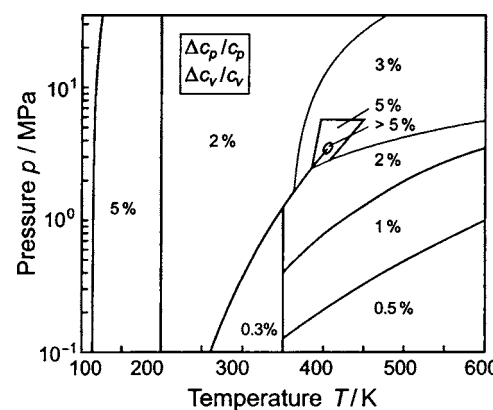


FIG. 40. Tolerance diagram for isobaric and isochoric heat capacities of isobutane calculated from the equation of state, Eq. (4.1).

7. Recommendations for Improving the Basis of the Experimental Data for *n*- and Isobutane

Since the data situation for *n*- and isobutane is very similar, the recommendations for both substances can be given in the same section.

As discussed at the end of Sec. 2.3, it would be helpful to have more accurate melting-pressure data for isobutane to better define the low-temperature boundary of the stable liquid phase of isobutane.

For the two substances the data situation regarding the thermal properties on the vapor–liquid phase boundary could be clearly improved by having very accurate vapor pressures and densities of the saturated liquid and vapor for temperatures from 340 K to the critical temperature. The accuracy of such data should be comparable to those measured by Glos *et al.* (2004) for the temperature range below 340 K.

For *n*-butane and isobutane, the data situation regarding the $p\rho T$ data in the single phase region could be significantly improved by measuring densities in the pressure range of the $p\rho T$ data of Glos *et al.* (2004), but for temperatures above 340 K possibly up to about 550 K. For pressures above 12

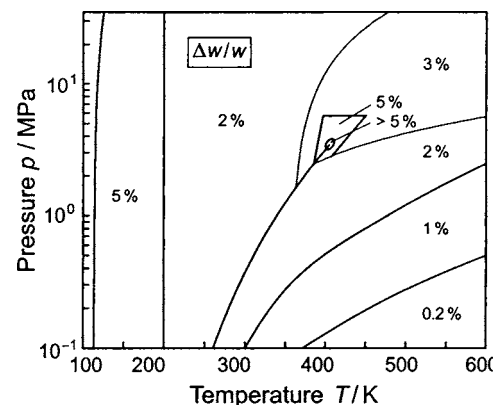


FIG. 41. Tolerance diagram for speeds of sound of isobutane calculated from the equation of state, Eq. (4.1).

TABLE 41. Coefficients for the correlation equations for the ideal-gas isobaric heat capacity c_p° and the ideal-gas part α° of the dimensionless Helmholtz energy of propane, Eqs. (4.5) and (4.6)

i	n_i°	θ_i°
1	10.14394256	—
2	-4.79513693	—
3	3.02256195	—
4	2.90591124	1.0515052038
5	4.68495401	3.0961635368
6	10.29711540	5.0845797877
7	8.08977905	11.4329447982

MPa up to about 50 MPa the entire temperature range from the melting line up to about 550 K should be measured. Such new $p\rho T$ data should have uncertainties in density not greater than about 0.02–0.05%. Figures 7 and 9 show that in the liquid region of *n*- and isobutane there are no $p\rho T$ data for pressures below 2 MPa. It is, however, not necessary to measure accurate $p\rho T$ data in this region because the thermal behavior of the two substances is sufficiently described by the existing $p\rho T$ data at higher pressures in combination with the saturated liquid densities measured by Glos *et al.* (2004).

The situation regarding the experimental data of the calorific properties in the single-phase region is rather bad for both butanes, particularly for isobutane. It would be very desirable to have very accurate measurements of the speed of sound in the liquid and in the gas phase. In the liquid phase the measurements should have an uncertainty of less than about 0.05%–0.1% and should cover the entire pressure range from 0.1 up to 40 MPa at temperatures up to the saturation state and for supercritical pressures up to about 450–500 K. In the gas phase, the speed of sound measurements with the spherical resonator should be extended to higher pressures at temperatures up to 500 K or above.

Experimental data of heat capacities are only really helpful if they are accurate enough. This means that measurements of the isochoric heat capacity should cover the liquid region up to possibly 50 MPa, where the experimental un-

TABLE 42. Coefficients of the equation of the residual part α^r of the dimensionless Helmholtz energy of propane, Eq. (4.12). The other parameters are identical to the values given in Table 39

i	n_i	i	n_i
1	$0.21933784906951 \times 10^1$	14	$-0.27766802597861 \times 10^{-1}$
2	$-0.38432884604893 \times 10^1$	15	-0.10523131087952
3	0.56820219711755	16	$0.97082793466314 \times 10^{-1}$
4	0.11235233289697	17	$0.20710537703751 \times 10^{-1}$
5	$-0.13246623110619 \times 10^{-1}$	18	$-0.54720320371501 \times 10^{-1}$
6	$0.14587076590314 \times 10^{-1}$	19	$0.64918009057295 \times 10^{-3}$
7	$0.19654925217128 \times 10^{-1}$	20	$0.74471355056336 \times 10^{-2}$
8	0.73811022854042	21	$-0.27504616979066 \times 10^{-3}$
9	-0.85976999811290	22	$-0.77693374632348 \times 10^{-2}$
10	0.14331675665712	23	$-0.17367624932157 \times 10^{-2}$
11	$-0.23280677426427 \times 10^{-1}$	24	$-0.38248057095416 \times 10^{-1}$
12	$-0.98713669399783 \times 10^{-4}$	25	$-0.68797254435490 \times 10^{-2}$
13	$0.45708225999895 \times 10^{-2}$		

TABLE 43. Coefficients for the correlation equations for the thermal properties on the vapor–liquid phase boundary of propane, Eqs. (9.2)–(9.4)

i	p_s , Eq. (9.2) n_i	p' , Eq. (9.3) n_i	p'' , Eq. (9.4) n_i
1	-6.75126926	1.68878288	-1.97376789
2	1.49720349	-0.589774828	-2.94776521
3	-1.46882321	0.189183445	0.214327267
4	-2.38157358	0.036669601	-1.178831790
5	0.075738439		-3.601452104
6			0.788655902

certainties should be 0.2%–0.4%. Concerning isobaric heat capacities, it would be desirable to have such data in the gas region and also in the supercritical range up to about 50 MPa and temperatures of up to 500 K or higher. However, these requirements on c_v and c_p measurements might probably be unrealistic. Therefore, it would be all the more important to get $p\rho T$ data and speed of sound data of very good quality that fill the gaps mentioned above.

8. Acknowledgments

We would like to express our gratitude to C. Guder for his many important contributions to this work and to E. W. Lemmon for his very valuable suggestions and advice. We are indebted to the Deutsche Forschungsgemeinschaft (German Research Association) for their financial support of this project.

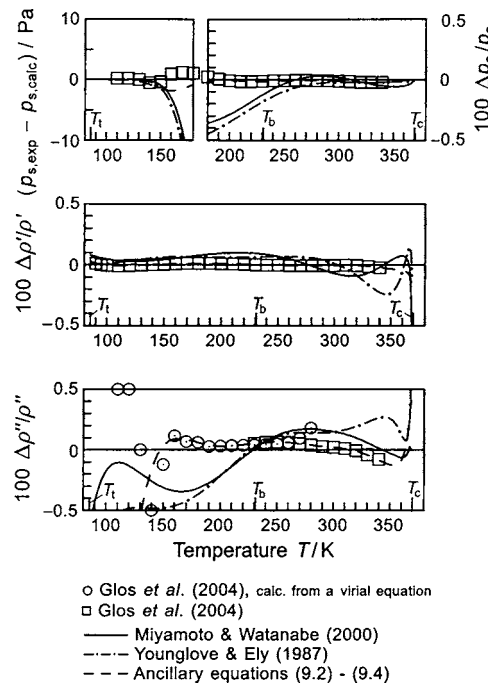


FIG. 42. Absolute deviations and percentage deviations [$100\Delta y/y = 100(y_{\text{exp}} - y_{\text{calc}})/y_{\text{exp}}$ with $y = p_s, p', p''$] of highly accurate thermal data for propane at saturation from values calculated from the equation of state, Eq. (4.1). Values calculated from the ancillary equations, Eqs. (9.2)–(9.4), and from the equations of state of Miyamoto and Watanabe (2000) and of Younglove and Ely (1987) are plotted for comparison.

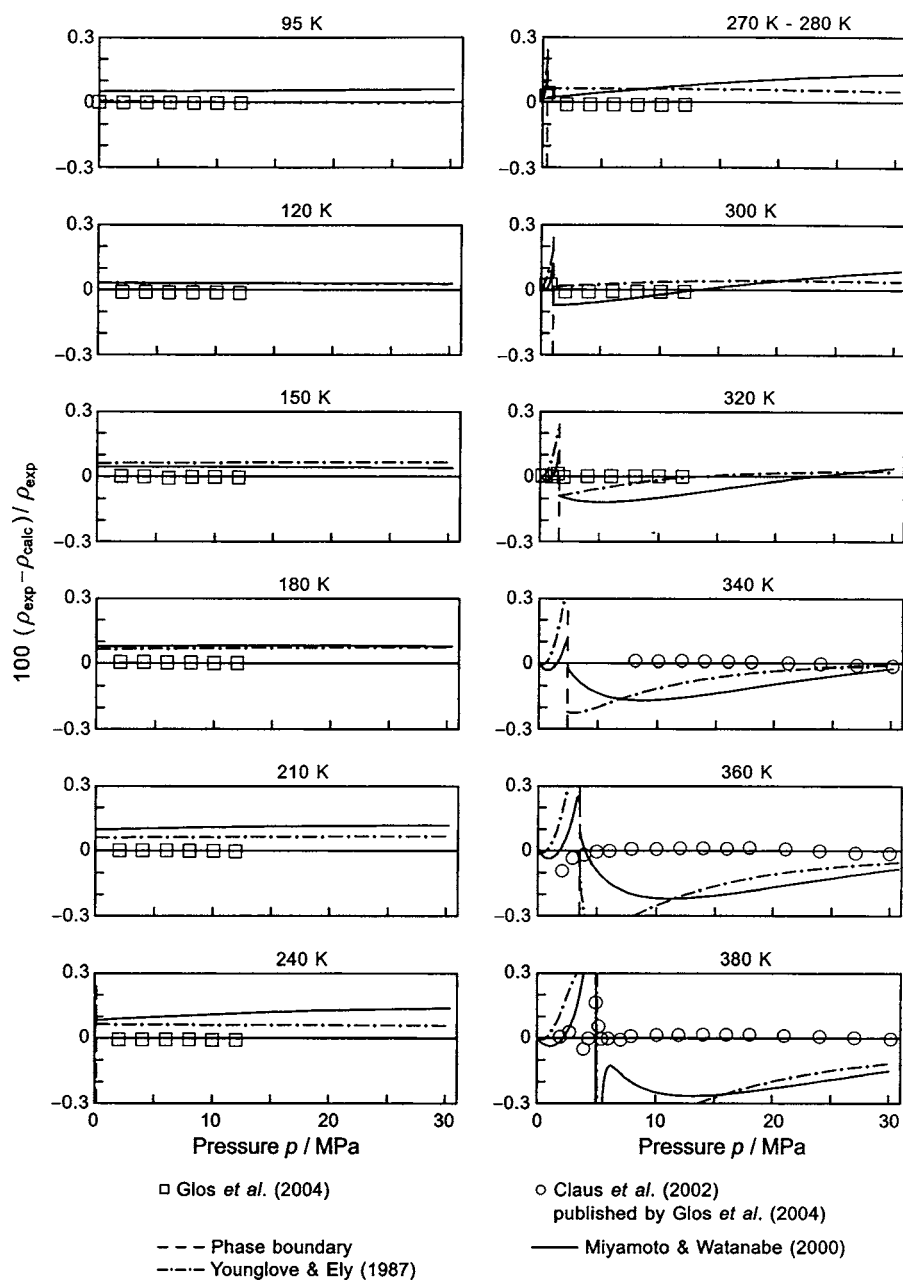


FIG. 43. Percentage density deviations of highly accurate $p\rho T$ data for propane (95–380 K) from values calculated from the equation of state, Eq. (4.1). Values calculated from the equations of state of Miyamoto and Watanabe (2000) and of Younglove and Ely (1987) are plotted for comparison.

9. Appendix 1: The Simultaneously Optimized Equation of State for Propane

In this Appendix, we summarize the coefficients and parameters for the ideal-gas part α° , Eq. (4.6), and the residual part α^r , Eq. (4.12), that are needed to calculate thermodynamic property values for propane. We also provide the corresponding reducing parameters and ancillary equations for the thermal properties on the vapor–liquid phase boundary of propane. All the equations and parameters given in this section should be regarded as preliminary. As mentioned in Sec. 4.2.2, a new reference quality equation of state for propane is being developed by researchers at the National Institute for Standards and Technology in Boulder at present. Once the results of their work are published, they will super-

sede the equations given in this section. However, the simultaneously optimized equation of state presented here is the only equation of state that has been developed on the basis of current data including new, highly accurate measurements of the thermal properties of propane carried out by Glos *et al.* (2004). Although the equation does not reproduce all the data within their expected experimental uncertainties, it gives a substantially better representation than any available equation of state.

The coefficients and parameters for the ideal-gas part α° , Eq. (4.6), are given in Table 41. The coefficients for the residual part α^r , Eq. (4.12), are summarized in Table 42. The other parameters for Eq. (4.12) are identical to the values for *n*- and isobutane and are given in Table 39. As for the butanes, we set the enthalpy and the entropy to zero in the

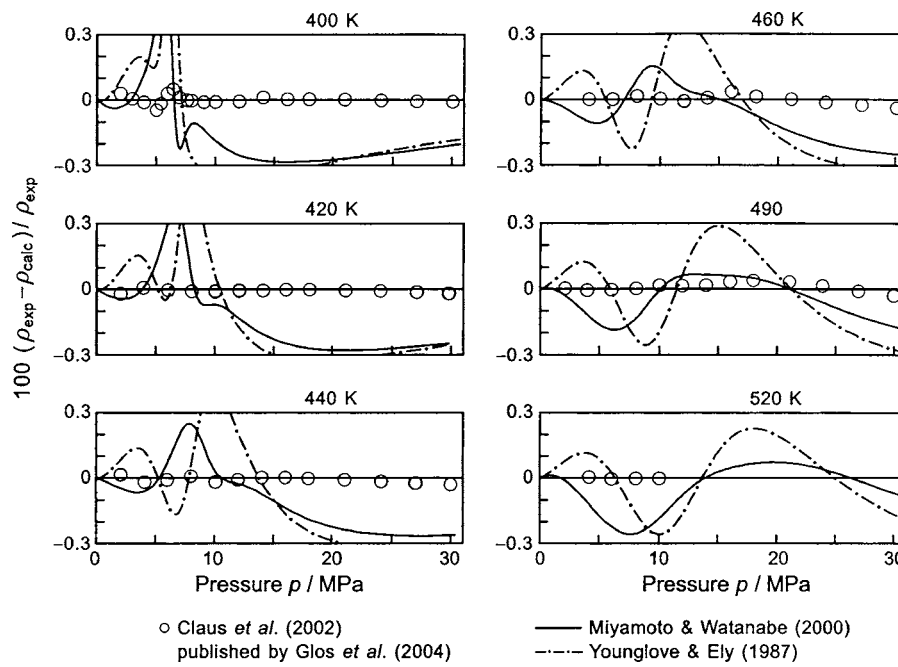


FIG. 44. Percentage density deviations of highly accurate $p\rho T$ data for propane (400–520 K) from values calculated from the equation of state, Eq. (4.1). Values calculated from the equations of state of Miyamoto and Watanabe (2000) and of Younglove and Ely (1987) are plotted for comparison.

ideal-gas state at $T_0 = 298.15$ K and $p_0 = 0.101325$ MPa. We adopted the critical parameters used by Younglove and Ely (1987), after transferring the critical temperature to ITS-90:

$$T_c = 369.825 \text{ K}, \quad (9.1a)$$

$$p_c = 4.24766 \text{ MPa}, \quad (9.1b)$$

$$\rho_c = 220.48 \text{ kg m}^{-3}. \quad (9.1c)$$

The critical temperature and density were used as reducing parameters for Eqs. (4.1), (4.6), and (4.12). We used a specific gas constant of $R = 0.188\,555\,51 \text{ kJ kg}^{-1} \text{ K}^{-1}$, which is obtained from the universal gas constant $R_m = 8.314\,472 \text{ J mol}^{-1} \text{ K}^{-1}$ as reported by Mohr and Taylor (1999) and a molar mass of $M = 44.095\,62 \text{ g mol}^{-1}$ as reported by Coplen (2001).

For a linearized solution of the Maxwell criterion, consistent $(T_s, p_s, \rho', \rho'')$ data are needed (see Wagner 1972). These values were calculated from ancillary equations for the vapor pressure and the saturated-liquid and saturated-vapor densities that were developed by Glos *et al.* (2004). These equations are:

$$\ln\left(\frac{p_s}{p_c}\right) = \frac{T_c}{T}(n_1\vartheta + n_2\vartheta^{1.5} + n_3\vartheta^{2.5} + n_4\vartheta^5 + n_5\vartheta^{7.5}) \quad (9.2)$$

$$\ln\left(\frac{\rho'}{\rho_c}\right) = (n_1\vartheta^{0.336} + n_2\vartheta^{4/6} + n_3\vartheta^{7/6} + n_4\vartheta^{4.5}) \quad (9.3)$$

$$\begin{aligned} \ln\left(\frac{\rho''}{\rho_c}\right) = \frac{T_c}{T}(n_1\vartheta^{0.348} + n_2\vartheta^{0.8} + n_3\vartheta^{1.8} + n_4\vartheta^{2.8} + n_5\vartheta^{4.8} \\ + n_6\vartheta^{6.8}) \end{aligned} \quad (9.4)$$

with $\vartheta = 1 - T/T_c$, and the values of the critical parameters as given in Eqs. (9.1a)–(9.1c). The coefficients n_i for the different equations are compiled in Table 43.

The data that were used in the simultaneous optimization and in the nonlinear fit of the coefficients of the formulation for the residual part α^r , Eq. (4.12), are given in Table 38. The thermal properties for pressures up to 12 MPa were measured by Glos *et al.* (2004) using a two-sinker densimeter, while the data for pressures up to 30 MPa were measured by Claus *et al.* (2002) using a single-sinker densimeter; the data measured by Claus *et al.* (2002) are published in the Appendix of the article by Glos *et al.* (2004).

Due to the temperature and pressure ranges of the experimental data used to develop this equation of state for propane, its range of validity is defined by the following region:

$$85.529 \text{ K} \leq T \leq 623 \text{ K} \text{ and } p \leq 100 \text{ MPa},$$

with the lowest temperature corresponding to the triple-point temperature.

Comparisons of these highly accurate data with results from the new simultaneously optimized equation of state for propane, Eq. (4.1), are shown in Fig. 42 for the properties on the vapor–liquid phase boundary, and in Figs. 43 and 44 for $p\rho T$ values in the homogenous fluid phase. Additionally, values calculated from the equation of state of Miyamoto and Watanabe (2000) and from the MBWR-type equation of state of Younglove and Ely (1987) are plotted as lines. In Fig. 42, results from the ancillary equations, Eqs. (9.2)–(9.4), are also shown.

10. Appendix 2: Tables of Thermodynamic Properties of *n*- and Isobutane

Tables 44 and 46 are given for the saturation properties of *n*- and isobutane as a function of temperature, Table 45 for single-phase state points of *n*-butane from 0.1 to 69 MPa from the melting line to 575 K and Table 47 for single-phase

state points of isobutane from 0.1 to 35 MPa from the melting line to 575 K. In order to preserve thermodynamic consistency, all values were calculated from the new equations of state given in Eqs. (4.1), (4.6), and (4.12). The saturation properties were calculated using the phase-equilibrium condition and are also shown in the single-phase tables to define the boundary between liquid and vapor states. The melting pressures were calculated from Eq. (2.1).

TABLE 44. Thermodynamic properties of *n*-butane on the vapor–liquid phase boundary as a function of temperature^a

<i>T</i> (K)	<i>p</i> (MPa)	ρ (kg m ⁻³)	<i>h</i> (kJ kg ⁻¹)	<i>s</i> (kJ kg ⁻¹ K ⁻¹)	c_v (kJ kg ⁻¹ K ⁻¹)	c_p (kJ kg ⁻¹ K ⁻¹)	<i>w</i> (m s ⁻¹)
134.895 ^b	0.00000067	734.9588 0.000034	-721.64 -225.72	-3.036 0.640	1.441 0.963	1.973 1.106	1826.82 148.87
136	0.00000082	733.9269 0.000042	-719.46 -224.49	-3.020 0.619	1.442 0.967	1.974 1.110	1819.41 149.44
138	0.0000012	732.0601 0.000060	-715.51 -222.26	-2.991 0.583	1.442 0.974	1.975 1.118	1806.14 150.46
140	0.0000017	730.1946 0.000084	-711.56 -220.02	-2.963 0.548	1.442 0.982	1.977 1.125	1793.06 151.48
142	0.0000024	728.330 0.00012	-707.61 -217.76	-2.935 0.515	1.442 0.988	1.979 1.131	1780.15 152.49
144	0.0000033	726.466 0.00016	-703.65 -215.50	-2.907 0.483	1.442 0.995	1.981 1.138	1767.38 153.49
146	0.0000046	724.603 0.00022	-699.68 -213.21	-2.880 0.452	1.442 1.002	1.982 1.145	1754.75 154.49
148	0.0000063	722.741 0.00030	-695.72 -210.92	-2.853 0.423	1.442 1.009	1.984 1.152	1742.24 155.48
150	0.0000086	720.878 0.00040	-691.75 -208.61	-2.826 0.395	1.442 1.015	1.986 1.158	1729.84 156.46
152	0.000012	719.016 0.00053	-687.77 -206.28	-2.800 0.368	1.443 1.022	1.988 1.165	1717.54 157.44
154	0.000015	717.154 0.00070	-683.79 -203.95	-2.774 0.342	1.443 1.028	1.990 1.171	1705.33 158.41
156	0.000020	715.291 0.00091	-679.81 -201.60	-2.748 0.317	1.443 1.034	1.992 1.178	1693.20 159.37
158	0.000027	713.429 0.00118	-675.83 -199.24	-2.723 0.294	1.443 1.041	1.994 1.184	1681.15 160.33
160	0.000035	711.565 0.00151	-671.83 -196.87	-2.698 0.271	1.444 1.047	1.997 1.190	1669.17 161.28
162	0.000045	709.701 0.00193	-667.84 -194.49	-2.673 0.249	1.444 1.053	1.999 1.197	1657.25 162.23
164	0.000057	707.837 0.00244	-663.84 -192.09	-2.648 0.228	1.445 1.060	2.001 1.203	1645.39 163.17
166	0.000073	705.971 0.00308	-659.83 -189.68	-2.624 0.208	1.446 1.066	2.004 1.209	1633.58 164.10
168	0.000092	704.105 0.00384	-655.82 -187.26	-2.600 0.189	1.446 1.072	2.006 1.215	1621.82 165.02
170	0.000116	702.237 0.00478	-651.81 -184.83	-2.576 0.171	1.447 1.078	2.009 1.221	1610.11 165.94
172	0.000145	700.368 0.00590	-647.79 -182.38	-2.553 0.153	1.448 1.084	2.012 1.228	1598.44 166.85

TABLE 44. Thermodynamic properties of *n*-butane on the vapor–liquid phase boundary as a function of temperature^a—Continued

<i>T</i> (K)	<i>p</i> (MPa)	ρ (kg m ⁻³)	<i>h</i> (kJ kg ⁻¹)	<i>s</i> (kJ kg ⁻¹ K ⁻¹)	<i>c_v</i> (kJ kg ⁻¹ K ⁻¹)	<i>c_p</i> (kJ kg ⁻¹ K ⁻¹)	<i>w</i> (m s ⁻¹)
174	0.000180	698.497	−643.76	−2.530	1.449	2.015	1586.81
		0.00725	−179.93	0.136	1.091	1.234	167.76
176	0.000223	696.625	−639.73	−2.506	1.450	2.018	1575.22
		0.00886	−177.46	0.120	1.097	1.240	168.66
178	0.000274	694.752	−635.69	−2.484	1.452	2.021	1563.66
		0.01076	−174.98	0.105	1.103	1.247	169.55
180	0.000335	692.876	−631.64	−2.461	1.453	2.024	1552.13
		0.01301	−172.50	0.090	1.109	1.253	170.43
182	0.000407	690.999	−627.59	−2.439	1.455	2.027	1540.63
		0.01565	−169.99	0.076	1.116	1.259	171.31
184	0.000493	689.120	−623.54	−2.417	1.456	2.031	1529.16
		0.01873	−167.48	0.062	1.122	1.266	172.18
186	0.000594	687.238	−619.47	−2.395	1.458	2.034	1517.71
		0.02233	−164.96	0.049	1.128	1.272	173.04
188	0.000712	685.354	−615.40	−2.373	1.460	2.038	1506.29
		0.02649	−162.43	0.037	1.135	1.278	173.90
190	0.000850	683.467	−611.32	−2.351	1.462	2.042	1494.89
		0.03130	−159.88	0.025	1.141	1.285	174.75
192	0.001010	681.578	−607.23	−2.330	1.464	2.045	1483.52
		0.03683	−157.33	0.013	1.148	1.292	175.59
194	0.001196	679.687	−603.14	−2.309	1.466	2.049	1472.16
		0.04316	−154.76	0.003	1.154	1.298	176.42
196	0.001410	677.792	−599.03	−2.288	1.468	2.054	1460.83
		0.05039	−152.19	−0.008	1.161	1.305	177.25
198	0.001657	675.894	−594.92	−2.267	1.471	2.058	1449.52
		0.05861	−149.60	−0.018	1.167	1.312	178.06
200	0.001939	673.993	−590.80	−2.246	1.473	2.062	1438.22
		0.06792	−147.01	−0.027	1.174	1.319	178.87
202	0.002261	672.089	−586.67	−2.225	1.476	2.067	1426.95
		0.07845	−144.40	−0.036	1.181	1.326	179.67
204	0.002628	670.181	−582.53	−2.205	1.479	2.071	1415.69
		0.09029	−141.78	−0.044	1.187	1.333	180.46
206	0.003043	668.270	−578.39	−2.185	1.482	2.076	1404.45
		0.10360	−139.16	−0.053	1.194	1.340	181.24
208	0.003513	666.354	−574.23	−2.165	1.485	2.081	1393.22
		0.11848	−136.52	−0.060	1.201	1.347	182.01
210	0.004043	664.435	−570.06	−2.145	1.488	2.086	1382.01
		0.13510	−133.88	−0.068	1.208	1.354	182.78
212	0.004638	662.512	−565.88	−2.125	1.491	2.091	1370.82
		0.15359	−131.22	−0.075	1.215	1.361	183.53
214	0.005305	660.585	−561.70	−2.105	1.494	2.096	1359.64
		0.17411	−128.56	−0.081	1.222	1.369	184.27
216	0.006050	658.653	−557.50	−2.086	1.498	2.102	1348.48
		0.19684	−125.89	−0.088	1.230	1.377	185.00
218	0.006881	656.716	−553.29	−2.066	1.501	2.107	1337.33
		0.22194	−123.21	−0.094	1.237	1.384	185.73
220	0.007805	654.775	−549.07	−2.047	1.505	2.113	1326.20
		0.24959	−120.52	−0.099	1.244	1.392	186.44

TABLE 44. Thermodynamic properties of *n*-butane on the vapor–liquid phase boundary as a function of temperature^a—Continued

<i>T</i> (K)	<i>p</i> (MPa)	<i>ρ</i> (kg m ⁻³)	<i>h</i> (kJ kg ⁻¹)	<i>s</i> (kJ kg ⁻¹ K ⁻¹)	<i>c_v</i> (kJ kg ⁻¹ K ⁻¹)	<i>c_p</i> (kJ kg ⁻¹ K ⁻¹)	<i>w</i> (m s ⁻¹)
222	0.008829	652.828 0.27998	-544.84 -117.82	-2.028 -0.104	1.509 1.252	2.119 1.400	1315.08 187.14
224	0.009962	650.877 0.31331	-540.59 -115.11	-2.009 -0.110	1.513 1.259	2.124 1.408	1303.98 187.82
226	0.011214	648.920 0.34979	-536.34 -112.40	-1.990 -0.114	1.517 1.267	2.130 1.416	1292.89 188.50
228	0.012592	646.958 0.38962	-532.07 -109.67	-1.971 -0.119	1.521 1.274	2.137 1.424	1281.81 189.16
230	0.014106	644.990 0.43303	-527.79 -106.94	-1.953 -0.123	1.525 1.282	2.143 1.433	1270.75 189.81
232	0.015766	643.016 0.48025	-523.49 -104.20	-1.934 -0.127	1.529 1.290	2.149 1.441	1259.70 190.45
234	0.017584	641.036 0.53151	-519.18 -101.46	-1.916 -0.130	1.534 1.298	2.156 1.450	1248.67 191.08
236	0.019568	639.050 0.58706	-514.86 -98.71	-1.897 -0.134	1.538 1.306	2.163 1.458	1237.65 191.69
238	0.021732	637.057 0.64715	-510.53 -95.95	-1.879 -0.137	1.543 1.314	2.169 1.467	1226.64 192.29
240	0.024086	635.058 0.71204	-506.18 -93.18	-1.861 -0.140	1.548 1.322	2.176 1.476	1215.65 192.87
242	0.026643	633.052 0.78200	-501.82 -90.41	-1.843 -0.143	1.553 1.330	2.184 1.485	1204.67 193.44
244	0.029415	631.038 0.85731	-497.44 -87.63	-1.825 -0.145	1.558 1.339	2.191 1.494	1193.70 194.00
246	0.032415	629.018 0.93825	-493.05 -84.84	-1.807 -0.147	1.563 1.347	2.198 1.504	1182.74 194.54
248	0.035656	626.99 1.0251	-488.64 -82.05	-1.789 -0.149	1.568 1.355	2.206 1.513	1171.80 195.06
250	0.039153	624.95 1.1182	-484.22 -79.25	-1.771 -0.151	1.573 1.364	2.213 1.523	1160.87 195.57
252	0.042919	622.91 1.2178	-479.78 -76.45	-1.754 -0.153	1.578 1.373	2.221 1.532	1149.95 196.06
254	0.046970	620.86 1.3243	-475.33 -73.64	-1.736 -0.155	1.584 1.381	2.229 1.542	1139.04 196.54
256	0.051319	618.80 1.4379	-470.86 -70.83	-1.718 -0.156	1.589 1.390	2.237 1.552	1128.15 197.00
258	0.055983	616.73 1.5590	-466.37 -68.02	-1.701 -0.157	1.595 1.399	2.245 1.562	1117.27 197.44
260	0.060978	614.65 1.6880	-461.87 -65.19	-1.684 -0.158	1.601 1.408	2.254 1.573	1106.40 197.86
262	0.066318	612.56 1.8251	-457.35 -62.37	-1.666 -0.159	1.606 1.417	2.262 1.583	1095.54 198.27
264	0.072022	610.46 1.9708	-452.81 -59.54	-1.649 -0.159	1.612 1.426	2.271 1.594	1084.69 198.66
266	0.078106	608.35 2.1254	-448.26 -56.70	-1.632 -0.160	1.618 1.435	2.279 1.604	1073.85 199.03
268	0.084586	606.23 2.2893	-443.68 -53.87	-1.615 -0.160	1.624 1.445	2.288 1.615	1063.02 199.38

TABLE 44. Thermodynamic properties of *n*-butane on the vapor–liquid phase boundary as a function of temperature^a—Continued

<i>T</i> (K)	<i>p</i> (MPa)	ρ (kg m ⁻³)	<i>h</i> (kJ kg ⁻¹)	<i>s</i> (kJ kg ⁻¹ K ⁻¹)	c_v (kJ kg ⁻¹ K ⁻¹)	c_p (kJ kg ⁻¹ K ⁻¹)	<i>w</i> (m s ⁻¹)
270	0.091481	604.11 2.4629	-439.09 -51.03	-1.598 -0.161	1.630 1.454	2.297 1.626	1052.20 199.71
272	0.098809	601.97 2.6465	-434.48 -48.18	-1.581 -0.161	1.636 1.463	2.307 1.637	1041.40 200.03
274	0.10659	599.82 2.8405	-429.85 -45.34	-1.564 -0.161	1.642 1.473	2.316 1.649	1030.60 200.32
276	0.11484	597.65 3.0454	-425.20 -42.49	-1.547 -0.161	1.649 1.482	2.325 1.660	1019.81 200.59
278	0.12357	595.48 3.2617	-420.54 -39.64	-1.530 -0.160	1.655 1.492	2.335 1.672	1009.03 200.84
280	0.13282	593.29 3.4896	-415.85 -36.79	-1.514 -0.160	1.662 1.501	2.345 1.684	998.26 201.08
282	0.14259	591.10 3.7297	-411.14 -33.94	-1.497 -0.159	1.668 1.511	2.355 1.695	987.49 201.29
284	0.15291	588.88 3.9824	-406.41 -31.08	-1.480 -0.159	1.675 1.521	2.365 1.708	976.74 201.47
286	0.16379	586.66 4.2481	-401.67 -28.23	-1.464 -0.158	1.681 1.531	2.375 1.720	965.99 201.64
288	0.17526	584.42 4.5275	-396.90 -25.37	-1.447 -0.157	1.688 1.541	2.385 1.732	955.24 201.78
290	0.18734	582.17 4.8208	-392.11 -22.51	-1.431 -0.156	1.695 1.551	2.396 1.745	944.51 201.90
292	0.20005	579.90 5.1287	-387.29 -19.66	-1.414 -0.155	1.701 1.561	2.407 1.758	933.77 202.00
294	0.21341	577.62 5.4517	-382.46 -16.80	-1.398 -0.154	1.708 1.571	2.417 1.771	923.04 202.08
296	0.22744	575.32 5.7903	-377.61 -13.95	-1.381 -0.153	1.715 1.581	2.429 1.784	912.32 202.13
298	0.24216	573.01 6.1450	-372.73 -11.10	-1.365 -0.152	1.722 1.591	2.440 1.798	901.60 202.15
300	0.25760	570.68 6.5164	-367.83 -8.24	-1.349 -0.150	1.729 1.602	2.451 1.811	890.88 202.15
302	0.27377	568.33 6.9051	-362.90 -5.40	-1.332 -0.149	1.736 1.612	2.463 1.825	880.16 202.13
304	0.29070	565.97 7.3116	-357.95 -2.55	-1.316 -0.147	1.744 1.623	2.475 1.839	869.44 202.08
306	0.30842	563.59 7.7367	-352.98 0.30	-1.300 -0.146	1.751 1.633	2.487 1.853	858.73 202.00
308	0.32694	561.19 8.1809	-347.98 3.14	-1.284 -0.144	1.758 1.644	2.499 1.868	848.01 201.89
310	0.34628	558.77 8.6450	-342.96 5.97	-1.268 -0.142	1.765 1.654	2.511 1.883	837.29 201.76
312	0.36648	556.33 9.1295	-337.92 8.81	-1.252 -0.140	1.773 1.665	2.524 1.898	826.57 201.61
314	0.38755	553.87 9.6352	-332.85 11.63	-1.236 -0.138	1.780 1.676	2.537 1.913	815.84 201.42
316	0.40952	551.39 10.163	-327.75 14.46	-1.219 -0.137	1.788 1.686	2.550 1.928	805.11 201.20

TABLE 44. Thermodynamic properties of *n*-butane on the vapor–liquid phase boundary as a function of temperature^a—Continued

<i>T</i> (K)	<i>p</i> (MPa)	ρ (kg m ⁻³)	<i>h</i> (kJ kg ⁻¹)	<i>s</i> (kJ kg ⁻¹ K ⁻¹)	c_v (kJ kg ⁻¹ K ⁻¹)	c_p (kJ kg ⁻¹ K ⁻¹)	<i>w</i> (m s ⁻¹)
318	0.43241	548.89	-322.62	-1.203	1.795	2.563	794.37
		10.713	17.27	-0.135	1.697	1.944	200.96
320	0.45624	546.36	-317.47	-1.187	1.803	2.577	783.62
		11.287	20.08	-0.133	1.708	1.960	200.69
322	0.48104	543.81	-312.30	-1.171	1.810	2.590	772.87
		11.885	22.89	-0.130	1.719	1.977	200.38
324	0.50684	541.24	-307.09	-1.155	1.818	2.604	762.10
		12.509	25.69	-0.128	1.730	1.993	200.05
326	0.53366	538.65	-301.86	-1.140	1.826	2.619	751.32
		13.158	28.47	-0.126	1.741	2.011	199.68
328	0.56152	536.02	-296.60	-1.124	1.833	2.634	740.53
		13.835	31.25	-0.124	1.752	2.028	199.28
330	0.59045	533.38	-291.31	-1.108	1.841	2.649	729.73
		14.540	34.02	-0.122	1.763	2.046	198.85
332	0.62047	530.70	-285.99	-1.092	1.849	2.664	718.90
		15.273	36.78	-0.120	1.774	2.064	198.38
334	0.65161	527.99	-280.63	-1.076	1.857	2.679	708.06
		16.037	39.53	-0.117	1.786	2.083	197.88
336	0.68390	525.26	-275.25	-1.060	1.865	2.695	697.19
		16.833	42.27	-0.115	1.797	2.102	197.35
338	0.71735	522.49	-269.84	-1.044	1.873	2.712	686.31
		17.660	45.00	-0.113	1.808	2.121	196.77
340	0.75201	519.69	-264.40	-1.028	1.881	2.729	675.39
		18.522	47.71	-0.110	1.820	2.142	196.17
342	0.78789	516.86	-258.92	-1.012	1.889	2.746	664.46
		19.419	50.40	-0.108	1.831	2.162	195.52
344	0.82501	514.00	-253.41	-0.997	1.897	2.764	653.49
		20.353	53.08	-0.106	1.843	2.183	194.83
346	0.86342	511.10	-247.87	-0.981	1.906	2.782	642.48
		21.324	55.75	-0.103	1.854	2.205	194.11
348	0.90313	508.16	-242.29	-0.965	1.914	2.800	631.45
		22.336	58.40	-0.101	1.866	2.227	193.35
350	0.94418	505.18	-236.68	-0.949	1.922	2.820	620.37
		23.389	61.02	-0.098	1.877	2.250	192.54
352	0.98658	502.16	-231.03	-0.933	1.931	2.840	609.25
		24.486	63.63	-0.096	1.889	2.274	191.69
354	1.0304	499.09	-225.34	-0.917	1.939	2.860	598.09
		25.627	66.22	-0.094	1.900	2.299	190.80
356	1.0756	495.99	-219.61	-0.901	1.948	2.881	586.88
		26.817	68.78	-0.091	1.912	2.324	189.86
358	1.1222	492.83	-213.85	-0.886	1.957	2.903	575.62
		28.056	71.31	-0.089	1.923	2.351	188.88
360	1.1704	489.63	-208.05	-0.870	1.965	2.926	564.31
		29.347	73.82	-0.087	1.935	2.379	187.85
362	1.2200	486.37	-202.20	-0.854	1.974	2.950	552.93
		30.694	76.30	-0.084	1.947	2.407	186.78
364	1.2712	483.06	-196.31	-0.838	1.983	2.974	541.49
		32.098	78.74	-0.082	1.958	2.438	185.65

TABLE 44. Thermodynamic properties of *n*-butane on the vapor–liquid phase boundary as a function of temperature^a—Continued

<i>T</i> (K)	<i>p</i> (MPa)	ρ (kg m ⁻³)	<i>h</i> (kJ kg ⁻¹)	<i>s</i> (kJ kg ⁻¹ K ⁻¹)	c_v (kJ kg ⁻¹ K ⁻¹)	c_p (kJ kg ⁻¹ K ⁻¹)	<i>w</i> (m s ⁻¹)
366	1.3240	479.69 33.563	-190.38 81.16	-0.822 -0.080	1.992 1.970	3.000 2.469	529.99 184.47
368	1.3783	476.26 35.092	-184.40 83.53	-0.806 -0.078	2.001 1.982	3.027 2.503	518.41 183.24
370	1.4343	472.76 36.689	-178.38 85.87	-0.790 -0.076	2.010 1.994	3.055 2.538	506.76 181.96
372	1.4920	469.20 38.358	-172.31 88.17	-0.774 -0.074	2.020 2.007	3.084 2.576	495.02 180.62
374	1.5513	465.57 40.104	-166.18 90.42	-0.758 -0.072	2.029 2.019	3.116 2.616	483.19 179.22
376	1.6124	461.85 41.931	-160.01 92.62	-0.742 -0.070	2.039 2.032	3.148 2.659	471.27 177.76
378	1.6753	458.06 43.845	-153.78 94.77	-0.725 -0.068	2.049 2.045	3.183 2.705	459.26 176.24
380	1.7399	454.17 45.851	-147.49 96.87	-0.709 -0.066	2.059 2.058	3.221 2.754	447.13 174.66
382	1.8065	450.20 47.958	-141.14 98.90	-0.693 -0.065	2.069 2.072	3.260 2.808	434.90 173.01
384	1.8749	446.12 50.171	-134.73 100.87	-0.677 -0.063	2.079 2.086	3.303 2.866	422.54 171.29
386	1.9452	441.92 52.500	-128.25 102.77	-0.660 -0.062	2.090 2.100	3.349 2.929	410.06 169.51
388	2.0175	437.61 54.955	-121.70 104.59	-0.644 -0.060	2.101 2.114	3.400 2.999	397.44 167.64
390	2.0918	433.17 57.546	-115.08 106.33	-0.627 -0.059	2.112 2.129	3.454 3.075	384.68 165.71
392	2.1682	428.59 60.286	-108.37 107.97	-0.610 -0.059	2.123 2.144	3.515 3.160	371.76 163.69
394	2.2467	423.84 63.191	-101.58 109.51	-0.594 -0.058	2.135 2.160	3.581 3.255	358.69 161.59
396	2.3274	418.93 66.276	-94.69 110.94	-0.577 -0.057	2.147 2.176	3.656 3.362	345.43 159.41
398	2.4103	413.81 69.563	-87.70 112.23	-0.560 -0.057	2.160 2.192	3.741 3.483	331.99 157.14
400	2.4954	408.48 73.077	-80.60 113.39	-0.542 -0.057	2.173 2.210	3.838 3.623	318.35 154.77
402	2.5830	402.90 76.846	-73.36 114.39	-0.525 -0.058	2.186 2.227	3.950 3.785	304.49 152.31
404	2.6729	397.02 80.908	-65.99 115.19	-0.507 -0.059	2.200 2.245	4.081 3.976	290.40 149.74
406	2.7653	390.82 85.307	-58.45 115.79	-0.489 -0.060	2.215 2.265	4.239 4.206	276.06 147.06
408	2.8602	384.21 90.102	-50.72 116.13	-0.471 -0.062	2.231 2.284	4.433 4.487	261.43 144.27
410	2.9578	377.13 95.371	-42.76 116.18	-0.452 -0.064	2.247 2.306	4.677 4.840	246.50 141.36
412	3.0582	369.45 101.22	-34.53 115.86	-0.432 -0.067	2.265 2.328	4.995 5.299	231.23 138.31

TABLE 44. Thermodynamic properties of *n*-butane on the vapor–liquid phase boundary as a function of temperature^a—Continued

<i>T</i> (K)	<i>p</i> (MPa)	<i>ρ</i> (kg m ⁻³)	<i>h</i> (kJ kg ⁻¹)	<i>s</i> (kJ kg ⁻¹ K ⁻¹)	<i>c_v</i> (kJ kg ⁻¹ K ⁻¹)	<i>c_p</i> (kJ kg ⁻¹ K ⁻¹)	<i>w</i> (m s ⁻¹)
414	3.1614	361.02	−25.95	−0.412	2.284	5.429	215.58
		107.79	115.08	−0.072	2.352	5.921	135.12
416	3.2676	351.59	−16.92	−0.391	2.305	6.057	199.49
		115.31	113.70	−0.077	2.379	6.814	131.77
418	3.3770	340.76	−7.26	−0.369	2.329	7.049	182.87
		124.16	111.50	−0.085	2.409	8.211	128.23
420	3.4897	327.77	3.37	−0.344	2.357	8.852	165.59
		135.00	108.06	−0.095	2.444	10.719	124.46
421	3.5474	320.01	9.25	−0.331	2.374	10.444	156.63
		141.59	105.62	−0.102	2.465	12.910	122.47
422	3.6060	310.91	15.74	−0.316	2.394	13.117	147.36
		149.41	102.42	−0.110	2.488	16.554	120.38
423	3.6656	299.64	23.20	−0.299	2.419	18.493	137.67
		159.25	98.01	−0.122	2.515	23.801	118.16
424	3.7262	284.03	32.66	−0.277	2.454	34.430	127.24
		173.21	91.15	−0.139	2.549	44.895	115.73
425	3.7881	250.17	50.78	−0.235	2.534	375.35	114.85
		205.54	73.93	−0.180	2.589	460.13	112.63
425.125 ^c	3.7960	228.00	62.09	−0.208			

^aFor each temperature, the values on the first line correspond to the saturated-liquid line and the values on the second line correspond to the saturated-vapor line.

^bTriple point.

^cCritical point.

TABLE 45. Thermodynamic properties of *n*-butane in the single-phase region

<i>T</i> (K)	<i>ρ</i> (kg m ⁻³)	<i>u</i> (kJ kg ⁻¹)	<i>h</i> (kJ kg ⁻¹)	<i>s</i> (kJ kg ⁻¹ K ⁻¹)	<i>c_v</i> (kJ kg ⁻¹ K ⁻¹)	<i>c_p</i> (kJ kg ⁻¹ K ⁻¹)	<i>w</i> (m s ⁻¹)
0.1 MPa							
134.91 ^a	734.98	−721.63	−721.50	−3.0362	1.4416	1.9728	1827.06
135	734.90	−721.46	−721.32	−3.0349	1.4416	1.9729	1826.47
140	730.24	−711.59	−711.45	−2.9631	1.4419	1.9771	1793.44
145	725.58	−701.69	−701.55	−2.8937	1.4421	1.9814	1761.44
150	720.92	−691.77	−691.64	−2.8264	1.4424	1.9861	1730.24
155	716.27	−681.83	−681.69	−2.7612	1.4430	1.9911	1699.68
160	711.61	−671.86	−671.72	−2.6979	1.4439	1.9965	1669.61
165	706.96	−661.87	−661.73	−2.6364	1.4454	2.0025	1639.93
170	702.29	−651.84	−651.70	−2.5765	1.4473	2.0090	1610.58
175	697.62	−641.78	−641.64	−2.5182	1.4500	2.0161	1581.50
180	692.93	−631.68	−631.54	−2.4613	1.4532	2.0239	1552.63
185	688.24	−621.54	−621.40	−2.4057	1.4572	2.0323	1523.95
190	683.53	−611.36	−611.21	−2.3514	1.4618	2.0414	1495.43
195	678.80	−601.13	−600.98	−2.2982	1.4672	2.0513	1467.05
200	674.06	−590.85	−590.70	−2.2462	1.4733	2.0620	1438.79
210	664.51	−570.11	−569.96	−2.1450	1.4877	2.0857	1382.60
220	654.85	−549.13	−548.97	−2.0474	1.5051	2.1125	1326.81
230	645.06	−527.85	−527.70	−1.9528	1.5252	2.1427	1271.35
240	635.13	−506.27	−506.11	−1.8609	1.5479	2.1762	1216.22
250	625.02	−484.32	−484.16	−1.7713	1.5731	2.2131	1161.36
260	614.69	−462.00	−461.83	−1.6838	1.6006	2.2534	1106.73
270	604.12	−439.25	−439.08	−1.5979	1.6301	2.2973	1052.28

TABLE 45. Thermodynamic properties of *n*-butane in the single-phase region—Continued

<i>T</i> (K)	ρ (kg m ⁻³)	<i>u</i> (kJ kg ⁻¹)	<i>h</i> (kJ kg ⁻¹)	<i>s</i> (kJ kg ⁻¹ K ⁻¹)	c_v (kJ kg ⁻¹ K ⁻¹)	c_p (kJ kg ⁻¹ K ⁻¹)	<i>w</i> (m s ⁻¹)
272.31 ^b	601.63	−433.92	−433.75	−1.5783	1.6372	2.3080	1039.70
272.31 ^c	2.6762	−85.104	−47.738	−0.16071	1.4647	1.6391	200.07
280	2.5924	−73.617	−35.042	−0.11473	1.4940	1.6648	203.31
290	2.4919	−58.347	−18.217	−0.055693	1.5335	1.7006	207.36
300	2.3998	−42.694	−1.0238	0.002591	1.5742	1.7383	211.28
310	2.3150	−26.642	16.555	0.060226	1.6160	1.7776	215.06
320	2.2365	−10.180	34.532	0.11730	1.6586	1.8181	218.74
330	2.1636	6.7009	52.920	0.17388	1.7018	1.8595	222.31
340	2.0957	24.007	71.725	0.23001	1.7454	1.9016	225.80
350	2.0321	41.743	90.953	0.28575	1.7892	1.9441	229.21
360	1.9726	59.912	110.61	0.34111	1.8331	1.9869	232.55
370	1.9166	78.515	130.69	0.39614	1.8770	2.0298	235.82
380	1.8638	97.551	151.20	0.45084	1.9208	2.0728	239.03
390	1.8140	117.02	172.15	0.50524	1.9644	2.1157	242.19
400	1.7669	136.92	193.52	0.55934	2.0077	2.1583	245.29
425	1.6596	188.54	248.80	0.69336	2.1144	2.2637	252.85
450	1.5649	242.78	306.68	0.82568	2.2183	2.3666	260.14
475	1.4806	299.56	367.10	0.95632	2.3190	2.4664	267.20
500	1.4052	358.81	429.98	1.0853	2.4162	2.5630	274.06
525	1.3371	420.44	495.22	1.2126	2.5098	2.6562	280.74
550	1.2755	484.36	562.76	1.3383	2.6000	2.7460	287.25
575	1.2193	550.48	632.50	1.4623	2.6869	2.8325	293.60
0.5 MPa							
134.98 ^a	735.09	−721.60	−720.92	−3.0359	1.4421	1.9727	1828.03
135	735.07	−721.55	−720.87	−3.0356	1.4421	1.9727	1827.88
140	730.41	−711.68	−711.00	−2.9638	1.4424	1.9769	1794.92
145	725.76	−701.79	−701.10	−2.8944	1.4425	1.9812	1762.99
150	721.11	−691.88	−691.19	−2.8271	1.4428	1.9858	1731.87
155	716.46	−681.94	−681.25	−2.7619	1.4434	1.9908	1701.37
160	711.81	−671.98	−671.28	−2.6986	1.4443	1.9962	1671.36
165	707.16	−661.99	−661.28	−2.6371	1.4457	2.0021	1641.75
170	702.50	−651.97	−651.26	−2.5773	1.4477	2.0086	1612.47
175	697.84	−641.91	−641.20	−2.5189	1.4503	2.0157	1583.45
180	693.16	−631.82	−631.10	−2.4620	1.4536	2.0234	1554.65
185	688.48	−621.69	−620.96	−2.4065	1.4575	2.0318	1526.03
190	683.78	−611.51	−610.78	−2.3522	1.4622	2.0409	1497.58
195	679.06	−601.29	−600.55	−2.2990	1.4675	2.0508	1469.27
200	674.33	−591.01	−590.27	−2.2470	1.4737	2.0614	1441.09
210	664.80	−570.29	−569.54	−2.1459	1.4881	2.0849	1385.06
220	655.17	−549.32	−548.56	−2.0483	1.5054	2.1117	1329.42
230	645.41	−528.07	−527.30	−1.9537	1.5255	2.1417	1274.15
240	635.51	−506.50	−505.72	−1.8619	1.5482	2.1751	1219.20
250	625.43	−484.58	−483.78	−1.7724	1.5734	2.2117	1164.55
260	615.15	−462.28	−461.47	−1.6849	1.6009	2.2518	1110.16
270	604.62	−439.56	−438.74	−1.5991	1.6304	2.2953	1055.98
280	593.81	−416.39	−415.55	−1.5148	1.6618	2.3425	1001.92
290	582.66	−392.73	−391.87	−1.4317	1.6949	2.3936	947.89
300	571.11	−368.54	−367.66	−1.3496	1.7295	2.4490	893.74
310	559.08	−343.77	−342.88	−1.2683	1.7655	2.5095	839.28
320	546.46	−318.37	−317.45	−1.1876	1.8027	2.5760	784.25
323.48 ^b	541.92	−309.38	−308.45	−1.1597	1.8160	2.6008	764.92
323.48 ^c	12.343	−15.553	24.955	−0.12895	1.7271	1.9891	200.14
330	11.971	−3.8062	37.960	−0.089143	1.7496	1.9990	203.83
340	11.458	14.412	58.048	−0.029173	1.7860	2.0198	209.14
350	11.001	32.921	78.371	0.029736	1.8239	2.0455	214.11
360	10.589	51.753	98.971	0.087764	1.8630	2.0749	218.79

TABLE 45. Thermodynamic properties of *n*-butane in the single-phase region—Continued

<i>T</i> (K)	<i>ρ</i> (kg m ⁻³)	<i>u</i> (kJ kg ⁻¹)	<i>h</i> (kJ kg ⁻¹)	<i>s</i> (kJ kg ⁻¹ K ⁻¹)	<i>c_v</i> (kJ kg ⁻¹ K ⁻¹)	<i>c_p</i> (kJ kg ⁻¹ K ⁻¹)	<i>w</i> (m s ⁻¹)
370	10.215	70.931	119.88	0.14505	1.9030	2.1071	223.23
380	9.8725	90.472	141.12	0.20169	1.9437	2.1412	227.47
390	9.5569	110.39	162.71	0.25776	1.9846	2.1766	231.54
400	9.2648	130.69	184.65	0.31333	2.0257	2.2130	235.46
425	8.6190	183.13	241.14	0.45027	2.1279	2.3062	244.71
450	8.0686	238.00	299.97	0.58476	2.2287	2.4006	253.34
475	7.5918	295.30	361.16	0.71707	2.3272	2.4942	261.48
500	7.1732	354.96	424.67	0.84735	2.4228	2.5861	269.22
525	6.8019	416.94	490.45	0.97571	2.5152	2.6757	276.62
550	6.4697	481.15	558.43	1.1022	2.6045	2.7627	283.75
575	6.1703	547.53	628.56	1.2269	2.6906	2.8470	290.62
1 MPa							
135.06 ^a	735.21	-721.55	-720.19	-3.0356	1.4426	1.9725	1829.23
140	730.62	-711.81	-710.44	-2.9647	1.4429	1.9766	1796.77
145	725.98	-701.92	-700.54	-2.8952	1.4430	1.9809	1764.93
150	721.34	-692.01	-690.63	-2.8280	1.4433	1.9855	1733.89
155	716.70	-682.08	-680.69	-2.7628	1.4438	1.9904	1703.47
160	712.06	-672.13	-670.72	-2.6995	1.4447	1.9958	1673.55
165	707.42	-662.14	-660.73	-2.6380	1.4462	2.0017	1644.02
170	702.77	-652.13	-650.71	-2.5782	1.4481	2.0081	1614.82
175	698.12	-642.08	-640.65	-2.5199	1.4507	2.0152	1585.88
180	693.45	-631.99	-630.55	-2.4630	1.4540	2.0228	1557.16
185	688.78	-621.87	-620.42	-2.4075	1.4579	2.0312	1528.63
190	684.09	-611.70	-610.24	-2.3532	1.4626	2.0403	1500.27
195	679.39	-601.49	-600.01	-2.3001	1.4680	2.0501	1472.04
200	674.67	-591.22	-589.74	-2.2480	1.4741	2.0606	1443.95
210	665.16	-570.52	-569.02	-2.1469	1.4885	2.0840	1388.11
220	655.56	-549.57	-548.05	-2.0494	1.5058	2.1107	1332.68
230	645.84	-528.34	-526.79	-1.9549	1.5259	2.1405	1277.62
240	635.98	-506.80	-505.23	-1.8631	1.5487	2.1736	1222.91
250	625.95	-484.91	-483.31	-1.7737	1.5739	2.2100	1168.52
260	615.72	-462.64	-461.01	-1.6862	1.6013	2.2498	1114.42
270	605.25	-439.96	-438.30	-1.6005	1.6309	2.2929	1060.56
280	594.51	-416.83	-415.14	-1.5163	1.6622	2.3396	1006.86
290	583.44	-393.21	-391.50	-1.4333	1.6953	2.3901	953.24
300	571.99	-369.08	-367.33	-1.3514	1.7299	2.4447	899.57
310	560.08	-344.37	-342.59	-1.2703	1.7658	2.5040	845.68
320	547.61	-319.05	-317.23	-1.1898	1.8030	2.5690	791.34
330	534.47	-293.06	-291.18	-1.1096	1.8414	2.6411	736.22
340	520.48	-266.30	-264.37	-1.0296	1.8811	2.7227	679.85
350	505.39	-238.66	-236.69	-0.94935	1.9223	2.8178	621.53
352.62 ^b	501.21	-231.26	-229.27	-0.92824	1.9334	2.8458	605.80
352.62 ^c	24.834	24.167	64.434	-0.095323	1.8921	2.2818	191.42
360	23.804	39.201	81.210	-0.048237	1.9129	2.2666	197.12
370	22.604	59.604	103.84	0.013775	1.9446	2.2625	204.07
380	21.573	80.146	126.50	0.074200	1.9792	2.2706	210.36
390	20.669	100.90	149.28	0.13337	2.0153	2.2864	216.13
400	19.867	121.91	172.25	0.19151	2.0522	2.3073	221.49
425	18.184	175.73	230.73	0.33330	2.1469	2.3739	233.55
450	16.831	231.62	291.03	0.47116	2.2429	2.4518	244.24
475	15.705	289.68	353.36	0.60593	2.3381	2.5345	253.96
500	14.745	349.95	417.77	0.73807	2.4314	2.6187	262.94
525	13.913	412.41	484.29	0.86787	2.5222	2.7027	271.35
550	13.182	477.03	552.89	0.99552	2.6102	2.7854	279.30
575	12.532	543.75	623.54	1.1211	2.6954	2.8663	286.87

TABLE 45. Thermodynamic properties of *n*-butane in the single-phase region—Continued

<i>T</i> (K)	<i>ρ</i> (kg m ⁻³)	<i>u</i> (kJ kg ⁻¹)	<i>h</i> (kJ kg ⁻¹)	<i>s</i> (kJ kg ⁻¹ K ⁻¹)	<i>c_v</i> (kJ kg ⁻¹ K ⁻¹)	<i>c_p</i> (kJ kg ⁻¹ K ⁻¹)	<i>w</i> (m s ⁻¹)
1.5 MPa							
135.15 ^a	735.34	-721.50	-719.46	-3.0352	1.4432	1.9723	1830.43
140	730.83	-711.93	-709.88	-2.9655	1.4434	1.9763	1798.62
145	726.20	-702.05	-699.98	-2.8961	1.4435	1.9806	1766.87
150	721.57	-692.15	-690.07	-2.8289	1.4438	1.9851	1735.91
155	716.94	-682.22	-680.13	-2.7637	1.4443	1.9901	1705.57
160	712.31	-672.27	-670.17	-2.7005	1.4452	1.9954	1675.73
165	707.67	-662.30	-660.18	-2.6390	1.4466	2.0013	1646.28
170	703.04	-652.29	-650.15	-2.5791	1.4486	2.0077	1617.16
175	698.39	-642.25	-640.10	-2.5208	1.4512	2.0147	1588.30
180	693.74	-632.17	-630.01	-2.4640	1.4544	2.0223	1559.66
185	689.07	-622.05	-619.87	-2.4085	1.4584	2.0306	1531.22
190	684.40	-611.89	-609.70	-2.3542	1.4630	2.0396	1502.94
195	679.71	-601.68	-599.48	-2.3011	1.4684	2.0494	1474.80
200	675.00	-591.43	-589.20	-2.2491	1.4745	2.0599	1446.80
210	665.53	-570.75	-568.49	-2.1480	1.4889	2.0832	1391.14
220	655.96	-549.82	-547.53	-2.0505	1.5063	2.1096	1335.91
230	646.27	-528.61	-526.29	-1.9561	1.5264	2.1393	1281.07
240	636.45	-507.09	-504.73	-1.8644	1.5491	2.1722	1226.60
250	626.46	-485.23	-482.83	-1.7750	1.5743	2.2084	1172.47
260	616.28	-462.99	-460.56	-1.6876	1.6018	2.2478	1118.64
270	605.87	-440.34	-437.87	-1.6020	1.6313	2.2906	1065.09
280	595.20	-417.25	-414.73	-1.5178	1.6627	2.3368	1011.75
290	584.21	-393.69	-391.12	-1.4350	1.6957	2.3867	958.53
300	572.86	-369.60	-366.99	-1.3532	1.7302	2.4405	905.33
310	561.06	-344.97	-342.29	-1.2722	1.7661	2.4988	851.98
320	548.74	-319.73	-316.99	-1.1919	1.8033	2.5624	798.29
330	535.78	-293.82	-291.02	-1.1120	1.8416	2.6325	743.98
340	522.02	-267.19	-264.31	-1.0322	1.8811	2.7112	688.63
350	507.25	-239.72	-236.76	-0.95239	1.9220	2.8018	631.67
360	491.14	-211.27	-208.22	-0.87199	1.9647	2.9105	572.19
370	473.15	-181.62	-178.45	-0.79043	2.0102	3.0500	508.67
372.27 ^b	468.71	-174.67	-171.47	-0.77163	2.0211	3.0885	493.40
372.27 ^c	38.593	49.613	88.480	-0.073352	2.0084	2.5814	180.43
380	36.498	67.054	108.15	-0.021049	2.0272	2.5173	188.38
390	34.300	89.350	133.08	0.043708	2.0552	2.4739	197.21
400	32.494	111.55	157.71	0.10607	2.0854	2.4556	204.92
425	29.027	167.44	219.12	0.25497	2.1689	2.4666	221.05
450	26.462	224.67	281.36	0.39726	2.2585	2.5165	234.40
475	24.436	283.69	345.07	0.53505	2.3498	2.5827	246.01
500	22.772	344.68	410.55	0.66937	2.4404	2.6562	256.43
525	21.367	407.71	477.91	0.80081	2.5293	2.7328	265.96
550	20.156	472.78	547.20	0.92973	2.6160	2.8102	274.81
575	19.096	539.87	618.42	1.0564	2.7002	2.8872	283.12
2 MPa							
135.23 ^a	735.46	-721.45	-718.73	-3.0348	1.4437	1.9722	1831.63
140	731.04	-712.05	-709.31	-2.9664	1.4439	1.9760	1800.47
145	726.42	-702.17	-699.42	-2.8970	1.4440	1.9803	1768.80
150	721.79	-692.28	-689.51	-2.8298	1.4442	1.9848	1737.92
155	717.17	-682.36	-679.57	-2.7646	1.4448	1.9897	1707.66
160	712.55	-672.42	-669.61	-2.7014	1.4457	1.9950	1677.90
165	707.93	-662.45	-659.62	-2.6399	1.4471	2.0008	1648.53
170	703.30	-652.45	-649.60	-2.5801	1.4490	2.0072	1619.49
175	698.67	-642.41	-639.55	-2.5218	1.4516	2.0142	1590.71
180	694.02	-632.34	-629.46	-2.4649	1.4549	2.0218	1562.16
185	689.37	-622.23	-619.33	-2.4094	1.4588	2.0300	1533.79

TABLE 45. Thermodynamic properties of *n*-butane in the single-phase region—Continued

<i>T</i> (K)	<i>ρ</i> (kg m ⁻³)	<i>u</i> (kJ kg ⁻¹)	<i>h</i> (kJ kg ⁻¹)	<i>s</i> (kJ kg ⁻¹ K ⁻¹)	<i>c_v</i> (kJ kg ⁻¹ K ⁻¹)	<i>c_p</i> (kJ kg ⁻¹ K ⁻¹)	<i>w</i> (m s ⁻¹)
190	684.71	-612.08	-609.16	-2.3552	1.4634	2.0390	1505.60
195	680.03	-601.88	-598.94	-2.3021	1.4688	2.0487	1477.55
200	675.33	-591.63	-588.67	-2.2501	1.4749	2.0591	1449.63
210	665.89	-570.97	-567.97	-2.1491	1.4894	2.0823	1394.16
220	656.35	-550.06	-547.01	-2.0516	1.5067	2.1086	1339.13
230	646.70	-528.88	-525.78	-1.9573	1.5268	2.1381	1284.50
240	636.91	-507.38	-504.24	-1.8656	1.5495	2.1708	1230.26
250	626.97	-485.55	-482.36	-1.7762	1.5747	2.2067	1176.38
260	616.84	-463.34	-460.10	-1.6889	1.6022	2.2459	1122.83
270	606.49	-440.72	-437.43	-1.6034	1.6317	2.2883	1069.59
280	595.88	-417.67	-414.32	-1.5194	1.6631	2.3340	1016.59
290	584.97	-394.15	-390.73	-1.4366	1.6961	2.3833	963.76
300	573.71	-370.13	-366.64	-1.3549	1.7306	2.4364	911.00
310	562.03	-345.55	-341.99	-1.2741	1.7665	2.4938	858.18
320	549.84	-320.38	-316.75	-1.1940	1.8036	2.5561	805.11
330	537.05	-294.57	-290.85	-1.1143	1.8418	2.6244	751.55
340	523.52	-268.05	-264.23	-1.0348	1.8811	2.7004	697.16
350	509.04	-240.74	-236.81	-0.95533	1.9218	2.7871	641.45
360	493.35	-212.50	-208.44	-0.87543	1.9641	2.8892	583.69
370	475.99	-183.14	-178.94	-0.79461	2.0087	3.0164	522.68
380	456.16	-152.35	-147.96	-0.71200	2.0571	3.1905	456.34
387.52 ^b	438.66	-127.84	-123.28	-0.64769	2.0982	3.3871	400.48
387.52 ^c	54.354	67.367	104.16	-0.060775	2.1106	2.9815	168.10
390	53.001	73.729	111.46	-0.041992	2.1139	2.9108	171.75
400	48.655	98.488	139.59	0.029236	2.1309	2.7376	184.18
425	41.696	157.90	205.86	0.18997	2.1950	2.6031	206.82
450	37.209	217.02	270.77	0.33839	2.2759	2.6008	223.72
475	33.913	277.27	336.24	0.47997	2.3623	2.6412	237.64
500	31.322	339.13	402.98	0.61688	2.4498	2.6997	249.70
525	29.201	402.81	471.30	0.75020	2.5367	2.7667	260.47
550	27.413	468.39	541.35	0.88053	2.6219	2.8375	270.29
575	25.876	535.89	613.18	1.0083	2.7050	2.9097	279.37
3 MPa							
135.40 ^a	735.72	-721.35	-717.27	-3.0341	1.4448	1.9718	1834.03
140	731.46	-712.29	-708.19	-2.9681	1.4449	1.9755	1804.14
145	726.85	-702.43	-698.30	-2.8987	1.4450	1.9797	1772.64
150	722.25	-692.54	-688.39	-2.8316	1.4452	1.9841	1741.92
155	717.64	-682.64	-678.46	-2.7664	1.4457	1.9890	1711.83
160	713.04	-672.71	-668.50	-2.7032	1.4466	1.9942	1682.22
165	708.44	-662.75	-658.51	-2.6417	1.4479	2.0000	1653.01
170	703.83	-652.76	-648.50	-2.5819	1.4499	2.0063	1624.13
175	699.21	-642.74	-638.45	-2.5237	1.4525	2.0132	1595.51
180	694.59	-632.68	-628.37	-2.4669	1.4557	2.0207	1567.12
185	689.96	-622.59	-618.24	-2.4114	1.4596	2.0289	1538.92
190	685.32	-612.45	-608.08	-2.3572	1.4643	2.0377	1510.89
195	680.66	-602.27	-597.86	-2.3041	1.4697	2.0473	1483.01
200	675.99	-592.04	-587.60	-2.2522	1.4758	2.0577	1455.27
210	666.60	-571.41	-566.91	-2.1512	1.4902	2.0806	1400.16
220	657.12	-550.54	-545.98	-2.0538	1.5075	2.1067	1345.52
230	647.54	-529.40	-524.77	-1.9596	1.5276	2.1358	1291.30
240	637.83	-507.96	-503.25	-1.8680	1.5504	2.1681	1237.51
250	627.97	-486.17	-481.40	-1.7788	1.5756	2.2036	1184.12
260	617.94	-464.02	-459.17	-1.6916	1.6030	2.2421	1131.11
270	607.70	-441.48	-436.54	-1.6062	1.6325	2.2838	1078.45
280	597.23	-418.51	-413.48	-1.5224	1.6639	2.3287	1026.11
290	586.47	-395.07	-389.96	-1.4398	1.6969	2.3770	974.03

TABLE 45. Thermodynamic properties of *n*-butane in the single-phase region—Continued

<i>T</i> (K)	<i>ρ</i> (kg m ⁻³)	<i>u</i> (kJ kg ⁻¹)	<i>h</i> (kJ kg ⁻¹)	<i>s</i> (kJ kg ⁻¹ K ⁻¹)	<i>c_v</i> (kJ kg ⁻¹ K ⁻¹)	<i>c_p</i> (kJ kg ⁻¹ K ⁻¹)	<i>w</i> (m s ⁻¹)
300	575.38	-371.15	-365.93	-1.3584	1.7314	2.4287	922.12
310	563.91	-346.69	-341.37	-1.2778	1.7672	2.4843	870.28
320	551.99	-321.67	-316.23	-1.1980	1.8042	2.5442	818.38
330	539.52	-296.03	-290.47	-1.1188	1.8422	2.6094	766.22
340	526.39	-269.72	-264.02	-1.0398	1.8814	2.6809	713.55
350	512.45	-242.68	-236.82	-0.96097	1.9216	2.7608	660.04
360	497.49	-214.80	-208.77	-0.88194	1.9631	2.8524	605.20
370	481.18	-185.95	-179.72	-0.80236	2.0064	2.9613	548.29
380	463.01	-155.93	-149.45	-0.72164	2.0523	3.0991	488.16
390	442.07	-124.34	-117.56	-0.63881	2.1025	3.2922	422.81
400	416.28	-90.374	-83.167	-0.55176	2.1613	3.6230	348.01
410.85 ^b	373.96	-47.336	-39.314	-0.44365	2.2544	4.8011	240.08
410.85 ^c	97.769	85.407	116.09	-0.065396	2.3149	5.0191	140.09
425	77.966	131.67	170.15	0.064116	2.2720	3.2856	170.11
450	63.746	198.71	245.77	0.23711	2.3178	2.8797	199.45
475	55.802	262.79	316.55	0.39020	2.3902	2.8046	219.69
500	50.326	327.03	386.64	0.53401	2.4700	2.8102	235.76
525	46.182	392.36	457.32	0.67194	2.5519	2.8477	249.35
550	42.869	459.17	529.15	0.80559	2.6339	2.9001	261.29
575	40.127	527.63	602.39	0.93581	2.7147	2.9599	272.03
4 MPa							
135.56 ^a	735.97	-721.25	-715.82	-3.0334	1.4459	1.9715	1836.44
140	731.88	-712.53	-707.06	-2.9699	1.4460	1.9750	1807.80
145	727.29	-702.68	-697.18	-2.9005	1.4460	1.9791	1776.46
150	722.70	-692.80	-687.27	-2.8333	1.4461	1.9835	1745.91
155	718.11	-682.91	-677.34	-2.7682	1.4466	1.9883	1715.97
160	713.53	-672.99	-667.39	-2.7050	1.4475	1.9935	1686.52
165	708.94	-663.05	-657.40	-2.6436	1.4488	1.9992	1657.47
170	704.35	-653.07	-647.39	-2.5838	1.4508	2.0054	1628.74
175	699.76	-643.07	-637.35	-2.5256	1.4533	2.0122	1600.27
180	695.15	-633.02	-627.27	-2.4688	1.4566	2.0196	1572.04
185	690.54	-622.95	-617.15	-2.4133	1.4605	2.0277	1544.00
190	685.93	-612.82	-606.99	-2.3591	1.4651	2.0365	1516.14
195	681.29	-602.66	-596.79	-2.3061	1.4705	2.0460	1488.42
200	676.65	-592.44	-586.53	-2.2542	1.4766	2.0563	1460.85
210	667.31	-571.85	-565.86	-2.1533	1.4910	2.0790	1406.10
220	657.89	-551.02	-544.94	-2.0560	1.5084	2.1047	1351.83
230	648.37	-529.92	-523.75	-1.9618	1.5285	2.1336	1298.03
240	638.74	-508.52	-502.26	-1.8704	1.5512	2.1655	1244.67
250	628.96	-486.79	-480.43	-1.7813	1.5764	2.2005	1191.74
260	619.03	-464.70	-458.24	-1.6942	1.6039	2.2386	1139.25
270	608.90	-442.22	-435.65	-1.6090	1.6334	2.2796	1087.16
280	598.54	-419.32	-412.64	-1.5253	1.6647	2.3237	1035.45
290	587.93	-395.97	-389.16	-1.4429	1.6977	2.3710	984.07
300	577.01	-372.14	-365.21	-1.3617	1.7322	2.4215	932.96
310	565.74	-347.79	-340.72	-1.2815	1.7679	2.4755	882.04
320	554.06	-322.90	-315.68	-1.2020	1.8048	2.5333	831.19
330	541.88	-297.42	-290.04	-1.1231	1.8428	2.5957	780.29
340	529.12	-271.31	-263.75	-1.0446	1.8817	2.6635	729.15
350	515.65	-244.51	-236.75	-0.96632	1.9216	2.7380	677.52
360	501.31	-216.94	-208.96	-0.88804	1.9626	2.8215	625.09
370	485.85	-188.51	-180.28	-0.80946	2.0049	2.9176	571.39
380	468.94	-159.07	-150.54	-0.73017	2.0491	3.0328	515.76
390	450.02	-128.41	-119.52	-0.64958	2.0960	3.1798	457.18
400	428.06	-96.091	-86.747	-0.56663	2.1476	3.3888	393.91
425	323.28	6.3288	18.702	-0.31172	2.3640	7.3685	173.79

TABLE 45. Thermodynamic properties of *n*-butane in the single-phase region—Continued

<i>T</i> (K)	<i>ρ</i> (kg m ⁻³)	<i>u</i> (kJ kg ⁻¹)	<i>h</i> (kJ kg ⁻¹)	<i>s</i> (kJ kg ⁻¹ K ⁻¹)	<i>c_v</i> (kJ kg ⁻¹ K ⁻¹)	<i>c_p</i> (kJ kg ⁻¹ K ⁻¹)	<i>w</i> (m s ⁻¹)
450	103.34	173.18	211.89	0.13415	2.3741	3.5686	171.01
475	83.422	245.34	293.29	0.31031	2.4223	3.0750	200.70
500	72.576	313.35	368.46	0.46457	2.4916	2.9647	221.71
525	65.226	380.96	442.29	0.60865	2.5677	2.9508	238.48
550	59.727	449.34	516.31	0.74639	2.6460	2.9751	252.67
575	55.370	518.95	591.19	0.87953	2.7242	3.0176	265.11
5 MPa							
135.73 ^a	736.22	-721.15	-714.36	-3.0327	1.4469	1.9711	1838.84
140	732.30	-712.76	-705.94	-2.9716	1.4470	1.9745	1811.44
145	727.72	-702.92	-696.05	-2.9022	1.4469	1.9785	1780.27
150	723.15	-693.06	-686.15	-2.8351	1.4471	1.9829	1749.87
155	718.58	-683.18	-676.22	-2.7700	1.4475	1.9876	1720.09
160	714.01	-673.28	-666.27	-2.7068	1.4483	1.9927	1690.80
165	709.44	-663.34	-656.30	-2.6454	1.4497	1.9983	1661.89
170	704.87	-653.38	-646.29	-2.5856	1.4516	2.0045	1633.32
175	700.29	-643.39	-636.25	-2.5274	1.4542	2.0113	1605.01
180	695.71	-633.36	-626.17	-2.4707	1.4574	2.0186	1576.93
185	691.13	-623.30	-616.06	-2.4153	1.4613	2.0266	1549.05
190	686.53	-613.19	-605.91	-2.3611	1.4660	2.0353	1521.34
195	681.92	-603.04	-595.71	-2.3081	1.4713	2.0447	1493.79
200	677.30	-592.84	-585.46	-2.2562	1.4775	2.0549	1466.39
210	668.01	-572.28	-564.80	-2.1554	1.4919	2.0774	1411.99
220	658.65	-551.49	-543.90	-2.0582	1.5092	2.1029	1358.09
230	649.20	-530.43	-522.73	-1.9641	1.5293	2.1314	1304.67
240	639.63	-509.08	-501.26	-1.8727	1.5521	2.1630	1251.73
250	629.94	-487.40	-479.46	-1.7838	1.5773	2.1976	1199.27
260	620.09	-465.36	-457.30	-1.6968	1.6047	2.2351	1147.27
270	610.07	-442.94	-434.75	-1.6117	1.6342	2.2756	1095.73
280	599.83	-420.11	-411.78	-1.5282	1.6656	2.3190	1044.62
290	589.35	-396.84	-388.36	-1.4460	1.6986	2.3653	993.90
300	578.60	-373.10	-364.46	-1.3650	1.7330	2.4147	943.54
310	567.52	-348.87	-340.06	-1.2850	1.7687	2.4672	893.47
320	556.05	-324.10	-315.11	-1.2058	1.8055	2.5233	843.60
330	544.15	-298.77	-289.58	-1.1272	1.8433	2.5833	793.83
340	531.72	-272.83	-263.43	-1.0492	1.8821	2.6479	744.04
350	518.67	-246.24	-236.60	-0.97142	1.9218	2.7180	694.05
360	504.86	-218.94	-209.04	-0.89378	1.9623	2.7952	643.65
370	490.12	-190.87	-180.66	-0.81604	2.0040	2.8818	592.54
380	474.21	-161.90	-151.36	-0.73790	2.0470	2.9817	540.35
390	456.75	-131.91	-120.96	-0.65895	2.0919	3.1017	486.52
400	437.17	-100.65	-89.216	-0.57858	2.1395	3.2553	430.26
425	368.63	-12.880	0.68419	-0.36083	2.2866	4.1643	268.65
450	181.40	129.67	157.23	-0.003956	2.4489	6.0356	147.05
475	120.32	223.58	265.14	0.22994	2.4572	3.5473	182.95
500	99.106	297.76	348.22	0.40048	2.5139	3.1801	208.77
525	86.713	368.53	426.20	0.55269	2.5835	3.0798	228.60
550	78.133	438.88	502.88	0.69538	2.6578	3.0632	244.93
575	71.657	509.87	579.65	0.83188	2.7335	3.0826	258.98
6 MPa							
135.90 ^a	736.47	-721.05	-712.90	-3.0320	1.4480	1.9708	1841.24
140	732.72	-713.00	-704.81	-2.9733	1.4480	1.9740	1815.06
145	728.15	-703.17	-694.93	-2.9039	1.4479	1.9780	1784.05
150	723.59	-693.32	-685.03	-2.8368	1.4480	1.9823	1753.82
155	719.04	-683.45	-675.11	-2.7717	1.4484	1.9869	1724.19
160	714.49	-673.56	-665.16	-2.7086	1.4492	1.9920	1695.04

TABLE 45. Thermodynamic properties of *n*-butane in the single-phase region—Continued

<i>T</i> (K)	<i>ρ</i> (kg m ⁻³)	<i>u</i> (kJ kg ⁻¹)	<i>h</i> (kJ kg ⁻¹)	<i>s</i> (kJ kg ⁻¹ K ⁻¹)	<i>c_v</i> (kJ kg ⁻¹ K ⁻¹)	<i>c_p</i> (kJ kg ⁻¹ K ⁻¹)	<i>w</i> (m s ⁻¹)
165	709.94	-663.64	-655.18	-2.6472	1.4506	1.9976	1666.29
170	705.38	-653.69	-645.18	-2.5875	1.4525	2.0037	1637.86
175	700.83	-643.71	-635.15	-2.5293	1.4550	2.0103	1609.71
180	696.27	-633.70	-625.08	-2.4726	1.4582	2.0176	1581.78
185	691.70	-623.64	-614.97	-2.4172	1.4622	2.0256	1554.05
190	687.13	-613.55	-604.82	-2.3630	1.4668	2.0342	1526.51
195	682.54	-603.42	-594.63	-2.3101	1.4722	2.0435	1499.12
200	677.94	-593.24	-584.38	-2.2582	1.4783	2.0535	1471.88
210	668.71	-572.71	-563.74	-2.1575	1.4927	2.0758	1417.82
220	659.40	-551.96	-542.86	-2.0604	1.5100	2.1011	1364.27
230	650.01	-530.94	-521.71	-1.9664	1.5302	2.1294	1311.24
240	640.52	-509.63	-500.26	-1.8751	1.5529	2.1606	1258.71
250	630.90	-488.00	-478.49	-1.7862	1.5781	2.1948	1206.69
260	621.14	-466.02	-456.36	-1.6994	1.6056	2.2318	1155.17
270	611.22	-443.66	-433.84	-1.6144	1.6351	2.2717	1104.15
280	601.09	-420.89	-410.91	-1.5311	1.6664	2.3144	1053.61
290	590.75	-397.70	-387.54	-1.4491	1.6994	2.3599	1003.53
300	580.14	-374.05	-363.70	-1.3682	1.7338	2.4082	953.87
310	569.24	-349.91	-339.37	-1.2885	1.7694	2.4596	904.59
320	557.99	-325.26	-314.50	-1.2095	1.8062	2.5140	855.63
330	546.33	-300.06	-289.08	-1.1313	1.8440	2.5720	806.90
340	534.21	-274.28	-263.05	-1.0536	1.8826	2.6338	758.32
350	521.53	-247.89	-236.38	-0.97629	1.9220	2.7003	709.77
360	508.19	-220.83	-209.03	-0.89923	1.9623	2.7724	661.11
370	494.07	-193.06	-180.91	-0.82220	2.0034	2.8518	612.15
380	478.96	-164.49	-151.96	-0.74499	2.0456	2.9407	562.68
390	462.64	-135.02	-122.05	-0.66732	2.0891	3.0431	512.40
400	444.73	-104.52	-91.030	-0.58878	2.1344	3.1659	460.93
425	388.16	-21.802	-6.3447	-0.38358	2.2619	3.6871	323.48
450	283.15	83.063	104.25	-0.13121	2.4274	5.4936	183.67
475	170.54	196.74	231.93	0.14529	2.4863	4.2388	173.78
500	130.83	280.19	326.05	0.33858	2.5344	3.4608	199.24
525	110.89	355.11	409.21	0.50092	2.5982	3.2340	220.82
550	98.146	427.86	488.99	0.64938	2.6689	3.1631	238.72
575	88.983	500.44	567.87	0.78964	2.7423	3.1539	254.03
7 MPa							
136.06 ^a	736.72	-720.95	-711.45	-3.0312	1.4490	1.9705	1843.65
140	733.13	-713.23	-703.68	-2.9750	1.4490	1.9735	1818.67
145	728.58	-703.41	-693.80	-2.9057	1.4489	1.9774	1787.82
150	724.04	-693.58	-683.91	-2.8385	1.4489	1.9817	1757.74
155	719.50	-683.72	-673.99	-2.7735	1.4493	1.9863	1728.26
160	714.97	-673.83	-664.04	-2.7104	1.4501	1.9913	1699.27
165	710.43	-663.93	-654.07	-2.6490	1.4514	1.9968	1670.66
170	705.90	-653.99	-644.08	-2.5893	1.4533	2.0028	1642.38
175	701.36	-644.03	-634.04	-2.5312	1.4559	2.0094	1614.38
180	696.82	-634.03	-623.98	-2.4744	1.4591	2.0166	1586.60
185	692.27	-623.99	-613.88	-2.4191	1.4630	2.0245	1559.02
190	687.72	-613.91	-603.73	-2.3650	1.4676	2.0331	1531.63
195	683.16	-603.79	-593.55	-2.3121	1.4730	2.0423	1504.40
200	678.58	-593.63	-583.31	-2.2602	1.4791	2.0522	1477.32
210	669.40	-573.14	-562.68	-2.1596	1.4935	2.0743	1423.59
220	660.15	-552.42	-541.81	-2.0625	1.5109	2.0993	1370.40
230	650.82	-531.44	-520.68	-1.9686	1.5310	2.1273	1317.74
240	641.39	-510.17	-499.26	-1.8774	1.5537	2.1583	1265.61
250	631.85	-488.59	-477.51	-1.7886	1.5789	2.1921	1214.01
260	622.18	-466.66	-455.41	-1.7019	1.6064	2.2287	1162.96

TABLE 45. Thermodynamic properties of *n*-butane in the single-phase region—Continued

<i>T</i> (K)	<i>ρ</i> (kg m ⁻³)	<i>u</i> (kJ kg ⁻¹)	<i>h</i> (kJ kg ⁻¹)	<i>s</i> (kJ kg ⁻¹ K ⁻¹)	<i>c_v</i> (kJ kg ⁻¹ K ⁻¹)	<i>c_p</i> (kJ kg ⁻¹ K ⁻¹)	<i>w</i> (m s ⁻¹)
270	612.35	-444.36	-432.93	-1.6171	1.6359	2.2680	1112.44
280	602.33	-421.66	-410.04	-1.5339	1.6672	2.3101	1062.44
290	592.11	-398.54	-386.71	-1.4520	1.7002	2.3548	1012.96
300	581.65	-374.97	-362.93	-1.3714	1.7346	2.4022	963.97
310	570.91	-350.92	-338.66	-1.2918	1.7702	2.4524	915.43
320	559.86	-326.38	-313.88	-1.2131	1.8069	2.5054	867.31
330	548.44	-301.31	-288.54	-1.1352	1.8446	2.5615	819.53
340	536.59	-275.68	-262.63	-1.0579	1.8831	2.6210	772.05
350	524.25	-249.46	-236.11	-0.98097	1.9224	2.6844	724.78
360	511.34	-222.62	-208.93	-0.90441	1.9624	2.7524	677.63
370	497.74	-195.11	-181.04	-0.82801	2.0031	2.8260	630.49
380	483.32	-166.87	-152.39	-0.75159	2.0447	2.9068	583.24
390	467.90	-137.84	-122.88	-0.67494	2.0872	2.9970	535.73
400	451.25	-107.91	-92.402	-0.59779	2.1310	3.1004	487.80
425	401.52	-28.161	-10.727	-0.39984	2.2488	3.4703	364.86
450	328.25	63.449	84.774	-0.18172	2.3853	4.2898	241.44
475	227.20	169.50	200.31	0.068085	2.4922	4.5411	185.34
500	167.34	261.28	303.11	0.27918	2.5490	3.7501	196.73
525	137.61	340.93	391.80	0.45233	2.6105	3.4007	216.59
550	119.65	416.40	474.91	0.60701	2.6787	3.2699	234.78
575	107.25	490.76	556.02	0.75124	2.7501	3.2290	250.72
8 MPa							
136.23 ^a	736.96	-720.85	-709.99	-3.0305	1.4501	1.9702	1846.05
140	733.54	-713.46	-702.55	-2.9767	1.4500	1.9730	1822.26
145	729.01	-703.65	-692.68	-2.9074	1.4498	1.9769	1791.57
150	724.48	-693.83	-682.79	-2.8403	1.4498	1.9811	1761.64
155	719.96	-683.98	-672.87	-2.7752	1.4502	1.9856	1732.31
160	715.44	-674.11	-662.93	-2.7121	1.4510	1.9906	1703.47
165	710.92	-664.22	-652.96	-2.6508	1.4523	1.9960	1675.01
170	706.41	-654.29	-642.97	-2.5911	1.4542	2.0020	1646.88
175	701.89	-644.34	-632.94	-2.5330	1.4567	2.0085	1619.01
180	697.37	-634.35	-622.88	-2.4763	1.4599	2.0157	1591.38
185	692.84	-624.33	-612.78	-2.4210	1.4638	2.0235	1563.96
190	688.31	-614.27	-602.65	-2.3669	1.4685	2.0320	1536.72
195	683.77	-604.16	-592.46	-2.3140	1.4738	2.0411	1509.64
200	679.21	-594.01	-582.23	-2.2622	1.4799	2.0510	1482.72
210	670.08	-573.56	-561.62	-2.1616	1.4944	2.0728	1429.31
220	660.88	-552.87	-540.77	-2.0646	1.5117	2.0977	1376.47
230	651.61	-531.93	-519.65	-1.9708	1.5318	2.1254	1324.17
240	642.25	-510.71	-498.25	-1.8797	1.5546	2.1560	1272.43
250	632.79	-489.17	-476.52	-1.7910	1.5798	2.1894	1221.24
260	623.19	-467.29	-454.45	-1.7044	1.6072	2.2256	1170.63
270	613.46	-445.04	-432.00	-1.6197	1.6367	2.2645	1120.59
280	603.55	-422.41	-409.15	-1.5366	1.6681	2.3059	1071.12
290	593.45	-399.36	-385.88	-1.4550	1.7010	2.3500	1022.22
300	583.12	-375.86	-362.15	-1.3745	1.7354	2.3965	973.86
310	572.55	-351.91	-337.94	-1.2951	1.7710	2.4456	926.02
320	561.67	-327.47	-313.22	-1.2167	1.8077	2.4973	878.67
330	550.47	-302.51	-287.98	-1.1390	1.8453	2.5518	831.77
340	538.88	-277.02	-262.18	-1.0620	1.8837	2.6093	785.29
350	526.85	-250.97	-235.78	-0.98548	1.9228	2.6701	739.16
360	514.31	-224.32	-208.76	-0.90936	1.9626	2.7347	693.34
370	501.18	-197.04	-181.08	-0.83351	2.0031	2.8037	647.77
380	487.34	-169.09	-152.67	-0.75776	2.0442	2.8782	602.38
390	472.68	-140.41	-123.49	-0.68196	2.0860	2.9595	557.10

TABLE 45. Thermodynamic properties of *n*-butane in the single-phase region—Continued

<i>T</i> (K)	ρ (kg m ⁻³)	<i>u</i> (kJ kg ⁻¹)	<i>h</i> (kJ kg ⁻¹)	<i>s</i> (kJ kg ⁻¹ K ⁻¹)	c_v (kJ kg ⁻¹ K ⁻¹)	c_p (kJ kg ⁻¹ K ⁻¹)	<i>w</i> (m s ⁻¹)
400	457.03	-110.96	-93.452	-0.60592	2.1287	3.0497	511.89
425	411.91	-33.246	-13.824	-0.41291	2.2408	3.3406	398.89
450	352.51	52.524	75.218	-0.20946	2.3628	3.8305	288.93
475	272.66	148.95	178.29	0.013324	2.4781	4.2991	214.33
500	205.16	242.87	281.86	0.22591	2.5541	3.9184	204.38
525	165.98	326.55	374.75	0.40726	2.6189	3.5500	217.43
550	142.26	404.76	460.99	0.56778	2.6865	3.3739	233.85
575	126.25	480.94	544.31	0.71593	2.7568	3.3035	249.45
10 MPa							
136.56 ^a	737.46	-720.64	-707.08	-3.0291	1.4521	1.9695	1850.85
140	734.35	-713.92	-700.30	-2.9800	1.4519	1.9720	1829.40
145	729.85	-704.13	-690.43	-2.9108	1.4517	1.9758	1799.01
150	725.35	-694.33	-680.54	-2.8437	1.4516	1.9799	1769.39
155	720.87	-684.50	-670.63	-2.7787	1.4519	1.9844	1740.35
160	716.38	-674.66	-660.70	-2.7156	1.4527	1.9892	1711.79
165	711.90	-664.79	-650.74	-2.6543	1.4540	1.9945	1683.62
170	707.42	-654.89	-640.75	-2.5947	1.4558	2.0004	1655.77
175	702.93	-644.96	-630.73	-2.5366	1.4584	2.0068	1628.20
180	698.45	-635.00	-620.68	-2.4800	1.4616	2.0139	1600.86
185	693.96	-625.00	-610.59	-2.4247	1.4655	2.0215	1573.72
190	689.47	-614.97	-600.47	-2.3707	1.4701	2.0298	1546.77
195	684.97	-604.89	-590.29	-2.3179	1.4754	2.0388	1520.00
200	680.46	-594.77	-580.08	-2.2661	1.4816	2.0485	1493.38
210	671.42	-574.38	-559.49	-2.1657	1.4960	2.0700	1440.61
220	662.33	-553.76	-538.67	-2.0688	1.5133	2.0944	1388.42
230	653.18	-532.90	-517.59	-1.9751	1.5334	2.1216	1336.82
240	643.95	-511.75	-496.22	-1.8842	1.5562	2.1517	1285.82
250	634.62	-490.30	-474.54	-1.7957	1.5814	2.1845	1235.43
260	625.19	-468.52	-452.53	-1.7094	1.6089	2.2199	1185.67
270	615.62	-446.38	-430.14	-1.6249	1.6384	2.2578	1136.54
280	605.92	-423.86	-407.36	-1.5420	1.6697	2.2982	1088.05
290	596.04	-400.94	-384.17	-1.4607	1.7026	2.3410	1040.22
300	585.97	-377.60	-360.53	-1.3805	1.7370	2.3860	993.02
310	575.69	-353.81	-336.44	-1.3015	1.7726	2.4333	946.46
320	565.15	-329.56	-311.86	-1.2235	1.8092	2.4828	900.52
330	554.34	-304.82	-286.78	-1.1463	1.8467	2.5345	855.19
340	543.21	-279.57	-261.16	-1.0699	1.8850	2.5886	810.46
350	531.73	-253.80	-235.00	-0.99402	1.9239	2.6452	766.31
360	519.84	-227.49	-208.25	-0.91868	1.9634	2.7044	722.73
370	507.48	-200.60	-180.90	-0.84374	2.0033	2.7666	679.71
380	494.61	-173.13	-152.91	-0.76910	2.0438	2.8321	637.27
390	481.14	-145.03	-124.24	-0.69465	2.0847	2.9014	595.40
400	466.99	-116.28	-94.864	-0.62027	2.1261	2.9752	554.16
425	427.92	-41.303	-17.934	-0.43378	2.2319	3.1867	454.17
450	381.75	38.769	64.965	-0.24432	2.3409	3.4571	360.83
475	326.38	124.68	155.32	-0.048978	2.4488	3.7644	283.79
500	267.88	213.86	251.19	0.14770	2.5435	3.8442	243.50
525	220.83	300.18	345.47	0.33172	2.6224	3.6837	236.18
550	187.96	382.25	435.45	0.49920	2.6947	3.5247	242.94
575	164.98	461.64	522.25	0.65355	2.7658	3.4297	254.32
15 MPa							
137.38 ^a	738.69	-720.12	-699.81	-3.0255	1.4569	1.9680	1862.83
140	736.36	-715.03	-694.66	-2.9883	1.4566	1.9698	1846.96
145	731.93	-705.29	-684.80	-2.9191	1.4562	1.9734	1817.32
150	727.51	-695.54	-674.92	-2.8521	1.4561	1.9772	1788.41

TABLE 45. Thermodynamic properties of *n*-butane in the single-phase region—Continued

<i>T</i> (K)	<i>ρ</i> (kg m ⁻³)	<i>u</i> (kJ kg ⁻¹)	<i>h</i> (kJ kg ⁻¹)	<i>s</i> (kJ kg ⁻¹ K ⁻¹)	<i>c_v</i> (kJ kg ⁻¹ K ⁻¹)	<i>c_p</i> (kJ kg ⁻¹ K ⁻¹)	<i>w</i> (m s ⁻¹)
155	723.09	-685.77	-665.03	-2.7872	1.4562	1.9814	1760.08
160	718.68	-675.98	-655.11	-2.7243	1.4569	1.9860	1732.21
165	714.28	-666.17	-645.17	-2.6631	1.4581	1.9911	1704.72
170	709.88	-656.33	-635.20	-2.6036	1.4599	1.9967	1677.55
175	705.49	-646.46	-625.20	-2.5456	1.4624	2.0029	1650.65
180	701.09	-636.56	-615.17	-2.4891	1.4656	2.0096	1623.99
185	696.70	-626.63	-605.10	-2.4339	1.4695	2.0169	1597.54
190	692.30	-616.66	-595.00	-2.3800	1.4741	2.0249	1571.29
195	687.90	-606.66	-584.85	-2.3273	1.4794	2.0336	1545.21
200	683.50	-596.61	-574.66	-2.2757	1.4855	2.0429	1519.31
210	674.68	-576.36	-554.13	-2.1755	1.5000	2.0636	1468.01
220	665.84	-555.91	-533.38	-2.0790	1.5173	2.0871	1417.36
230	656.95	-535.21	-512.38	-1.9857	1.5375	2.1132	1367.36
240	648.01	-514.25	-491.11	-1.8951	1.5602	2.1421	1318.05
250	639.01	-493.00	-469.53	-1.8071	1.5855	2.1734	1269.45
260	629.93	-471.44	-447.63	-1.7212	1.6130	2.2073	1221.58
270	620.76	-449.54	-425.38	-1.6372	1.6425	2.2433	1174.47
280	611.49	-427.29	-402.75	-1.5549	1.6738	2.2816	1128.13
290	602.11	-404.65	-379.74	-1.4742	1.7067	2.3218	1082.60
300	592.59	-381.62	-356.31	-1.3948	1.7410	2.3639	1037.88
310	582.93	-358.19	-332.46	-1.3165	1.7765	2.4077	993.98
320	573.10	-334.33	-308.15	-1.2394	1.8130	2.4532	950.91
330	563.09	-310.02	-283.39	-1.1632	1.8504	2.5002	908.70
340	552.88	-285.27	-258.14	-1.0878	1.8885	2.5486	867.35
350	542.45	-260.06	-232.41	-1.0132	1.9271	2.5983	826.88
360	531.78	-234.38	-206.17	-0.93932	1.9662	2.6494	787.32
370	520.84	-208.22	-179.42	-0.86602	2.0056	2.7016	748.70
380	509.62	-181.57	-152.14	-0.79326	2.0452	2.7550	711.06
390	498.10	-154.43	-124.31	-0.72100	2.0851	2.8095	674.46
400	486.25	-126.79	-95.943	-0.64917	2.1251	2.8651	638.95
425	455.08	-55.501	-22.539	-0.47121	2.2251	3.0081	555.43
450	421.55	18.918	54.501	-0.29511	2.3247	3.1557	480.47
475	385.71	96.351	135.24	-0.12053	2.4224	3.3024	415.81
500	348.26	176.39	219.46	0.052246	2.5166	3.4296	364.35
525	311.23	258.09	306.28	0.22167	2.6058	3.5054	329.52
550	277.44	340.18	394.25	0.38535	2.6895	3.5242	311.03
575	248.60	421.92	482.26	0.54185	2.7684	3.5148	304.22
20 MPa							
138.20 ^a	739.89	-719.59	-692.55	-3.0219	1.4615	1.9666	1874.77
140	738.32	-716.10	-689.01	-2.9964	1.4612	1.9678	1864.15
145	733.95	-706.41	-679.16	-2.9273	1.4606	1.9711	1835.21
150	729.60	-696.71	-669.30	-2.8604	1.4603	1.9748	1806.98
155	725.26	-686.99	-659.42	-2.7956	1.4604	1.9787	1779.31
160	720.92	-677.25	-649.51	-2.7327	1.4610	1.9832	1752.08
165	716.60	-667.49	-639.58	-2.6716	1.4621	1.9880	1725.23
170	712.28	-657.71	-629.63	-2.6122	1.4639	1.9934	1698.69
175	707.96	-647.90	-619.65	-2.5543	1.4663	1.9993	1672.42
180	703.65	-638.06	-609.64	-2.4979	1.4695	2.0058	1646.39
185	699.34	-628.19	-599.59	-2.4428	1.4733	2.0129	1620.58
190	695.04	-618.28	-589.51	-2.3891	1.4779	2.0206	1594.96
195	690.73	-608.34	-579.38	-2.3365	1.4833	2.0289	1569.53
200	686.43	-598.35	-569.22	-2.2850	1.4894	2.0379	1544.29
210	677.81	-578.25	-548.74	-2.1851	1.5038	2.0580	1494.32
220	669.18	-557.94	-528.05	-2.0888	1.5212	2.0806	1445.05
230	660.54	-537.40	-507.12	-1.9958	1.5414	2.1059	1396.49

TABLE 45. Thermodynamic properties of *n*-butane in the single-phase region—Continued

<i>T</i> (K)	<i>ρ</i> (kg m ⁻³)	<i>u</i> (kJ kg ⁻¹)	<i>h</i> (kJ kg ⁻¹)	<i>s</i> (kJ kg ⁻¹ K ⁻¹)	<i>c_v</i> (kJ kg ⁻¹ K ⁻¹)	<i>c_p</i> (kJ kg ⁻¹ K ⁻¹)	<i>w</i> (m s ⁻¹)
240	651.86	-516.60	-485.92	-1.9056	1.5642	2.1338	1348.67
250	643.14	-495.53	-464.43	-1.8179	1.5894	2.1641	1301.63
260	634.37	-474.16	-442.63	-1.7324	1.6169	2.1966	1255.40
270	625.55	-452.47	-420.49	-1.6488	1.6464	2.2313	1210.01
280	616.65	-430.43	-398.00	-1.5670	1.6778	2.2679	1165.48
290	607.68	-408.04	-375.13	-1.4868	1.7107	2.3064	1121.84
300	598.62	-385.28	-351.87	-1.4079	1.7450	2.3464	1079.12
310	589.46	-362.13	-328.20	-1.3303	1.7805	2.3879	1037.34
320	580.20	-338.58	-304.11	-1.2538	1.8169	2.4306	996.50
330	570.81	-314.62	-279.58	-1.1784	1.8542	2.4745	956.64
340	561.29	-290.24	-254.61	-1.1038	1.8922	2.5194	917.76
350	551.63	-265.45	-229.19	-1.0301	1.9307	2.5652	879.90
360	541.83	-240.22	-203.31	-0.95722	1.9696	2.6117	843.08
370	531.86	-214.56	-176.95	-0.88502	2.0087	2.6588	807.33
380	521.73	-188.46	-150.13	-0.81348	2.0481	2.7063	772.69
390	511.43	-161.93	-122.83	-0.74257	2.0875	2.7542	739.20
400	500.95	-134.97	-95.042	-0.67223	2.1270	2.8023	706.89
425	473.97	-65.679	-23.482	-0.49873	2.2253	2.9224	631.64
450	445.92	6.2068	51.058	-0.32834	2.3223	3.0403	564.80
475	417.01	80.529	128.49	-0.16091	2.4173	3.1532	506.91
500	387.62	157.04	208.64	0.003511	2.5094	3.2566	458.47
525	358.40	235.38	291.19	0.16460	2.5981	3.3440	420.11
550	330.27	315.10	375.65	0.32176	2.6832	3.4097	392.21
575	304.14	395.73	461.49	0.47438	2.7647	3.4544	374.06
25 MPa							
139.01 ^a	741.09	-719.04	-685.31	-3.0183	1.4658	1.9653	1886.67
140	740.24	-717.13	-683.36	-3.0043	1.4656	1.9659	1880.99
145	735.94	-707.49	-673.52	-2.9353	1.4649	1.9690	1852.72
150	731.65	-697.84	-663.67	-2.8685	1.4644	1.9725	1825.13
155	727.37	-688.17	-653.80	-2.8037	1.4644	1.9763	1798.07
160	723.11	-678.48	-643.91	-2.7409	1.4649	1.9805	1771.45
165	718.85	-668.77	-633.99	-2.6799	1.4660	1.9852	1745.19
170	714.60	-659.04	-624.05	-2.6206	1.4677	1.9904	1719.24
175	710.36	-649.28	-614.09	-2.5628	1.4701	1.9961	1693.56
180	706.13	-639.49	-604.09	-2.5065	1.4733	2.0024	1668.12
185	701.90	-629.68	-594.06	-2.4515	1.4771	2.0092	1642.90
190	697.68	-619.83	-584.00	-2.3979	1.4817	2.0167	1617.87
195	693.46	-609.95	-573.89	-2.3454	1.4871	2.0248	1593.04
200	689.24	-600.02	-563.75	-2.2940	1.4932	2.0335	1568.39
210	680.82	-580.04	-543.32	-2.1943	1.5076	2.0530	1519.64
220	672.39	-559.86	-522.68	-2.0983	1.5250	2.0750	1471.63
230	663.96	-539.46	-501.81	-2.0055	1.5452	2.0996	1424.36
240	655.52	-518.82	-480.68	-1.9156	1.5680	2.1267	1377.88
250	647.05	-497.91	-459.27	-1.8282	1.5933	2.1560	1332.22
260	638.56	-476.70	-437.55	-1.7431	1.6208	2.1876	1287.42
270	630.03	-455.19	-415.51	-1.6599	1.6503	2.2212	1243.52
280	621.46	-433.35	-393.12	-1.5785	1.6817	2.2566	1200.54
290	612.85	-411.17	-370.37	-1.4986	1.7146	2.2936	1158.51
300	604.17	-388.62	-347.25	-1.4202	1.7489	2.3321	1117.46
310	595.43	-365.71	-323.73	-1.3431	1.7844	2.3719	1077.40
320	586.62	-342.42	-299.80	-1.2672	1.8208	2.4128	1038.37
330	577.74	-318.74	-275.47	-1.1923	1.8581	2.4546	1000.36
340	568.77	-294.66	-250.71	-1.1184	1.8960	2.4972	963.41
350	559.72	-270.19	-225.52	-1.0454	1.9344	2.5404	927.53
360	550.57	-245.31	-199.90	-0.97318	1.9732	2.5841	892.74
370	541.33	-220.02	-173.84	-0.90178	2.0122	2.6281	859.07

TABLE 45. Thermodynamic properties of *n*-butane in the single-phase region—Continued

<i>T</i> (K)	<i>ρ</i> (kg m ⁻³)	<i>u</i> (kJ kg ⁻¹)	<i>h</i> (kJ kg ⁻¹)	<i>s</i> (kJ kg ⁻¹ K ⁻¹)	<i>c_v</i> (kJ kg ⁻¹ K ⁻¹)	<i>c_p</i> (kJ kg ⁻¹ K ⁻¹)	<i>w</i> (m s ⁻¹)
380	531.99	-194.33	-147.33	-0.83110	2.0514	2.6724	826.53
390	522.55	-168.23	-120.39	-0.76111	2.0907	2.7166	795.16
400	513.01	-141.73	-93.003	-0.69178	2.1299	2.7608	764.98
425	488.75	-73.764	-22.613	-0.52112	2.2275	2.8700	694.92
450	463.97	-3.4123	50.470	-0.35405	2.3235	2.9759	632.80
475	438.86	69.175	126.14	-0.19043	2.4174	3.0766	578.80
500	413.69	143.81	204.24	-0.030200	2.5086	3.1704	532.85
525	388.79	220.28	284.58	0.12657	2.5969	3.2551	494.83
550	364.59	298.34	366.91	0.27975	2.6819	3.3289	464.56
575	341.52	377.73	450.93	0.42914	2.7638	3.3910	441.70
30 MPa							
139.82 ^a	742.27	-718.48	-678.07	-3.0147	1.4699	1.9640	1898.53
140	742.11	-718.13	-677.70	-3.0121	1.4699	1.9641	1897.50
145	737.87	-708.53	-667.88	-2.9431	1.4689	1.9671	1869.86
150	733.65	-698.92	-658.03	-2.8764	1.4684	1.9704	1842.87
155	729.43	-689.30	-648.17	-2.8117	1.4683	1.9741	1816.40
160	725.23	-679.66	-638.29	-2.7490	1.4687	1.9781	1790.35
165	721.05	-670.00	-628.39	-2.6881	1.4698	1.9827	1764.65
170	716.87	-660.31	-618.46	-2.6288	1.4715	1.9877	1739.26
175	712.70	-650.60	-608.51	-2.5711	1.4738	1.9932	1714.13
180	708.54	-640.87	-598.53	-2.5149	1.4769	1.9993	1689.23
185	704.38	-631.11	-588.52	-2.4600	1.4808	2.0059	1664.55
190	700.24	-621.31	-578.47	-2.4064	1.4854	2.0132	1640.08
195	696.10	-611.48	-568.38	-2.3540	1.4907	2.0211	1615.80
200	691.97	-601.61	-558.26	-2.3027	1.4968	2.0296	1591.70
210	683.71	-581.75	-537.87	-2.2033	1.5113	2.0485	1544.08
220	675.47	-561.69	-517.28	-2.1075	1.5287	2.0700	1497.21
230	667.24	-541.42	-496.46	-2.0149	1.5489	2.0940	1451.11
240	659.01	-520.91	-475.39	-1.9253	1.5717	2.1204	1405.83
250	650.77	-500.14	-454.04	-1.8381	1.5970	2.1491	1361.41
260	642.53	-479.09	-432.40	-1.7533	1.6246	2.1799	1317.88
270	634.26	-457.74	-410.44	-1.6704	1.6541	2.2126	1275.28
280	625.98	-436.07	-388.14	-1.5893	1.6855	2.2470	1233.65
290	617.67	-414.07	-365.50	-1.5098	1.7184	2.2830	1193.00
300	609.32	-391.71	-342.48	-1.4318	1.7527	2.3203	1153.37
310	600.94	-369.01	-319.08	-1.3551	1.7882	2.3588	1114.78
320	592.52	-345.93	-295.30	-1.2796	1.8246	2.3984	1077.23
330	584.05	-322.48	-271.11	-1.2052	1.8619	2.4387	1040.76
340	575.54	-298.65	-246.52	-1.1318	1.8998	2.4797	1005.36
350	566.97	-274.43	-221.52	-1.0593	1.9381	2.5212	971.05
360	558.35	-249.83	-196.10	-0.98767	1.9769	2.5630	937.86
370	549.67	-224.84	-170.26	-0.91688	2.0158	2.6050	905.78
380	540.94	-199.46	-144.00	-0.84685	2.0550	2.6471	874.84
390	532.15	-173.69	-117.32	-0.77754	2.0941	2.6892	845.05
400	523.31	-147.54	-90.216	-0.70893	2.1332	2.7310	816.42
425	501.00	-80.525	-20.645	-0.54025	2.2304	2.8342	750.03
450	478.47	-11.234	51.466	-0.37541	2.3260	2.9339	691.11
475	455.87	60.205	126.01	-0.21421	2.4194	3.0290	639.65
500	433.38	133.64	202.87	-0.056550	2.5102	3.1182	595.43
525	411.22	208.91	281.87	0.097616	2.5981	3.2009	558.10
550	389.64	285.86	362.85	0.24829	2.6830	3.2763	527.27
575	368.89	364.30	445.62	0.39545	2.7650	3.3442	502.52
35 MPa							
140.62 ^a	743.43	-717.91	-670.84	-3.0111	1.4738	1.9629	1910.32
145	739.77	-709.54	-662.22	-2.9508	1.4729	1.9654	1886.65

TABLE 45. Thermodynamic properties of *n*-butane in the single-phase region—Continued

<i>T</i> (K)	<i>ρ</i> (kg m ⁻³)	<i>u</i> (kJ kg ⁻¹)	<i>h</i> (kJ kg ⁻¹)	<i>s</i> (kJ kg ⁻¹ K ⁻¹)	<i>c_v</i> (kJ kg ⁻¹ K ⁻¹)	<i>c_p</i> (kJ kg ⁻¹ K ⁻¹)	<i>w</i> (m s ⁻¹)
150	735.60	-699.97	-652.39	-2.8842	1.4722	1.9686	1860.24
155	731.45	-690.39	-642.54	-2.8196	1.4720	1.9721	1834.32
160	727.31	-680.79	-632.67	-2.7569	1.4724	1.9760	1808.81
165	723.18	-671.18	-622.78	-2.6960	1.4734	1.9803	1783.64
170	719.07	-661.54	-612.86	-2.6368	1.4751	1.9852	1758.77
175	714.97	-651.88	-602.93	-2.5792	1.4774	1.9906	1734.15
180	710.88	-642.19	-592.96	-2.5231	1.4805	1.9965	1709.77
185	706.79	-632.48	-582.96	-2.4683	1.4844	2.0030	1685.60
190	702.72	-622.73	-572.93	-2.4148	1.4889	2.0101	1661.64
195	698.66	-612.95	-562.86	-2.3624	1.4943	2.0178	1637.87
200	694.60	-603.14	-552.75	-2.3113	1.5004	2.0261	1614.29
210	686.51	-583.38	-532.40	-2.2120	1.5149	2.0446	1567.70
220	678.44	-563.44	-511.85	-2.1164	1.5323	2.0657	1521.88
230	670.39	-543.29	-491.08	-2.0240	1.5525	2.0891	1476.85
240	662.35	-522.90	-470.06	-1.9346	1.5754	2.1150	1432.67
250	654.32	-502.26	-448.77	-1.8477	1.6007	2.1431	1389.36
260	646.29	-481.34	-427.19	-1.7631	1.6282	2.1732	1346.96
270	638.27	-460.14	-405.30	-1.6804	1.6578	2.2052	1305.53
280	630.24	-438.62	-383.08	-1.5996	1.6892	2.2388	1265.08
290	622.20	-416.77	-360.52	-1.5205	1.7221	2.2740	1225.64
300	614.14	-394.59	-337.60	-1.4428	1.7564	2.3104	1187.24
310	606.07	-372.05	-314.31	-1.3664	1.7919	2.3480	1149.90
320	597.98	-349.16	-290.63	-1.2913	1.8284	2.3865	1113.62
330	589.87	-325.91	-266.57	-1.2172	1.8656	2.4257	1078.42
340	581.73	-302.28	-242.12	-1.1442	1.9035	2.4655	1044.32
350	573.56	-278.28	-217.26	-1.0722	1.9418	2.5058	1011.31
360	565.37	-253.91	-192.00	-1.0010	1.9805	2.5463	979.41
370	557.15	-229.16	-166.34	-0.93069	2.0195	2.5869	948.62
380	548.91	-204.03	-140.26	-0.86116	2.0585	2.6276	918.94
390	540.64	-178.52	-113.78	-0.79238	2.0976	2.6682	890.40
400	532.34	-152.65	-86.899	-0.72432	2.1367	2.7086	862.98
425	511.53	-86.359	-17.936	-0.55711	2.2337	2.8080	799.38
450	490.67	-17.858	53.473	-0.39387	2.3290	2.9041	742.84
475	469.88	52.747	127.23	-0.23437	2.4221	2.9960	693.22
500	449.29	125.33	203.23	-0.078466	2.5127	3.0829	650.25
525	429.06	199.76	281.33	0.073944	2.6004	3.1644	613.52
550	409.36	275.91	361.41	0.22293	2.6852	3.2403	582.59
575	390.34	353.64	443.30	0.36853	2.7671	3.3104	556.98
40 MPa							
141.41 ^a	744.58	-717.34	-663.62	-3.0076	1.4775	1.9618	1922.06
145	741.62	-710.51	-656.57	-2.9584	1.4767	1.9638	1903.12
150	737.51	-700.98	-646.74	-2.8918	1.4759	1.9668	1877.25
155	733.42	-691.44	-636.90	-2.8272	1.4757	1.9702	1851.85
160	729.34	-681.89	-627.04	-2.7646	1.4760	1.9740	1826.85
165	725.27	-672.31	-617.16	-2.7038	1.4770	1.9782	1802.19
170	721.22	-662.72	-607.26	-2.6447	1.4786	1.9829	1777.80
175	717.18	-653.10	-597.33	-2.5871	1.4809	1.9882	1753.67
180	713.15	-643.46	-587.38	-2.5310	1.4840	1.9940	1729.77
185	709.13	-633.80	-577.39	-2.4763	1.4878	2.0003	1706.08
190	705.13	-624.10	-567.37	-2.4229	1.4924	2.0072	1682.60
195	701.13	-614.37	-557.32	-2.3707	1.4978	2.0148	1659.30
200	697.15	-604.60	-547.22	-2.3196	1.5039	2.0229	1636.20
210	689.21	-584.94	-526.90	-2.2204	1.5184	2.0411	1590.57
220	681.30	-565.10	-506.39	-2.1250	1.5358	2.0618	1545.72
230	673.41	-545.06	-485.66	-2.0329	1.5560	2.0848	1501.68

TABLE 45. Thermodynamic properties of *n*-butane in the single-phase region—Continued

<i>T</i> (K)	<i>ρ</i> (kg m ⁻³)	<i>u</i> (kJ kg ⁻¹)	<i>h</i> (kJ kg ⁻¹)	<i>s</i> (kJ kg ⁻¹ K ⁻¹)	<i>c_v</i> (kJ kg ⁻¹ K ⁻¹)	<i>c_p</i> (kJ kg ⁻¹ K ⁻¹)	<i>w</i> (m s ⁻¹)
240	665.55	-524.79	-464.69	-1.9436	1.5789	2.1102	1458.49
250	657.71	-504.27	-443.45	-1.8569	1.6043	2.1378	1416.19
260	649.89	-483.48	-421.93	-1.7725	1.6318	2.1674	1374.82
270	642.07	-462.39	-400.10	-1.6901	1.6614	2.1988	1334.43
280	634.27	-441.01	-377.95	-1.6096	1.6928	2.2318	1295.03
290	626.47	-419.31	-355.46	-1.5306	1.7258	2.2663	1256.66
300	618.67	-397.27	-332.62	-1.4532	1.7601	2.3020	1219.34
310	610.87	-374.89	-309.41	-1.3771	1.7956	2.3388	1183.09
320	603.07	-352.16	-285.84	-1.3023	1.8320	2.3765	1147.91
330	595.26	-329.08	-261.88	-1.2286	1.8692	2.4149	1113.81
340	587.44	-305.63	-237.54	-1.1559	1.9071	2.4539	1080.80
350	579.62	-281.81	-212.80	-1.0842	1.9454	2.4932	1048.89
360	571.79	-257.63	-187.67	-1.0134	1.9841	2.5327	1018.07
370	563.95	-233.07	-162.14	-0.94347	2.0231	2.5724	988.35
380	556.11	-208.15	-136.22	-0.87434	2.0621	2.6121	959.72
390	548.26	-182.86	-109.90	-0.80597	2.1012	2.6517	932.18
400	540.41	-157.21	-83.189	-0.73834	2.1402	2.6911	905.74
425	520.79	-91.502	-14.696	-0.57228	2.2370	2.7879	844.38
450	501.24	-23.619	56.183	-0.41025	2.3322	2.8818	789.71
475	481.84	46.346	129.36	-0.25201	2.4252	2.9717	741.53
500	462.70	118.28	204.73	-0.097386	2.5155	3.0573	699.52
525	443.93	192.08	282.19	0.053755	2.6031	3.1381	663.29
550	425.64	267.62	361.60	0.20151	2.6878	3.2142	632.38
575	407.96	344.81	442.86	0.34598	2.7697	3.2855	606.31
50 MPa							
142.98 ^a	746.84	-716.15	-649.20	-3.0006	1.4845	1.9599	1945.32
145	745.22	-712.35	-645.25	-2.9731	1.4840	1.9610	1935.14
150	741.21	-702.90	-635.44	-2.9066	1.4831	1.9638	1910.28
155	737.23	-693.44	-625.61	-2.8421	1.4827	1.9669	1885.86
160	733.26	-683.96	-615.77	-2.7796	1.4829	1.9705	1861.80
165	729.30	-674.47	-605.91	-2.7189	1.4838	1.9745	1838.05
170	725.36	-664.96	-596.02	-2.6599	1.4854	1.9790	1814.57
175	721.44	-655.42	-586.12	-2.6025	1.4877	1.9841	1791.33
180	717.53	-645.87	-576.18	-2.5465	1.4907	1.9896	1768.31
185	713.63	-636.28	-566.22	-2.4919	1.4945	1.9957	1745.49
190	709.75	-626.67	-556.22	-2.4386	1.4991	2.0024	1722.88
195	705.88	-617.03	-546.19	-2.3865	1.5045	2.0097	1700.45
200	702.03	-607.35	-536.13	-2.3355	1.5106	2.0176	1678.22
210	694.36	-587.87	-515.87	-2.2367	1.5251	2.0352	1634.32
220	686.73	-568.22	-495.42	-2.1416	1.5426	2.0552	1591.20
230	679.15	-548.38	-474.75	-2.0497	1.5629	2.0776	1548.91
240	671.60	-528.31	-453.86	-1.9608	1.5858	2.1022	1507.47
250	664.10	-507.99	-432.70	-1.8744	1.6112	2.1290	1466.95
260	656.62	-487.42	-411.27	-1.7904	1.6388	2.1578	1427.36
270	649.18	-466.56	-389.54	-1.7084	1.6684	2.1883	1388.76
280	641.76	-445.41	-367.50	-1.6282	1.6998	2.2204	1351.17
290	634.37	-423.94	-345.13	-1.5497	1.7328	2.2540	1314.61
300	627.01	-402.16	-322.41	-1.4727	1.7671	2.2887	1279.11
310	619.66	-380.04	-299.35	-1.3971	1.8026	2.3244	1244.67
320	612.34	-357.58	-275.92	-1.3227	1.8391	2.3610	1211.31
330	605.03	-334.77	-252.13	-1.2495	1.8763	2.3982	1179.01
340	597.75	-311.61	-227.96	-1.1773	1.9141	2.4359	1147.79
350	590.48	-288.09	-203.41	-1.1062	1.9525	2.4740	1117.64
360	583.23	-264.21	-178.48	-1.0360	1.9911	2.5123	1088.55
370	576.00	-239.97	-153.16	-0.96660	2.0300	2.5507	1060.51

TABLE 45. Thermodynamic properties of *n*-butane in the single-phase region—Continued

<i>T</i> (K)	ρ (kg m ⁻³)	<i>u</i> (kJ kg ⁻¹)	<i>h</i> (kJ kg ⁻¹)	<i>s</i> (kJ kg ⁻¹ K ⁻¹)	c_v (kJ kg ⁻¹ K ⁻¹)	c_p (kJ kg ⁻¹ K ⁻¹)	<i>w</i> (m s ⁻¹)
380	568.78	-215.37	-127.46	-0.89807	2.0690	2.5891	1033.52
390	561.59	-190.41	-101.38	-0.83032	2.1081	2.6274	1007.57
400	554.42	-165.10	-74.917	-0.76332	2.1470	2.6655	982.64
425	536.61	-100.28	-7.1014	-0.59889	2.2437	2.7594	924.72
450	519.00	-33.311	63.029	-0.43858	2.3387	2.8505	872.89
475	501.63	35.722	135.40	-0.28209	2.4314	2.9384	826.87
500	484.57	106.73	209.92	-0.12921	2.5216	3.0225	786.33
525	467.89	179.63	286.49	0.020211	2.6090	3.1027	750.88
550	451.64	254.31	365.02	0.16633	2.6936	3.1791	720.10
575	435.90	330.71	445.41	0.30926	2.7753	3.2516	693.56
60 MPa							
144.54 ^a	749.05	-714.94	-634.83	-2.9936	1.4910	1.9583	1968.29
145	748.68	-714.07	-633.93	-2.9873	1.4909	1.9585	1966.04
150	744.77	-704.69	-624.13	-2.9209	1.4898	1.9612	1942.10
155	740.88	-695.30	-614.31	-2.8565	1.4893	1.9642	1918.55
160	737.01	-685.89	-604.48	-2.7941	1.4894	1.9676	1895.35
165	733.16	-676.47	-594.64	-2.7335	1.4902	1.9715	1872.43
170	729.32	-667.04	-584.77	-2.6746	1.4918	1.9758	1849.76
175	725.50	-657.58	-574.88	-2.6173	1.4941	1.9807	1827.32
180	721.70	-648.10	-564.96	-2.5614	1.4971	1.9860	1805.09
185	717.91	-638.59	-555.02	-2.5069	1.5010	1.9920	1783.05
190	714.14	-629.06	-545.04	-2.4537	1.5055	1.9984	1761.21
195	710.38	-619.49	-535.03	-2.4017	1.5109	2.0055	1739.55
200	706.65	-609.89	-524.98	-2.3508	1.5170	2.0132	1718.08
210	699.21	-590.58	-504.77	-2.2522	1.5316	2.0304	1675.70
220	691.84	-571.09	-484.37	-2.1573	1.5491	2.0499	1634.10
230	684.51	-551.42	-463.76	-2.0657	1.5694	2.0718	1593.32
240	677.24	-531.52	-442.92	-1.9770	1.5924	2.0960	1553.39
250	670.02	-511.38	-421.84	-1.8909	1.6178	2.1222	1514.37
260	662.85	-490.99	-400.47	-1.8071	1.6454	2.1504	1476.29
270	655.71	-470.33	-378.82	-1.7254	1.6751	2.1803	1439.19
280	648.62	-449.37	-356.86	-1.6456	1.7065	2.2118	1403.10
290	641.57	-428.10	-334.58	-1.5674	1.7395	2.2446	1368.04
300	634.56	-406.52	-311.97	-1.4907	1.7738	2.2786	1334.02
310	627.59	-384.61	-289.01	-1.4154	1.8093	2.3136	1301.04
320	620.65	-362.37	-265.69	-1.3414	1.8458	2.3494	1269.13
330	613.74	-339.78	-242.02	-1.2686	1.8830	2.3859	1238.26
340	606.87	-316.84	-217.97	-1.1968	1.9209	2.4229	1208.45
350	600.04	-293.55	-193.56	-1.1260	1.9592	2.4602	1179.67
360	593.23	-269.91	-168.77	-1.0562	1.9978	2.4977	1151.92
370	586.47	-245.91	-143.60	-0.98725	2.0367	2.5354	1125.18
380	579.73	-221.56	-118.06	-0.91914	2.0757	2.5730	1099.44
390	573.03	-196.85	-92.142	-0.85181	2.1147	2.6106	1074.69
400	566.37	-171.79	-65.849	-0.78525	2.1536	2.6479	1050.91
425	549.89	-107.61	1.5057	-0.62194	2.2502	2.7401	995.56
450	533.66	-41.295	71.136	-0.46277	2.3451	2.8299	945.85
475	517.73	27.084	142.97	-0.30743	2.4377	2.9166	901.45
500	502.13	97.450	216.94	-0.15569	2.5277	3.0001	862.03
525	486.90	169.72	292.95	-0.007361	2.6150	3.0801	827.21
550	472.08	243.82	370.92	0.13771	2.6994	3.1567	796.61
575	457.70	319.66	450.76	0.27965	2.7810	3.2299	769.85
69 MPa							
145.92 ^a	750.99	-713.81	-621.93	-2.9874	1.4965	1.9571	1988.69
150	747.86	-706.20	-613.94	-2.9334	1.4955	1.9592	1969.79
155	744.05	-696.87	-604.14	-2.8691	1.4949	1.9621	1946.97

TABLE 45. Thermodynamic properties of *n*-butane in the single-phase region—Continued

<i>T</i> (K)	<i>ρ</i> (kg m ⁻³)	<i>u</i> (kJ kg ⁻¹)	<i>h</i> (kJ kg ⁻¹)	<i>s</i> (kJ kg ⁻¹ K ⁻¹)	<i>c_v</i> (kJ kg ⁻¹ K ⁻¹)	<i>c_p</i> (kJ kg ⁻¹ K ⁻¹)	<i>w</i> (m s ⁻¹)
160	740.26	-687.53	-594.32	-2.8067	1.4950	1.9654	1924.46
165	736.49	-678.17	-584.48	-2.7462	1.4958	1.9692	1902.23
170	732.74	-668.79	-574.62	-2.6874	1.4973	1.9734	1880.23
175	729.00	-659.40	-564.75	-2.6301	1.4996	1.9781	1858.44
180	725.29	-649.98	-554.84	-2.5743	1.5027	1.9834	1836.85
185	721.59	-640.53	-544.91	-2.5199	1.5065	1.9892	1815.45
190	717.91	-631.06	-534.95	-2.4667	1.5111	1.9955	1794.23
195	714.25	-621.56	-524.96	-2.4148	1.5164	2.0025	1773.19
200	710.60	-612.03	-514.92	-2.3640	1.5226	2.0100	1752.34
210	703.36	-592.84	-494.74	-2.2656	1.5372	2.0269	1711.18
220	696.19	-573.49	-474.38	-2.1708	1.5547	2.0461	1670.79
230	689.07	-553.95	-453.81	-2.0794	1.5750	2.0677	1631.21
240	682.02	-534.19	-433.02	-1.9909	1.5980	2.0915	1592.47
250	675.02	-514.20	-411.98	-1.9050	1.6235	2.1173	1554.64
260	668.08	-493.95	-390.67	-1.8214	1.6511	2.1451	1517.73
270	661.19	-473.43	-369.07	-1.7399	1.6808	2.1746	1481.80
280	654.35	-452.62	-347.17	-1.6603	1.7123	2.2056	1446.86
290	647.56	-431.51	-324.95	-1.5823	1.7453	2.2380	1412.93
300	640.82	-410.08	-302.40	-1.5059	1.7796	2.2716	1380.04
310	634.12	-388.33	-279.52	-1.4309	1.8151	2.3062	1348.17
320	627.47	-366.24	-256.28	-1.3571	1.8516	2.3415	1317.34
330	620.87	-343.82	-232.68	-1.2845	1.8888	2.3775	1287.55
340	614.31	-321.05	-208.73	-1.2130	1.9267	2.4140	1258.77
350	607.79	-297.93	-184.40	-1.1424	1.9650	2.4509	1231.00
360	601.31	-274.46	-159.71	-1.0729	2.0036	2.4880	1204.23
370	594.88	-250.63	-134.64	-1.0042	2.0425	2.5251	1178.44
380	588.49	-226.45	-109.20	-0.93638	2.0814	2.5623	1153.62
390	582.15	-201.92	-83.395	-0.86934	2.1204	2.5995	1129.73
400	575.84	-177.04	-57.216	-0.80306	2.1593	2.6364	1106.77
425	560.29	-113.31	9.8387	-0.64048	2.2558	2.7276	1053.28
450	545.03	-47.450	79.148	-0.48204	2.3506	2.8166	1005.10
475	530.09	20.482	150.65	-0.32743	2.4431	2.9028	961.89
500	515.49	90.412	224.26	-0.17641	2.5330	2.9860	923.31
525	501.25	162.26	299.92	-0.028773	2.6202	3.0659	888.99
550	487.40	235.97	377.53	0.11564	2.7045	3.1426	858.58
575	473.95	311.44	457.02	0.25697	2.7860	3.2162	831.74

^aTemperature on the melting curve.^bSaturated liquid.^cSaturated vapor.TABLE 46. Thermodynamic properties of isobutane on the vapor–liquid phase boundary as a function of temperature^a

<i>T</i> (K)	<i>p</i> (MPa)	<i>ρ</i> (kg m ⁻³)	<i>h</i> (kJ kg ⁻¹)	<i>s</i> (kJ kg ⁻¹ K ⁻¹)	<i>c_v</i> (kJ kg ⁻¹ K ⁻¹)	<i>c_p</i> (kJ kg ⁻¹ K ⁻¹)	<i>w</i> (m s ⁻¹)
113.730 ^b	0.00000002	740.33876	-714.04	-3.199	1.174	1.689	1999.81
		0.0000014	-233.34	1.028	0.737	0.880	139.39
114	0.00000002	740.08373	-713.59	-3.195	1.175	1.690	1997.42
		0.0000015	-233.11	1.020	0.738	0.881	139.53
116	0.00000004	738.19490	-710.20	-3.165	1.179	1.696	1979.82
		0.0000025	-231.34	0.963	0.747	0.890	140.61
118	0.00000007	736.30640	-706.80	-3.136	1.183	1.702	1962.46
		0.0000039	-229.55	0.908	0.756	0.899	141.68
120	0.00000011	734.41812	-703.39	-3.108	1.187	1.709	1945.35
		0.0000062	-227.74	0.856	0.766	0.909	142.74

TABLE 46. Thermodynamic properties of isobutane on the vapor–liquid phase boundary as a function of temperature^a—Continued

T (K)	p (MPa)	ρ (kg m ⁻³)	h (kJ kg ⁻¹)	s (kJ kg ⁻¹ K ⁻¹)	c_v (kJ kg ⁻¹ K ⁻¹)	c_p (kJ kg ⁻¹ K ⁻¹)	w (m s ⁻¹)
122	0.00000017	732.52996	−699.97	−3.079	1.191	1.715	1928.49
		0.0000096	−225.91	0.806	0.775	0.918	143.79
124	0.00000026	730.6418	−696.53	−3.051	1.196	1.721	1911.87
		0.000015	−224.07	0.759	0.784	0.927	144.83
126	0.00000040	728.7535	−693.08	−3.024	1.200	1.728	1895.49
		0.000022	−222.21	0.713	0.793	0.936	145.87
128	0.00000059	726.8649	−689.62	−2.996	1.204	1.734	1879.34
		0.000032	−220.33	0.670	0.801	0.944	146.90
130	0.00000088	724.9759	−686.14	−2.970	1.209	1.741	1863.41
		0.000047	−218.43	0.628	0.810	0.953	147.92
132	0.0000013	723.0864	−682.66	−2.943	1.213	1.747	1847.70
		0.000068	−216.51	0.588	0.819	0.962	148.93
134	0.0000019	721.1963	−679.16	−2.917	1.217	1.754	1832.19
		0.000097	−214.58	0.550	0.827	0.971	149.94
136	0.0000027	719.305	−675.64	−2.891	1.222	1.760	1816.87
		0.00014	−212.63	0.514	0.836	0.979	150.94
138	0.0000037	717.414	−672.11	−2.865	1.226	1.767	1801.74
		0.00019	−210.66	0.479	0.845	0.988	151.94
140	0.0000052	715.521	−668.58	−2.839	1.230	1.773	1786.79
		0.00026	−208.68	0.446	0.853	0.996	152.92
142	0.0000072	713.627	−665.02	−2.814	1.234	1.779	1772.01
		0.00036	−206.68	0.414	0.861	1.004	153.90
144	0.0000099	711.732	−661.46	−2.789	1.239	1.786	1757.38
		0.00048	−204.67	0.383	0.870	1.013	154.88
146	0.000013	709.836	−657.88	−2.765	1.243	1.792	1742.91
		0.00064	−202.63	0.354	0.878	1.021	155.84
148	0.000018	707.938	−654.29	−2.740	1.247	1.798	1728.58
		0.00085	−200.58	0.325	0.886	1.029	156.80
150	0.000024	706.038	−650.69	−2.716	1.251	1.805	1714.39
		0.00111	−198.52	0.299	0.894	1.037	157.76
152	0.000031	704.137	−647.07	−2.692	1.255	1.811	1700.33
		0.00145	−196.44	0.273	0.903	1.046	158.71
154	0.000041	702.234	−643.44	−2.668	1.260	1.817	1686.40
		0.00187	−194.34	0.248	0.911	1.054	159.65
156	0.000053	700.329	−639.80	−2.645	1.264	1.824	1672.58
		0.00240	−192.23	0.224	0.919	1.062	160.58
158	0.000069	698.422	−636.15	−2.622	1.268	1.830	1658.87
		0.00305	−190.10	0.202	0.927	1.070	161.51
160	0.000088	696.513	−632.48	−2.598	1.272	1.836	1645.26
		0.00385	−187.95	0.180	0.935	1.078	162.43
162	0.000112	694.602	−628.80	−2.576	1.276	1.843	1631.76
		0.00484	−185.79	0.159	0.943	1.086	163.35
164	0.000141	692.688	−625.11	−2.553	1.281	1.849	1618.35
		0.00603	−183.62	0.139	0.951	1.094	164.26
166	0.000177	690.772	−621.41	−2.531	1.285	1.855	1605.03
		0.00747	−181.43	0.120	0.959	1.102	165.16
168	0.000221	688.854	−617.69	−2.508	1.289	1.862	1591.80
		0.00920	−179.22	0.102	0.967	1.110	166.06

TABLE 46. Thermodynamic properties of isobutane on the vapor-liquid phase boundary as a function of temperature^a—Continued

T (K)	p (MPa)	ρ (kg m ⁻³)	h (kJ kg ⁻¹)	s (kJ kg ⁻¹ K ⁻¹)	c_v (kJ kg ⁻¹ K ⁻¹)	c_p (kJ kg ⁻¹ K ⁻¹)	w (m s ⁻¹)
170	0.000274	686.932 0.01127	-613.96 -177.00	-2.486 0.084	1.293 0.975	1.868 1.118	1578.65 166.95
172	0.000337	685.008 0.01372	-610.22 -174.77	-2.464 0.067	1.298 0.983	1.874 1.126	1565.57 167.83
174	0.000413	683.081 0.01662	-606.46 -172.52	-2.443 0.051	1.302 0.991	1.881 1.134	1552.58 168.70
176	0.000504	681.151 0.02003	-602.69 -170.25	-2.421 0.036	1.307 0.999	1.887 1.142	1539.65 169.57
178	0.000611	679.218 0.02402	-598.91 -167.97	-2.400 0.021	1.311 1.006	1.894 1.150	1526.79 170.43
180	0.000737	677.281 0.02867	-595.12 -165.68	-2.379 0.007	1.315 1.014	1.900 1.158	1514.00 171.29
182	0.000886	675.341 0.03406	-591.31 -163.38	-2.357 -0.006	1.320 1.022	1.907 1.166	1501.27 172.13
184	0.001059	673.397 0.04028	-587.49 -161.06	-2.337 -0.019	1.324 1.030	1.913 1.174	1488.60 172.97
186	0.001260	671.450 0.04744	-583.66 -158.72	-2.316 -0.031	1.329 1.038	1.920 1.183	1475.98 173.80
188	0.001494	669.499 0.05563	-579.81 -156.38	-2.295 -0.043	1.334 1.046	1.927 1.191	1463.42 174.63
190	0.001763	667.544 0.06499	-575.95 -154.02	-2.275 -0.054	1.338 1.055	1.933 1.199	1450.92 175.44
192	0.002072	665.585 0.07563	-572.08 -151.64	-2.255 -0.065	1.343 1.063	1.940 1.207	1438.46 176.25
194	0.002427	663.622 0.08768	-568.19 -149.26	-2.234 -0.075	1.348 1.071	1.947 1.216	1426.06 177.05
196	0.002832	661.655 0.10129	-564.29 -146.86	-2.214 -0.085	1.353 1.079	1.954 1.224	1413.70 177.83
198	0.003292	659.683 0.11660	-560.37 -144.45	-2.195 -0.094	1.358 1.087	1.961 1.232	1401.39 178.61
200	0.003814	657.706 0.13378	-556.44 -142.03	-2.175 -0.103	1.363 1.095	1.968 1.241	1389.12 179.38
202	0.004403	655.725 0.15300	-552.50 -139.59	-2.155 -0.111	1.368 1.103	1.975 1.249	1376.89 180.14
204	0.005067	653.738 0.17443	-548.54 -137.14	-2.136 -0.119	1.373 1.112	1.982 1.258	1364.70 180.89
206	0.005813	651.747 0.19826	-544.57 -134.69	-2.116 -0.127	1.378 1.120	1.989 1.267	1352.56 181.63
208	0.006648	649.750 0.22469	-540.58 -132.22	-2.097 -0.134	1.383 1.128	1.996 1.275	1340.45 182.36
210	0.007581	647.748 0.25392	-536.58 -129.74	-2.078 -0.141	1.388 1.137	2.004 1.284	1328.38 183.08
212	0.008620	645.741 0.28617	-532.57 -127.25	-2.059 -0.147	1.394 1.145	2.011 1.293	1316.35 183.78
214	0.009773	643.727 0.32166	-528.54 -124.75	-2.040 -0.153	1.399 1.154	2.018 1.302	1304.35 184.48
216	0.011052	641.708 0.36063	-524.49 -122.23	-2.021 -0.159	1.404 1.162	2.026 1.311	1292.39 185.16

TABLE 46. Thermodynamic properties of isobutane on the vapor–liquid phase boundary as a function of temperature^a—Continued

T (K)	p (MPa)	ρ (kg m ⁻³)	h (kJ kg ⁻¹)	s (kJ kg ⁻¹ K ⁻¹)	c_v (kJ kg ⁻¹ K ⁻¹)	c_p (kJ kg ⁻¹ K ⁻¹)	w (m s ⁻¹)
218	0.012465	639.683 0.40331	-520.43 -119.71	-2.003 -0.164	1.410 1.171	2.034 1.320	1280.45 185.83
220	0.014023	637.651 0.44997	-516.35 -117.18	-1.984 -0.170	1.415 1.180	2.041 1.330	1268.56 186.48
222	0.015736	635.613 0.50086	-512.26 -114.64	-1.965 -0.174	1.421 1.188	2.049 1.339	1256.69 187.12
224	0.017618	633.568 0.55625	-508.15 -112.09	-1.947 -0.179	1.427 1.197	2.057 1.348	1244.85 187.75
226	0.019678	631.517 0.61643	-504.03 -109.53	-1.929 -0.183	1.433 1.206	2.065 1.358	1233.04 188.37
228	0.021930	629.458 0.68168	-499.89 -106.96	-1.910 -0.187	1.438 1.215	2.073 1.368	1221.26 188.97
230	0.024387	627.392 0.75229	-495.73 -104.39	-1.892 -0.191	1.444 1.224	2.081 1.377	1209.51 189.56
232	0.027061	625.319 0.82857	-491.56 -101.80	-1.874 -0.194	1.450 1.233	2.089 1.387	1197.79 190.13
234	0.029967	623.238 0.91085	-487.37 -99.21	-1.856 -0.198	1.456 1.242	2.098 1.397	1186.09 190.68
236	0.033118	621.149 0.99943	-483.16 -96.61	-1.838 -0.201	1.462 1.251	2.106 1.407	1174.42 191.22
238	0.036530	619.05 1.0947	-478.94 -94.01	-1.821 -0.203	1.469 1.260	2.115 1.417	1162.78 191.75
240	0.040218	616.95 1.1969	-474.70 -91.39	-1.803 -0.206	1.475 1.270	2.123 1.428	1151.15 192.25
242	0.044196	614.83 1.3064	-470.44 -88.77	-1.785 -0.208	1.481 1.279	2.132 1.438	1139.56 192.74
244	0.048482	612.71 1.4237	-466.16 -86.15	-1.768 -0.210	1.487 1.288	2.141 1.449	1127.98 193.22
246	0.053092	610.58 1.5490	-461.87 -83.51	-1.750 -0.212	1.494 1.298	2.150 1.460	1116.43 193.67
248	0.058042	608.44 1.6827	-457.56 -80.88	-1.733 -0.214	1.500 1.307	2.159 1.470	1104.90 194.11
250	0.063350	606.28 1.8253	-453.22 -78.23	-1.715 -0.215	1.507 1.317	2.168 1.481	1093.39 194.52
252	0.069033	604.12 1.9771	-448.87 -75.58	-1.698 -0.217	1.513 1.327	2.177 1.492	1081.90 194.92
254	0.075109	601.95 2.1386	-444.51 -72.93	-1.681 -0.218	1.520 1.336	2.186 1.504	1070.43 195.30
256	0.081597	599.77 2.3100	-440.12 -70.27	-1.664 -0.219	1.527 1.346	2.196 1.515	1058.98 195.66
258	0.088516	597.58 2.4920	-435.71 -67.61	-1.647 -0.220	1.534 1.356	2.206 1.527	1047.54 196.00
260	0.095885	595.37 2.6848	-431.28 -64.94	-1.630 -0.221	1.541 1.366	2.215 1.538	1036.13 196.32
262	0.10372	593.16 2.8890	-426.84 -62.27	-1.613 -0.221	1.548 1.376	2.225 1.550	1024.73 196.62
264	0.11205	590.93 3.1050	-422.37 -59.60	-1.596 -0.222	1.555 1.386	2.235 1.562	1013.35 196.89

TABLE 46. Thermodynamic properties of isobutane on the vapor–liquid phase boundary as a function of temperature^a—Continued

<i>T</i> (K)	<i>p</i> (MPa)	ρ (kg m ⁻³)	<i>h</i> (kJ kg ⁻¹)	<i>s</i> (kJ kg ⁻¹ K ⁻¹)	c_v (kJ kg ⁻¹ K ⁻¹)	c_p (kJ kg ⁻¹ K ⁻¹)	<i>w</i> (m s ⁻¹)
266	0.12089	588.69 3.3332	-417.88 -56.92	-1.579 -0.222	1.562 1.396	2.245 1.574	1001.98 197.15
268	0.13025	586.44 3.5742	-413.37 -54.24	-1.562 -0.222	1.569 1.406	2.256 1.587	990.63 197.38
270	0.14017	584.17 3.8285	-408.84 -51.56	-1.545 -0.222	1.576 1.417	2.266 1.599	979.29 197.59
272	0.15066	581.89 4.0964	-404.29 -48.87	-1.528 -0.222	1.583 1.427	2.277 1.612	967.96 197.78
274	0.16174	579.60 4.3787	-399.72 -46.19	-1.512 -0.222	1.590 1.437	2.287 1.625	956.65 197.94
276	0.17344	577.29 4.6757	-395.12 -43.50	-1.495 -0.221	1.598 1.448	2.298 1.638	945.35 198.08
278	0.18577	574.97 4.9881	-390.51 -40.81	-1.479 -0.221	1.605 1.458	2.309 1.651	934.06 198.20
280	0.19876	572.64 5.3164	-385.87 -38.12	-1.462 -0.220	1.613 1.469	2.320 1.664	922.77 198.29
282	0.21243	570.28 5.6611	-381.21 -35.43	-1.446 -0.219	1.620 1.480	2.332 1.678	911.50 198.35
284	0.22681	567.91 6.0229	-376.52 -32.74	-1.429 -0.219	1.628 1.490	2.343 1.691	900.23 198.39
286	0.24192	565.53 6.4024	-371.81 -30.06	-1.413 -0.218	1.635 1.501	2.355 1.705	888.97 198.41
288	0.25777	563.13 6.8002	-367.08 -27.37	-1.396 -0.217	1.643 1.512	2.367 1.720	877.72 198.39
290	0.27440	560.71 7.2170	-362.32 -24.68	-1.380 -0.216	1.651 1.523	2.379 1.734	866.47 198.35
292	0.29183	558.27 7.6534	-357.54 -22.00	-1.364 -0.214	1.659 1.534	2.391 1.749	855.22 198.29
294	0.31008	555.81 8.1101	-352.74 -19.32	-1.347 -0.213	1.666 1.545	2.403 1.764	843.98 198.19
296	0.32917	553.34 8.5879	-347.91 -16.64	-1.331 -0.212	1.674 1.556	2.416 1.779	832.74 198.07
298	0.34914	550.84 9.0875	-343.05 -13.96	-1.315 -0.210	1.682 1.567	2.429 1.794	821.50 197.92
300	0.37000	548.32 9.6096	-338.17 -11.29	-1.299 -0.209	1.690 1.578	2.442 1.810	810.25 197.74
302	0.39177	545.78 10.155	-333.26 -8.63	-1.282 -0.207	1.698 1.589	2.456 1.826	799.01 197.52
304	0.41450	543.22 10.725	-328.32 -5.96	-1.266 -0.206	1.706 1.601	2.469 1.842	787.76 197.28
306	0.43819	540.63 11.320	-323.36 -3.31	-1.250 -0.204	1.715 1.612	2.483 1.859	776.50 197.01
308	0.46288	538.02 11.941	-318.37 -0.66	-1.234 -0.202	1.723 1.623	2.497 1.876	765.24 196.70
310	0.48858	535.39 12.589	-313.35 1.99	-1.218 -0.201	1.731 1.635	2.512 1.893	753.97 196.37
312	0.51534	532.73 13.264	-308.30 4.62	-1.202 -0.199	1.739 1.647	2.526 1.911	742.69 196.00

TABLE 46. Thermodynamic properties of isobutane on the vapor-liquid phase boundary as a function of temperature^a—Continued

T (K)	p (MPa)	ρ (kg m ⁻³)	h (kJ kg ⁻¹)	s (kJ kg ⁻¹ K ⁻¹)	c_v (kJ kg ⁻¹ K ⁻¹)	c_p (kJ kg ⁻¹ K ⁻¹)	w (m s ⁻¹)
314	0.54317	530.04 13.969	-303.22 7.25	-1.186 -0.197	1.748 1.658	2.541 1.929	731.40 195.59
316	0.57209	527.33 14.704	-298.12 9.87	-1.170 -0.195	1.756 1.670	2.557 1.947	720.10 195.15
318	0.60215	524.58 15.470	-292.98 12.48	-1.154 -0.193	1.765 1.682	2.573 1.966	708.78 194.68
320	0.63335	521.81 16.269	-287.81 15.08	-1.138 -0.191	1.773 1.694	2.589 1.985	697.45 194.17
322	0.66573	519.00 17.101	-282.61 17.67	-1.122 -0.189	1.782 1.705	2.605 2.005	686.10 193.62
324	0.69932	516.16 17.968	-277.38 20.25	-1.106 -0.187	1.790 1.717	2.622 2.025	674.72 193.04
326	0.73415	513.29 18.872	-272.11 22.82	-1.090 -0.185	1.799 1.729	2.639 2.046	663.33 192.41
328	0.77023	510.38 19.814	-266.81 25.37	-1.074 -0.183	1.808 1.741	2.657 2.068	651.91 191.75
330	0.80761	507.43 20.795	-261.48 27.90	-1.058 -0.181	1.817 1.753	2.676 2.089	640.46 191.05
332	0.84630	504.44 21.818	-256.11 30.42	-1.042 -0.179	1.826 1.765	2.695 2.112	628.99 190.31
334	0.88635	501.42 22.884	-250.71 32.92	-1.026 -0.177	1.835 1.777	2.714 2.135	617.48 189.52
336	0.92776	498.35 23.995	-245.27 35.41	-1.010 -0.174	1.844 1.790	2.734 2.159	605.94 188.69
338	0.97059	495.23 25.153	-239.79 37.87	-0.994 -0.172	1.853 1.802	2.755 2.184	594.36 187.82
340	1.0148	492.07 26.361	-234.27 40.31	-0.978 -0.170	1.862 1.814	2.777 2.209	582.74 186.90
342	1.0606	488.86 27.620	-228.71 42.72	-0.962 -0.168	1.871 1.826	2.799 2.236	571.08 185.94
344	1.1078	485.60 28.934	-223.11 45.11	-0.946 -0.166	1.880 1.838	2.822 2.264	559.37 184.92
346	1.1565	482.28 30.305	-217.47 47.47	-0.930 -0.164	1.890 1.850	2.846 2.293	547.62 183.86
348	1.2068	478.90 31.736	-211.78 49.81	-0.914 -0.162	1.899 1.862	2.872 2.323	535.81 182.75
350	1.2587	475.47 33.230	-206.05 52.10	-0.897 -0.160	1.909 1.874	2.898 2.355	523.94 181.59
352	1.3123	471.97 34.792	-200.28 54.36	-0.881 -0.158	1.918 1.887	2.926 2.389	512.02 180.38
354	1.3674	468.40 36.424	-194.45 56.59	-0.865 -0.156	1.928 1.900	2.955 2.425	500.02 179.11
356	1.4243	464.75 38.132	-188.58 58.77	-0.849 -0.154	1.938 1.913	2.985 2.463	487.96 177.78
358	1.4829	461.03 39.919	-182.65 60.91	-0.833 -0.152	1.948 1.926	3.017 2.504	475.82 176.40
360	1.5433	457.23 41.791	-176.66 63.00	-0.816 -0.151	1.958 1.939	3.052 2.548	463.60 174.96

TABLE 46. Thermodynamic properties of isobutane on the vapor-liquid phase boundary as a function of temperature^a—Continued

T (K)	p (MPa)	ρ (kg m ⁻³)	h (kJ kg ⁻¹)	s (kJ kg ⁻¹ K ⁻¹)	c_v (kJ kg ⁻¹ K ⁻¹)	c_p (kJ kg ⁻¹ K ⁻¹)	w (m s ⁻¹)
362	1.6054	453.33	-170.62	-0.800	1.968	3.088	451.29
		43.754	65.04	-0.149	1.953	2.596	173.45
364	1.6694	449.34	-164.53	-0.784	1.978	3.127	438.89
		45.814	67.03	-0.147	1.968	2.647	171.89
366	1.7352	445.25	-158.36	-0.767	1.989	3.168	426.38
		47.979	68.96	-0.146	1.982	2.703	170.25
368	1.8030	441.05	-152.13	-0.751	2.000	3.213	413.76
		50.255	70.82	-0.145	1.998	2.764	168.55
370	1.8727	436.72	-145.83	-0.734	2.011	3.262	401.01
		52.652	72.61	-0.144	2.013	2.831	166.77
372	1.9444	432.27	-139.46	-0.717	2.022	3.315	388.14
		55.180	74.32	-0.142	2.030	2.905	164.92
374	2.0181	427.67	-133.01	-0.700	2.033	3.373	375.12
		57.851	75.95	-0.142	2.047	2.987	163.00
376	2.0939	422.91	-126.47	-0.683	2.045	3.437	361.94
		60.678	77.49	-0.141	2.064	3.078	160.99
378	2.1718	417.97	-119.84	-0.666	2.057	3.508	348.59
		63.677	78.93	-0.140	2.082	3.181	158.90
380	2.2519	412.85	-113.11	-0.649	2.069	3.588	335.05
		66.867	80.25	-0.140	2.101	3.298	156.73
382	2.3343	407.50	-106.26	-0.632	2.082	3.678	321.32
		70.269	81.45	-0.140	2.120	3.431	154.46
384	2.4189	401.91	-99.30	-0.614	2.095	3.783	307.36
		73.909	82.51	-0.141	2.140	3.586	152.10
386	2.5058	396.03	-92.20	-0.596	2.110	3.904	293.15
		77.820	83.40	-0.141	2.162	3.768	149.63
388	2.5951	389.84	-84.95	-0.578	2.125	4.048	278.69
		82.042	84.10	-0.142	2.184	3.984	147.06
390	2.6869	383.26	-77.53	-0.559	2.141	4.221	263.93
		86.625	84.58	-0.144	2.207	4.248	144.37
392	2.7812	376.24	-69.90	-0.541	2.158	4.436	248.86
		91.634	84.80	-0.146	2.232	4.577	141.57
394	2.8782	368.67	-62.03	-0.521	2.177	4.710	233.42
		97.159	84.71	-0.149	2.258	4.999	138.63
396	2.9778	360.43	-53.86	-0.501	2.198	5.073	217.58
		103.32	84.23	-0.153	2.287	5.563	135.56
398	3.0802	351.32	-45.32	-0.480	2.222	5.582	201.26
		110.30	83.25	-0.157	2.318	6.356	132.32
400	3.1856	341.03	-36.27	-0.459	2.250	6.349	184.38
		118.39	81.59	-0.164	2.354	7.555	128.90
402	3.2940	329.04	-26.51	-0.435	2.285	7.647	166.79
		128.07	78.95	-0.173	2.396	9.588	125.27
403	3.3494	322.11	-21.23	-0.422	2.306	8.709	157.65
		133.80	77.09	-0.178	2.420	11.246	123.35
404	3.4057	314.25	-15.57	-0.409	2.331	10.344	148.23
		140.39	74.71	-0.185	2.448	13.789	121.33
405	3.4629	305.04	-9.33	-0.394	2.362	13.190	138.43
		148.28	71.55	-0.194	2.481	18.178	119.17

TABLE 46. Thermodynamic properties of isobutane on the vapor–liquid phase boundary as a function of temperature^a—Continued

T (K)	p (MPa)	ρ (kg m ⁻³)	h (kJ kg ⁻¹)	s (kJ kg ⁻¹ K ⁻¹)	c_v (kJ kg ⁻¹ K ⁻¹)	c_p (kJ kg ⁻¹ K ⁻¹)	w (m s ⁻¹)
406	3.5210	293.52	-2.12	-0.376	2.402	19.368	128.12
		158.36	67.07	-0.206	2.521	27.552	116.78
407	3.5801	276.83	7.30	-0.354	2.465	42.319	116.97
		173.46	59.64	-0.225	2.575	61.185	113.83
407.810 ^c	3.6290	225.50	32.27	-0.293			

^aFor each temperature, the values on the first line correspond to the saturated-liquid line and the values on the second line correspond to the saturated-vapor line.

^bTriple point.

^cCritical point.

TABLE 47. Thermodynamic properties of isobutane in the single-phase region

T (K)	ρ (kg m ⁻³)	u (kJ kg ⁻¹)	h (kJ kg ⁻¹)	s (kJ kg ⁻¹ K ⁻¹)	c_v (kJ kg ⁻¹ K ⁻¹)	c_p (kJ kg ⁻¹ K ⁻¹)	w (m s ⁻¹)
0.1 MPa							
113.77 ^a	740.33	-713.99	-713.85	-3.1982	1.1744	1.6889	1999.64
115	739.18	-711.91	-711.78	-3.1801	1.1769	1.6927	1988.81
120	734.46	-703.41	-703.28	-3.1077	1.1873	1.7086	1945.60
125	729.74	-694.83	-694.69	-3.0377	1.1981	1.7246	1903.92
130	725.02	-686.17	-686.03	-2.9697	1.2089	1.7408	1863.70
135	720.29	-677.42	-677.29	-2.9037	1.2196	1.7569	1824.81
140	715.57	-668.60	-668.46	-2.8395	1.2303	1.7729	1787.12
145	710.83	-659.70	-659.56	-2.7770	1.2408	1.7888	1750.48
150	706.09	-650.72	-650.57	-2.7161	1.2513	1.8046	1714.76
155	701.33	-641.65	-641.51	-2.6567	1.2618	1.8204	1679.86
160	696.57	-632.51	-632.37	-2.5987	1.2723	1.8362	1645.67
165	691.79	-623.29	-623.15	-2.5419	1.2829	1.8520	1612.11
170	686.99	-613.99	-613.85	-2.4864	1.2936	1.8679	1579.10
175	682.18	-604.62	-604.47	-2.4320	1.3045	1.8839	1546.58
180	677.34	-595.16	-595.01	-2.3787	1.3156	1.9002	1514.49
185	672.49	-585.62	-585.47	-2.3264	1.3269	1.9166	1482.80
190	667.61	-575.99	-575.84	-2.2751	1.3385	1.9333	1451.45
195	662.71	-566.29	-566.13	-2.2247	1.3505	1.9502	1420.42
200	657.78	-556.49	-556.34	-2.1751	1.3627	1.9676	1389.68
210	647.82	-536.64	-536.49	-2.0782	1.3884	2.0034	1328.97
220	637.73	-516.42	-516.27	-1.9841	1.4155	2.0411	1269.15
230	627.47	-495.82	-495.66	-1.8925	1.4443	2.0808	1210.08
240	617.01	-474.80	-474.64	-1.8031	1.4748	2.1229	1151.64
250	606.33	-453.36	-453.19	-1.7155	1.5069	2.1676	1093.71
260	595.38	-431.45	-431.28	-1.6296	1.5406	2.2153	1036.17
261.07 ^b	594.19	-429.08	-428.92	-1.6205	1.5443	2.2205	1030.06
261.07 ^c	2.7921	-99.333	-63.518	-0.22090	1.3713	1.5446	196.48
270	2.6871	-86.787	-49.572	-0.16838	1.4082	1.5775	200.26
280	2.5798	-72.367	-33.603	-0.11031	1.4509	1.6166	204.32
290	2.4816	-57.531	-17.234	-0.052872	1.4947	1.6575	208.25
300	2.3913	-42.267	-0.44894	0.004030	1.5394	1.6998	212.04
310	2.3080	-26.562	16.766	0.060473	1.5849	1.7433	215.73
320	2.2307	-10.410	34.420	0.11652	1.6308	1.7876	219.32
330	2.1587	6.1960	52.520	0.17221	1.6772	1.8325	222.83
340	2.0915	23.260	71.072	0.22759	1.7237	1.8779	226.26
350	2.0286	40.784	90.079	0.28268	1.7704	1.9235	229.61
360	1.9695	58.769	109.54	0.33751	1.8170	1.9692	232.90
370	1.9140	77.216	129.46	0.39209	1.8635	2.0149	236.13
380	1.8616	96.123	149.84	0.44643	1.9097	2.0604	239.30
390	1.8121	115.49	170.67	0.50054	1.9556	2.1057	242.43
400	1.7653	135.31	191.95	0.55442	2.0011	2.1507	245.50

TABLE 47. Thermodynamic properties of isobutane in the single-phase region—Continued

<i>T</i> (K)	<i>ρ</i> (kg m ⁻³)	<i>u</i> (kJ kg ⁻¹)	<i>h</i> (kJ kg ⁻¹)	<i>s</i> (kJ kg ⁻¹ K ⁻¹)	<i>c_v</i> (kJ kg ⁻¹ K ⁻¹)	<i>c_p</i> (kJ kg ⁻¹ K ⁻¹)	<i>w</i> (m s ⁻¹)
425	1.6584	186.81	247.11	0.68814	2.1129	2.2614	252.99
450	1.5640	241.06	305.00	0.82045	2.2212	2.3688	260.23
475	1.4800	297.96	365.52	0.95133	2.3257	2.4726	267.26
500	1.4048	357.41	428.59	1.0807	2.4261	2.5726	274.09
525	1.3369	419.31	494.12	1.2086	2.5226	2.6685	280.74
550	1.2753	483.58	561.99	1.3348	2.6150	2.7607	287.23
575	1.2192	550.10	632.12	1.4595	2.7037	2.8491	293.57
0.5 MPa							
113.95 ^a	740.31	-713.77	-713.10	-3.1964	1.1753	1.6893	1998.99
115	739.32	-711.99	-711.32	-3.1808	1.1775	1.6925	1989.71
120	734.61	-703.50	-702.82	-3.1084	1.1879	1.7083	1946.57
125	729.90	-694.92	-694.23	-3.0384	1.1987	1.7244	1904.98
130	725.18	-686.26	-685.57	-2.9704	1.2095	1.7405	1864.84
135	720.47	-677.52	-676.83	-2.9044	1.2202	1.7566	1826.04
140	715.75	-668.70	-668.01	-2.8403	1.2308	1.7726	1788.43
145	711.02	-659.81	-659.10	-2.7778	1.2414	1.7884	1751.88
150	706.28	-650.83	-650.12	-2.7169	1.2518	1.8043	1716.25
155	701.54	-641.77	-641.06	-2.6575	1.2623	1.8200	1681.43
160	696.78	-632.64	-631.92	-2.5994	1.2728	1.8358	1647.32
165	692.01	-623.43	-622.70	-2.5427	1.2834	1.8516	1613.84
170	687.22	-614.13	-613.41	-2.4872	1.2941	1.8674	1580.92
175	682.42	-604.76	-604.03	-2.4328	1.3050	1.8834	1548.48
180	677.59	-595.31	-594.57	-2.3796	1.3161	1.8996	1516.48
185	672.75	-585.78	-585.03	-2.3273	1.3274	1.9160	1484.87
190	667.89	-576.16	-575.41	-2.2760	1.3390	1.9326	1453.62
195	662.99	-566.46	-565.71	-2.2256	1.3510	1.9495	1422.68
200	658.08	-556.67	-555.91	-2.1760	1.3632	1.9668	1392.04
210	648.15	-536.84	-536.07	-2.0792	1.3888	2.0025	1331.53
220	638.09	-516.64	-515.86	-1.9851	1.4160	2.0400	1271.92
230	627.86	-496.06	-495.26	-1.8936	1.4448	2.0796	1213.07
240	617.44	-475.07	-474.26	-1.8042	1.4752	2.1214	1154.88
250	606.81	-453.65	-452.82	-1.7167	1.5073	2.1659	1097.23
260	595.91	-431.77	-430.93	-1.6309	1.5410	2.2132	1040.00
270	584.71	-409.41	-408.55	-1.5464	1.5762	2.2637	983.05
280	573.14	-386.52	-385.65	-1.4631	1.6129	2.3179	926.22
290	561.14	-363.07	-362.18	-1.3808	1.6510	2.3765	869.32
300	548.61	-339.01	-338.10	-1.2991	1.6904	2.4405	812.07
310	535.42	-314.28	-313.34	-1.2180	1.7311	2.5114	754.15
310.86 ^b	534.24	-312.11	-311.17	-1.2110	1.7347	2.5179	749.11
310.86 ^c	12.877	-35.703	3.1265	-0.19992	1.6400	1.9006	196.21
320	12.322	-20.015	20.563	-0.14464	1.6742	1.9171	201.39
330	11.786	-2.5722	39.852	-0.085287	1.7136	1.9418	206.66
340	11.308	15.198	59.414	-0.026892	1.7546	1.9712	211.58
350	10.878	33.325	79.289	0.030719	1.7968	2.0043	216.22
360	10.487	51.833	99.509	0.087678	1.8400	2.0401	220.64
370	10.130	70.738	120.10	0.14408	1.8837	2.0777	224.85
380	9.8008	90.050	141.07	0.20000	1.9275	2.1164	228.90
390	9.4962	109.77	162.43	0.25549	1.9714	2.1558	232.81
400	9.2132	129.91	184.18	0.31057	2.0152	2.1959	236.58
425	8.5838	182.09	240.34	0.44672	2.1236	2.2969	245.54
450	8.0443	236.87	299.03	0.58087	2.2296	2.3976	253.96
475	7.5747	294.20	360.21	0.71315	2.3323	2.4964	261.93
500	7.1613	354.00	423.82	0.84366	2.4316	2.5925	269.54
525	6.7936	416.21	489.80	0.97241	2.5270	2.6855	276.84
550	6.4641	480.72	558.07	1.0994	2.6188	2.7753	283.88
575	6.1667	547.46	628.54	1.2247	2.7069	2.8618	290.69

TABLE 47. Thermodynamic properties of isobutane in the single-phase region—Continued

<i>T</i> (K)	<i>ρ</i> (kg m ⁻³)	<i>u</i> (kJ kg ⁻¹)	<i>h</i> (kJ kg ⁻¹)	<i>s</i> (kJ kg ⁻¹ K ⁻¹)	<i>c_v</i> (kJ kg ⁻¹ K ⁻¹)	<i>c_p</i> (kJ kg ⁻¹ K ⁻¹)	<i>w</i> (m s ⁻¹)
1 MPa							
114.16 ^a	740.29	-713.51	-712.16	-3.1941	1.1766	1.6897	1998.20
115	739.50	-712.09	-710.74	-3.1817	1.1783	1.6923	1990.82
120	734.80	-703.60	-702.24	-3.1093	1.1887	1.7081	1947.79
125	730.09	-695.03	-693.66	-3.0393	1.1994	1.7241	1906.30
130	725.39	-686.38	-685.00	-2.9713	1.2102	1.7402	1866.27
135	720.68	-677.64	-676.26	-2.9054	1.2209	1.7562	1827.58
140	715.97	-668.83	-667.44	-2.8412	1.2315	1.7722	1790.07
145	711.25	-659.94	-658.54	-2.7787	1.2420	1.7880	1753.62
150	706.53	-650.97	-649.56	-2.7178	1.2525	1.8038	1718.09
155	701.79	-641.92	-640.50	-2.6584	1.2630	1.8195	1683.38
160	697.04	-632.80	-631.36	-2.6004	1.2735	1.8353	1649.38
165	692.28	-623.59	-622.14	-2.5437	1.2840	1.8510	1616.00
170	687.51	-614.30	-612.85	-2.4882	1.2947	1.8668	1583.18
175	682.72	-604.94	-603.48	-2.4339	1.3056	1.8828	1550.85
180	677.91	-595.50	-594.02	-2.3806	1.3167	1.8989	1518.96
185	673.08	-585.97	-584.49	-2.3284	1.3280	1.9152	1487.46
190	668.23	-576.37	-574.87	-2.2771	1.3396	1.9318	1456.32
195	663.35	-566.68	-565.17	-2.2267	1.3516	1.9487	1425.50
200	658.45	-556.90	-555.38	-2.1771	1.3638	1.9659	1394.97
210	648.56	-537.09	-535.55	-2.0803	1.3894	2.0014	1334.70
220	638.53	-516.91	-515.35	-1.9864	1.4166	2.0387	1275.35
230	628.35	-496.36	-494.77	-1.8949	1.4454	2.0781	1216.79
240	617.98	-475.40	-473.78	-1.8056	1.4758	2.1196	1158.91
250	607.40	-454.01	-452.37	-1.7182	1.5079	2.1637	1101.60
260	596.57	-432.17	-430.50	-1.6324	1.5415	2.2106	1044.74
270	585.45	-409.85	-408.14	-1.5481	1.5767	2.2606	988.22
280	573.97	-387.02	-385.27	-1.4649	1.6134	2.3141	931.89
290	562.08	-363.63	-361.85	-1.3827	1.6514	2.3718	875.56
300	549.69	-339.64	-337.82	-1.3012	1.6908	2.4345	819.00
310	536.68	-315.00	-313.14	-1.2203	1.7314	2.5035	761.91
320	522.89	-289.64	-287.72	-1.1396	1.7733	2.5809	703.88
330	508.12	-263.45	-261.48	-1.0589	1.8167	2.6701	644.33
339.34 ^b	493.13	-238.13	-236.10	-0.98306	1.8587	2.7694	586.60
339.34 ^c	25.955	0.97325	39.502	-0.17087	1.8096	2.2009	187.21
340	25.846	2.2717	40.962	-0.16657	1.8114	2.1988	187.76
350	24.378	21.822	62.843	-0.10314	1.8423	2.1816	195.45
360	23.146	41.454	84.658	-0.041688	1.8780	2.1839	202.25
370	22.086	61.279	106.56	0.018312	1.9161	2.1973	208.41
380	21.156	81.360	128.63	0.077166	1.9553	2.2175	214.08
390	20.330	101.73	150.92	0.13508	1.9953	2.2425	219.35
400	19.586	122.43	173.49	0.19221	2.0358	2.2711	224.30
425	18.003	175.71	231.26	0.33227	2.1385	2.3522	235.61
450	16.710	231.31	291.15	0.46919	2.2408	2.4401	245.77
475	15.622	289.27	353.28	0.60354	2.3411	2.5303	255.09
500	14.687	349.58	417.67	0.73561	2.4386	2.6202	263.78
525	13.873	412.20	484.28	0.86560	2.5328	2.7086	271.97
550	13.154	477.06	553.08	0.99361	2.6236	2.7949	279.74
575	12.513	544.09	624.00	1.1197	2.7109	2.8786	287.16
1.5 MPa							
114.37 ^a	740.27	-713.25	-711.22	-3.1918	1.1778	1.6901	1997.44
115	739.68	-712.19	-710.16	-3.1825	1.1790	1.6921	1991.94
120	734.99	-703.70	-701.66	-3.1102	1.1895	1.7078	1949.01
125	730.29	-695.14	-693.08	-3.0401	1.2002	1.7238	1907.62
130	725.60	-686.49	-684.43	-2.9722	1.2110	1.7399	1867.70

TABLE 47. Thermodynamic properties of isobutane in the single-phase region—Continued

T (K)	ρ (kg m ⁻³)	u (kJ kg ⁻¹)	h (kJ kg ⁻¹)	s (kJ kg ⁻¹ K ⁻¹)	c_v (kJ kg ⁻¹ K ⁻¹)	c_p (kJ kg ⁻¹ K ⁻¹)	w (m s ⁻¹)
135	720.90	-677.77	-675.69	-2.9063	1.2216	1.7559	1829.11
140	716.20	-668.96	-666.87	-2.8421	1.2322	1.7718	1791.71
145	711.49	-660.08	-657.97	-2.7797	1.2427	1.7876	1755.36
150	706.77	-651.11	-648.99	-2.7188	1.2532	1.8034	1719.94
155	702.05	-642.07	-639.93	-2.6594	1.2636	1.8191	1685.32
160	697.31	-632.95	-630.80	-2.6014	1.2741	1.8347	1651.42
165	692.56	-623.75	-621.59	-2.5447	1.2847	1.8505	1618.15
170	687.80	-614.48	-612.29	-2.4892	1.2953	1.8662	1585.44
175	683.02	-605.12	-602.92	-2.4349	1.3062	1.8821	1553.21
180	678.22	-595.68	-593.47	-2.3817	1.3173	1.8982	1521.43
185	673.40	-586.17	-583.94	-2.3294	1.3286	1.9145	1490.04
190	668.57	-576.57	-574.33	-2.2781	1.3402	1.9310	1459.00
195	663.70	-566.89	-564.63	-2.2278	1.3521	1.9478	1428.30
200	658.82	-557.13	-554.85	-2.1782	1.3644	1.9649	1397.88
210	648.96	-537.34	-535.02	-2.0815	1.3900	2.0003	1337.86
220	638.97	-517.18	-514.84	-1.9876	1.4172	2.0375	1278.76
230	628.83	-496.65	-494.27	-1.8962	1.4459	2.0766	1220.48
240	618.51	-475.72	-473.30	-1.8070	1.4764	2.1179	1162.90
250	607.99	-454.37	-451.90	-1.7196	1.5084	2.1616	1105.92
260	597.22	-432.57	-430.06	-1.6339	1.5421	2.2081	1049.44
270	586.18	-410.29	-407.73	-1.5497	1.5772	2.2575	993.34
280	574.79	-387.51	-384.90	-1.4666	1.6139	2.3104	937.48
290	563.01	-364.18	-361.51	-1.3846	1.6519	2.3671	881.70
300	550.75	-340.26	-337.54	-1.3033	1.6911	2.4286	825.79
310	537.91	-315.71	-312.92	-1.2226	1.7317	2.4960	769.49
320	524.34	-290.45	-287.59	-1.1422	1.7735	2.5709	712.44
330	509.85	-264.41	-261.47	-1.0618	1.8166	2.6563	654.16
340	494.16	-237.45	-234.42	-0.98107	1.8613	2.7572	593.92
350	476.78	-209.39	-206.24	-0.89941	1.9081	2.8832	530.58
358.57 ^b	459.95	-184.20	-180.94	-0.82800	1.9507	3.0270	472.33
358.57 ^c	40.446	24.429	61.515	-0.15183	1.9297	2.5165	175.99
360	39.978	27.574	65.095	-0.14187	1.9333	2.4999	177.62
370	37.176	49.316	89.665	-0.074544	1.9618	2.4238	187.73
380	34.966	70.808	113.71	-0.010425	1.9929	2.3895	196.24
390	33.141	92.269	137.53	0.051457	2.0260	2.3781	203.69
400	31.587	113.83	161.32	0.11168	2.0613	2.3813	210.38
425	28.491	168.67	221.32	0.25716	2.1556	2.4247	224.85
450	26.120	225.32	282.75	0.39760	2.2532	2.4923	237.16
475	24.209	284.05	346.01	0.53440	2.3505	2.5700	248.07
500	22.617	344.96	411.28	0.66829	2.4459	2.6516	257.97
525	21.259	408.04	478.60	0.79966	2.5387	2.7342	267.11
550	20.082	473.29	547.98	0.92875	2.6284	2.8162	275.66
575	19.046	540.64	619.40	1.0557	2.7150	2.8967	283.72
2 MPa							
114.58 ^a	740.26	-712.99	-710.29	-3.1895	1.1790	1.6905	1996.70
115	739.86	-712.29	-709.59	-3.1834	1.1798	1.6918	1993.05
120	735.18	-703.81	-701.09	-3.1111	1.1903	1.7076	1950.23
125	730.49	-695.25	-692.51	-3.0410	1.2009	1.7235	1908.94
130	725.80	-686.61	-683.85	-2.9731	1.2117	1.7396	1869.12
135	721.11	-677.89	-675.11	-2.9072	1.2223	1.7556	1830.63
140	716.42	-669.09	-666.30	-2.8430	1.2329	1.7714	1793.34
145	711.72	-660.21	-657.40	-2.7806	1.2434	1.7872	1757.09
150	707.01	-651.25	-648.42	-2.7197	1.2539	1.8029	1721.77
155	702.30	-642.22	-639.37	-2.6604	1.2643	1.8186	1687.26
160	697.57	-633.11	-630.24	-2.6024	1.2747	1.8342	1653.47

TABLE 47. Thermodynamic properties of isobutane in the single-phase region—Continued

<i>T</i> (K)	<i>p</i> (kg m ⁻³)	<i>u</i> (kJ kg ⁻¹)	<i>h</i> (kJ kg ⁻¹)	<i>s</i> (kJ kg ⁻¹ K ⁻¹)	<i>c_v</i> (kJ kg ⁻¹ K ⁻¹)	<i>c_p</i> (kJ kg ⁻¹ K ⁻¹)	<i>w</i> (m s ⁻¹)
165	692.83	-623.91	-621.03	-2.5457	1.2853	1.8499	1620.30
170	688.08	-614.65	-611.74	-2.4902	1.2960	1.8656	1587.68
175	683.32	-605.30	-602.37	-2.4359	1.3068	1.8815	1555.56
180	678.53	-595.87	-592.92	-2.3827	1.3179	1.8975	1523.88
185	673.73	-586.36	-583.40	-2.3305	1.3292	1.9137	1492.60
190	668.90	-576.78	-573.79	-2.2792	1.3408	1.9302	1461.68
195	664.06	-567.11	-564.09	-2.2289	1.3527	1.9469	1431.08
200	659.18	-557.35	-554.32	-2.1794	1.3650	1.9640	1400.78
210	649.36	-537.58	-534.50	-2.0827	1.3906	1.9993	1340.99
220	639.41	-517.45	-514.33	-1.9888	1.4177	2.0362	1282.16
230	629.31	-496.95	-493.77	-1.8975	1.4465	2.0751	1224.15
240	619.04	-476.05	-472.82	-1.8083	1.4769	2.1161	1166.86
250	608.57	-454.73	-451.44	-1.7211	1.5090	2.1596	1110.21
260	597.87	-432.96	-429.62	-1.6355	1.5426	2.2056	1054.09
270	586.90	-410.73	-407.32	-1.5513	1.5778	2.2546	998.39
280	575.60	-387.99	-384.51	-1.4684	1.6144	2.3068	942.99
290	563.93	-364.72	-361.17	-1.3865	1.6523	2.3627	887.74
300	551.80	-340.87	-337.25	-1.3054	1.6915	2.4231	832.46
310	539.11	-316.40	-312.69	-1.2249	1.7320	2.4888	776.91
320	525.75	-291.25	-287.45	-1.1447	1.7736	2.5615	720.78
330	511.53	-265.34	-261.43	-1.0647	1.8166	2.6436	663.66
340	496.21	-238.56	-234.53	-0.98438	1.8609	2.7390	604.95
350	479.39	-210.75	-206.58	-0.90337	1.9071	2.8554	543.77
360	460.41	-181.65	-177.30	-0.82090	1.9560	3.0083	478.61
370	437.98	-150.73	-146.16	-0.73560	2.0095	3.2386	406.45
373.51 ^b	428.80	-139.25	-134.58	-0.70445	2.0303	3.3580	378.30
373.51 ^c	57.188	40.594	75.566	-0.14182	2.0425	2.9661	163.47
380	53.482	56.722	94.118	-0.092573	2.0508	2.7747	172.92
390	49.272	80.448	121.04	-0.022635	2.0691	2.6288	184.56
400	46.082	103.55	146.95	0.042963	2.0943	2.5614	194.12
425	40.396	160.76	210.27	0.19654	2.1755	2.5242	213.09
450	36.438	218.83	273.72	0.34158	2.2669	2.5576	228.12
475	33.419	278.52	338.36	0.48137	2.3605	2.6169	240.87
500	30.993	340.12	404.65	0.61736	2.4536	2.6873	252.12
525	28.976	403.74	472.76	0.75028	2.5447	2.7624	262.29
550	27.258	469.41	542.78	0.88056	2.6333	2.8392	271.66
575	25.769	537.11	614.72	1.0085	2.7190	2.9159	280.39
3 MPa							
115.00 ^a	740.23	-712.49	-708.44	-3.1851	1.1814	1.6913	1995.31
115	740.22	-712.48	-708.43	-3.1851	1.1814	1.6913	1995.28
120	735.55	-704.01	-699.94	-3.1128	1.1918	1.7070	1952.65
125	730.88	-695.47	-691.36	-3.0428	1.2024	1.7230	1911.57
130	726.21	-686.84	-682.71	-2.9749	1.2131	1.7390	1871.96
135	721.54	-678.13	-673.97	-2.9090	1.2238	1.7549	1833.68
140	716.86	-669.34	-665.16	-2.8449	1.2343	1.7707	1796.59
145	712.18	-660.48	-656.26	-2.7824	1.2448	1.7864	1760.55
150	707.50	-651.53	-647.29	-2.7216	1.2552	1.8021	1725.43
155	702.80	-642.51	-638.24	-2.6623	1.2656	1.8177	1691.12
160	698.10	-633.41	-629.12	-2.6043	1.2760	1.8332	1657.53
165	693.38	-624.24	-619.91	-2.5477	1.2866	1.8488	1624.56
170	688.65	-614.98	-610.63	-2.4922	1.2972	1.8645	1592.16
175	683.91	-605.65	-601.27	-2.4380	1.3081	1.8803	1560.24
180	679.15	-596.24	-591.82	-2.3848	1.3191	1.8962	1528.77
185	674.37	-586.75	-582.30	-2.3326	1.3304	1.9123	1497.70
190	669.57	-577.18	-572.70	-2.2814	1.3420	1.9286	1466.99
195	664.76	-567.53	-563.02	-2.2311	1.3539	1.9453	1436.61

TABLE 47. Thermodynamic properties of isobutane in the single-phase region—Continued

T (K)	ρ (kg m ⁻³)	u (kJ kg ⁻¹)	h (kJ kg ⁻¹)	s (kJ kg ⁻¹ K ⁻¹)	c_v (kJ kg ⁻¹ K ⁻¹)	c_p (kJ kg ⁻¹ K ⁻¹)	w (m s ⁻¹)
200	659.91	-557.79	-553.25	-2.1816	1.3662	1.9622	1406.54
210	650.15	-538.07	-533.45	-2.0850	1.3917	1.9972	1347.22
220	640.28	-517.98	-513.30	-1.9913	1.4189	2.0338	1288.88
230	630.26	-497.53	-492.77	-1.9000	1.4476	2.0722	1231.40
240	620.09	-476.69	-471.85	-1.8110	1.4780	2.1128	1174.69
250	609.72	-455.43	-450.51	-1.7239	1.5101	2.1556	1118.67
260	599.15	-433.73	-428.73	-1.6385	1.5437	2.2009	1063.24
270	588.31	-411.58	-406.48	-1.5545	1.5788	2.2489	1008.32
280	577.19	-388.94	-383.74	-1.4718	1.6153	2.2999	953.80
290	565.71	-365.77	-360.47	-1.3902	1.6532	2.3543	899.56
300	553.83	-342.06	-336.64	-1.3094	1.6923	2.4126	845.45
310	541.44	-317.74	-312.20	-1.2293	1.7326	2.4756	791.28
320	528.46	-292.78	-287.11	-1.1496	1.7741	2.5444	736.83
330	514.74	-267.12	-261.29	-1.0702	1.8166	2.6208	681.79
340	500.07	-240.66	-234.66	-0.99066	1.8604	2.7074	625.77
350	484.19	-213.29	-207.09	-0.91076	1.9057	2.8089	568.19
360	466.65	-184.83	-178.40	-0.82995	1.9529	2.9341	508.19
370	446.70	-154.99	-148.27	-0.74741	2.0030	3.1014	444.33
380	422.83	-123.18	-116.08	-0.66158	2.0586	3.3595	373.75
390	391.03	-87.871	-80.199	-0.56840	2.1283	3.9078	289.24
396.44 ^b	358.51	-60.392	-52.024	-0.49677	2.2028	5.1698	214.04
396.44 ^c	104.77	55.430	84.063	-0.15349	2.2933	5.7129	134.86
400	95.405	69.772	101.22	-0.11041	2.2417	4.2367	145.97
425	71.152	140.91	183.08	0.088439	2.2280	2.9007	185.60
450	60.780	203.86	253.22	0.24884	2.2988	2.7514	208.63
475	54.137	266.30	321.72	0.39699	2.3825	2.7401	226.04
500	49.287	329.72	390.59	0.53829	2.4698	2.7744	240.43
525	45.496	394.66	460.60	0.67491	2.5572	2.8282	252.88
550	42.404	461.33	532.07	0.80790	2.6432	2.8911	263.99
575	39.806	529.82	605.18	0.93788	2.7272	2.9581	274.10
4 MPa							
115.40 ^a	740.21	-712.00	-706.59	-3.1809	1.1837	1.6921	1994.01
120	735.93	-704.22	-698.78	-3.1145	1.1933	1.7065	1955.07
125	731.27	-695.68	-690.21	-3.0445	1.2039	1.7224	1914.19
130	726.62	-687.06	-681.56	-2.9767	1.2146	1.7384	1874.79
135	721.97	-678.37	-672.83	-2.9107	1.2252	1.7542	1836.71
140	717.31	-669.59	-664.02	-2.8467	1.2357	1.7700	1799.82
145	712.65	-660.74	-655.13	-2.7843	1.2461	1.7857	1763.98
150	707.98	-651.81	-646.16	-2.7235	1.2565	1.8013	1729.07
155	703.30	-642.80	-637.11	-2.6642	1.2669	1.8168	1694.96
160	698.62	-633.72	-627.99	-2.6062	1.2773	1.8323	1661.57
165	693.92	-624.56	-618.79	-2.5496	1.2878	1.8478	1628.80
170	689.22	-615.32	-609.51	-2.4942	1.2984	1.8634	1596.60
175	684.50	-606.00	-600.16	-2.4400	1.3093	1.8790	1564.89
180	679.76	-596.61	-590.72	-2.3868	1.3203	1.8949	1533.62
185	675.01	-587.14	-581.21	-2.3347	1.3316	1.9109	1502.76
190	670.24	-577.58	-571.61	-2.2835	1.3432	1.9271	1472.26
195	665.45	-567.95	-561.94	-2.2332	1.3551	1.9436	1442.10
200	660.64	-558.23	-552.18	-2.1838	1.3673	1.9605	1412.24
210	650.94	-538.55	-532.40	-2.0873	1.3929	1.9951	1353.38
220	641.13	-518.51	-512.27	-1.9937	1.4200	2.0314	1295.52
230	631.20	-498.10	-491.77	-1.9026	1.4487	2.0695	1238.55
240	621.11	-477.31	-470.87	-1.8137	1.4791	2.1096	1182.40
250	610.85	-456.12	-449.57	-1.7267	1.5111	2.1518	1126.98
260	600.39	-434.49	-427.83	-1.6414	1.5447	2.1964	1072.22
270	589.70	-412.41	-405.63	-1.5577	1.5798	2.2436	1018.04

TABLE 47. Thermodynamic properties of isobutane in the single-phase region—Continued

T (K)	ρ (kg m ⁻³)	u (kJ kg ⁻¹)	h (kJ kg ⁻¹)	s (kJ kg ⁻¹ K ⁻¹)	c_v (kJ kg ⁻¹ K ⁻¹)	c_p (kJ kg ⁻¹ K ⁻¹)	w (m s ⁻¹)
280	578.73	-389.86	-382.95	-1.4752	1.6163	2.2935	964.35
290	567.45	-366.80	-359.75	-1.3938	1.6541	2.3465	911.04
300	555.79	-343.20	-336.01	-1.3133	1.6932	2.4030	858.01
310	543.68	-319.03	-311.68	-1.2335	1.7333	2.4636	805.10
320	531.04	-294.25	-286.72	-1.1543	1.7746	2.5291	752.14
330	517.75	-268.80	-261.07	-1.0754	1.8169	2.6008	698.92
340	503.66	-242.62	-234.67	-0.99657	1.8602	2.6806	645.15
350	488.55	-215.61	-207.43	-0.91759	1.9048	2.7714	590.48
360	472.13	-187.67	-179.19	-0.83806	1.9508	2.8784	534.39
370	453.90	-158.58	-149.77	-0.75746	1.9988	3.0111	476.14
380	433.07	-128.06	-118.82	-0.67493	2.0501	3.1895	414.52
390	408.03	-95.474	-85.671	-0.58883	2.1073	3.4646	347.41
400	374.74	-59.311	-48.637	-0.49510	2.1788	4.0279	270.30
425	125.28	108.62	140.54	-0.037133	2.3178	4.3537	150.66
450	92.889	185.00	228.06	0.16327	2.3382	3.1117	187.69
475	78.875	252.20	302.91	0.32519	2.4071	2.9218	211.15
500	70.023	318.25	375.38	0.47386	2.4869	2.8885	229.14
525	63.629	384.90	447.77	0.61514	2.5700	2.9083	244.05
550	58.670	452.80	520.98	0.75136	2.6532	2.9512	256.96
575	54.649	522.22	595.42	0.88371	2.7352	3.0054	268.45
5 MPa							
115.80 ^a	740.20	-711.52	-704.76	-3.1767	1.1861	1.6929	1992.81
120	736.30	-704.42	-697.63	-3.1162	1.1948	1.7060	1957.47
125	731.66	-695.89	-689.06	-3.0463	1.2054	1.7219	1916.80
130	727.03	-687.29	-680.41	-2.9784	1.2160	1.7378	1877.60
135	722.39	-678.60	-671.68	-2.9125	1.2266	1.7536	1839.73
140	717.75	-669.84	-662.88	-2.8485	1.2370	1.7693	1803.04
145	713.11	-661.00	-653.99	-2.7861	1.2474	1.7849	1767.40
150	708.46	-652.08	-645.03	-2.7253	1.2578	1.8004	1732.69
155	703.80	-643.09	-635.99	-2.6661	1.2681	1.8159	1698.78
160	699.14	-634.02	-626.87	-2.6082	1.2785	1.8313	1665.58
165	694.46	-624.87	-617.67	-2.5516	1.2890	1.8468	1633.02
170	689.78	-615.65	-608.40	-2.4962	1.2997	1.8623	1601.01
175	685.08	-606.35	-599.05	-2.4420	1.3105	1.8779	1569.49
180	680.37	-596.97	-589.62	-2.3889	1.3215	1.8936	1538.43
185	675.64	-587.51	-580.11	-2.3368	1.3328	1.9095	1507.77
190	670.90	-577.98	-570.53	-2.2856	1.3443	1.9257	1477.48
195	666.14	-568.36	-560.86	-2.2354	1.3562	1.9421	1447.53
200	661.35	-558.66	-551.10	-2.1860	1.3685	1.9588	1417.89
210	651.72	-539.02	-531.35	-2.0896	1.3940	1.9932	1359.47
220	641.98	-519.02	-511.24	-1.9961	1.4211	2.0291	1302.08
230	632.12	-498.67	-490.76	-1.9051	1.4498	2.0669	1245.61
240	622.13	-477.93	-469.89	-1.8163	1.4802	2.1065	1190.00
250	611.97	-456.79	-448.62	-1.7294	1.5122	2.1482	1135.16
260	601.62	-435.23	-426.92	-1.6443	1.5458	2.1922	1081.04
270	591.06	-413.23	-404.77	-1.5607	1.5808	2.2385	1027.55
280	580.24	-390.76	-382.14	-1.4785	1.6173	2.2874	974.64
290	569.13	-367.80	-359.01	-1.3973	1.6550	2.3392	922.21
300	557.68	-344.31	-335.35	-1.3171	1.6940	2.3941	870.18
310	545.83	-320.28	-311.12	-1.2376	1.7341	2.4526	818.42
320	533.50	-295.65	-286.28	-1.1588	1.7751	2.5154	766.80
330	520.60	-270.40	-260.79	-1.0804	1.8172	2.5832	715.17
340	507.01	-244.46	-234.59	-1.0022	1.8602	2.6575	663.34
350	492.56	-217.76	-207.61	-0.92395	1.9042	2.7403	611.08
360	477.04	-190.23	-179.75	-0.84546	1.9494	2.8346	558.07
370	460.11	-161.73	-150.87	-0.76633	1.9961	2.9458	503.94

TABLE 47. Thermodynamic properties of isobutane in the single-phase region—Continued

<i>T</i> (K)	<i>ρ</i> (kg m ⁻³)	<i>u</i> (kJ kg ⁻¹)	<i>h</i> (kJ kg ⁻¹)	<i>s</i> (kJ kg ⁻¹ K ⁻¹)	<i>c_v</i> (kJ kg ⁻¹ K ⁻¹)	<i>c_p</i> (kJ kg ⁻¹ K ⁻¹)	<i>w</i> (m s ⁻¹)
380	441.29	-132.08	-120.75	-0.68601	2.0447	3.0835	448.12
390	419.77	-100.96	-89.047	-0.60368	2.0967	3.2667	389.89
400	394.05	-67.804	-55.115	-0.51779	2.1541	3.5415	328.20
425	270.12	40.202	58.713	-0.24266	2.3658	6.8137	159.53
450	139.29	159.80	195.69	0.071658	2.3829	3.8489	168.79
475	109.14	235.74	281.55	0.25750	2.4332	3.1911	197.65
500	93.684	305.60	358.97	0.41636	2.5044	3.0356	219.06
525	83.540	374.47	434.32	0.56342	2.5827	3.0039	236.29
550	76.103	443.85	509.55	0.70341	2.6630	3.0197	250.88
575	70.293	514.35	585.48	0.83842	2.7430	3.0575	263.66
6 MPa							
116.20 ^a	740.19	-711.05	-702.94	-3.1727	1.1884	1.6937	1991.71
120	736.67	-704.62	-696.48	-3.1179	1.1963	1.7056	1959.87
125	732.05	-696.11	-687.91	-3.0480	1.2068	1.7214	1919.40
130	727.43	-687.51	-679.26	-2.9802	1.2174	1.7372	1880.40
135	722.81	-678.84	-670.54	-2.9143	1.2280	1.7529	1842.73
140	718.19	-670.09	-661.73	-2.8503	1.2384	1.7686	1806.25
145	713.56	-661.26	-652.85	-2.7879	1.2488	1.7842	1770.81
150	708.93	-652.36	-643.89	-2.7272	1.2591	1.7996	1736.29
155	704.30	-643.38	-634.86	-2.6679	1.2694	1.8150	1702.57
160	699.65	-634.32	-625.74	-2.6101	1.2798	1.8304	1669.57
165	695.00	-625.19	-616.55	-2.5535	1.2903	1.8458	1637.20
170	690.33	-615.98	-607.29	-2.4982	1.3009	1.8612	1605.39
175	685.66	-606.69	-597.94	-2.4440	1.3117	1.8767	1574.07
180	680.97	-597.33	-588.52	-2.3909	1.3227	1.8924	1543.20
185	676.27	-587.89	-579.02	-2.3388	1.3339	1.9082	1512.74
190	671.55	-578.37	-569.44	-2.2877	1.3455	1.9242	1482.66
195	666.82	-568.77	-559.77	-2.2376	1.3574	1.9405	1452.91
200	662.06	-559.09	-550.03	-2.1882	1.3696	1.9571	1423.48
210	652.49	-539.48	-530.29	-2.0919	1.3951	1.9913	1365.49
220	642.82	-519.53	-510.20	-1.9985	1.4222	2.0269	1308.56
230	633.04	-499.22	-489.74	-1.9075	1.4509	2.0643	1252.58
240	623.12	-478.54	-468.91	-1.8189	1.4813	2.1035	1197.49
250	613.06	-457.45	-447.67	-1.7322	1.5133	2.1448	1143.21
260	602.82	-435.96	-426.00	-1.6472	1.5468	2.1881	1089.69
270	592.38	-414.03	-403.90	-1.5638	1.5818	2.2337	1036.88
280	581.71	-391.64	-381.32	-1.4817	1.6182	2.2818	984.70
290	570.77	-368.77	-358.25	-1.4007	1.6560	2.3324	933.09
300	559.52	-345.39	-334.67	-1.3208	1.6948	2.3859	881.98
310	547.91	-321.48	-310.53	-1.2416	1.7348	2.4426	831.28
320	535.86	-297.00	-285.80	-1.1631	1.7758	2.5029	780.88
330	523.32	-271.92	-260.45	-1.0851	1.8176	2.5675	730.67
340	510.16	-246.20	-234.43	-1.0075	1.8604	2.6374	680.53
350	496.28	-219.77	-207.68	-0.92993	1.9040	2.7139	630.29
360	481.50	-192.59	-180.13	-0.85230	1.9485	2.7990	579.80
370	465.60	-164.55	-151.67	-0.77433	1.9942	2.8957	528.84
380	448.25	-135.54	-122.16	-0.69564	2.0412	3.0091	477.18
390	429.00	-105.39	-91.399	-0.61575	2.0902	3.1479	424.56
400	407.10	-73.802	-59.064	-0.53390	2.1421	3.3282	370.77
425	329.94	15.576	33.761	-0.30908	2.2922	4.2887	233.44
450	205.38	127.86	157.08	-0.027314	2.4100	4.7477	167.66
475	146.24	216.77	257.80	0.19080	2.4569	3.5505	189.04
500	120.58	291.78	341.54	0.36270	2.5209	3.2150	211.60
525	105.28	363.40	420.39	0.51660	2.5948	3.1137	230.33
550	94.678	434.52	497.90	0.66082	2.6722	3.0953	246.18

TABLE 47. Thermodynamic properties of isobutane in the single-phase region—Continued

T (K)	ρ (kg m ⁻³)	u (kJ kg ⁻¹)	h (kJ kg ⁻¹)	s (kJ kg ⁻¹ K ⁻¹)	c_v (kJ kg ⁻¹ K ⁻¹)	c_p (kJ kg ⁻¹ K ⁻¹)	w (m s ⁻¹)
7 MPa							
575	86.692	506.24	575.45	0.79873	2.7504	3.1135	259.99
116.58 ^a	740.19	-710.59	-701.14	-3.1688	1.1907	1.6944	1990.69
120	737.04	-704.82	-695.32	-3.1196	1.1978	1.7051	1962.26
125	732.44	-696.32	-686.76	-3.0497	1.2083	1.7208	1921.99
130	727.83	-687.73	-678.12	-2.9819	1.2188	1.7366	1883.19
135	723.23	-679.07	-669.39	-2.9161	1.2293	1.7523	1845.72
140	718.62	-670.33	-660.59	-2.8521	1.2397	1.7679	1809.44
145	714.02	-661.52	-651.71	-2.7897	1.2501	1.7834	1774.19
150	709.40	-652.63	-642.76	-2.7290	1.2604	1.7988	1739.87
155	704.79	-643.66	-633.73	-2.6698	1.2707	1.8142	1706.35
160	700.16	-634.61	-624.62	-2.6120	1.2810	1.8295	1673.54
165	695.53	-625.50	-615.43	-2.5554	1.2915	1.8448	1641.36
170	690.89	-616.30	-606.17	-2.5001	1.3021	1.8601	1609.74
175	686.24	-607.03	-596.83	-2.4460	1.3128	1.8756	1578.61
180	681.57	-597.68	-587.41	-2.3929	1.3238	1.8911	1547.94
185	676.89	-588.26	-577.92	-2.3409	1.3351	1.9069	1517.68
190	672.20	-578.76	-568.34	-2.2898	1.3466	1.9228	1487.79
195	667.49	-569.18	-558.69	-2.2397	1.3585	1.9390	1458.25
200	662.76	-559.52	-548.95	-2.1904	1.3707	1.9555	1429.02
210	653.25	-539.95	-529.23	-2.0942	1.3962	1.9894	1371.46
220	643.65	-520.04	-509.16	-2.0008	1.4233	2.0248	1314.97
230	633.94	-499.77	-488.73	-1.9100	1.4520	2.0618	1259.46
240	624.11	-479.13	-467.92	-1.8214	1.4823	2.1007	1204.87
250	614.14	-458.11	-446.71	-1.7348	1.5143	2.1414	1151.13
260	604.00	-436.67	-425.08	-1.6500	1.5478	2.1842	1098.19
270	593.68	-414.81	-403.02	-1.5668	1.5828	2.2292	1046.01
280	583.15	-392.49	-380.49	-1.4848	1.6192	2.2764	994.54
290	572.37	-369.71	-357.48	-1.4041	1.6569	2.3260	943.70
300	561.30	-346.43	-333.96	-1.3244	1.6957	2.3782	893.46
310	549.91	-322.64	-309.91	-1.2455	1.7356	2.4333	843.72
320	538.13	-298.29	-285.29	-1.1673	1.7764	2.4915	794.43
330	525.90	-273.38	-260.06	-1.0897	1.8181	2.5534	745.50
340	513.14	-247.84	-234.20	-1.0125	1.8606	2.6197	696.84
350	499.75	-221.66	-207.65	-0.93558	1.9039	2.6912	648.35
360	485.61	-194.77	-180.36	-0.85869	1.9480	2.7692	599.95
370	470.54	-167.12	-152.24	-0.78166	1.9929	2.8556	551.54
380	454.33	-138.62	-123.21	-0.70424	2.0388	2.9532	503.02
390	436.70	-109.16	-93.126	-0.62610	2.0860	3.0663	454.37
400	417.22	-78.586	-61.808	-0.54682	2.1348	3.2018	405.61
425	355.89	4.4293	24.099	-0.33866	2.2663	3.7326	285.85
450	265.55	101.47	127.83	-0.10171	2.3963	4.4799	197.97
475	188.56	196.55	233.68	0.12736	2.4707	3.8686	190.96
500	150.36	277.15	323.70	0.31217	2.5343	3.4046	208.81
525	128.66	351.87	406.28	0.47336	2.6053	3.2307	227.11
550	114.26	424.93	486.19	0.62208	2.6805	3.1748	243.37
575	103.74	497.97	565.45	0.76300	2.7571	3.1717	257.74
8 MPa							
116.96 ^a	740.20	-710.15	-699.34	-3.1649	1.1930	1.6951	1989.76
120	737.41	-705.02	-694.17	-3.1213	1.1992	1.7046	1964.64
125	732.82	-696.53	-685.61	-3.0514	1.2097	1.7203	1924.57
130	728.23	-687.95	-676.97	-2.9836	1.2202	1.7360	1885.97
135	723.65	-679.30	-668.25	-2.9178	1.2307	1.7517	1848.70
140	719.06	-670.58	-659.45	-2.8538	1.2411	1.7673	1812.61
145	714.47	-661.77	-650.58	-2.7916	1.2514	1.7827	1777.56

TABLE 47. Thermodynamic properties of isobutane in the single-phase region—Continued

<i>T</i> (K)	<i>ρ</i> (kg m ⁻³)	<i>u</i> (kJ kg ⁻¹)	<i>h</i> (kJ kg ⁻¹)	<i>s</i> (kJ kg ⁻¹ K ⁻¹)	<i>c_v</i> (kJ kg ⁻¹ K ⁻¹)	<i>c_p</i> (kJ kg ⁻¹ K ⁻¹)	<i>w</i> (m s ⁻¹)
150	709.87	-652.89	-641.62	-2.7309	1.2616	1.7981	1743.43
155	705.28	-643.94	-632.60	-2.6716	1.2719	1.8133	1710.10
160	700.67	-634.91	-623.49	-2.6138	1.2822	1.8286	1677.48
165	696.06	-625.80	-614.31	-2.5573	1.2927	1.8438	1645.49
170	691.44	-616.62	-605.05	-2.5021	1.3032	1.8591	1614.06
175	686.81	-607.37	-595.72	-2.4480	1.3140	1.8745	1583.13
180	682.16	-598.03	-586.31	-2.3949	1.3250	1.8900	1552.65
185	677.51	-588.63	-576.82	-2.3429	1.3362	1.9056	1522.58
190	672.84	-579.14	-567.25	-2.2919	1.3478	1.9215	1492.88
195	668.16	-569.58	-557.60	-2.2418	1.3596	1.9376	1463.54
200	663.46	-559.93	-547.87	-2.1925	1.3718	1.9539	1434.51
210	654.00	-540.40	-528.17	-2.0964	1.3973	1.9876	1377.36
220	644.46	-520.53	-508.12	-2.0031	1.4244	2.0228	1321.31
230	634.83	-500.31	-487.71	-1.9124	1.4531	2.0595	1266.26
240	625.08	-479.72	-466.92	-1.8239	1.4834	2.0979	1212.15
250	615.19	-458.75	-445.74	-1.7375	1.5153	2.1382	1158.93
260	605.16	-437.37	-424.15	-1.6528	1.5488	2.1805	1106.55
270	594.96	-415.57	-402.13	-1.5697	1.5838	2.2248	1054.98
280	584.56	-393.33	-379.65	-1.4879	1.6202	2.2713	1004.16
290	573.93	-370.63	-356.69	-1.4074	1.6578	2.3200	954.06
300	563.04	-347.45	-333.24	-1.3279	1.6966	2.3710	904.62
310	551.85	-323.76	-309.26	-1.2493	1.7364	2.4247	855.79
320	540.31	-299.54	-284.74	-1.1714	1.7771	2.4811	807.51
330	528.37	-274.77	-259.63	-1.0942	1.8187	2.5407	759.73
340	515.97	-249.42	-233.91	-1.0174	1.8610	2.6039	712.39
350	503.02	-223.44	-207.54	-0.94095	1.9040	2.6714	665.43
360	489.42	-196.81	-180.47	-0.86469	1.9477	2.7439	618.81
370	475.05	-169.48	-152.64	-0.78845	1.9920	2.8226	572.49
380	459.76	-141.39	-123.99	-0.71205	2.0371	2.9092	526.47
390	443.36	-112.47	-94.424	-0.63526	2.0831	3.0058	480.79
400	425.59	-82.626	-63.829	-0.55780	2.1301	3.1158	435.59
425	372.86	-3.1339	18.322	-0.35870	2.2525	3.4834	326.96
450	303.11	85.369	111.76	-0.14521	2.3760	3.9923	238.78
475	229.40	178.09	212.97	0.073676	2.4714	3.9528	205.99
500	181.46	262.49	306.58	0.26584	2.5426	3.5568	212.58
525	153.10	340.19	392.44	0.43345	2.6136	3.3408	227.61
550	134.54	415.22	474.68	0.58649	2.6876	3.2528	242.99
575	121.25	489.63	555.61	0.73040	2.7630	3.2294	257.22
10 MPa							
117.70 ^a	740.24	-709.28	-695.77	-3.1576	1.1974	1.6965	1988.14
120	738.15	-705.41	-691.86	-3.1247	1.2021	1.7037	1969.38
125	733.59	-696.94	-683.31	-3.0548	1.2125	1.7193	1929.71
130	729.03	-688.39	-674.67	-2.9871	1.2230	1.7349	1891.50
135	724.48	-679.76	-665.96	-2.9213	1.2334	1.7505	1854.62
140	719.92	-671.06	-657.17	-2.8574	1.2437	1.7660	1818.92
145	715.37	-662.28	-648.30	-2.7951	1.2539	1.7813	1784.25
150	710.81	-653.42	-639.35	-2.7345	1.2641	1.7966	1750.50
155	706.25	-644.49	-630.33	-2.6753	1.2744	1.8117	1717.55
160	701.68	-635.49	-621.24	-2.6176	1.2846	1.8268	1685.30
165	697.11	-626.41	-612.06	-2.5611	1.2950	1.8419	1653.68
170	692.53	-617.26	-602.82	-2.5059	1.3056	1.8571	1622.62
175	687.94	-608.03	-593.49	-2.4519	1.3163	1.8723	1592.06
180	683.34	-598.73	-584.09	-2.3989	1.3273	1.8877	1561.95
185	678.73	-589.35	-574.62	-2.3470	1.3385	1.9032	1532.26
190	674.11	-579.90	-565.06	-2.2960	1.3500	1.9189	1502.95

TABLE 47. Thermodynamic properties of isobutane in the single-phase region—Continued

T (K)	ρ (kg m ⁻³)	u (kJ kg ⁻¹)	h (kJ kg ⁻¹)	s (kJ kg ⁻¹ K ⁻¹)	c_v (kJ kg ⁻¹ K ⁻¹)	c_p (kJ kg ⁻¹ K ⁻¹)	w (m s ⁻¹)
195	669.48	-570.36	-555.43	-2.2460	1.3618	1.9348	1473.98
200	664.83	-560.75	-545.71	-2.1968	1.3740	1.9510	1445.35
210	655.49	-541.29	-526.04	-2.1008	1.3995	1.9842	1389.00
220	646.07	-521.50	-506.02	-2.0077	1.4265	2.0188	1333.78
230	636.57	-501.37	-485.66	-1.9172	1.4552	2.0550	1279.61
240	626.97	-480.87	-464.92	-1.8289	1.4855	2.0927	1226.42
250	617.26	-460.00	-443.80	-1.7427	1.5174	2.1323	1174.19
260	607.42	-438.73	-422.27	-1.6583	1.5508	2.1736	1122.87
270	597.43	-417.06	-400.32	-1.5754	1.5858	2.2168	1072.43
280	587.28	-394.95	-377.93	-1.4940	1.6221	2.2619	1022.84
290	576.93	-372.41	-355.07	-1.4138	1.6596	2.3090	974.08
300	566.36	-349.40	-331.74	-1.3347	1.6983	2.3580	926.11
310	555.55	-325.91	-307.91	-1.2566	1.7380	2.4093	878.90
320	544.45	-301.92	-283.55	-1.1792	1.7786	2.4627	832.42
330	533.02	-277.40	-258.64	-1.1026	1.8199	2.5185	786.64
340	521.23	-252.35	-233.17	-1.0265	1.8619	2.5770	741.55
350	509.02	-226.74	-207.10	-0.95097	1.9045	2.6383	697.13
360	496.32	-200.54	-180.39	-0.87575	1.9476	2.7028	653.38
370	483.07	-173.73	-153.03	-0.80078	1.9912	2.7710	610.34
380	469.19	-146.27	-124.96	-0.72593	2.0352	2.8433	568.06
390	454.57	-118.14	-96.144	-0.65109	2.0797	2.9205	526.64
400	439.11	-89.303	-66.530	-0.57611	2.1246	3.0033	486.23
425	396.01	-13.836	11.416	-0.38717	2.2383	3.2401	391.31
450	345.26	66.863	95.826	-0.19425	2.3517	3.5155	310.82
475	288.94	151.94	186.55	0.001897	2.4561	3.7060	257.74
500	238.30	236.82	278.78	0.19116	2.5439	3.6366	239.25
525	201.23	318.02	367.71	0.36475	2.6217	3.4813	241.31
550	175.32	396.28	453.32	0.52406	2.6970	3.3777	250.77
575	156.60	473.21	537.07	0.67298	2.7719	3.3304	262.29
15 MPa							
119.45 ^a	740.44	-707.28	-687.02	-3.1407	1.2081	1.6998	1985.41
120	739.95	-706.36	-686.09	-3.1330	1.2092	1.7015	1981.09
125	735.47	-697.94	-677.55	-3.0632	1.2194	1.7169	1942.39
130	730.99	-689.44	-668.92	-2.9956	1.2297	1.7323	1905.15
135	726.52	-680.87	-660.22	-2.9299	1.2399	1.7477	1869.23
140	722.04	-672.22	-651.45	-2.8661	1.2500	1.7629	1834.46
145	717.57	-663.50	-642.59	-2.8039	1.2601	1.7780	1800.72
150	713.10	-654.70	-633.67	-2.7434	1.2702	1.7930	1767.88
155	708.62	-645.83	-624.66	-2.6844	1.2803	1.8079	1735.83
160	704.15	-636.89	-615.59	-2.6267	1.2905	1.8228	1704.48
165	699.67	-627.88	-606.44	-2.5704	1.3008	1.8376	1673.74
170	695.18	-618.79	-597.21	-2.5153	1.3112	1.8525	1643.57
175	690.69	-609.63	-587.91	-2.4614	1.3218	1.8674	1613.89
180	686.20	-600.40	-578.54	-2.4086	1.3327	1.8824	1584.66
185	681.70	-591.09	-569.09	-2.3568	1.3439	1.8975	1555.86
190	677.19	-581.71	-559.56	-2.3060	1.3553	1.9128	1527.44
195	672.68	-572.26	-549.96	-2.2561	1.3671	1.9284	1499.37
200	668.15	-562.73	-540.28	-2.2071	1.3793	1.9441	1471.65
210	659.07	-543.44	-520.68	-2.1115	1.4047	1.9764	1417.16
220	649.95	-523.82	-500.74	-2.0188	1.4316	2.0100	1363.85
230	640.76	-503.88	-480.47	-1.9287	1.4602	2.0449	1311.68
240	631.51	-483.59	-459.84	-1.8409	1.4905	2.0813	1260.58
250	622.18	-462.95	-438.84	-1.7551	1.5223	2.1191	1210.54
260	612.77	-441.93	-417.45	-1.6713	1.5557	2.1586	1161.54
270	603.25	-420.53	-395.66	-1.5890	1.5906	2.1996	1113.56

TABLE 47. Thermodynamic properties of isobutane in the single-phase region—Continued

T (K)	ρ (kg m ⁻³)	u (kJ kg ⁻¹)	h (kJ kg ⁻¹)	s (kJ kg ⁻¹ K ⁻¹)	c_v (kJ kg ⁻¹ K ⁻¹)	c_p (kJ kg ⁻¹ K ⁻¹)	w (m s ⁻¹)
280	593.63	-398.73	-373.46	-1.5083	1.6268	2.2421	1066.60
290	583.88	-376.51	-350.82	-1.4288	1.6642	2.2861	1020.65
300	573.98	-353.86	-327.73	-1.3506	1.7027	2.3316	975.70
310	563.93	-330.78	-304.18	-1.2733	1.7422	2.3786	931.74
320	553.71	-307.24	-280.15	-1.1971	1.7824	2.4269	888.77
330	543.29	-283.25	-255.64	-1.1216	1.8234	2.4766	846.80
340	532.66	-258.78	-230.62	-1.0469	1.8649	2.5277	805.83
350	521.80	-233.83	-205.08	-0.97292	1.9069	2.5800	765.89
360	510.68	-208.38	-179.01	-0.89949	1.9493	2.6336	727.01
370	499.28	-182.45	-152.40	-0.82659	1.9919	2.6884	689.22
380	487.58	-156.00	-125.24	-0.75415	2.0346	2.7444	652.59
390	475.55	-129.05	-97.512	-0.68213	2.0774	2.8014	617.21
400	463.19	-101.59	-69.209	-0.61047	2.1203	2.8593	583.15
425	430.73	-30.714	4.1106	-0.43272	2.2269	3.0066	504.59
450	396.09	43.243	81.114	-0.25671	2.3316	3.1527	436.99
475	359.85	119.96	161.64	-0.082585	2.4326	3.2857	382.45
500	323.48	198.74	245.11	0.088655	2.5280	3.3843	343.01
525	289.30	278.56	330.41	0.25512	2.6171	3.4312	319.23
550	259.36	358.50	416.33	0.41500	2.7005	3.4380	308.43
575	234.35	438.20	502.21	0.56769	2.7798	3.4319	306.18
20 MPa							
121.09 ^a	740.77	-705.47	-678.47	-3.1258	1.2182	1.7027	1984.31
125	737.32	-698.91	-671.78	-3.0714	1.2261	1.7147	1954.88
130	732.91	-690.46	-663.17	-3.0038	1.2361	1.7299	1918.57
135	728.51	-681.94	-654.48	-2.9383	1.2462	1.7451	1883.56
140	724.11	-673.34	-645.72	-2.8745	1.2561	1.7601	1849.69
145	719.72	-664.67	-636.88	-2.8125	1.2661	1.7750	1816.84
150	715.33	-655.93	-627.97	-2.7521	1.2760	1.7898	1784.86
155	710.93	-647.12	-618.98	-2.6932	1.2860	1.8045	1753.66
160	706.54	-638.23	-609.92	-2.6356	1.2960	1.8191	1723.15
165	702.15	-629.28	-600.79	-2.5794	1.3062	1.8337	1693.25
170	697.76	-620.25	-591.59	-2.5245	1.3166	1.8483	1663.90
175	693.36	-611.15	-582.31	-2.4707	1.3271	1.8629	1635.05
180	688.97	-601.99	-572.96	-2.4180	1.3380	1.8776	1606.64
185	684.57	-592.75	-563.53	-2.3664	1.3491	1.8925	1578.66
190	680.16	-583.44	-554.03	-2.3157	1.3605	1.9075	1551.06
195	675.76	-574.05	-544.46	-2.2659	1.3722	1.9227	1523.82
200	671.34	-564.60	-534.81	-2.2171	1.3843	1.9381	1496.92
210	662.50	-545.46	-515.27	-2.1218	1.4096	1.9697	1444.11
220	653.63	-526.01	-495.41	-2.0294	1.4365	2.0023	1392.52
230	644.72	-506.24	-475.22	-1.9396	1.4650	2.0363	1342.10
240	635.78	-486.14	-454.68	-1.8522	1.4952	2.0716	1292.83
250	626.78	-465.69	-433.78	-1.7669	1.5270	2.1082	1244.68
260	617.73	-444.89	-412.51	-1.6835	1.5604	2.1462	1197.64
270	608.62	-423.71	-390.85	-1.6018	1.5952	2.1856	1151.71
280	599.43	-402.16	-368.79	-1.5215	1.6313	2.2263	1106.90
290	590.17	-380.21	-346.32	-1.4427	1.6686	2.2683	1063.19
300	580.82	-357.86	-323.42	-1.3651	1.7070	2.3114	1020.60
310	571.37	-335.09	-300.09	-1.2886	1.7463	2.3556	979.12
320	561.81	-311.91	-276.31	-1.2131	1.7864	2.4008	938.76
330	552.14	-288.29	-252.07	-1.1385	1.8272	2.4470	899.53
340	542.34	-264.24	-227.37	-1.0647	1.8685	2.4939	861.43
350	532.40	-239.75	-202.19	-0.99176	1.9102	2.5415	824.48
360	522.33	-214.82	-176.53	-0.91949	1.9521	2.5898	788.70
370	512.10	-189.45	-150.39	-0.84787	1.9942	2.6385	754.14

TABLE 47. Thermodynamic properties of isobutane in the single-phase region—Continued

T (K)	ρ (kg m ⁻³)	u (kJ kg ⁻¹)	h (kJ kg ⁻¹)	s (kJ kg ⁻¹ K ⁻¹)	c_v (kJ kg ⁻¹ K ⁻¹)	c_p (kJ kg ⁻¹ K ⁻¹)	w (m s ⁻¹)
380	501.71	-163.63	-123.76	-0.77685	2.0365	2.6875	720.81
390	491.16	-137.36	-96.641	-0.70641	2.0787	2.7368	688.77
400	480.45	-110.65	-69.027	-0.63649	2.1208	2.7861	658.06
425	452.98	-41.996	2.1557	-0.46391	2.2251	2.9081	587.48
450	424.66	29.246	76.343	-0.29433	2.3272	3.0258	526.33
475	395.82	102.85	153.37	-0.12776	2.4262	3.1349	475.18
500	367.06	178.49	232.97	0.035535	2.5212	3.2305	434.25
525	339.13	255.77	314.75	0.19511	2.6118	3.3079	403.50
550	312.87	334.28	398.20	0.35039	2.6980	3.3652	382.36
575	288.97	413.66	482.87	0.50092	2.7801	3.4059	369.47
25 MPa							
122.61 ^a	741.21	-703.82	-670.09	-3.1124	1.2278	1.7054	1984.60
125	739.13	-699.83	-666.01	-3.0794	1.2325	1.7126	1967.18
130	734.79	-691.43	-657.41	-3.0120	1.2423	1.7277	1931.78
135	730.46	-682.96	-648.73	-2.9465	1.2522	1.7427	1897.65
140	726.14	-674.41	-639.98	-2.8828	1.2620	1.7575	1864.65
145	721.82	-665.79	-631.16	-2.8209	1.2717	1.7722	1832.63
150	717.50	-657.11	-622.26	-2.7606	1.2815	1.7868	1801.48
155	713.19	-648.35	-613.29	-2.7017	1.2914	1.8013	1771.09
160	708.87	-639.52	-604.25	-2.6443	1.3013	1.8157	1741.38
165	704.56	-630.62	-595.13	-2.5882	1.3114	1.8301	1712.27
170	700.26	-621.65	-585.95	-2.5334	1.3217	1.8445	1683.69
175	695.95	-612.61	-576.69	-2.4797	1.3322	1.8589	1655.60
180	691.64	-603.51	-567.36	-2.4271	1.3429	1.8734	1627.96
185	687.33	-594.33	-557.96	-2.3756	1.3540	1.8880	1600.74
190	683.03	-585.08	-548.48	-2.3251	1.3653	1.9027	1573.89
195	678.72	-575.76	-538.93	-2.2755	1.3770	1.9177	1547.41
200	674.41	-566.37	-529.30	-2.2267	1.3891	1.9328	1521.28
210	665.78	-547.37	-509.82	-2.1317	1.4143	1.9637	1469.99
220	657.14	-528.07	-490.02	-2.0396	1.4411	1.9957	1419.95
230	648.49	-508.45	-469.90	-1.9501	1.4696	2.0289	1371.11
240	639.81	-488.52	-449.44	-1.8631	1.4998	2.0633	1323.44
250	631.11	-468.25	-428.63	-1.7781	1.5315	2.0990	1276.94
260	622.37	-447.63	-407.46	-1.6951	1.5648	2.1359	1231.59
270	613.60	-426.65	-385.91	-1.6138	1.5995	2.1741	1187.41
280	604.79	-405.31	-363.97	-1.5340	1.6356	2.2135	1144.40
290	595.94	-383.59	-341.64	-1.4556	1.6729	2.2540	1102.55
300	587.03	-361.48	-318.89	-1.3785	1.7112	2.2954	1061.87
310	578.07	-338.97	-295.73	-1.3025	1.7504	2.3378	1022.37
320	569.04	-316.07	-272.13	-1.2276	1.7904	2.3809	984.04
330	559.95	-292.75	-248.10	-1.1537	1.8310	2.4248	946.90
340	550.78	-269.03	-223.64	-1.0807	1.8721	2.4692	910.94
350	541.54	-244.88	-198.72	-1.0084	1.9136	2.5140	876.19
360	532.22	-220.33	-173.35	-0.93699	1.9554	2.5591	842.63
370	522.83	-195.35	-147.54	-0.86626	1.9973	2.6045	810.30
380	513.35	-169.96	-121.26	-0.79620	2.0392	2.6499	779.21
390	503.79	-144.16	-94.538	-0.72678	2.0811	2.6953	749.38
400	494.15	-117.95	-67.360	-0.65797	2.1228	2.7404	720.84
425	469.73	-50.675	2.5468	-0.48848	2.2261	2.8515	655.22
450	444.99	18.999	75.180	-0.32244	2.3271	2.9582	598.03
475	420.15	90.898	150.40	-0.15979	2.4252	3.0582	549.36
500	395.54	164.81	228.02	-0.000561	2.5197	3.1496	509.02
525	371.53	240.51	307.79	0.15512	2.6104	3.2308	476.64
550	348.54	317.74	389.46	0.30707	2.6972	3.3009	451.68
575	326.92	396.28	472.75	0.45516	2.7803	3.3605	433.44

TABLE 47. Thermodynamic properties of isobutane in the single-phase region—Continued

T (K)	ρ (kg m ⁻³)	u (kJ kg ⁻¹)	h (kJ kg ⁻¹)	s (kJ kg ⁻¹ K ⁻¹)	c_v (kJ kg ⁻¹ K ⁻¹)	c_p (kJ kg ⁻¹ K ⁻¹)	w (m s ⁻¹)
30 MPa							
124.05 ^a	741.73	-702.32	-661.87	-3.1004	1.2368	1.7078	1986.08
125	740.91	-700.73	-660.24	-3.0873	1.2386	1.7107	1979.32
130	736.64	-692.37	-651.65	-3.0199	1.2483	1.7256	1944.79
135	732.38	-683.94	-642.98	-2.9545	1.2579	1.7404	1911.51
140	728.12	-675.45	-634.24	-2.8909	1.2676	1.7551	1879.34
145	723.87	-666.88	-625.43	-2.8291	1.2772	1.7697	1848.13
150	719.62	-658.24	-616.55	-2.7689	1.2868	1.7841	1817.77
155	715.38	-649.53	-607.59	-2.7101	1.2966	1.7984	1788.15
160	711.14	-640.75	-598.56	-2.6528	1.3064	1.8126	1759.19
165	706.91	-631.90	-589.46	-2.5968	1.3164	1.8268	1730.82
170	702.68	-622.99	-580.29	-2.5421	1.3266	1.8410	1702.97
175	698.46	-614.01	-571.05	-2.4885	1.3370	1.8553	1675.61
180	694.23	-604.96	-561.74	-2.4360	1.3477	1.8696	1648.68
185	690.01	-595.84	-552.36	-2.3846	1.3587	1.8839	1622.16
190	685.79	-586.65	-542.90	-2.3342	1.3700	1.8985	1596.03
195	681.57	-577.39	-533.37	-2.2847	1.3816	1.9131	1570.25
200	677.36	-568.06	-523.77	-2.2360	1.3936	1.9280	1544.81
210	668.93	-549.19	-504.34	-2.1412	1.4188	1.9584	1494.93
220	660.50	-530.02	-484.60	-2.0494	1.4456	1.9899	1446.29
230	652.07	-510.55	-464.54	-1.9602	1.4740	2.0224	1398.87
240	643.64	-490.76	-444.15	-1.8735	1.5041	2.0561	1352.64
250	635.20	-470.64	-423.41	-1.7888	1.5358	2.0911	1307.59
260	626.74	-450.19	-402.32	-1.7061	1.5690	2.1272	1263.73
270	618.27	-429.39	-380.86	-1.6251	1.6037	2.1645	1221.06
280	609.79	-408.23	-359.03	-1.5457	1.6397	2.2029	1179.58
290	601.28	-386.70	-336.80	-1.4677	1.6769	2.2422	1139.30
300	592.75	-364.79	-314.18	-1.3911	1.7152	2.2825	1100.22
310	584.18	-342.50	-291.15	-1.3155	1.7544	2.3235	1062.34
320	575.59	-319.83	-267.71	-1.2411	1.7943	2.3653	1025.67
330	566.97	-296.76	-243.84	-1.1677	1.8348	2.4075	990.20
340	558.31	-273.29	-219.56	-1.0952	1.8758	2.4502	955.93
350	549.62	-249.42	-194.84	-1.0235	1.9172	2.4933	922.87
360	540.89	-225.15	-169.69	-0.95269	1.9588	2.5365	891.01
370	532.12	-200.49	-144.11	-0.88261	2.0005	2.5798	860.36
380	523.31	-175.42	-118.09	-0.81323	2.0423	2.6230	830.92
390	514.47	-149.96	-91.649	-0.74454	2.0840	2.6661	802.70
400	505.60	-124.11	-64.773	-0.67650	2.1255	2.7090	775.70
425	483.31	-57.799	4.2736	-0.50910	2.2282	2.8142	713.58
450	460.95	10.820	75.903	-0.34535	2.3287	2.9154	659.15
475	438.70	81.612	150.00	-0.18514	2.4262	3.0111	612.29
500	416.74	154.41	226.40	-0.028395	2.5203	3.1002	572.71
525	395.32	229.06	304.94	0.12487	2.6110	3.1819	539.95
550	374.67	305.36	385.43	0.27464	2.6979	3.2561	513.45
575	355.01	383.18	467.69	0.42088	2.7814	3.3229	492.62
35 MPa							
125.40 ^a	742.32	-700.93	-653.78	-3.0895	1.2453	1.7100	1988.58
130	738.45	-693.28	-645.88	-3.0277	1.2540	1.7236	1957.62
135	734.25	-684.89	-637.23	-2.9624	1.2634	1.7383	1925.16
140	730.06	-676.44	-628.50	-2.8989	1.2729	1.7529	1893.79
145	725.87	-667.91	-619.70	-2.8371	1.2824	1.7673	1863.35
150	721.70	-659.32	-610.82	-2.7770	1.2919	1.7815	1833.74
155	717.52	-650.66	-601.88	-2.7183	1.3015	1.7957	1804.86
160	713.36	-641.93	-592.87	-2.6611	1.3113	1.8098	1776.62
165	709.20	-633.14	-583.78	-2.6052	1.3212	1.8239	1748.95

TABLE 47. Thermodynamic properties of isobutane in the single-phase region—Continued

<i>T</i> (K)	<i>ρ</i> (kg m ⁻³)	<i>u</i> (kJ kg ⁻¹)	<i>h</i> (kJ kg ⁻¹)	<i>s</i> (kJ kg ⁻¹ K ⁻¹)	<i>c_v</i> (kJ kg ⁻¹ K ⁻¹)	<i>c_p</i> (kJ kg ⁻¹ K ⁻¹)	<i>w</i> (m s ⁻¹)
170	705.04	-624.27	-574.63	-2.5505	1.3313	1.8379	1721.79
175	700.89	-615.34	-565.40	-2.4970	1.3416	1.8520	1695.11
180	696.75	-606.34	-556.11	-2.4447	1.3522	1.8661	1668.85
185	692.61	-597.28	-546.74	-2.3933	1.3631	1.8803	1643.00
190	688.47	-588.14	-537.31	-2.3430	1.3744	1.8946	1617.52
195	684.34	-578.94	-527.80	-2.2936	1.3860	1.9091	1592.39
200	680.21	-569.67	-518.22	-2.2451	1.3980	1.9238	1567.61
210	671.96	-550.91	-498.83	-2.1505	1.4231	1.9538	1519.01
220	663.73	-531.87	-479.14	-2.0589	1.4498	1.9847	1471.66
230	655.50	-512.52	-459.13	-1.9700	1.4782	2.0167	1425.52
240	647.29	-492.87	-438.80	-1.8835	1.5082	2.0499	1380.59
250	639.08	-472.89	-418.13	-1.7991	1.5399	2.0843	1336.84
260	630.87	-452.59	-397.11	-1.7166	1.5731	2.1197	1294.29
270	622.67	-431.94	-375.73	-1.6360	1.6078	2.1563	1252.94
280	614.47	-410.94	-353.98	-1.5569	1.6437	2.1939	1212.80
290	606.26	-389.58	-331.85	-1.4792	1.6809	2.2325	1173.87
300	598.05	-367.85	-309.33	-1.4029	1.7191	2.2718	1136.15
310	589.83	-345.75	-286.41	-1.3277	1.7582	2.3119	1099.64
320	581.61	-323.27	-263.09	-1.2537	1.7980	2.3526	1064.35
330	573.37	-300.40	-239.36	-1.1807	1.8385	2.3938	1030.26
340	565.13	-277.14	-215.21	-1.1086	1.8794	2.4353	997.36
350	556.88	-253.50	-190.65	-1.0374	1.9207	2.4771	965.67
360	548.62	-229.46	-165.67	-0.96701	1.9622	2.5190	935.16
370	540.35	-205.04	-140.27	-0.89742	2.0038	2.5610	905.84
380	532.07	-180.23	-114.45	-0.82857	2.0455	2.6028	877.69
390	523.78	-155.03	-88.212	-0.76042	2.0870	2.6445	850.71
400	515.50	-129.46	-61.560	-0.69295	2.1284	2.6859	824.91
425	494.79	-63.872	6.8650	-0.52705	2.2308	2.7876	765.44
450	474.18	3.9758	77.788	-0.36492	2.3309	2.8856	713.10
475	453.76	73.972	151.10	-0.20638	2.4280	2.9789	667.65
500	433.69	145.98	226.69	-0.051328	2.5220	3.0667	628.75
525	414.12	219.87	304.39	0.10030	2.6124	3.1486	595.95
550	395.19	295.50	384.07	0.24855	2.6994	3.2245	568.73
575	377.06	372.74	465.57	0.39345	2.7830	3.2945	546.53

^aTemperature on the melting curve.^bSaturated liquid.^cSaturated vapor.

11. References

- Ababio, B. D., P. J. McElroy, and A. G. Williamson, Fluid Phase Equilib. **95**, 329 (1994).
- Abdulagatov, I. M., L. N. Levina, Z. R. Zakaryaev, and O. N. Mamchenkova, Fluid Phase Equilib. **127**, 205 (1997).
- Ambrose, D. and C. Tsionopoulos, J. Chem. Eng. Data **40**, 531 (1995).
- Aston, J. G., R. M. Kennedy, and S. C. Schuman, J. Am. Chem. Soc. **62**, 2059 (1940).
- Aston, J. G. and G. H. Messerly, J. Am. Chem. Soc. **62**, 1917 (1940).
- Beattie, J. A., G. L. Simard, and G.-J. Su, J. Am. Chem. Soc. **61**, 26 (1939a).
- Beattie, J. A., G. L. Simard, and G.-J. Su, J. Am. Chem. Soc. **61**, 24 (1939b).
- Beattie, J. A., G.-J. Su, and G. L. Simard, J. Am. Chem. Soc. **61**, 926 (1939c).
- Beattie, J. A. and W. H. Stockmayer, J. Chem. Phys. **10**, 473 (1942).
- Beattie, J. A., D. G. Edward, and M. Stanley, Jr., J. Chem. Phys. **17**, 576 (1949).
- Beattie, J. A., M. Stanley, Jr., and D. G. Edward, J. Chem. Phys. **18**, 127 (1950).
- Bedford, R. E., and C. G. M. Kirby, Metrologia **5**, 83 (1969).
- Beeck, O., J. Chem. Phys. **4**, 680 (1936).
- Bender, R., Ph.D. thesis, Universität Karlsruhe, 1982.
- Benoliel, R. W., M.Sc. thesis, Pennsylvania State College, 1941.
- Berestov, A. T., M. S. Giterman, and N. G. Shmakov, Zh. Eksp. Teor. Fiz. **64**, 2232 (1973); [Sov. Phys. JETP **37**, 1128 (1973)].
- Bottomley, G. A. and D. B. Nairn, Aust. J. Chem. **30**, 1645 (1977).
- Bottomley, G. A. and T. H. Spurling, Aust. J. Chem. **17**, 501 (1964).
- Boyes, S. J., Ph.D. thesis, University of London, 1992.
- Browstow, W., D. M. McEachern, and S. Perez-Gutierrez, J. Chem. Phys. **71**, 2716 (1979).
- Brunner, E., J. Chem. Thermodyn. **20**, 273 (1988).
- Bücker, D. and W. Wagner, J. Phys. Chem. Ref. Data **35**, 205 (2006).
- Burrell, G. A. and I. W. Robertson, J. Am. Chem. Soc. **37**, 2188 (1915a).
- Burrell, G. A. and I. W. Robertson, J. Am. Chem. Soc. **37**, 2482 (1915b).
- Carmichael, L. T., K. C. Hwang, V. M. Berry, and B. H. Sage, J. Chem. Eng. Data **7**, 331 (1962).
- Carney, B. R., Petrol. Refin. **21**, 84 (1942).
- Carruth, G. F. and R. Kobayashi, J. Chem. Eng. **18**, 115 (1973).
- Chen, S. S., R. C. Wilhout, and B. J. Zwolinski, J. Phys. Chem. Ref. Data **4**, 859 (1975).
- Claus, P., G. Schilling, R. Kleinrahm, and W. Wagner (private communication), Ruhr-Universität Bochum, 2002.

- Claus, P., R. Kleinrahm, and W. Wagner, *J. Chem. Thermodyn.* **35**, 159 (2003).
- Coffin, C. and O. Maass, *J. Am. Chem. Soc.* **50**, 1427 (1928).
- Colgate, S. O., C. F. Sona, K. R. Reed, and A. Sivaraman, *J. Chem. Eng. Data* **35**, 1 (1990).
- Connolly, J. F., *Ind. Eng. Chem.* **48**, 813 (1956).
- Connolly, J. F., *J. Phys. Chem.* **66**, 1082 (1962).
- Coplen, T. B., *J. Phys. Chem. Ref. Data* **30**, 701 (2001).
- Dailey, B. P. and W. A. Felsing, *J. Am. Chem. Soc.* **65**, 44 (1943).
- Dana, L. I., A. C. Jenkins, J. N. Burdick, and R. C. Timm, *Ref. Eng.* **12**, 387 (1926).
- Das, T. R., C. O. Reed, Jr., and P. T. Eubank, *J. Chem. Eng. Data* **18**, 244 (1973a).
- Das, T. R., C. O. Reed, Jr., and P. T. Eubank, *J. Chem. Eng. Data* **18**, 253 (1973b).
- Daubert, T. E., *J. Chem. Eng. Data* **41**, 365 (1996).
- Dobratz, C. J., *Ind. Eng. Chem.* **33**, 759 (1941).
- Douslin, D. R. and R. H. Harrison, *J. Chem. Thermodyn.* **5**, 491 (1973).
- Dawson, P. P., Jr. and J. J. McKetta, *Pet. Ref.* **39**, 151 (1960).
- Ely, J. F. and R. Kobayashi, *J. Chem. Eng. Data* **23**, 221 (1978).
- Ernst, G. and J. Büscher, *J. Chem. Thermodyn.* **2**, 787 (1970).
- Ernst, G. and U. E. Hochberg, *J. Chem. Thermodyn.* **21**, 407 (1989).
- Estrada-Alexanders, A. F. and J. P. M. Trusler, *J. Chem. Thermodyn.* **29**, 991 (1997).
- Ewers, J. and W. Wagner, *A method for optimizing the structure of equations of state and its application to an equation of state for oxygen*, Proceedings of the 8th Symposium on Thermophysical Properties, edited by J. V. Sengers (Am. Soc. of Mech. Engineers, New York, 1982), p. 78.
- Ewing, M. B. and A. R. H. Goodwin, *J. Chem. Thermodyn.* **23**, 1107 (1991).
- Ewing, M. B., A. R. H. Goodwin, M. L. McGlashan, and J. P. M. Trusler, *J. Chem. Thermodyn.* **20**, 243 (1988).
- Flebbe, J. L., D. A. Barclay, and D. B. Manley, *J. Chem. Eng. Data* **27**, 405 (1982).
- Francis, A. W., *Ind. Eng. Chem.* **33**, 554 (1941).
- Funke, M., R. Kleinrahm, and W. Wagner, *J. Chem. Thermodyn.* **34**, 2001 (2002a).
- Funke, M., R. Kleinrahm, and W. Wagner, *J. Chem. Thermodyn.* **34**, 2017 (2002b).
- Gainer, I. and G. Anitescu, *An. Univ. Bucuresti, Chim.* **91** (1992).
- Gilliland, E. R. and H. W. Scheeline, *Ind. Eng. Chem.* **32**, 48 (1940).
- Glos, S., R. Kleinrahm, and W. Wagner, *J. Chem. Thermodyn.* **36**, 1037 (2004).
- Golovskii, E. A., V. A. Zagoruchenko, and E. P. Mizevich, *Measurement of n-butane density in the range 135.29–273.00 K up to pressure 608.40 bar* (VNIIE Gazprom Depos. No. 50M, 1978a).
- Golovskii, Y. A., E. P. Mitsevich, and V. A. Tsymarny, *Measurement of the density of ethane at 90.24–270.21 K and at pressures to 604.09 bar* (VNIIE Gazprom Depos. No. 39M, 1978b).
- Gonzalez, M. H. and A. L. Lee, *J. Chem. Eng. Data* **11**, 357 (1966).
- Goodwin, R. D. and W. M. Haynes, *Thermophysical properties of isobutane from 114 to 700 K at pressures to 70 MPa* (NBS Tech. Note 1051, Boulder, 1982).
- Gunn, R. D., M.Sc. thesis, University of California, Berkley, 1958.
- Gupta, D. and P. T. Eubank, *J. Chem. Eng. Data* **42**, 961 (1997).
- Haase, R. and W. Tillmann, *Z. Phys. Chem.* **186**, 99 (1994).
- Händel, G., R. Kleinrahm, and W. Wagner, *J. Chem. Thermodyn.* **24**, 685 (1992).
- Hamann, S. D. and W. J. McManamey, *Trans. Faraday Soc.* **49**, 149 (1953).
- Harand, J., *Monatsh. Chem.* **65**, 153 (1935).
- Haynes, W. M., *J. Chem. Thermodyn.* **15**, 801 (1983a).
- Haynes, W. M., *J. Chem. Eng. Data* **28**, 367 (1983b).
- Haynes, W. M., *J. Chem. Thermodynamics* **15**, 419 (1983c).
- Haynes, W. M. and R. D. Goodwin, *Thermophysical properties of normal butane from 135 to 700 K at pressures to 70 MPa* (NBS Monograph 169, Boulder, 1982).
- Haynes, W. M. and M. J. Hiza, *J. Chem. Thermodyn.* **9**, 179 (1977).
- Hirata, M. and S. Suda, *J. Japan Petrol. Inst.* **9**, 885 (1966).
- Hirschfelder, J. O., F. T. McClure, and I. F. Weeks, *J. Chem. Phys.* **10**, 201 (1942).
- Holcomb, C. D., J. W. Magee, and W. M. Haynes, *Density measurements on natural gas liquids*, Research Report RR-147 (Gas Processors Association, Tulsa, 1995).
- Holldorf, H. and H. Knapp, *Fluid Phase Equilib.* **40**, 113 (1988).
- Hsu, J. J. C., N. Nagarajan, and R. L. Robinson, Jr., *J. Chem. Eng. Data* **30**, 485 (1985).
- Huff, J. A. and T. M. Reed, *J. Chem. Eng. Data* **8**, 306 (1963).
- Huffman, H. M., G. S. Parks, and M. Barnmore, *J. Am. Chem. Soc.* **53**, 3876 (1931).
- Jones, A. E. and W. B. Kay, *AIChE J.* **13**, 720 (1967).
- Kahre, L. C., *J. Chem. Eng. Data* **18**, 267 (1973).
- Kaminishi, G.-I., C. Yokoyama, and S. Takahashi, *Sekiyu Gakkaishi* **31**, 433 (1988).
- Kappallo, W., N. Lund, and K. Schäfer, *Z. Phys. Chem.* **37**, 196 (1963).
- Kay, W. B., *Ind. Eng. Chem.* **32**, 358 (1940).
- Kay, W. B., *Ind. Eng. Chem.* **33**, 590 (1941).
- Kay, W. B., *J. Phys. Chem.* **68**, 827 (1964).
- Kay, W. B., *J. Chem. Eng. Data* **15**, 46 (1970).
- Kayukawa, Y., Ph.D. thesis, Keio University, 2002.
- Kiran, E. and Y. L. Sen, *Int. J. Thermophys.* **13**, 411 (1992).
- Kleinrahm, R. and W. Wagner, *J. Chem. Thermodyn.* **18**, 739 (1986).
- Klipping, G. and F. Schmidt, *Kältetechnik* **17**, 382 (1965).
- Kratzke, H., *J. Chem. Thermodyn.* **12**, 305 (1980).
- Kratzke, H. and S. Müller, *J. Chem. Thermodyn.* **16**, 1157 (1984).
- Kratzke, H., E. Spillner, and S. Müller, *J. Chem. Thermodyn.* **14**, 1175 (1982).
- Kreglewski, A. and W. B. Kay, *J. Phys. Chem.* **73**, 3359 (1969).
- Kuenen, J. P., *Communications from the Kamerlingh Onnes Laboratory of the University of Leiden*, 1911.
- Kumar, B., Thesis, Brown University, Providence, 1979.
- Kurnik, R. T. and A. J. Barduhn, *Desalination* **26**, 211 (1978).
- Laurance, D. R. and G. W. Swift, *J. Chem. Eng. Data* **19**, 61 (1974).
- Lemming, W., *Fortschr.-Ber. VDI*, Reihe 19, Nr. 32 (VDI-Verlag, Düsseldorf, 1989).
- Lemmon, E. W., M. O. McLinden, and W. Wagner (unpublished).
- Levett Sengers, J. M. H., B. Kamgar-Parsi, and J. V. Sengers, *J. Chem. Eng. Data* **28**, 354 (1983).
- Li, L. and E. Kiran, *J. Chem. Eng. Data* **33**, 342 (1988).
- M'Hirsi, A., *Comptes Rendus Hebdomadaires de Séances de Académie Sciences* **246**, 2355 (1958).
- Machin, W. D. and P. D. Golding, *J. Chem. Soc. Faraday Trans.* **85**, 2229 (1989).
- Magee, J. W. and T. O. D. Lüddecke, *Int. J. Thermophys.* **19**, 129 (1998).
- Mansoorian, H., K. R. Hall, J. C. Holste, and P. T. Eubank, *J. Chem. Thermodyn.* **13**, 1001 (1981).
- Martinez-Ortiz, J. A. and D. B. Manley, *J. Chem. Eng. Data* **23**, 165 (1978).
- Masui, R., H. A. Davis, and J. M. H. Levett Sengers, "A new magnetic suspension densimeter for determining fluid densities by weighing," in *Proceedings of the 8th Symposium on Thermophysical Properties*, Vol. 1, edited by J. V. Sengers (American Society of Mechanical Engineers, New York, 1982), p. 128.
- McClune, C. R., *Cryogenics* **16**, 289 (1976).
- McGlashan, M. L. and D. J. B. Potter, *Proc. Roy. Soc. A* **267**, 478 (1962).
- Mertes, T. S. and A. P. Colburn, *Ind. Eng. Chem.* **39**, 787 (1947).
- Miyamoto, H. and K. Watanabe, *Int. J. Thermophys.* **21**, 1045 (2000).
- Miyamoto, H. and K. Watanabe, *Int. J. Thermophys.* **22**, 459 (2001).
- Miyamoto, H. and K. Watanabe, *Int. J. Thermophys.* **23**, 477 (2002).
- Miyamoto, H., J. Takemura, and M. Uematsu, *J. Chem. Thermodyn.* **36**, 919 (2004).
- Mohr, P. J. and B. N. Taylor, *J. Phys. Chem. Ref. Data* **28**, 1713 (1999).
- Morris, W. M., B. H. Sage, and W. N. Lacey, *Tech. Pub. No. 1128, Am. Inst. Mining and Metallurgical Engineers*, New York (1939).
- NGAA, Tech. Committee, *Natural Gasoline Assoc. Am. Ind. Eng. Chem.* **34**, 1240 (1942).
- Niepmann, R., *J. Chem. Thermodyn.* **16**, 851 (1984).
- Olds, R. H., H. H. Reamer, B. H. Sage, and W. N. Lacey, *Ind. Eng. Chem.* **36**, 282 (1944).
- Orrit, J. E. and J. M. Laupretre, *Adv. Cryog. Eng.* **23**, 573 (1978).
- Pal, A. K., G. A. Pope, Y. Arai, N. F. Carnahan, and R. Kobayashi, *J. Chem. Eng. Data* **21**, 394 (1976).
- Parks, G. S., C. H. Shomate, W. D. Kennedy, and B. L. Crawford, *J. Chem. Phys.* **5**, 359 (1937).
- Pitzer, K. S., *Ind. Eng. Chem.* **36**, 829 (1944).
- Polt, A., B. Platzer, and G. Maurer, *Chem. Technik* **22**, 216 (1992).

- Preston-Thomas, H., *Metrologia* **27**, 3 (1990).
- Rao, M. G. S., *Ind. J. Pure Appl. Phys.* **9**, 169 (1971).
- Reeves, L. E., G. J. Scott, and S. E. Babb, *J. Chem. Phys.* **40**, 3662 (1964).
- Roder, H. M., *J. Res. NBS* **80A**, 739 (1976).
- Rodosevich, J. B. and R. C. Miller, *AIChE J.* **19**, 729 (1973).
- Rossini, F. D., K. S. Pitzer, R. L. Arnett, R. M. Braun, and G. C. Pimentel, *Selected Values of Physical and Thermodynamic Properties of Hydrocarbons and Related Compounds* (American Petroleum Institute, Carnegie Press, Pittsburgh, 1953).
- Rusby, R. L., *J. Chem. Thermodyn.* **23**, 1153 (1991).
- Sage, B. H. and W. N. Lacey, *Ind. Eng. Chem.* **30**, 673 (1938).
- Sage, B. H., D. C. Webster, and W. N. Lacey, *Ind. Eng. Chem.* **29**, 1188 (1937a).
- Sage, B. H., D. C. Webster, and W. N. Lacey, *Ind. Eng. Chem.* **29**, 1309 (1937b).
- Sako, T. and S. Horiguchi, *J. Chem. Eng. Data* **42**, 169 (1997).
- Schäfer, K. and W. Auer, *Werte der thermodynamischen Funktionen bei Standarddruecken in Abhängigkeit von der Temperatur für ausgewählte Stoffe*, Landolt-Börnstein (Springer, Berlin, 1961), Vol. 2.
- Schäfer, K., B. Schramm, and J. S. Urieta Navarro, *Z. Phys. Chem.* **93**, 203 (1974).
- Seibert, F. M. and G. A. Burrell, *J. Am. Chem. Soc.* **37**, 2683 (1915).
- Setzmann, U. and W. Wagner, *Int. J. Thermophys.* **10**, 1103 (1989).
- Setzmann, U. and W. Wagner, *J. Phys. Chem. Ref. Data* **20**, 1061 (1991).
- Sliwinski, P., *Z. Phys. Chem. Neue Folge* **63**, 263 (1969).
- Span, R., *Multiparameter Equations of State—An Accurate Source of Thermodynamic Property Data* (Springer, Berlin, 2000).
- Span, R., H.-J. Collmann, and W. Wagner, *Int. J. Thermophys.* **19**, 491 (1998).
- Span, R. and W. Wagner, *Int. J. Thermophys.* **18**, 1415 (1997).
- Span, R. and W. Wagner, *Int. J. Thermophys.* **24**, 1 (2003a).
- Span, R. and W. Wagner, *Int. J. Thermophys.* **24**, 41 (2003b).
- Span, R. and W. Wagner, *Int. J. Thermophys.* **24**, 111 (2003c).
- Steele, K., B. E. Polling, and D. B. Manley, *J. Chem. Eng. Data* **21**, 399 (1976).
- Straty, G. C. and R. Tsumura, *J. Res. NBS* **80A**, 35 (1976).
- Strein, K., R. N. Lichtenhaler, B. Schramm, and K. Schäfer, *Ber. Bunsenges. Phys. Chem.* **75**, 1308 (1971).
- Sychev, V. V., A. A. Vasserman, A. D. Kozlov, and V. A. Tsymarny, *Thermodynamic Properties of Butane* (Begell House, New York, 1995).
- Tegeler, C., R. Span, and W. Wagner, *Fortschr.-Ber. VDI*, Reihe 3, Nr. 480 (VDI-Verlag, Düsseldorf, 1997).
- Thomas, R. H. P. and R. H. Harrison, *J. Chem. Eng. Data* **27**, 1 (1982).
- Tickner, A. W. and F. P. Lossing, *J. Phys. Colloid Chem.* **55**, 733 (1951).
- Tripp, T. B. and R. D. Dunlap, *J. Phys. Chem.* **66**, 635 (1962).
- Trusler, J. P. M. and M. F. Costa Gomez, *The speed of sound in nitrogen and ethane*, Research report for the GERG-project “Fundamental equations for calorific properties,” London, 1996.
- Trusler, J. P. M. and M. P. Zarari, *J. Chem. Thermodyn.* **28**, 329 (1996).
- Tsiklis, D. S., A. I. Semenova, S. S. Tsimmermann, and E. A. Emel’yanova, *Russ. J. Phys. Chem.* **46**, 1677 (1972).
- Tsumura, R. and G. C. Straty, *Cryogenics* **17**, 195 (1977).
- van der Vet, A. P., *Density, Compressibility, Expansion of Light Hydrocarbons and of Light Hydrocarbon Blends* (Congress Mondial du Petrole, Paris II, 1937), Vol. 11, p. 515.
- Vangeel, E. (private communication with NBS, Boulder). Data published in Goodwin *et al.*, 1976.
- Visser, S. W., Ph.D. thesis, Universität Leiden, 1913.
- Wacker, P. F., R. K. Cheney, and R. B. Scott, *J. Res. Natl. Bur. Stand.* **38**, 651 (1947).
- Wackher, R. C., C. B. Linn, and A. V. Grosse, *Ind. Eng. Chem.* **37**, 464 (1945).
- Wagner, W., *Cryogenics* **12**, 214 (1972).
- Wagner, W., *Fortschr.-Ber. VDI-Z.*, Reihe 3, Nr. 39 (VDI-Verlag, Düsseldorf, 1974).
- Wagner, W. and A. Prüß, *J. Phys. Chem. Ref. Data* **31**, 387 (2002).
- Wagner, W. and R. Kleinrahm, *Metrologia* **41** (issue 2), S24 (2004).
- Waxman, M. (private communication with NBS, Boulder, 1980). Data published in: Goodwin and Haynes (1982).
- Waxman, M. and J. S. Gallagher, *Am. Chem. Soc.* **28**, 224 (1983).
- Weber, L. A., *Cryogenics* **25**, 338 (1985).
- Weber, L. A., *J. Chem. Eng. Data* **34**, 171 (1989).
- Yesavage, V. F., K. L. Katz, and J. E. Powers, *Proceedings 4th Symposium on Thermodynamic Properties* (A.S.M.E., New York, 1968), p. 45.
- Younglove, B. A., *J. Res. Natl. Bur. Stand.* **86**, 165 (1981).
- Younglove, B. A. and J. F. Ely, *J. Phys. Chem. Ref. Data* **16**, 577 (1987).